Evaluation of nitrate fluxes into a coastal lagoon through Submarine Groundwater Discharge (SGD)

A Thesis Presented to the Academic Faculty in Fulfilment of the

Requirements for the Degree of Doctor of Philosophy

2016

Shan Jiang

School of Natural Sciences

Discipline of Geography

Biogeochemistry Research Group

The University of Dublin

Trinity College

I declare that this thesis has not been submitted as an exercise for a degree at this or any other university and it is entirely my own work.

I agree to deposit this thesis in the University's open access institutional repository or allow the library to do so on my behalf, subject to Irish Copyright Legislation and Trinity College Library conditions of use and acknowledgement.

Shan Jiang

Summary

Submarine Groundwater Discharge (SGD) delivers substantial land-derived nitrate (NO_3^-) to coastal regions, which potentially influences the environmental status and ecological balance in the receiving water. A systematic study of NO_3^- discharge from SGD on a regional scale is however limited. In this thesis, distribution, turnover and circulation of SGD-borne NO_3^- in one semi-enclosed coastal system, the Ria Formosa lagoon (Portugal) were studied. The research in this thesis comprises an examination of NO_3^- transformation within the subterranean estuary, a regional quantification of NO_3^- input from SGD to the lagoon, and an evaluation of nutrient ratios and limiting nutrient in the case of N, P, and Si in SGD.

A combination of i*n-situ* sampling and laboratory simulation experiments under controlled conditions with deterministic modelling techniques was employed in order to quantify NO_3^- reduction/accumulation rates and to parameterise key factors affecting N processing in the benthic compartment. In particular, to separate the effects of chemical reactions from those of physical transport on porewater concentrations of N at the subterranean estuary, a 2-D Advection-Reaction model was used to describe the *in-situ* N-transformation rate. Results indicated that the subterranean estuary in the Ria Formosa lagoon is an important biogeochemical reactor, with clear effects on N turnover on a regional scale. The transformation rates varied from -0.69 mmol m^{-3} h^{-1} to 2.44 mmol m^{-3} h^{-1} for NO_3^- in different seasons.

As a potential electron donor to both NO_3^- reductions and benthic respiration, labile dissolved organic matter (DOM) may play an important role in the modulation of SGD-borne NO_3^-. Flow-Through Reactor (FTR) experiments with sediment collected at a sandy beach site within the Ria Formosa lagoon were performed under different labile DOM and NO_3^- input conditions. Results suggest that more than 70% of glucose added to porewater was utilised by aerobic respiration, while the stimulation of NO_3^- reduction in the sediment was limited compared with the enhancement of respiration.

This suggests that an enrichment of labile DOM in the subterranean estuary may lead to an increase in the magnitude of NO_3^- fluxes in SGD due to the significant stimulation of respiration and presence of nitrification.

The regional survey based on the NO_3^- concentration in endmembers and ^{222}Rn activity revealed that NO_3^- fluxes associated with SGD may reach $1.3(\pm1.0)\times10^3$ kg day^{-1}, even though a substantial amount of NO_3^- might be reduced in the subterranean estuary prior to discharge. Compared to the entire NO_3^- input into the lagoon, the magnitude of NO_3^- fluxes from SGD accounted for 89%. Furthermore, in the total NO_3^- budget of SGD, approximately 98% NO_3^- was derived from fresh groundwater. The exogenous NO_3^- from SGD was rapidly removed from the lagoon system. In particular, the reduction rate reached 69.9±68.5 μmol $N\text{-}NO_3^-$ m^2 h^{-1}. Such high reduction may reflect the assimilation potential from the lagoon algae.

As an important nutrient source in coastal regions, nutrient structure in SGD may influence ecological balance in the receiving water. To understand variations of nutrient structure in SGD, database established by previous annual field survey in the barrier island at the Ria Formosa lagoon was revaluated. Limiting nutrient along the mixing gradient was examined via a combination of frequency analysis and Dirichlet regression. Results showed that limiting nutrient in SGD can vary between N and P in both spring term and autumn term. Furthermore, in the autumn survey, the occurrence of Si-limitation in SGD was observed which may result from an increase of NO_3^- concentration in terrestrial groundwater and the presence of a spectrum of biogeochemical reactions in the subterranean estuary. To constrain the impact of SGD on the ecological balance in the lagoon, two possible regulation methods, further reduction of the NO_3^- concentration in terrestrial groundwater and proper management of groundwater sources, should be included in future regulation.

This work is dedicated to my parents, Minzhi Jiang and Lihui Zhan.

慈母吟

孟郊

慈母手中线，游子身上衣。
临行密密缝，意恐迟迟归。
谁言寸草心，报得三春晖。

Acknowledgements

In acknowledgements, I would like to use Chinese (my mother language) to express my gratitude to those people that offered me great help during my PhD study.

当博士毕业论文写到这里，意味着我即将完成在爱尔兰 Trinity College 的博士学习。四年前，我从中国“211 工程”和“985 工程”重点大学——厦门大学，来到有四百多年历史的 Trinity College Dublin。四年中，我一路走来，Trinity College 悠久的历史文化令我着迷，导师的谆谆教诲让我终身受益，同窗之谊、朋友之情让我永世难忘……

在 Trinity College Dublin 学习的四年，我首先要感谢导师 Prof. Carlos Rocha。遇见他，是我的幸运。四年来，他给与我学业上的指导、生活上的关心，使我能很快地适应新的学习环境，并找到研究的方向。Prof. Carlos Rocha 以严谨的态度对待科研和教学，不仅秉承了 Trinity College 优良的治学传统，也是 Prof. Carlos Rocha 人格魅力所在。Prof. Carlos Rocha 对我的引领已超越了专业范围，还包括为人处世的指引和关怀。

亦师亦友的 Mark Kavanagh 研究员，尽自己的最大努力为我的实验提供帮助。在我困惑的时候，他都会无私地伸出援助之手。

Centre for the Environment 和 School for the Natural Sciences 的老师们，在我实验进行和论文写作过程中，谆谆教导、指点迷津，显现了良好的师德和风范。

我读博士期间的好友和同伴：Dr. Tengwen Long, Dr. Xin Zhao, Kathyrn Woods, Dr.

Acknowledgement

Junfang Cui, Louise Esmonde, Qiang Yang, Feifei Zhang, Xiaoli Huang，有多少个日子，我们探讨学业，交流生活的感受，结下了兄弟姐妹般的友谊。

我还要感谢 Biogeochemistry 实验小组的同仁。在这个集体里，我们有各自独立的研究项目和方向，在自由而舒畅的环境中，大家有争论、有共鸣，彼此取长补短、共促成长。他们的名字将永存我的记忆里：Dr. Dannielle Green, Dr. Jean Wilson, Dr. Laura Foley, Dr. Alexandra Oppelt, and Tara Kelly。

Liliana Carvalho 在我来 Trinity College 之初，为了帮助我顺利地得到实验所需的数据，她将自己多年积累的经验和心得，毫无保留地拿出来与我分享。

本论文由 Prof. Ian Donohue 和 Prof. Yaqian Zhao 评审。我在这里对他们表示由衷的感谢。感谢他们在百忙之中抽出时间阅读，并提出诸多宝贵的意见。

最后，我由衷地感谢我远在故乡西安的父母，他们在经济和精神上的支持，使我有了到 Trinity College 学习的条件。

谨以我的博士论文，献给一直以来关爱、支持和帮助我的亲人、导师和同学、朋友！

Table of Contents

List of Figures

List of Tables

Chapter I

General Introduction

I.1 Nitrogen in the environment

Nitrogen (N) is an essential element for life. It presents in a spectrum of compounds and oxidation states range from +5 to -3 (NO_3^- to NH_4^+) in the biosphere. Apart from N_2, N is chemically active, and can easily be involved in a variety of reactions. Biological compounds, such as proteins, enzymes, cell membranes and DNA/RNA contain N. In addition, compounds of N have been widely used in fertilisers, pesticides, water softeners, food preservatives, chemical buffers, fungicides and anti-corrosion agents. To meet the needs of a growing human population, the application of the Haber-Bosch process for NH_4^+ synthesis from atmospheric N_2 and subsequent transformation into NO_3^- has significantly changed the global N cycle. It is estimated that the application of synthesised bioactive N to the Earth's ecosystems reached 100 Tg N yr^{-1} in the 1990s, and will, according to recent predictions, increase to 165 Tg N yr^{-1} by 2050 (Galloway et al. 2004). In addition, the cultivation of N-fixing crops and combustion of fossil fuel and subsequent deposition also provide a large contribution to the reactive N budget on a global scale (Wakida and Lerner 2005; Huettel et al. 2014). Therefore, human activities now introduce more bioavailable N into the biosphere than all natural N-fixing processes combined (Galloway et al. 2004; Huettel et al. 2014). Enrichment of N in water due to human activity in the environment results in numerous problems and poses health risks to humans. For instance, high concentrations of NO_3^- and NO_2^- in drinking water are likely to trigger digestive cancer and infant methemoglobinemia (Powlson et al. 2008). High concentrations of NH_4^+ in aquatic systems can also be toxic for seagrass and diatom populations (Natarajan 1970; Källqvist and Svenson 2003). Release of N_2O, mainly from combustion of fossil fuel, directly increases the atmospheric level of the greenhouse gas, likely aggravating global warming and depleting ozone (Ravishankara et al. 2007). In addition, deterioration of coastal ecosystems is also a major effect of increasing N concentrations (Galloway et al. 2003; Camargo and Alonso 2006).

Indeed, a drastic increase in N inventory in coastal zones has been observed, resulting from the anthropogenic N introduced by human activities (Mackenzie et al. 2002; Smith et al. 2003). Moreover, projections based on the current terrestrial N budget suggest more than a 30% N increase in N transfer to the coastal regions by 2050 (Galloway et al. 2004). Since N is assumed to be the limiting factor that constrains biomass increase of algae in coastal environments (Howarth and Paerl 2008) and the mean temperature in coastal waters keeps increasing, elevations of N in coastal waters enhance the likelihood of eutrophication events, increasing the likelihood of harmful algal blooms (HABs) occurring, leading to the local accumulation of organic matter and the increase of oxygen consumption; consequently, a reduction in water quality and consequent economic loss is likely (Rabouille et al. 2001; Howarth and Paerl 2008). Such events in coastal regions have been reported worldwide (Howarth and Paerl 2008; Rabalais et al. 2009). To prevent further deterioration of coastal ecosystems and in anticipation of the negative effects of global change, the scientific community has promoted control over the introduction of reactive N in ecosystems two decades ago (e.g. Galloway et al. 2003; Howarth and Marino 2006; Leote et al. 2008; Rocha et al. 2015). In response, the European Union launched a series of regulations aiming to control the reactive N levels in inland and coastal waters through Nitrate Directive (1991) and the European Union Water Framework Directive (Council of the European Communities 1991; 2000). The primary requisite to support the overall aim of these programmes is to understand and predict the distribution, reactive patterns and resulting fluxes of reactive N compounds within fragile ecosystems (Ibánhez 2012).

I.2 N to coastal zones

Atmospheric deposition is one of the main sources that transfer anthropogenic N to the oceans (Kim et al. 2011). It has been estimated to account for 30% of the external N inputs to the ocean (Duce et al. 2008). The remaining 70% of the exogenous N inputs are assumed to be derived from N in coastal inventories (Huettel et al. 2014).

They have been shown to be by-products of human activities in the near-shore, such as, aquaculture, waste water treatment or run-off from agriculture which can enter the coastal seas by direct disposal or riverine (Howarth et al. 1996) and subsurface transport (Moore 2010). Comparing with well-documented surface loading via estuarine outflows, the diffuse sources arising from subsurface transport (groundwater discharge) have only recently been recorded (Moore and Church 1996; Moore 1999; Burnett et al. 2003). The lack of literature support on fresh groundwater input to coasts is likely due to the difficulty in identifying source, quantifying discharge and variability on spatial and temporal scales (Burnett et al. 2006). Global estimates suggest that terrestrial groundwater discharge accounts for a small fraction (5% to 10%) of the total freshwater input to the coastal ocean (Zektser and Loaiciga 1993). However, the concentration of solutes, including nutrients, in terrestrial groundwater can be higher than those in seawater by several orders of magnitude (Moore 1999). Because of this, groundwater discharge is deemed responsible for more than 50% of the total dissolved salt load crossing the land-ocean interface (Zektser and Loaiciga 1993). Hence, even a small discharge volume of terrestrial groundwater can significantly influence the nutrient inventory in the receiving system.

Groundwater with high N concentrations is reported worldwide, with particular incidence in contaminated aquifers (Beusen et al. 2013). The main inorganic form of N in groundwater is NO_3^- resulting from application of fertilizers and subsequent leakage into aquifers (Foster 2000). Other sources also increase NO_3^- concentrations in coastal aquifers, such as leakage from septic tanks and/or sewage pipes, industrial spillages and overuse of manure (Wakida and Lerner 2005). From entry-point to coastal aquifers, the NO_3^- concentrations in groundwater can be altered in subsurface transport via NO_3^- reduction pathways (Rivett et al. 2008; Beusen et al. 2013; Huettel et al. 2014). However, the potential for the significant NO_3^- removal along the groundwater transit pathway to the sea occur prior to arrival at the coastal zone is limited, mainly because of the lack of reactive organic matter (Slater and Capone 1987; Cable et al. 1997; Shaw

2003). Indeed, denitrification in continental aquifers only accounts of 11.7% of total global NO_3^- reduction (Galloway et al. 2004; Huettel et al. 2014). Therefore, groundwater discharge could be an important source of NO_3^- to coastal waters, and indeed it is the dominant source in contaminated systems (Cable et al. 1997; Ullman et al. 2003; Bowen et al. 2007; Moore 2010; Santos et al. 2011; Rocha et al. 2015). Due to the potential impact on the ecological status of the receiving coastal systems, quantification of groundwater-derived NO_3^- fluxes to the receiving ecosystems, as well as a deeper understanding of its contribution to local biogeochemical budgets becomes an important task in support of coastal management (Moore 1999; Moore 2010; Rocha et al. 2015).

I.3 NO_3^- fluxes associated with coastal groundwater discharge

1.3.1 Submarine Groundwater Discharge and subterranean estuary

The discharge of coastal groundwater usually occurs as diffusive flow into the coast wherever a costal aquifer is connected to the sea with a positive head relative to sea level (Johannes 1980). On a global scale, direct freshwater input into oceans was usually defined as Submarine Groundwater Discharge (SGD, Zektser and Loaicga 1993). However, in order to understand nutrient contribution from freshwater to marine chemistry and interactions of these two components in coastal permeable aquifers (Moore 1996; Taniguchi et al. 2002), a more broad concept of SGD was established by Burnett et al. (2003), as 'the flow of water on continental margins from the seabed to the coastal ocean, regardless of fluid composition or driving force' (Moore 2010). Comparing with traditional perspective in hydrogeology, the definition of SGD is not limited to fresh groundwater discharge but includes recirculation of seawater in coastal aquifers by seasonal variation of saline/fresh interface, tidal pumping, and wave setup (Santos et al. 2012b). Literally, SGD can be consisting of two different scenarios. Firstly, SGD is only recycled seawater. In this scenario, though dissolved nutrient can be

generated from degradation of pelagic particle organic matter in permeable sediments, the total nutrient budget within the system has not been altered and therefore the ecological and environmental balance tends to be stable. Consequently, this type of SGD (seawater recirculation only) poses a limited risk to the coastal system. In comparison, the second type of SGD, comprising recycled saline water and terrestrial groundwater (Taniguchi et al. 2002); introduces land-derived nutrients into the receiving water, thereby being a potential threat to marine ecosystem health and function (Schubert et al. 2015), which is current focus of environmental research (Slomp and Van Cappellen 2004). As a result, in this thesis, SGD is referring the combination of terrestrial groundwater and recirculation of seawater.

Three main propagation pathways of SGD have been identified by Burnett et al. (2001), as can be seen in Fig.I.1. In particular, they are nearshore discharge from unconfined aquifers, offshore seepage discharge and submarine spring from artesian aquifers (confined). Generally, the offshore discharge, seepage from fracture zones to permeable beaches (2 in in Fig.I.1) and discharge as deep sea springs (3 in in Fig.I.1), occur in deeper regions of the coastal shelf. In these two pathways, the mixing degree between fresh groundwater and intruded seawater is low; hence, the hydrological compositions of SGD are recycled seawater and fresh groundwater in a separated status (e.g. Corbett et al. 1999; Schubert et al. 2015).

In comparison, in the near shore, SGD happens through the lower intertidal and subtidal area of permeable beaches; therefore, seawater can easily infiltrate the aquifer via tidal pumping or wave-set up (Santos et al. 2012b), developing a larger mixing zone (Fig.I.1) and resulting in the mixed beach porewater seeping out at discharge sites. In 1999, Moore (1999) established the concept of subterranean estuary applied to this subsurface mixing region due to the similarities of this mixing area with surface estuaries. Notably, under this circumstance, SGD is brackish water, a good mixture between fresh groundwater and saline water.

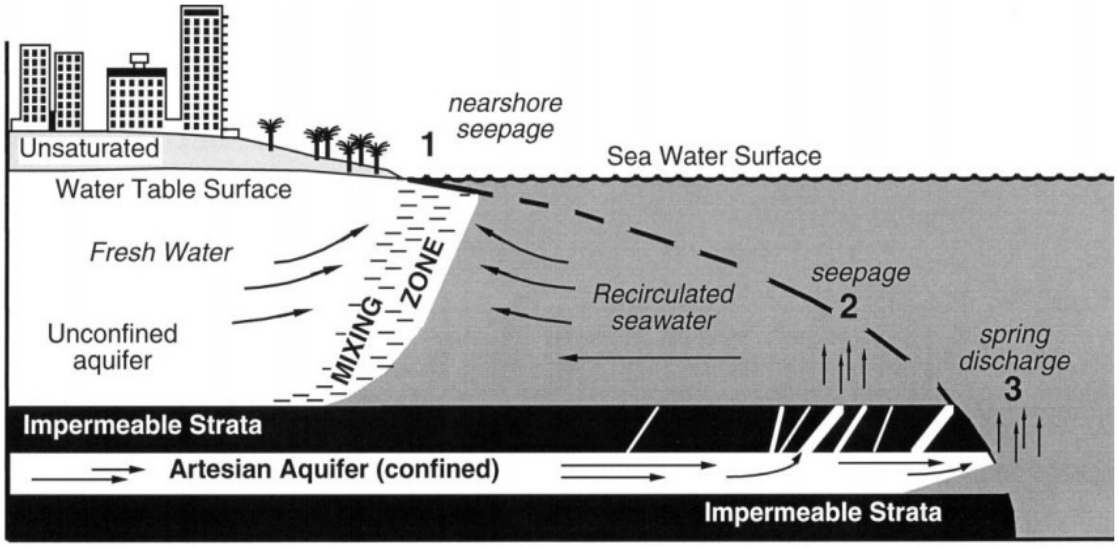

Figure I.1 Schematic view of mixing processes and SGD, the mixing zone between coastal aquifers and sea water is a subterranean estuary. Dark region is seawater and water in white zone is fresh groundwater. Taken from Burnett et al. (2001).

1.3.2 Determination of SGD rate and NO_3^- fluxes from SGD

The magnitude of the SGD rates has been estimated by a variety of methodologies, mainly direct measurement via deployment of seepage meters (e.g. Leote et al. 2008; Loveless and Oldham 2010), and determination of radiogenic tracer activity, usually, radon (e.g. Santos et al. 2008) and radium (e.g. Kim et al. 2005; Paytan et al. 2006). While direct measurement using seepage meters is straightforward, it can usually only be carried out in small areas and thus it is difficult to confidently up-scale to system level regions. In addition, deployment of seepage meters is labour intensive. Consequently, the majority of scientific workers have instead used radioactive tracers to reach an in-depth understanding of SGD in basin scale investigations (Schubert et al. 2015). Among the available radioactive tracers, 222-radon (^{222}Rn, hereafter referred to as 'radon') is often used in SGD monitoring programmes (e.g. Garrison et al. 2003; Charette and Buesseler 2004; Kim et al. 2005; Paytan et al. 2006; Shellenbarger et al. 2006; Kroeger et al. 2007; Knee et al. 2008; Hwang et al. 2010; Waska and Kim 2011; Tait et al. 2014). Radon is a product of the natural uranium-238 decay chain (Schubert et al. 2015). It is constantly generated in natural mineral matrix by the radioactive

decay of radium-226 and then dissolved into the interstitial water. Consequently, concentration of radon in groundwater and porewater is orders of magnitude higher than in seawater. Accordingly, SGD usually leads to patches of detectably elevated radon concentrations where groundwater injects into the coastal waters. In practice, excess radon fluxes detected along a coastline can be used as a good indicator of SGD. The magnitude of excess radon flux can be determined by mass balance approach. As Fig.I.2 shows, in a steady state, the SGD-derived radon flux (identified as excess radon flux here) is equal to the addition of radon loss via decay and radon input from sediment. Combining with the proper defined endmember radon concentration, the magnitude of excess radon flux in coastal waters can be transformed into a discharge rate (e.g. Tait et al. 2013; Rocha et al. 2015). Subsequently, the magnitude of NO_3^- fluxes delivered by SGD can be determined from NO_3^- concentrations (e.g. Tait et al. 2014).

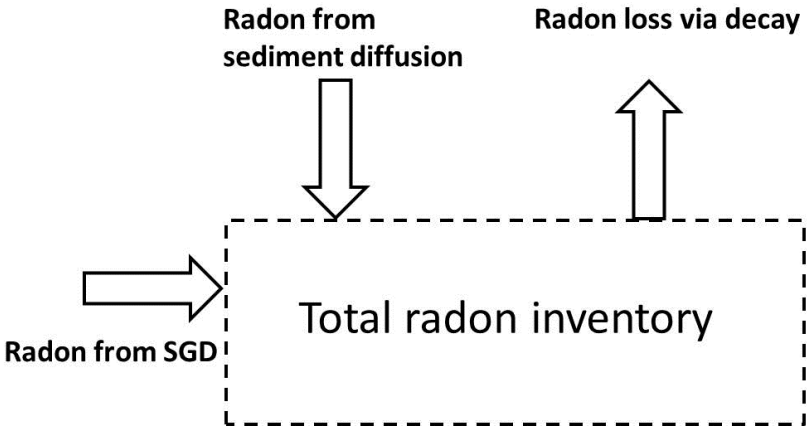

Figure I.2 A simple sketch to describe the input and output pathways in total radon inventory in coastal systems. In this figure, radon flux from SGD (excess radon) can be defined as the addition of loss via decay and contribution from sediment in a steady state.

1.3.3 Current research in NO_3^- fluxes associated with SGD

SGD has frequently been ignored in local NO_3^- mass balances, (Burnett et al. 2003) due to the character of invisibility (Finkl and Krupa 2003) and spatially dispersed nature. However, growing evidence suggests that SGD can be an important source of

NO_3^- to coastal systems, particularly when discharging from contaminated continental aquifers (e.g. Leote et al. 2008). To date, NO_3^- fluxes into the coastal water column via the SGD pathway have been monitored in more than 40 sites worldwide (Zhang and Mandal 2012). In the majority of research locations, evaluations confirm that substantial NO_3^- fluxes can in fact be delivered by SGD.

Table I.1 Comparison of NO_3^- inputs in some coastal systems (bays and lagoons) worldwide. Proportion indicates the contribution of SGD to the total N input by all identified sources.

Site	NO_3^- flux	Proportion	Reference
Gulf of Aqaba (Israel)	1×10^4 μmol $m^{-1}h^{-1}$	32% - 46%	Shellenbarger et al. 2006
Hanalei Bay (U.S.)	12.4 kg d^{-1}	73%	Knee et al. 2008
Florida Bay (U.S.)	4.3×10^3	38%	Santos et al. 2008
Patos Lagoon (Brazil)	9.4×10^3 kg d^{-1}	55%	Niencheski et al. 2007
Wenchang Lagoon (China)	1.5×10^2 kg d^{-1}	51%	Liu et al. 2011
Tolo Harbour (China)	1.0×10^4 kg d^{-1}	99%	Lee et al. 2012
Rhode Island	181 μmol m^{-2} h^{-1}	84%	Moran et al. 2014
Werribee Estuary (Australia)	170 μmol m^{-2} h^{-1}	60% -76%	Wong et al. 2014
Kinvarra Bay (Ireland)	2.7×10^2 kg d^{-1}	99%	Rocha et al. 2015

In Table I.1, I displayed the results on the magnitude of NO_3^- fluxes and the proportion of SGD-borne NO_3^- fluxes within total NO_3^- contributions on the local scale (e.g. riverine input, input from sediment and sewage flow) from previous research records. For example, in the Patos lagoon, Brazil, NO_3^- fluxes can reach 9.4×10^3 kg d^{-1}, accounting for 55% in total NO_3^- inputs into the system (Niencheski et al. 2007). In regions that are scarce in surface loading vectors, such as the Kinvarra Bay (Ireland), NO_3^- contribution from SGD can be as high as 99% of total NO_3^- flux to coastal waters (Rocha et al. 2015). Even in regions with substantial riverine loadings, such as the Wenchang Lagoon (China) and the Werribee Estuary (Australia), SGD is still an important carrier of NO_3^- to the coast (Liu et al. 2011; Wong et al. 2014). On the broader scale, Moore (2010) suggested that terrigenous NO_3^- delivered via SGD may be responsible for 56% of total N inputs to the Atlantic Ocean which is greater than the combined contributions from atmospheric deposition and surface water. The estimate

by Moore (2010) is consistent with the independent estimate by Zektser and Loaiciga (1993), who suggested that the SGD pathway can be deemed responsible for 52% of the total dissolved salt (including NO_3^-) crossing the land-ocean interface.

SGD-borne NO_3^- fluxes may act as an important support for local food webs. Indeed, the NO_3^- fluxes delivered from SGD can boost primary productivity in receiving waters (Kroeger et al. 2007), which may benefit benthic fish communities (Miller and Ullman 2004) and might also be important in sustaining tropical coral systems (Johannes and Hearn 1985). However, field survey results derived from the majority of sites suggest that NO_3^- supplied by the SGD pathway substantially exceeds that needed to support food webs and this can lead to a series of environmental problems. For example, in the Gamak Bay, an important fishing ground in Korea, excessive NO_3^- from SGD leads to eutrophication and frequent hypoxia events, as well as red tide outbreaks (Hwang et al. 2010). Frequent algal blooms owing to eutrophication have already been reported in the aquaculture areas of Bolinao which is a coastal zone that is strongly influenced by SGD in the Philippines (Senal et al. 2011). For the Tolo Harbour in Hong Kong (China), even though the Tolo Harbour Action Plan was implemented by the local government in 1987 to reduce nutrient loading from surface water, algal blooms are still frequently reported due to NO_3^- pollution from SGD (Lee et al. 2012). In the Tampa Bay, though stream water greatly diluted NO_3^- fluxes driven by SGD, this subtropical estuary has still been classified as eutrophic (Kroeger et al. 2007). In the Kinvarra bay (West of Ireland), though residence time of bay water is only seven days due to rapid hydraulic exchange between Kinvarra bay and adjacent ocean region, occasional hypoxia was still found, potentially harming local aquiculture (Rocha et al. 2015).

Despite the fact that the magnitude of NO_3^- fluxes from SGD and its subsequent influences have been investigated in a number of study sites (Zhang and Mandal 2012), the understanding of NO_3^- fluxes from SGD pathway remains incomplete. Firstly, current research sites are concentrated in fewer than 20 countries. Elsewhere, data on

nutrient loading (including NO_3^-) associated with SGD are largely unavailable. In addition, even in countries such as the U.S. where extensive measurements have been made; there are still broad coastal regions without any data on SGD (e.g. east coast of the U.S.). Data on SGD and associated NO_3^- loading is urgently needed from such regions, especially those with aquifers that are polluted with NO_3^-.

The second deficiency in current research is the lack of discrimination between NO_3^- that is of fresh SGD origin and NO_3^- that is from recycled SGD (see Fig.I.3). Because radon is the most frequently employed in SGD studies, the entire causal chain (Fig.I.3) can be demonstrated from radon measurements. In brief, the first difficulty in the evaluation of SGD-borne chemical loading is to identify the radon source or sources. Both seawater recirculation in permeable beaches (Burnett et al. 2003) and injection of terrestrial groundwater (Moore 2010) can lead to a building up of radon activity in coastal waters. Accordingly, two distinct scenarios are generated to explain the origination of excess radon (Problem 1 in Fig.I.3): (1) recycled seawater only or (2) SGD. Many researchers have assumed SGD to be the radon source without verification by other techniques, such as determination of pH, salinity or stable isotopes, like ^2H, ^3H, ^{18}O (e.g. Knee et al. 2008; Hwang et al. 2010; Waska and Kim 2011). Lack of such verification potentially leads to errors in calculating the discharge rate and magnitude of NO_3^- fluxes.

In studies with clear identification of excess radon (e.g. Tait et al. 2013), the determination of the composition of fresh and saline compartments in total SGD is problematic (Problem 2 in Fig.I.3). Since terrestrial groundwater in total SGD is exogenous, it is the main target in coastal evaluation (Howarth and Marino 2006). The majority of case studies omitted contribution from saline SGD to radon inventory and treated radon flux from SGD as radon flux from terrestrial groundwater. This approach possibly leads to an exaggeration of the magnitude of fresh SGD rate. Subsequently, the overestimation on allochthonous pollution from SGD and the resulting

uncertainties will affect subsequent management and regulation. In addition, there is another challenge concerning determination accuracy, which is to pinpoint radon activity in terrestrial groundwater, since concentrations of radon in terrestrial groundwater can vary significantly in different adjacent aquifers due to heterogeneity of bedrock. Previous research defined radon activity in the fresh groundwater endmember by averaging the concentration from all the borehole and well survey results (e.g. Lee et al. 2012; Tait et al. 2013). This approach possibly generates a large statistical uncertainty. For instance, Kroeger et al. (2007) found a standard deviation in the terrestrial groundwater endmember five times larger than the mean value. This high variation significantly affects the reliability of SGD solute loading calculations.

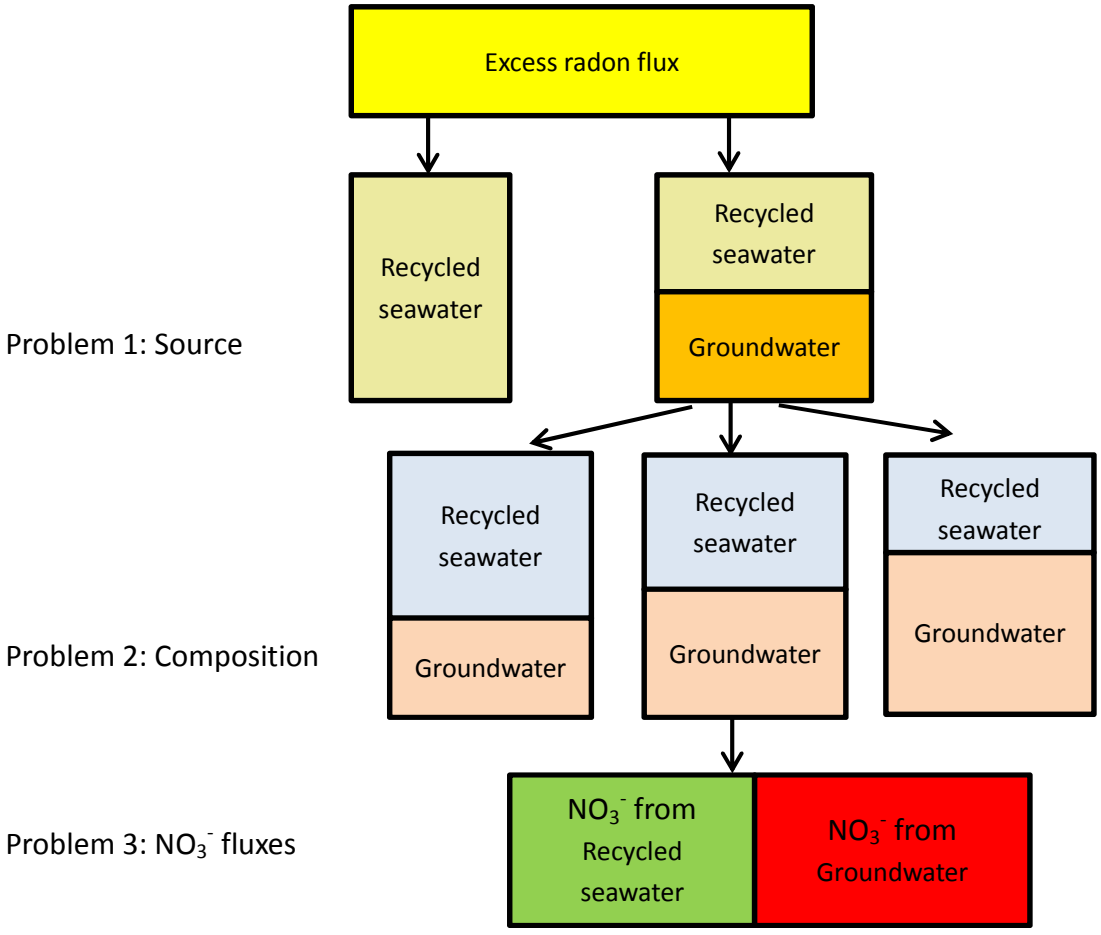

Figure I.3 The causal chain in current research of SGD-borne NO_3^- fluxes. Problem 1 (Source) is to define the source or sources of radon (recycled seawater solely or a combination of seawater and groundwater); Problem 2 (Composition) is to understand compositions of recycled seawater and groundwater in total SGD, it displays 3 different ratios, from groundwater dominance to recycled seawater dominance; Problem 3 (NO_3^- fluxes) is to quantify NO_3^- fluxes from groundwater and recycled seawater individually.

The final problem (Problem 3 in Fig.I.3) in current approaches is to quantify contributions of NO_3^- from the two hydraulic components in total SGD. As pointed out, SGD is the outflow of porewater from permeable sediment to the receiving water. In coastal zones, permeable sediment in subterranean estuaries, is active in NO_3^- processing (Kuwae et al. 2003; Rocha et al. 2009; Santos et al. 2009; Ibánhez et al. 2011; Ibánhez et al. 2013; Erler et al. 2014a); therefore, the magnitude of NO_3^- fluxes from both the fresh endmember and the saline endmember can be significantly altered in this porous media via a number of biogeochemical pathways (Santoro 2010). However, current quantification of NO_3^- fluxes associated with SGD takes little account of NO_3^- processing in subterranean estuaries. The common method for estimating SGD-derived NO_3^- exports to coastal systems barely considers the modification when NO_3^- plumes flow through subterranean estuaries. In particular, a number of studies simply multiply the average NO_3^- concentrations in endmembers by the SGD rate in their research (e.g. Tse and Jiao 2008; Senal et al. 2011; Lee et al. 2012). As a consequence, estimations of NO_3^- fluxes from SGD can be inaccurate. To conclude, these problems introduce uncertainties in quantification of NO_3^- fluxes via SGD pathway to coastal waters; improvements are urgently needed so that reliable estimates of NO_3^- loading to coastal waters via SGD can be made.

I.4 Objectives and thesis content

1.4.1 Research aim, hypotheses and objectives

The work presented in this thesis was part of the NITROLINKS project (funded by EU (FEDER), National Science and Technology Foundation (FCT) and the Portuguese Government, 2008-2011) and its extension. The study site is located in the Ria Formosa lagoon, one of the largest lagoons in the E.U. (Barnes 1980). Previous field work (Leote et al. 2008) suggests SGD in the Ria Formosa carries substantial land-derived NO_3^-. However, regional evaluation of the magnitude of NO_3^- fluxes via

the SGD pathway to the lagoon is currently unavailable. Hence, the central research aim in this thesis is to determine modulating process in the subterranean estuary, evaluate the magnitude of NO_3^- fluxes from SGD on a system scale and also to assess potential influences from excessive NO_3^- in SGD. Accordingly, three related hypotheses and objectives were designed for the thesis (Fig.I.4). This thesis will: (1) contribute to the current knowledge on NO_3^- fluxes from SGD in a region where there is a lack of data on the subject; (2) improve current determination approaches, especially with regard to the three problems in Fig.I.3; and (3) provide suggestions to local management on the basis of the results.

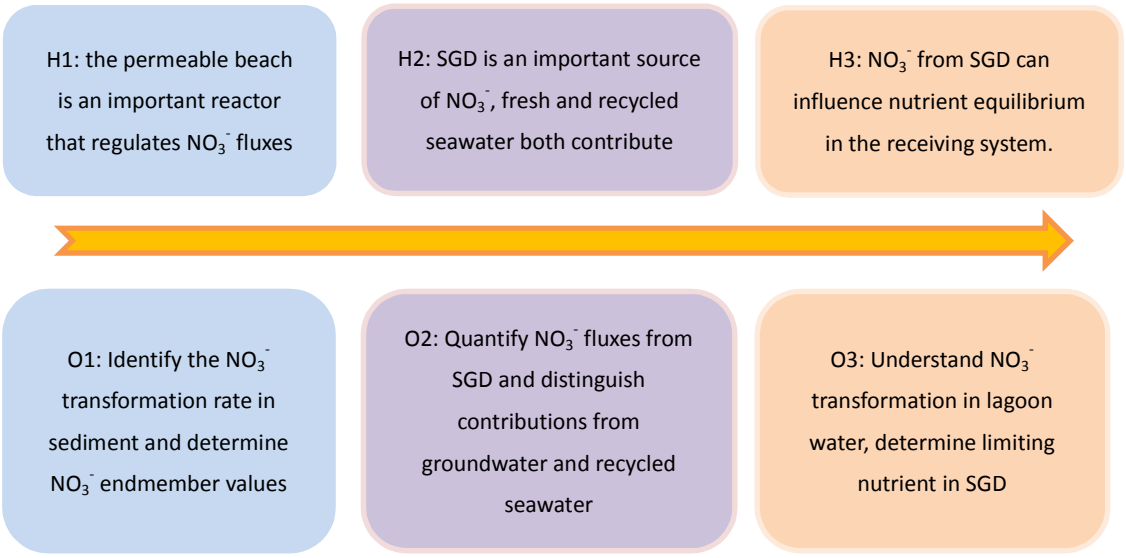

Figure I.4 Three hypotheses and objectives in the thesis, H is hypothesis and O is objective.

I.4.2 Thesis content

Chapter I is general introduction. This chapter demonstrates the background of N pollution in coastal regions and potential sources of N contamination. Subsequently, it highlights the influence of SGD to local NO_3^- inventory and potential threats introduced by SGD to receiving waters. At the end, this chapter displays current uncertainties in quantification of NO_3^- from SGD and links to the research work in this thesis.

Chapter II briefly illustrates the study site, i.e. Ria Formosa lagoon (Portugal). It

demonstrates the geological background and reasons of high NO_3^- pollution in terrestrial groundwater. It also shows the ecological and economical importance of the lagoon and previous research on SGD in the study site.

In **Chapter III**, an observation on NO_3^- transformation in subterranean estuaries on a global scale is provided. In particular, the distribution of NO_3^- concentration along salinity gradients in distinct subterranean estuaries was analysed via a fractional mixing model. It provides global scale insights into the dominant NO_3^- transformation trend and the magnitude of NO_3^- fluxes generated/reduced in subterranean estuaries, which serves as important evidence to support one of the key hypotheses in the thesis that coastal permeable sediments in subterranean estuaries are active in NO_3^- processing.

There is more than 100 km of coast line in Ria Formosa with the potential to act as a subterranean estuary. Given the connection to groundwater aquifers on its hinterland, the transformations related with NO_3^- circulation and turnover occurring there and affecting the NO_3^- levels in the seepage water could be extremely important to the lagoon ecosystem. To follow NO_3^- circulation and processing in subterranean estuaries, researchers have developed two distinct methodologies, namely, quantification from in-situ sampling and determination by laboratory experiment. The first method can provide a detailed reaction map for NO_3^- transformation in the subterranean estuary. The laboratory simulation has advantages of rapid determination key parameters such as temperature, concentration of substrate, flow rate, to reaction rate; while the *in-situ* quantification is understood as a better methodology for investigating the distribution of NO_3^- in benthic environment and establishing endmember concentrations for regional estimation. To reach a clear understanding on biogeochemical process and dynamics of NO_3^- transformation in sediment, a combination of these two approaches is recommended (Ibánhez 2012). In this thesis, **Chapter V is** focused on in-situ determination while **Chapter VI** is based on laboratory simulation.

During field work, nutrient sample storage has become an acute problem that befalls scientific researchers (Batley 1989). In the field campaign, non-additive vacutainers were employed for collection of lagoon water and porewater. In order to precisely reproduce N species distribution in the research location with a high degree of confidence, the uncertainties of sample storage affecting accuracy of analyte determination should be minimised. To understand the potential disturbance caused by the vacutainer and subsequent storage within on the analyte determination result and to decrease uncertainties, analytical suitability was evaluated for this type of vacutainer in **Chapter IV**. In particular, the performance of vacutainers for different chemical solutes was tested, including NO_3^-, ammonium (NH_4^+), soluble reactive phosphorus (SRP) and dissolved organic carbon (DOC). Based on the result, adjusted operational protocols were applied during the work to minimise potential artefacts.

The advective movement of porewater in SGD sites promotes interfacial fluxes of solutes that are orders of magnitude higher than diffusion transport and which are very important in determining the distribution of solutes (Rocha 2008). Thus, sampling techniques that are used should avoid interfering with the main transport mechanisms in the benthic environment. In the work described here, piezometers were deployed for seven months in the beach sands of Ria Formosa lagoon. The depth of piezometers ranged from 0.5 m to 3.5 m beneath the beach surface. A field survey, covering winter, spring and summer seasons, was conducted to observe the distribution and variation of NO_3^- ,NH_4^+, NO_2^- and total dissolved nitrogen (TDN) in porewater (**Chapter V)**. Through a combination of benthic reaction modelling and N distribution in the subterranean estuary, the benthic N reaction rates and the dominant N processing pathway were determined. In addition, the N concentration in freshwater endmember was deduced from regressions, which was used in the regional quantification of N fluxes in **Chapter VII**.

Total SGD includes comprises two components, namely, recycled seawater and

fresh groundwater. Each contributes differently to coastal systems. In general, freshwater-borne NO_3^- makes a substantial contribution to the total NO_3^- in SGD (Leote et al. 2008). An important parameter controlling benthic NO_3^- reactivity in sediments is the availability of dissolved organic matter (DOM, Fitzsimons et al. 2006; Rivett et al. 2008). Previous research reported that the potential for significant NO_3^- removal in continental aquifers is limited, mainly because of the lack of reactive organic matter (Desimone and Howes 1996; Shaw 2003; Ibánhez et al. 2013). In subterranean estuaries, the intrusion of seawater introduces pelagic DOM that can be highly reactive. Hence, the distribution of labile DOM might be a key factor that influences the magnitude of NO_3^- fluxes from fresh SGD. To gain further insight into the relationship between DOM and NO_3^- turnover in a subterranean estuary, a series of Flow-Through Reactor (FTR) experiments were carried out to explore the relationship between NO_3^- reduction and distribution of dissolved labile organic matter (**Chapter VI**).

Quantification of daily NO_3^- loading from terrestrial groundwater and recycled saline water is the key research aim in the thesis. In **Chapter VII**, the N (NO_3^- and DON) fluxes via the SGD pathway to the Ria Formosa lagoon were examined on the basis of three important sources of information: (1) the volume of terrestrial groundwater present as estimated by ^{222}Rn excess flux and fraction of fresh compartment in total SGD; (2) a precise definition of the terrestrial groundwater radon activity using stable isotopes and (3) knowledge of the influence of N transformations in the subterranean estuary on the magnitude of N fluxes. The combination of these approaches can be used to quantify the separate contributions in NO_3^- from terrestrial groundwater and recycled seawater in total SGD. In addition, a comprehensive comparison of the magnitude of N fluxes from distinct inputs, such as stream, waste water, and fluxes via sediment diffusion is made to highlight importance of NO_3^- fluxes associated with SGD in the lagoon NO_3^- budget. The comparison results can be used as a reference for future lagoon management. Enhanced NO_3^- loading to the lagoon may trigger an

undesirable level of algae biomass which poses ecological risks to the lagoon (Stigter et al. 2013). Generally, a high removal rate of NO_3^- from the lagoon water is potentially related to rapid biomass increase (Loureiro et al. 2005). Consequently, the N (NH_4^+, NO_3^- and DON) biogeochemical transformation rate in the lagoon water was determined via fixed site monitoring and mass balance approach in **Chapter VII.**

Previous research (Stiger et al. 2006a; Leote et al. 2008) and this study (**Chapter VII)** underline the importance of dissolved inorganic nitrogen (DIN, mainly as NO_3^-), inputs to the lagoon via the SGD pathway. Enrichment by DIN in terrestrial groundwater may alter nutrient ratios (N:P:Si) and mediate a shift in the nutrient that limits algal biomass. Such a shift may cause a series of ecological effects, such as altered succession of algal communities which may lead to harmful algae blooms (HABs, Justić et al. 1995a; Rabalais et al. 1996).

As one of the most important nutrient carriers, nutrient status and structure in SGD significantly influences the nutrient equilibrium in the lagoon water. SGD in Ria Formosa is a mixture between groundwater and recycled seawater. Variations in the proportion of terrestrial groundwater in total SGD may consequently cause oscillations in the nutrient that limits algal biomass. In addition, biogeochemical transformations in the subterranean estuary increase uncertainties in nutrient structure in SGD. Given the widespread occurrence of nutrient delivery from SGD and the potential linkage between nutrient structure and transition of algae community in the receiving water, a comprehensive research on nutrient ratios and limiting nutrient in SGD is highly necessary. In **Chapter VIII,** based on a metadatabase established in O-DOIS project (funded by National Science and Technology Foundation (FCT) and the Portuguese Government, 2005-2007), the nutrient ratios (N, P, and Si) and limiting nutrients in SGD were calculated on the basis of frequency analysis and Redfield ratio. In addition, Dirichlet regression was carried out to elucidate the relationship between limiting nutrient and proportion of freshwater in SGD.

Chapter IX is a summary and conclusions of the thesis. It also includes suggestions for the regulation and management of Ria Formosa lagoon. At the end of **Chapter IX**, suggestions are made for future coastal management as well as research on the sources and behaviour of NO_3^- in SGD to the Ria Formosa lagoon.

Chapter II

Study site: Ria Formosa coastal lagoon

II.1 Hydraulic setting and geomorphology

The Ria Formosa is a coastal lagoon, 110 Km^2 in area. It spans from 36°58'N 8°20'W to 37°30'N 7°32'W and covers the majority of the coast of Algarve (SW Iberian peninsula). The lagoon is separated from the Atlantic Ocean by a multi-inlet barrier island and two peninsulas. The lagoon system comprises channels, salt marshes, tidal creeks, sandy deposits, and two cities. The volume of the lagoon approximates 210×10^6 m^3 during spring high tides (Ferreira et al. 2003). Water exchange between the lagoon and the surrounding ocean is mainly depending on the tidal prism of the six inlets (Pacheco et al. 2007). The daily tidal flux is estimated to be 8×10^6 m^3 (Balouin et al. 2001).

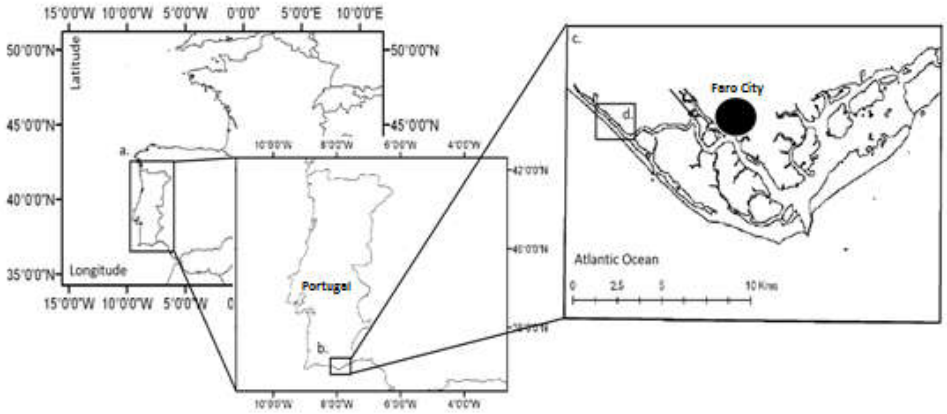

Figure II.1 Location of Portuguese beach face field site; a. – Portugal; b. –Algarve ; c. – the region of the Ria Formosa lagoon; d. – Studied subterranean estuary, Praia de Faro beach

The adjacent coastal area has a semidiurnal, meso-tidal regime. Tidal amplitude ranges from 1.3 m at neap tides to 2.8 m during spring tides, with extreme amplitude of 3.5 m (Vila-Concejo et al. 2004). The submerged area in the lagoon amounts to 55 km^2 at high spring tide and between 14 and 22 km^2 at low spring tide (Tett et al. 2003). The intertidal permeable beach in the lagoon is extensive due to the low depth of lagoon water (2m, Andrade et al. 2004) and relative large tidal regime.

The climate in the Ria Formosa region is controlled by Mediterranean weather (Newton and Mudge 2003). Annual precipitation is 480 mm in the Faro (West Boundary), and it increases to 580 mm in the East Limit (Salles 2001). The surface loading to the lagoon includes four rivers and fourteen streams (Synthesis Report 2003). Most of them are seasonal and limited. The average annual water temperature in the lagoon fell in the range of 18.1°C in the East to 20.6°C in the West.

The lagoon lies on sandy barrier platforms that approximately formed to a prism 6000 years ago due to influences from (1) decreases in rate of sea-level rise; (2) differences in ocean wave and current on two boundaries of the lagoon and (3) the effect of storms (Bettencourt 1994; Dias et al. 2000; Ibánhez 2012). The origin of Ria Formosa lagoon is assumed to be the product of flooding of ancient dune deposits during the last deglaciation (Pilkey et al. 1989). This conclusion has been confirmed by Bettencourt (1994) via determination of homogeneity of sandy deposits in the lagoon. Furthermore, after analysis of sediment cores collected from the Ancão inlet that reaches a depth of 5m (Western sector), Andrade et al. (2004) displayed that sedimentary homogeneity could extend to deeper layers. Their work also showed the absence of carbonate fossils in the upper layer of the sandy corers, which is a typical character of the sandy dune. In addition, they highlighted that the diatoms indicated the freshwater inputs and the authors suggested that the results were an evidence of freshwater injection on a seasonal scale.

II.2 Importance in economics and ecology

As one of the largest coastal lagoons in Europe, the Ria Formosa plays an important role in economics and ecology. It offers plenty of goods, services and buffer effects to local residence and especially it is a highly productive ground for the local fishery (Smith and Atkinson 1994; Leote et al. 2008), which is the largest commercial fishery in Portugal. The production is approximately 4000 to 7000 tons per year

(Mudge and Bebianno 1997), accounting for approximately 27% of the cultured seafood in Portugal (Ibánhez 2012). The lagoon is also a famous for the tourism and salt extraction in the Europe. These activates occupied up to 10% of the lagoon surface (Ibánhez 2012). Currently, it is estimated that 10, 000 people directly/indirectly rely on the natural resources of the lagoon (Ibánhez 2012).

In terms of ecology, the Ria Formosa has been identified as an important transferring location for several migratory bird species (Cunha et al. 2009). It also serves as a ground of breeding and nursing for a wide range of mollusc and fish species due to the abundant seagrass resource in the lagoon (Cunha et al. 2009). Because of ecological importance, Portuguese legislation has signed the protection for the Ria Formosa under the National Park designation. It is also catalogued as a Ramsar wetland, a protected area for birds (Videira et al. 2003) and a site of the Natural 2000 Network (Ibánhez 2012).

II.3 History of NO_3^- pollution and current problems

The lagoon is surrounded by a coastal plain where intensive agriculture activities are conducted. This region is named 'Campina' (Newton and Mudge 2005). The Campina de Faro is the most adjacent to the lagoon with two aquifers. The deeper aquifer is formed by Cretaceous limestone and the surficial contains sands and gravels from Pilo-Quaternary. Between two aquifers, there are Miocene sandy layers, which are permeable (Almeida et al. 2000). Since the early 1980s, the local vegetation cover in coastal plain was replaced by olive trees, farmland of tomato and citric trees. To meet the demands of agriculture and public water supply, groundwater was extensively used in the aquifer system. Heavy NO_3^- pollution in the surficial aquifer system was then been determined (Almeida and Silva 1987), where NO_3^- concentrations in the groundwater rising to 2.1 mM on average (Ferreira et al. 2007), with a maximum value of 6.5 mM. The ratio between NO_3^- and SO_4^{2-} in the

groundwater samples within the Campina de Fara indicated that excessive NO_3^- in the aquifer was a result of the application of inorganic fertilisers (Almeida and Silva 1987). Specifically, direct infiltration of NO_3^- enriched in the Pilo-Quaternary aquifer, subsequently polluting the underlying Miocentic strata via diffusion effect. In 2001, the Campina de Faro aquifer system was defined as a Nitrate Vulnerable Zone (NVZ) in compliance with European Union Nitrate Directive (91/676/ECC), aiming to control NO_3^- levels in the area. In 2005, Campina da Luz aquifer system, another aquifer system that surrounds the Ria Formosa coastal lagoon, has been listed as the other NVZ (Stigter et al. 2006b).

The influences of intensive human activities have extended from inland to the lagoon. Numerous pollutants in the lagoon have been reported since the 1990s, for instance, different types of fatty acid (Mudge et al. 1999), organic matter (Gamito 2008), microorganisms (Dionisio et al. 2000), polychlorinated biphenyls (Barreira et al. 2005), heavy metals (Bebianno 1995) and nutrients (Newton et al. 2005; Stigter et al. 2006a). The lagoon ecosystem was deeply influenced by anthropogenic activities. For example, human activities have altered the sedimentary balance in the muddy marshes and accelerated erosive rates of sandy beaches (Ibánhez 2012). Several species were dismissed (Arnaud-Fassetta et al. 2006). The lagoon was also frequently documented to host macroalgae blooms (*Enteromorpha/Ulvae* spp.) since the winter of 1988 (Aníbal et al. 2004). These macroalgae blooms potentially led to declining in marine spermatophytes (Padinha et al. 2000), which in turn affected local aquaculture (Aníbal 2007). In particular, decline in clam harvesting and extensive fish deaths due to anoxia associated with eutrophication has been reported (Leote et al. 2008).

To improve water quality in the lagoon and the hydraulic circulation of between lagoon water and adjacent seawater, a special project was launched in 1997 with direct implications for the ecological status of the Ria Formosa (Vila-Concejo et al. 2003; Vila-Concejo et al. 2004). The project dredged the lagoon channels and reconstructed

dunes and beaches .It also relocated the Ancão inlet at the West and the Fuzeta inlet at the East.

Despite great effort, several characters of eutrophication were still determined like the high concentrations of nutrient solutes in lagoon water (Ferreira et al. 2003; Newton et al. 2003; Newton and Mudge 2005). To pinpoint the nutrient status of the lagoon, researchers carried out a series of studies. Newton et al. (2003) revealed that dissolved inorganic nitrogen levels were consistently higher in lagoon water than the adjacent ocean water. Newton and Mudge (2005) showed that the lagoon continuously transports dissolved inorganic nitrogen to adjacent ocean. Ferreira et al. (2003) estimated that the unknown DIN source to the lagoon accounted for 600 ton N yr^{-1}. In 2006, Stigter et al. (2006a) draw a NW-SE pathway for groundwater flowing from the Campina de Faro to the lagoon. They suggested the potential importance of groundwater in nutrient budget, because of the high NO_3^- concentration determined in the subsurface of Campina de Faro zone. Stigter et al. (2013) further highlighted that researchers may underestimate nutrient fluxes from groundwater. Leote et al. (2008) suggested that seeped groundwater may potentially be responsible for the missing N budget described by Ferreira et al. (2003) .

II.4 Previous study of SGD

SGD was first discovered and determined at the Ria Formosa coastal lagoon during the research project “O-DOIS” (Leote et al. 2008). From November 2005 to January 2007, the biogeochemical research team performed more than 20 monthly sampling works in the intertidal area of Ancão peninsula. They found that brackish porewater (Fig.II.2) contained high NO_3^- concentrations and it travels across the permeable intertidal area to the lagoon.

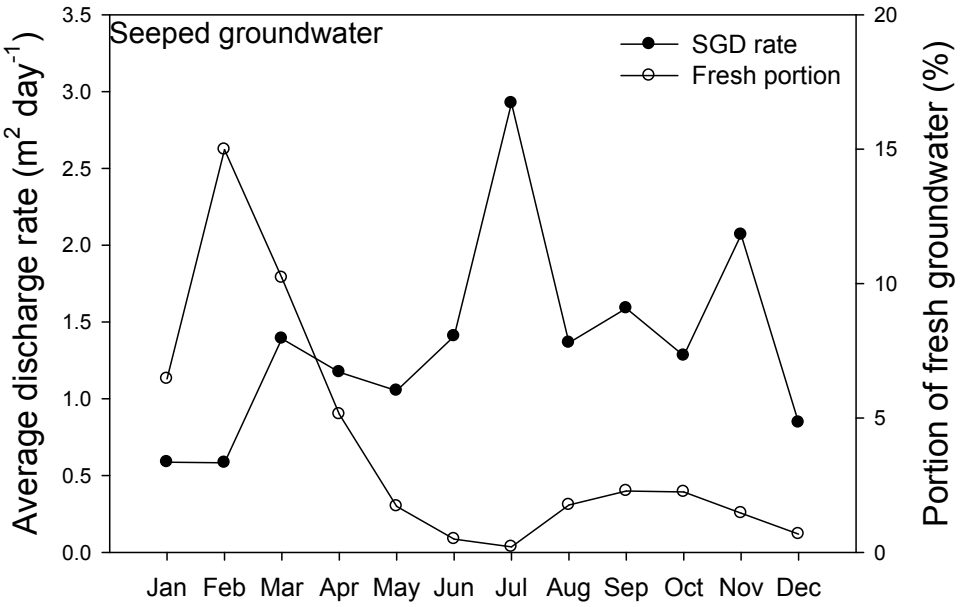

Figure II.2 Discharge rate on seepage faces in Ria Formosa lagoon, the figure also shows the portion of terrestrial groundwater in total discharge

At the permeable area, the seepage rates were peaked during low tides and showed a minimum or absent during high tides (Rocha et al. 2009). The discharge rate followed tidal oscillation and exhibited a cyclic, reproducible pattern. The mean discharge rate in the lagoon was assumed to be 3.6 m^3 m^{-1} day^{-1} derived from the deployment of seepage meters (Leote et al. 2008). Moreover, the concentrations of NO_3^- in porewater showed a seasonal fluctuation, which suggests the change of land use in adjacent regions (Leote et al. 2008), further indicating the hydraulic connection between the sandy beach and in-land aquifers (Rocha et al. 2009). Consequently, SGD in the lagoon was assumed to be an important delivery pathway that introduces substantial NO_3^- into the lagoon. In this thesis, this offers evidence for the regional survey.

Preliminary analysis of porewater profiles collected *in-situ* at the seepage face showed the presence of significant vertical NO_3^- concentration gradients during active seepage (Rocha et al. 2009). Based on these observations, Ibánhez et al. (2011; 2013)

revealed that the surface layer of the seepage face in sandy sediment is biogeochemically active in NO_3^- processing via advection-diffusion-reaction modelling (beach in Fig.II.3). The rates of nitrification and NO_3^- reduction in the sediment ranged from 0.05 to 1.9 (mmol m^{-2} h^{-1}) and 0.03 to 2.14 (mmol m^{-2} h^{-1}), respectively. The results suggest the subterranean estuary in the lagoon has high potential in NO_3^- processing.

Figure II.3 The sandy beach near the research location

Chapter III

Subterranean estuaries as highly efficient nitrate reactors: a global perspective

III.1 Abstract

The role that subterranean estuaries play in nitrate (NO_3^-) circulation and turnover has been underestimated in previous sediment research, as well as in regional quantification work on NO_3^- fluxes associated with terrestrial groundwater discharge. To investigate the importance of subterranean estuaries in NO_3^- transformation, I normalised NO_3^- attenuation along the salinity gradient and then estimated NO_3^- reaction proportions in different subterranean estuaries via a fraction mixing model. The magnitude of NO_3^- fluxes processed in subterranean estuaries was also examined. The results suggest that subterranean estuaries are currently dominated by NO_3^- reductions. On a global scale, the mean nitrate removal process in subterranean estuaries contributes to a loss of 22% of groundwater-borne NO_3^- prior to discharge under a steady state. At a conservative estimate, subterranean estuaries can reduce 0.34 to 0.61 Tg N-NO_3^- every year when combined with estimations of NO_3^- fluxes from subsurface loading. Compared with rivers, coastal permeable sediments, oceans and other systems from previous research, subterranean estuaries showed the highest NO_3^- reduction rate. In addition, subterranean estuaries could enhance magnitude of NO_3^- fluxes, reaching a ratio of 102% when compared with the concentration in the fresh endmembers. These results indicate that subterranean estuaries are one of the most important reactors in global NO_3^- circulation and transformation, which should not be omitted in future N budget estimations.

III.2 Introduction

Groundwater with high N concentrations in coastal aquifers is found worldwide (Beusen et al. 2013). The main chemical composition of N in groundwater is NO_3^-, originating from infiltration of chemical fertiliser (Ibánhez et al. 2011; Beusen et al. 2013). Other sources such as leakage of septic tanks, industrial spillages or the use of manure and sewage sludge inland also increase NO_3^- availability in coastal aquifers (Wakida and Lerner 2005). As a consequence, injection of groundwater introduces substantial NO_3^- into coastal systems, which has been reported in a number of research sites (e.g. Shellenbarger et al. 2006; Lee et al. 2009; Kim et al. 2013; Lee et al. 2012; Tait et al. 2014; Wong et al. 2014).

Prior to discharge into the sea, terrestrial groundwater is intercepted by permeable zones, usually a part of coastal aquifers, and often configuring a subterranean estuary (Moore 1999), where terrestrial groundwater gradually mixes with seawater. In benthic biogeochemistry, a large portion of organic matter is a crucial factor for the occurrence of significant reactions affecting porewater solute concentrations and sediment-water fluxes. Therefore, a number of studies assumed that cohesive sediments in the coastal region are the sole important medium to mitigate excess NO_3^- (e.g. Seitzinger et al. 2006). Here, the main solute transport processes are molecular diffusion (Ibánhez 2012), bioturbation and bioirrigation (Santos et al. 2012a). Given the low organic stock, the biogeochemical role of permeable sediments (Boudreau et al. 2001; Rocha 2008), especially subterranean estuaries (Moore 1999; Moore 2010), in NO_3^- transformation has been largely underestimated. Therefore, NO_3^- fluxes generated or reduced in subterranean estuaries have been excluded from a number of assessments of NO_3^- derived from terrestrial groundwater discharge (e.g. Tse and Jiao 2008; Senal et al. 2011; Lee et al. 2012).

In subterranean estuaries and permeable sandy sediment, infiltrated seawater delivers labile organic matter and dissolved oxygen (DO) to deep zones (Santos et al. 2009; Ibánhez and Rocha 2014a). Due to the high permeability, solute transport in porewater via advection can be orders of magnitude faster than that of transport caused by diffusion dispersion, which significantly stimulates the biogeochemical reaction potential in sediment mediated by benthic microorganism communities (Rocha et al. 2009). In addition, a spectrum of NO_3^- transformation pathways in subterranean estuaries have been found, comprising denitrification, dissimilatory nitrate reduction to ammonium (DNRA), and nitrification, among others (Burgin and Hamilton 2007; Santoro 2010). Consequently, subterranean estuaries can be an important NO_3^- reactor in coastal zones, which has been evidenced by numerous research efforts at local scales (e.g. Ullman et al. 2003; Dollhopf et al. 2005; Kroeger et al. 2008; Rocha et al. 2009; Ibánhez et al. 2011; 2013; Erler et al. 2014a). However, an overall picture of the behaviour of NO_3^- in subterranean estuaries is not available on a global scale.

Here, I evaluate the distribution of NO_3^- concentration along salinity gradients in 16 distinct subterranean estuaries, from North America, Pacific islands, Europe, and Australia, via a fractional mixing model. I then combined the results derived from individual study sites to provide global scale insights into the dominant NO_3^- transformation trend and the magnitude of NO_3^- fluxes generated/reduced in subterranean estuaries. In addition, I compared NO_3^- transformation rates between subterranean estuaries and other important regions, such as rivers, coastal sediments and oceans. Though this work, I aim to show the pivotal role that subterranean estuaries play in NO_3^- circulation and turnover in biosphere.

III.3 Methods

III.3.1 Concept of fractional mixing modelling

Fractional mixing modelling has been universally practised in predicating solute dispersion in a fresh-saline mixing region, such as well-mixed estuaries (e.g. Sinha et al. 1996; Koutitonsky et al. 2004) and subterranean estuaries (e.g. Beck et al. 2007a; Santos et al. 2009), since the method was developed by Ketchum (1951). This linear model is based on salinity, being an index of mixing status between fresh and saline water masses. It can determine the trend of solute dispersion and potential loss/generation during the mixing. In particular, if the solute in the fresh-saline interaction zone behaves as though it is chemically inert, the distribution along longitudinal curvilinear follows the conservative mixing curve in Fig.III.1. In comparison, if the solute associated with freshwater is reactive; an inward or outward curve long the mixing gradient can be observed, shown as the 'Observed mixing state' in the same figure. The enclosed region (shaded in Fig.III.1) between the two curves is the portion that is reduced or accumulation due to non-conservative mixing. More information on mathematic expression and application is reviewed by Regnier and O'Kane (2005).

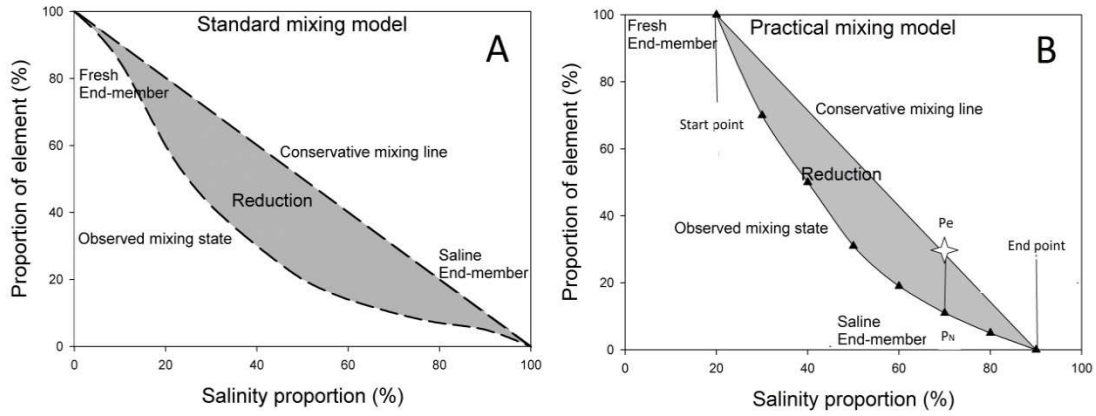

Figure III.1 (A): schematic diagram illustrating the models for solute reductions, straight line and curve indicate conservative mixing and the observed mixing along salinity gradient, respectively, the shaded region is the reduction portion due to reactions; (B): schematic diagram of fractional modelling for the water samples derived from research on subterranean estuaries. It shows the start point and end point as boundaries for integration, proportion of NO_3^- located in the observed mixing curve (P_N) and proportion of NO_3^- located in the conservative mixing curve (Pe).

III.3.2 Establishment of dataset

The global raw data to model distribution of NO_3^- concentration and concomitant salinity in subterranean estuaries were collected from the 13 individual studies in Table III.1 and cover 16 different beaches, situated in areas of North America, Pacific islands, Europe, and Australia (Fig.III.2). The majority of water samples were collected from benthic sediment via piezometers or artificial wells. The remaining were outflowing beach groundwater collected during ebbing tide.

Figure III.2 Distribution of research locations involved in the data collection in this study. The red point in the figure is the distinct study site.

III.3.3 Normalisation and reacted ratio calculation

For the fractional method, salinity ranges derived from each survey (original data in Appendix A) were normalised (Regnier and O'Kane 2005). In brief, the fresh endmember (salinity is 0) was set to 0 in each sampling site (or sub-location in one site). Conversely, the seawater endmember was 100% in portion. For the rest, the normalisation can be expressed in the function of salinity as following:

$$P_s = \frac{Sal_t}{Sal_{sea}} \times 100\% \quad (1)$$

where P_s is the proportion of seawater in different water samples, Sal_{sea} is the salinity in the seawater end member, which can be calculated by regession if determination of salinity in the seawater sample was excluded in the literature, and $\mathrm{Sal_t}$ is the salinity in the distinct water sample.

To normalise the NO_3^- concentration recorded in water samples, the definition of the endmembers were altered. In particular, due to salinisation in terrestrial groundwater and the difficulty of acquiring interstitial water samples in coastal beaches, the salinity interval of water samples in the research literature is only part of the complete fresh-saline range. For instance, in Ria Formosa, the 'most fresh' sample showed a salinity of 21 psu, which is a typical brackish mixture. For the calculation of NO_3^- reaction trends, I define the water sample with the minimum salinity as the fresh endmember for NO_3^- (100% in NO_3^- portion), and the sample with the maximum salinity contains 0 of NO_3^- (seawater endmember), though this might lead to decreases in reaction ratios. For the remaining water samples, normalisation procedure can be:

$$P_N = \frac{N_t - N_{min}}{N_{max} - N_{min}} \times 100\% \quad (2)$$

where P_N is the normalised proportion of NO_3^- concentration in water samples, N_{max} is the NO_3^- concentration in the lowest salinity water sample, N_{min} is the NO_3^- concentration in the highest salinity water sample, and N_t is NO_3^- concentration in each water sample. Based on these conditions, proportion of NO_3^- loss or generation in subterranean estuary during mixing can be calculated by integration. Here, I illustrate a case with regards to investigation of the nitrate reduction ratio (NRR) along the mixing gradient. I established a concept of P_e as the concentration of solute from conservative mixing in each salinity portion, shown as the star symbol in the righthand side of figure of Fig.III.1; therefore, the ratio of NO_3^- loss along mixing gradient is:

$$R_r = \int_{P_S=start}^{P_S=end} \frac{(P_e - P_N)}{P_e}\, d\, P_S \quad (3)$$

where R_r is NRR in subterranean estuaries. $P_s = \text{start}$ defines the lower limit of integration and $P_s = \text{end}$ defines the upper limit. Theoretically, the integration should cover the region between $P_s = 0$ and $P_s = 100$. The salinity of the fresh endmember in subterranean estuaries usually is above 0, and the salinity of the seawater endmember in calculation is possibly below that of water in adjacent ocean. For instance, in the practical case demonstrated in Fig.III.1, the start point is 20 in P_s value and end point is 90. Consequently, the calculating approach should only focus on the interval 20-90 instead of 0-100, i.e. the section between start point and end point. In light of the calculation for NO_3^- accumulation ratio, the mathmatical expression is indentical to Eq.(3), except for converting the term $(P_e - P_N)$ into $(P_N - P_e)$ to avoid generation of a negative value.

Table.III.1. Detailed information of distinct subterranean estuaries derived from previous research that can be used in the fraction mixing model. These study sites are located in different continents. The salinity and concentrations of NO_3^- are used as the raw data for my modelling.

Location	Sample type	Salinity range (psu)	NO_3^- range (μM)	Sample size	Reference
Marmion Lagoon, Australia	Seeped groundwater	4-34.2	10-365	10	Johannes and Hearn 1985
Woods Hole, USA	Porewater/Sea	3-32	0-400	13	Maier and Pregnall 1990
Mariana Islands, Guam	Porewater/Sea	17.76-36.15 [a]	10-66	10	Matson 1993
Cape Henlopen, USA	Porewater/Sea[b]	0-31.2	3.7-216	8	Ullman et al. 2003
Huntington beach, USA	Porewater	8.7-33.7	0.5-337	4	Santoro et al. 2006
Shelter Island, USA	Porewater/Sea	1-30	0-457	5	Beck et al. 2007b
Lynch Cove, USA	Seeped groundwater	14.5-25.9	0.8-30.2	10	Swarzenski et al. 2007
Ria Formosa lagoon, Portugal	Seeped groundwater	21-37	8-170	10	Leote et al. 2008
Stinson Beach, USA	Porewater/Sea	0.22-32.02	15-76	4	Sieyes et al. 2008
Concepcion Bay, USA	Porewater/Seeped	0.6-32	20.7-745	7	Santos et al. 2011
Puerto Morelos, Mexico	Porewater	1.64-33.75	0.15-268.6	4	Terrones et al. 2011
Dor Bay, Israel	Seeped/Sea	2-38	5-330	10	Weinstein et al. 2011
Truc Vert beach, France	Porewater	12-35	5-48	6	Charbonnier et al. 2013

a: Originally given as the concentration of chloride, I then transformed into salinity

b: The deep groundwater samples showed limited NO_3^- content and small fluctuations during the mixing process. I selected the water samples that represented mixing between shallow groundwater and seawater

III.4 Results and discussion

III.4.1 NO_3^- transformation in subterranean estuaries

On a global scale, two distinct patterns related to NO_3^- distribution in subterranean estuaries were observed derived from my calculations. In particular, the subterranean estuary at the Cape Henlopen, USA (Ullman et al. 2003) showed strong NO_3^- production, as can be seen in case of Fig.III.2. Beaches in Lynch Cove (Swarzenski et al. 2007) and Huntington (Santoro et al. 2006) were dominated by similar increasing trend during mixing processes. The maximum increase in magnitude of NO_3^- fluxes can be witnessed in Huntington beach, reaching a level of 102% (Fig.III.3). The mean production ratio in subterranean estuaries derived from the fraction modelling is approximately 73%. More importantly, subterranean estuaries could efficiently reduce terrestrial groundwater-borne NO_3^-. Distribution patterns derived from research works by Matson (1993), Beck et al. (2007b) and Santos et al. (2011) revealed a significant NO_3^- decline along the salinity gradient, indicating that the NO_3^- reduction process overwhelmed generation. The remaining sites also manifested a net loss of NO_3^- in beach groundwater prior to discharging to the sea with reduction ratios between 1.2% and 43%.

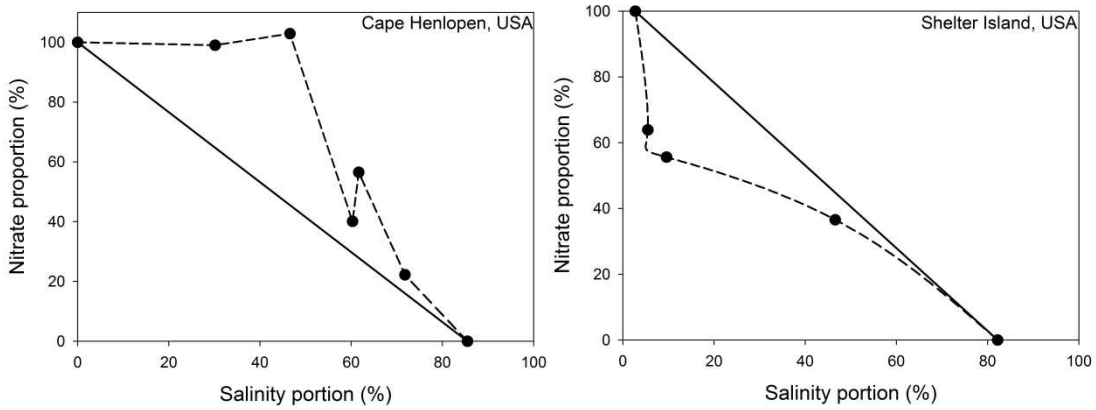

Figure III.3 Examples of normalisation for two cases, subterranean estuaries in Cape Henlopen (Ullman et al. 2003) and Shelter Island (Beck et al. 2007b), the straight line indicates conservative mixing, the bent curve is derived from observed distribution of NO_3^- in porewater

Previous studies usually expected the benthic sediment to act as a net sink of reactive N (Herbert 1999; Erler et al. 2014a). However, the results presented here show subterranean estuaries can shift between a sink and a source of NO_3^- over spatial and temporal scales. The coexistence of addition and removal indicated that the NO_3^- balance in subterranean estuaries is sensitive and can be influenced by availability of substrate, such as NO_3^-, labile carbon and ammonium (NH_4^+); community structure of microorganism, and hydraulic circulation rate (Ibánhez 2012; Santos et al. 2012b). In some sites where NO_3^- addition overwhelmed NO_3^- removal, terrestrial groundwater usually contained high concentration of NH_4^+ (e.g. Santoro et al. 2006), which facilitated nitrification. However, NH_4^+ in terrestrial groundwater is often limited since it has been consumed by oxidising reactions and biological assumptions before reaching the coastal beach. Hence, subterranean estuaries in the majority of sites (13 in 16) were dominated by NO_3^- reduction with large differences in reaction rates. Overall, approximately 22% of groundwater-borne NO_3^- can be reduced in subterranean estuaries. Though a large variation derived from my calculation can be observed; this estimation allies with the prediction of the NO_3^- reduction percentage in subsurface system prior to discharge (20% to 40%), estimated by Beusen et al. (2013).

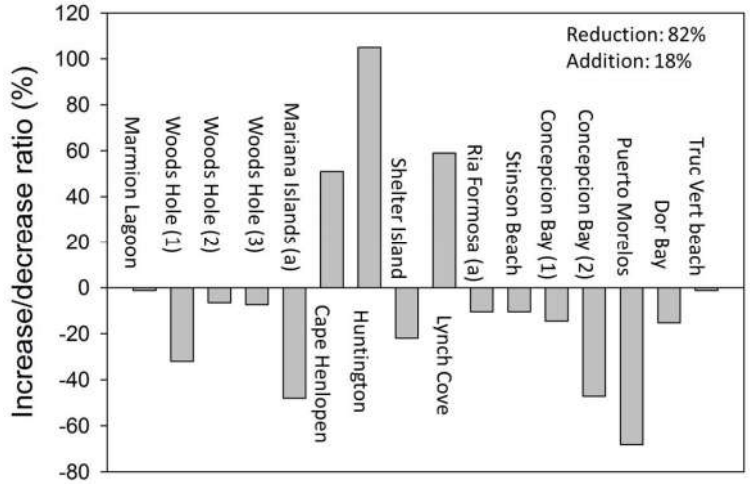

Figure III.4 Increase/decrease ratio of magnitude of NO_3^- fluxes flowing through subterranean estuaries. Positive value indicates net addition while negative value is net removal. The number in brackets indicates number of different sub-locations. Character 'a' indicates average value of a site, where samples were collected in different seasons or with different groundwater input.

III.4.2 Magnitude of NO_3^- fluxes from subterranean estuaries

Previous studies have emphasised the importance of cohesive sediment in NO_3^- transformation (e.g. Sigman et al. 2003; Lehmann et al. 2007). However, my results suggest that subterranean estuaries, which are highly permeable, are actively involved in NO_3^- circulation and transformation. In order to understand contributions of subterranean estuaries to NO_3^- turnover on a global scale, I formulated two scenarios to estimate the magnitude of reacted NO_3^- fluxes. The first scenario was based on the estimation of Zhang and Mandal (2012). They conservatively projected injection magnitude of groundwater associated with NO_3^- was approximately 1.9 Tg N-NO_3^- yr^{-1}. If the temporal and spatial variability of NO_3^- reactions within subterranean estuaries can be omitted (under a steady state), I can assume 82% of terrigenous NO_3^- was attributed to reducing subterranean estuaries since 13 sites or sub-sites among 16 locations showed NO_3^- decrease during mixing, 0.34 Tg N-NO_3^- yr^{-1} can be reduced in subterranean estuaries. The input for the second scenario was invoked from the calculation of the NO_3^- global budget (Galloway et al. 2004). Based on the NO_3^- balance on the continent, approximately 33.5 Tg N-NO_3^- yr^{-1} was delivered by the subsurface pathway to the coastal region. Beusen et al. (2013) conservatively presumed that 10% of groundwater associated NO_3^- fluxes was injected into the ocean via subterranean estuaries, which generated a value of 3.4 Tg N-NO_3^- yr^{-1} as groundwater input. Consequently, annual reduction fluxes in subterranean estuaries reached 0.61 Tg N-NO_3^- yr^{-1}. In terms of NO_3^- generation, subterranean estuaries could contribute 0.25 Tg N-NO_3^- yr^{-1} and 0.45 Tg N-NO_3^- yr^{-1} in two scenarios.

III.4.3 Comparison of NO_3^- transformation rate

Transformation rate, namely, the amount of reacted substrate in a unit area over specified length of time, reflected the capability of biogeochemical reaction within a specific system. Because previous research mainly focused on NO_3^- loss via

denitrification (Galloway et al. 2004; Huettel et al. 2014), I chose to compare NO_3^- removal rates between subterranean estuaries and other important systems, such as rivers, continental areas, and coastal sediments. The area of subterranean estuaries in the globe is approximately 3.0×10^4 km^2 on the basis of length of coastal line (6×10^5 km, Santos et al. 2012a) and portion of permeable sediment (50%, Hall 2002).

Table III.2. Reduction of NO_3^- and area in different regions. Notably, the reduction and rate in subterranean estuaries are based on two sceneries. The reduction rate is the quotient between reduction and area. The comparison in the table is the ratio of reaction rates between subterranean estuaries (two modes) and other systems. In the table, coast sediment (t) indicates the total sediment in the coastal shelf, while coast sediment (p) is permeable sediment. The average depth of river was assumed to be 10 m (Galloway et al. 2004). References are designated by number as follows: (1) Huettel et al. 2014; (2) Galloway et al. 2004; (3) Nilsson et al. 2005.

Region	Reduction (Tg)	Area (km^2)	Rate (Tg $km^{-2}yr^{-1}$)	Comparison
Subterranean estuaries	0.25/0.61	3.0×10^4	$(1.2/4.8)\times10^{-5}$	-----
Coast sediment$^{(p)}$	37.8 (1)	7.4×10^6 (1)	5.1×10^{-6}	2.2/4.0
Coast sediment$^{(t)}$	252 (1)	2.4×10^7 (1)	1.1×10^{-5}	1.1/1.9
River	47.8 (2)	4.3×10^6 (3)	1.1×10^{-5}	1.0/1.8
Land	67 (2)	1.5×10^8	4.5×10^{-7}	25.4/45.5
Continent	115 (2)	1.5×10^8	7.6×10^{-7}	14.8/26.5
Open Ocean	145 (2)	3.6×10^8	4.0×10^{-7}	28.1/50.5
Globe	572.7 (1)	5.1×10^8	1.1×10^{-6}	10.1/18.1

In Table III.2, permeable sediment in coastal region contributes to a reduction of 67 Tg N-NO_3^- yr^{-1}, but subterranean estuaries are removing NO_3^- at a 2.2 to 4.0 times higher rate on the basis of two scenarios in III.4.2 (the removing capability in subterranean estuaries was assumed to be constant). Compared with the reducing ability of all coastal sediments, most of which are cohesive, the removal rate in subterranean estuaries is still 1.1 and 1.9 times higher. The reduction capability in subterranean estuaries also exceeds that of rivers which have been treated as an important sink for NO_3^- due to intensive denitrification (Galloway et al. 2004). In comparison with the continents and oceans, subterranean estuaries are orders of magnitude higher in efficiency at removing NO_3^- under the steady state I assumed. On a global scale, NO_3^- removal rates in subterranean estuaries can be an order of

magnitude higher than the average level. In addition, our comparison is based on the unit of area (m^2). If the depth is taken into consideration, subterranean estuaries can be much more efficient in NO_3^- transformation due to a smaller volume. Specifically, the mean depth of subterranean estuaries in coastal aquifers is estimated to be 5 meters (Beusen et al. 2013); whereas depth of oceans and continent can extend to kilometres.

The comparison in the table is based on NO_3^- reduction, but it is worth noting that subterranean estuaries host high reaction potential in both accumulation and reduction (Fig.III.3). In my calculations, the ratio between NO_3^- reduction and accumulation in subterranean estuaries was assumed to be a constant. However, the circulation of NO_3^- may vary drastically on a large temporal and spatial scale, which adds uncertainties in the calculation. Moreover, the introduction of NO_3^- into coasts via biogeochemical reactions in subterranean estuaries is also highly efficient. In this circumstance, neglecting the NO_3^- contribution from subterranean estuaries in budget calculations may result in underestimation of NO_3^- loadings to coastal systems. Subsequently, it may hamper predication of occurrence of coastal events related with NO_3^- enrichment, such as harmful algae blooms, causing ecological and economical losses.

III.4.4 Limitations and implications

In this study, due to the quantity of sampling sites, the estimated reaction capability in subterranean estuaries may not be accurate. In addition, current measurements in subterranean estuaries have not fully captured water samples with the entire salinity range, i.e. from fresh to saline, as displayed in Table III.1. Consequently, the fraction mixing model embodied in this study possibly underestimates the NO_3^- transformation potential in subterranean estuaries due to the setting of endmembers, leading to additional uncertainties in the global budget estimation.

I am the first to study NO_3^- transformation patterns in subterranean estuaries on a global scale. The removal and addition ratio in our results can be served as a reference for future research on NO_3^- circulation in subterranean estuaries and NO_3^- mass balance estimation in coastal zones. Moreover, our results may also benefit research on global NO_3^- budget calculations.

III.5 Conclusions

Subterranean estuaries are important zones in circulation of NO_3^-. My results suggest that subterranean estuaries are dominated by NO_3^- reduction, probably due to high concentration of NO_3^- in porewater, suggesting subterranean estuaries are serving as barriers to protect the nutrient balance in coastal waters. Nevertheless, the NO_3^- circulation in subterranean estuaries is sensitive. Subterranean estuaries can shift to the source of NO_3^- in different environmental conditions, such as enrichment of NH_4^+ and dissolved organic matter. Both NO_3^- addition and reduction subterranean estuaries can lead to significant change of NO_3^- fluxes. Compared with NO_3^- removal capability in other systems, subterranean estuaries showed the highest reducing efficiency in transformation of NO_3^-, which suggests that subterranean estuaries are a highly active and sensitive reactor in NO_3^- transformation; therefore, they should not be omitted in future studies of NO_3^- circulation and budget estimation, as well as coastal management that focuses on reducing reactive nitrogen inputs via SGD pathway.

Chapter IV

Evaluation of vacutainers as to their suitability for sampling, storage and assessment of nutrient analytes in water samples

IV.1 Abstract

Vacutainers have been widely used for sample storage in surface water collection and porewater extraction in various environmental surveys and studies reported recently in the literature. However, possible interferences due to adsorption/desorption at the surface of vacutainers could impede accurate measurement of concentrations of solutes in filtrates. To understand their suitability for the collection and storage conventional natural nutrient analytes in water samples, the chemical stability of four nutrient analytes, NO_3^-, NH_4^+, soluble reactive phosphorus (SRP), and dissolved organic carbon (DOC) within different water samples, preserved in vacutainers, were examined in this study via incubation in controlled temperature conditions. The incubation time length ranged from 3 days to 30 days. In addition, borosilicate glass vials, the other storage vessels, were employed in the study in order to verify the storage performance of vacutainers by comparing nutrient concentrations. Results revealed that vacutainers are suitable for NO_3^- measured in all types of filtered water samples due to insignificant variations in concentration. Vacutainers are also an appropriate storage approach for water samples containing NH_4^+, especially for saline or brackish water samples. However, vacutainers need to be conditionally applied in determination of SRP and DOC since both solutes can be trapped by the surface of vacutainer hence affecting the accuracy of the analysis. The adsorbed amount depends on several factors, including solute concentration, temperature, ionic strength of the solution, and the presence or absence of complex dissolved organic matter (DOM). To minimise the analysis uncertainties introduced by using vacutainers, recommendations regarding the vacutainers operational use, including sample storage time and the use of process blanks are made. The safe operational time intervals for NH_4^+, SRP and DOC, between collection and analysis, where storage artefacts do not significantly affect (5%) the final results, is limited to a time period ranging from 1 day to approximately 2 weeks.

IV.2 Introduction

With the fast development of urbanisation, industry and agriculture, nutrient concentrations have increased significantly in surface, ground and coastal waters (Beusen et al. 2013), resulting in increased eutrophication, more frequent development of harmful algae blooms (HABs) and a general degradation of the natural environment. Hence, monitoring of nutrient concentrations in surface and groundwaters is listed as one of the most important tasks within environmental surveys aiming to evaluate and assess issues of potential nutrient pollution (Bende-Michl et al. 2013). Monitoring of these waters and their associated catchment areas requires a large suite of environmental samples and analytes be taken to characterise, document and evaluate trends of environmental status (Rocha and Woodward 2011). Due to the ensuing drastic increase in sampling tasks and requirements of accuracy in nutrient determination protocols, nutrient sample storage has become a real problem that befalls scientific researchers (Rocha and Woodward 2011).

In traditional methods, water samples were mainly stored in different kinds of conical flasks, test tubes and sample bottles. However, due to the large number of samples usually collected in the field, the traditional methodology has disadvantages associated with the labour-intensive preparation, risk of bacterial contamination, and possibility of leakage during transportation. These might all contribute to the introduction of significant bias reproducing nutrient status at the original research locations. Thus, environmental researchers have looked for other appropriate solutions for sample storage in order to standardise sample collection procedures and increase uniformity of sampling protocols. As a basic tool in medical and clinical research, vacutainers have been widely accepted as a collector for blood and urine samples for several decades (Pragay et al. 1971; Thomson et al. 1983; Toffaletti et al. 1984). Commonly, a vacutainer consists of a polyethylene tube and air tight plastic lid with

rubber septum (Fig.IV.1). The storage volume of vacutainers ranges from 5 to 10 millilitres (ml) depending on brand and type. A label is pre-attached onto the surface for recording sample information. The use of vacutainers for porewater extraction, collection of surface water and coastal water has several operational advantages compared to the traditionally employed sample storage. It is an inexpensive and portable way to preserve water samples, which significantly benefits field campaigns taking place on large temporal and/or spatial scales. In addition, vacutainers are sterile, which improves sample preservation by reducing the number of bacteria present. They are also disposable; hence, labour-intensive cleaning processes can be avoided. More importantly, the septum in the lid can be easily pierced by a syringe needle. A variety of filter holders and filtering membranes can be directly connected to vacutainers (Fig.IV.1). Water samples can be filtered and preserved in a closed environment, avoiding unnecessary contact with its surroundings before storage. Therefore, contamination possibilities can be diminished. These advantages are highly desirable for environmental researches to solve the conundrum of proper storage for liquid samples prior to analysis. Hence, an increasing number of field workers have included vacutainers in their operational sampling procedures. For instance, Cuffrey and Kemp (1992) determined nitrogen concentrations and stable isotope signatures in porewater samples which were stored in vacutainers. Corbett et al. (2000) utilised vacutainers to collect water samples from shallow groundwater boreholes. Leote et al. (2008) used vacutainers as sampling tools and for storage of porewater samples taken from seepage locations at a sandy beach. Berg and McGlathery (2001) and Ibánhez et al. (2011) employed vacutainers for porewater extraction and collection procedures from coastal sandy sediments. Carvalho et al. (2013) used vacutainers for the collection of coastal saline waters.

Previous testing proved their suitability of these vials in clinical and medical research (Reimold and Besch 1978; Chance et al. 2009). However, documented support for the performance of vacutainers in environmental research is limited. Prior studies

focused on blank tests for trace metals and nutrient elements (Helman et al. 1971; Kurkjian and Flegal 2003; Dong et al. 2008), but have not addressed the issue of prolonged storage of samples within the vials and its effects on analyte concentrations after sample collection. However, investigators have reported on sorption of different forms of nitrogen, phosphorus and carbon on other plastic tubes and sample vials (Jarvie et al. 2002; Shah et al. 2006). These results suggest that interferences on nutrient concentrations in water samples were likely following contact between the water sample and the vial internal walls.

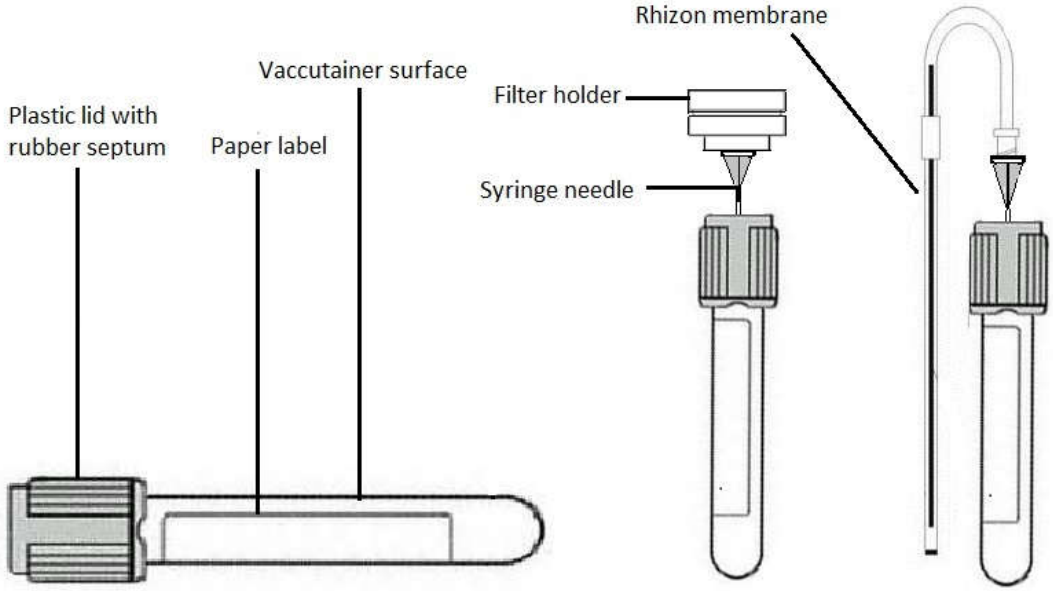

Figure IV.1 Sketch of the vacutainers employed in environmental surveys. This also illustrates the connections between a Rhizon membrane and a filter holder with the vacutainer via a syringe needle.

It is important to produce a comprehensive evaluation of the analytical suitability of vacutainers for conventional nutrient analytes and assess potential artefacts introduced from sample storage prior to analysis. To fill this knowledge gap, Greiner VACUETTE® No Additive vacutainers, were evaluated with respect to their analytical performance. Four distinct nutrient species, nitrate (NO_3^-), ammonium (NH_4^+), soluble reactive phosphate (SRP), and dissolved organic carbon (DOC) were studied. The major objectives are: (1) to determine nutrient analyte increases resulting from chemical release from the vacutainer surface; (2) to evaluate adsorption dynamics of nutrient

analytes onto the vacutainers; (3) to assess preservation time length, types of water and temperature on solute desorption/adsorption and (4) to provide practical recommendations for the operational use of vacutainers.

IV.3 Material and processes

IV.3.1 Preparation of water samples

The sorption characteristics of the four target analytes were examined by incubating water samples with distinct concentrations in vacutainers under constant temperature conditions (4°C and 20°C). To reach a comprehensive understanding on the sorption dynamics of analytes in different types of water samples, five types of aliquots were tested, comprising blank water, single-compound solutions, multi-compound standard solutions, fresh groundwater, and saline water samples.

Table IV. 1 Nominal concentrations of different nutrient in the test solutions. In the table, L signifies low concentrations, H indicates high concentrations, MDL is method detection limit.

Solutions	Concentrations of Analytes (unit mg l^{-1})			
	$N\text{-}NO_3^-$	$N\text{-}NH_4^+$	SRP	DOC
L-Single NO_3^-	0.1			
L-Single NH_4^+		0.1		
L-Single SRP			0.05	
L-Single DOC				2
H-Single NO_3^-	2			
H-Single NH_4^+		2		
H-Single SRP			0.2	
H-Single DOC				10
L-Multi standard	0.1	0.1	0.05	2
H-Multi standard	2	2	0.2	10
Groundwater	0.62	0.03	0.03	9.0
Spiked groundwater	2.62	2.03	0.23	19.0
Saline water	0.20	0.02	0.01	1.6
Spiked saline water	2.20	2.02	0.21	11.6
MDL	1.3×10^{-3}	1.5×10^{-3}	2.8×10^{-3}	0.021

Water employed in blank tests and dilution was produced from a Millipore Gradient system. Single-compound standard solutions were made from dilution of commercial certified standard stock solutions (NO_3^-, and NH_4^+ from AccuStandard®, SRP from ROMIL®, DOC from Reagecon®). Multi-compound standard solutions were produced from mixtures of four individual standard stocks (NO_3^-, NH_4^+, SRP and DOC). In order to identify any artefact due to the influence of analytes being present at different concentration levels, standard solutions were prepared at two concentration levels (Table IV.1) on the basis of nutrient concentration results derived from previous surveys in our research group. In addition to artificial sample solutions prepared from standards, two kinds of natural waters were employed to determine vacutainer performance in natural waters. Saline water samples were collected from the Atlantic Ocean. Fresh groundwater samples were gathered from Dunguaire Castle in Kinvarra, Co Galway, Ireland. Both water samples were pre-filtered through 0.2 μm pore size poly-ether-sulfone (PES) filter paper to reduce bacterial amounts. After filtration, samples were divided into two portions, one to be injected into the vacutainers and the other to be spiked with standard nutrient compounds (concentrations shown in Table IV.1) before injection.

IV.3.2 Treatment factors

There were two treatment factors tested, namely, storage temperature and length of storage period. Storage temperatures were set at 20°C (incubator) and 4°C (fridge) to simulate different sample preservation conditions in field work. Storage period length was divided into 'instantaneous' and 'long-term' storage in the collection vials. The instantaneous determination was divided into two subgroups to assess any putative effects of rapid sorption. The first subgroup was analysed immediately after filtration, which was identified as the initial group in the following statistical analysis, while the other was kept in the vacutainer for approximately 1 hour before analysis was carried out, which was treated as the instant group. All the remaining test samples

were stored for periods for 3 days, 10 days and 30 days at both 4°C and 20°C conditions, respectively. In each test, triplicate samples were prepared. Notably, the volume of filtrate in each vacutainer is 9 ml in order to minimise the uncertainties in the following dynamic sorption simulation. Detailed information about factor levels and experimental sequence is illustrated by the flow chart in Fig.IV.2.

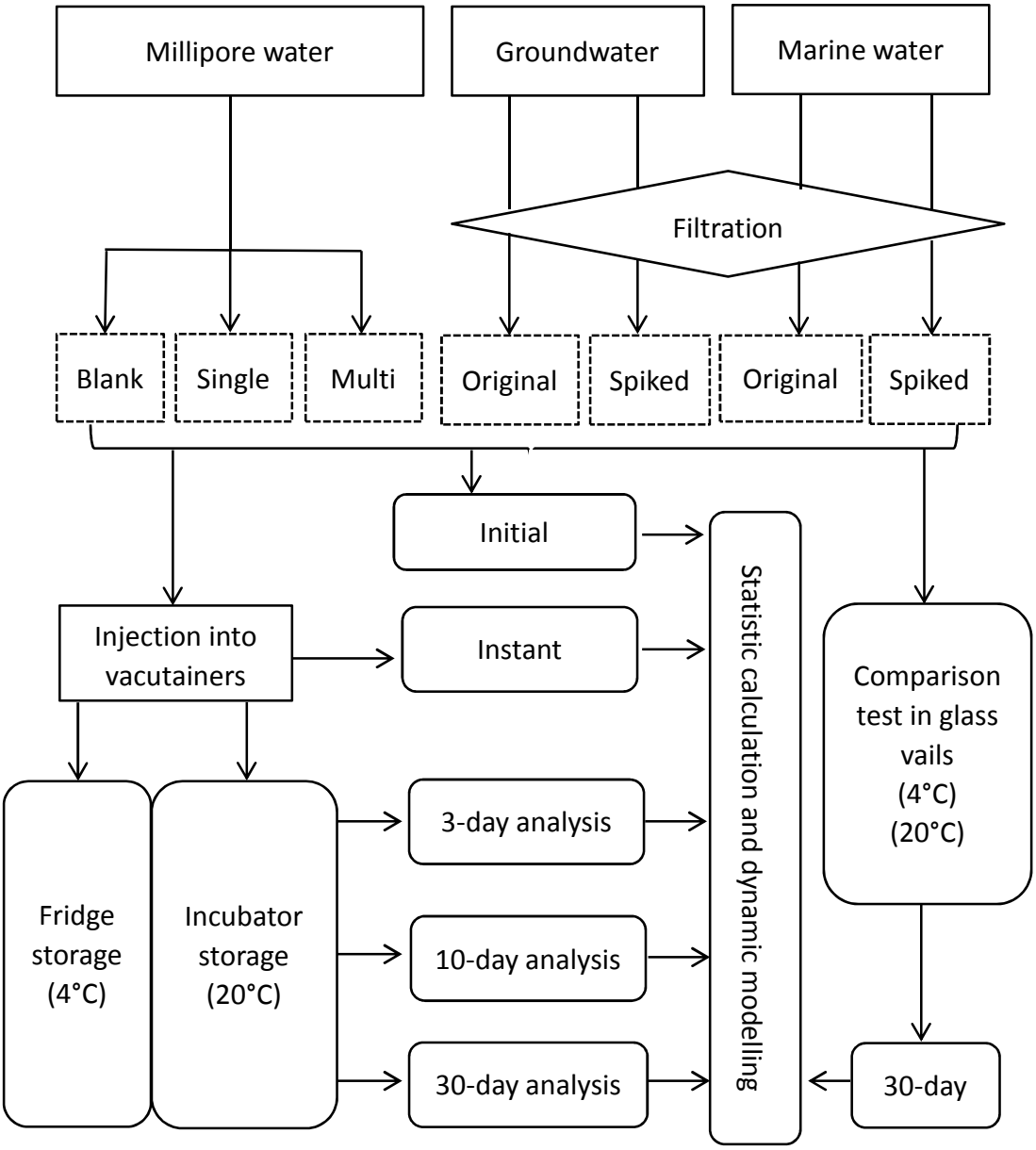

Figure IV.2 Flow chart of entire experiment, it shows the process from water sample preparation to data analysis. Each analysis included triplicate samples.

IV.3.3 Comparison test

Apart from the time sequential adsorption test, samples preserved in the vacutainers have been compared to those stored in traditional borosilicate glass vials to examine the analytical performance of the vacutainers. Chromacol 12-SV(A)-CP vials (Elementar®) have been applied for the comparison test. Identical water samples were injected and kept in the glass vials for 30 days within two preserving environments (4°C and 20°C). These water samples were analysed simultaneously with samples kept in the vacutainers.

IV.3.4 Analytical techniques

Concentrations of NO_3^- and NH_4^+ for all water samples were determined with a LACHAT Quickchem 8500 Flow Injection Analysis system following standard colorimetric methods (Grasshoff et al. 2009) as adapted for automated sequential analysis by the manufacturer. Concentrations of DOC were determined using an Elementar Vario TOC Cube at 680°C. The determination method for SRP is based on colorimetric methods (Eisenreich et al. 1975) at wavelength 882 nm on a Hach DR5000 spectrophotometer. The method detection limit (MDL) for each analyte determination was calculated on the basis of US EPA recommendations (e.g. Clayton et al. 1987), shown in Table IV.1.

IV.3.5 Statistical process

All statistical data analysis was done using SPSS®. The data was screened for normality and homogeneity of variance to ascertain assumptions for t-test and one way ANOVA. The design was asymmetrical (i.e. a single group for control and instant); therefore the data was analysed by using a combination of both ANOVA and t-test. In brief, it included calculating (1) a one-way ANOVA to determine influences from the

temporal treatment; when significant difference was determined via ANOVA, Tukey Honest Stand Deviation (HSD) test was applied to contrast differences between multiple groups (dependent variable: time length); and (2) a paired t-test to determine temperature influences in those groups with evident sorption effects without the control and instant samples. These allowed the variation associated with two treatment factors to be distinguished. To confirm and compare the suitability of vacutainers and glass vials for sample storage, paired t-test was used to compare mean values for all batches where adsorption was insignificant due to smaller variations within group (vacutainer or glass vials). For those groups with distinct adsorption effects, student t-test was used to determine whether there is a significant difference in analytical performance between groups. In all statistical calculations, the significant threshold was set at level of 0.05.

IV.3.6 Dynamic modelling

A comprehensive, rigorous theory of large compound solute exchange with solid surfaces is still pending (Ruthven 1984; Israelachvili 2011). The substance exchanges between liquid and solid surfaces lead to desorption and adsorption. For simplicity, adsorption and desorption are assumed to be independent. The desorption process can be treated as decomposition and dissolution of surface material from the vacutainer surface into the filtrate, while adsorption might result from establishment of chemical bonds between solute molecules and container surface (Gregg et al. 1967). The instant adsorption can be derived from direct addition or reduction in solute concentrations. For long-term dynamics, lumped kinetic models show how the averaged surface adsorption amount changes with time. These are much simpler and easier to apply for practical operations (e.g. Gil et al. 2011). I used a first order reaction model to describe the adsorption/release dynamics in those groups with statistical differences in concentration. The model assumes that the difference between the surface adsorption amount and the equilibrium adsorption amount is the driving force

and that the overall adsorption rate is proportional to this. It has been widely applied to explain the experimental results obtained for aqueous pollutants, such as dyes and metal ions (Ho and McKay 1999; Liu and Shen 2008; Gil et al. 2011).

In brief, the amount of solute adsorbed to the surface can be calculated as the change in the aqueous-phase concentration observed from the initial value, according to the following equation:

$$Q_t = \frac{V(C_0 - C)}{S} \quad (1)$$

where C_0 is the initial concentration, *C* is the concentration at time t, V is the water sample volume inside the vacutainer, *S* is the inner surface area of the vacutainer and Q_t is surface adsorption amount. When all the surface adsorption sites are saturated, adsorption equilibrium is reached. At this stage, we may write:

$$Q_e = \frac{V(C_0 - C_e)}{S} \quad (2)$$

where C_e is the solute equilibrium concentration, and Q_e is the equilibrium amount of solute adsorbed to the surface. The Lagergren pseudo first order equation (Azizian 2004) was used to fit the experimental results:

$$\frac{\mathrm{dQ}}{\mathrm{dt}} = k\,(Q_e - Q_t) \quad (3)$$

Integration of equation (3) for the boundary conditions at t=0 and t=t gives:

$$Q_t = Q_e[1 - exp(-kt)] \quad (4)$$

where k is the rate constant, and t is time. Due to all the vacutainers being identical

in sample volume and surface area, the volume and area terms contained in the expression for the adsorbed amount may be eliminated and equation (4) can be transformed to:

$$\ln\left(\frac{C-C_e}{C_0-C_e}\right) = -kt \quad (5)$$

which describes the sorption dynamics. When solute releases, the change of analyte concentration in solution with time can be described as:

$$\ln\left(\frac{C_e-C}{C_e-C_0}\right) = -kt \quad (6)$$

The Eq.5 and Eq.6 were modelled by fitting the rate constant and equilibrium concentration with the aid of Matlab®. When the minimum sum of squared standard deviations between modelled and measured concentrations were observed by a specific set of values, these numbers were then defined as the output parameters (detailed information in Ibánhez et al. 2011).

IV.4 Results and Discussion

IV.4.1 Blank test

In blank testing, concentrations of NO_3^-, NH_4^+ and SRP in all samples were below the method detection limits (MDL; detailed information in Appendix A). This showed that analyte leakage from the inner surface of vacutainers is low for those nutrient analytes. In comparison, leakage from vacutainers instantly increased DOC concentrations in blanks to a level of 0.45 mg l^{-1}. The analysis derived from 30-day incubation demonstrated a continuous increase of DOC in blank samples, as can be seen in Fig.IV.3. Specifically, after 30 days, the concentration of DOC in pure water

reached 1.86 mg l^{-1} and 1.79 mg l^{-1} at the low and high temperature treatments, respectively. Results from the one-way ANOVA (variable: time length) confirmed a significant difference in concentration between different time lengths ($F_{2,12}$= 26.01, P<0.001). Tukey post-hoc test indicated that DOC concentration steadily increased with sample storage from 3 days to 30 days at both temperatures, revealing both instant and long-term DOC release from the inner surface of vacutainers and into the sample solution. Though the concentration of DOC was higher after 30 days incubation in water samples stored at 4°C, a paired t-test indicated insignificant difference (t=1.14, P=0.34) in DOC concentrations accumulated within the Millipore water between vacutainers stored in 4°C and 20°C conditions, suggesting temperature is not an important factor for DOC release from the internal surface of the vacutainers.

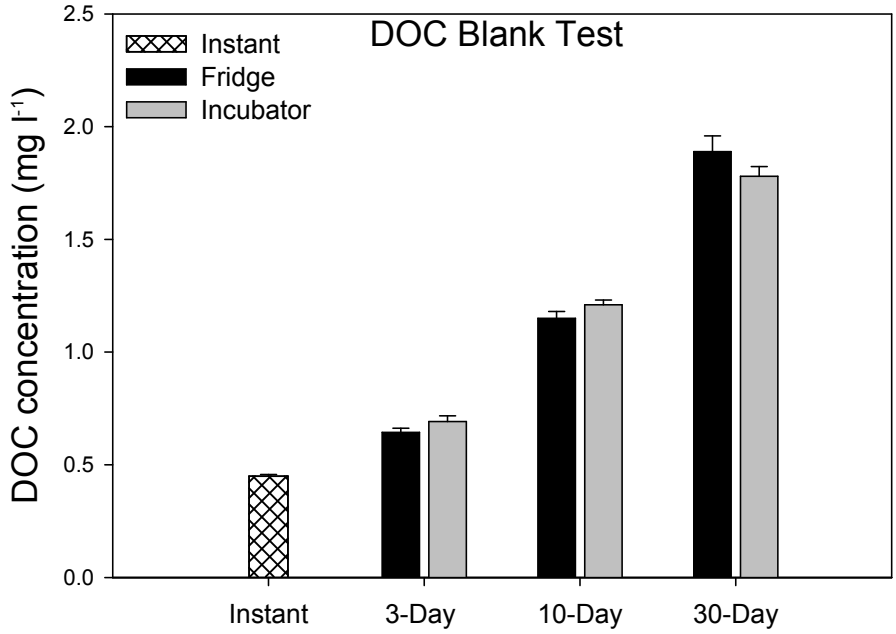

Figure IV.3 Temporal change of DOC concentrations in blank water samples, from instant determination (1 hour after injection) to 30 days, the figure displays results from two incubation temperatures, 4 °C and 20°C. Data are means ± standard deviations of three replicates.

A model simulation was run on the basis of temporal changes of DOC concentration for storage at 20°C. It suggests theoretical equilibrium (the maximum) concentrations of DOC in blank samples may reach 1.96 mg l^{-1} in maximum with a rate

constant of 0.07 day^{-1}. The non-additive vacutainer employed tested is made from polyethylene. The majority of desorbed carbon may be debris from the inner surface which increases organic carbon content in water samples.

IV.4.2 Adsorption of NO_3^-

The results of storage stability testing for NO_3^- are shown in Fig.IV.4. ANOVA indicates insignificant ($F_{2,12}$=1.18, P=0.34) concentration changes among all the samples at both temperature storage conditions. It confirmed that NO_3^- is the one analyte for which storage in vacutainers introduces no artefacts, which adds to findings of previous research showing adsorption of NO_3^- on polyethersulfone membrane filter surface to be negligible (Ibánhez and Rocha 2014b).

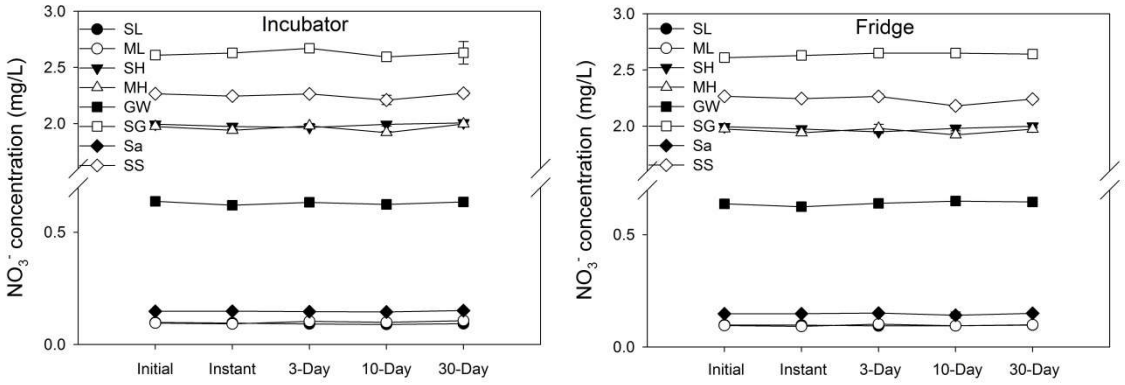

Figure IV.4 Temporal changes in NO_3^- concentrations in different water samples at 4 °C (Fridge) and 20°C (Incubator). Data are means ± standard deviations of three replicates. In the figures, SL represents low concentration of single-compound standard, ML is low concentration of multi-compound standard, SH is high concentration of single-compound, MH is high concentration of multi-compound standard, GW is groundwater, SG is spiked groundwater, Sa is saline water, SS is spiked saline water. In the following figures, definitions of abbreviations are the same.

IV.4.3 Adsorption of NH_4^+

After 30 days of incubation, a decline in NH_4^+ concentrations was observed in both multi-compound standard solutions and natural water samples (Fig.IV.5). For instance, the initial concentration of NH_4^+ in groundwater was 0.033 mg l^{-1}. At temperature of

20°C, the concentration gradually declined to 0.006 mg l^{-1} after 10 days. Afterwards, it stayed stably around that level. This sequential decrease was determined to be statistically significant via one-way ANOVA ($F_{2,12}$=8.51, P=0.005). Significant decreases in NH_4^+ concentration were also observed for analysis carried out in the spiked groundwater samples. For spiked groundwater samples, after 30 days, the total reduction in concentration was approximately 0.17 mg l^{-1}, approximately 8.3%, on for both treatments. Temperature influence on NH_4^+ adsorption was insignificant except when groundwater samples are concerned (t=3.48, P=0.04). Results suggested that more rapid reduction of NH_4^+ determined in groundwater samples stored in vacutainers at higher temperatures. In dynamic simulation, dynamic factor *k* in adsorption of NH_4^+ (groundwater) is larger than 1 in the incubator (20°C) while it decreases to 0.19 at 4°C (Table IV.2). In terms of the remaining groups, concentration variations were random under both temperature treatments.

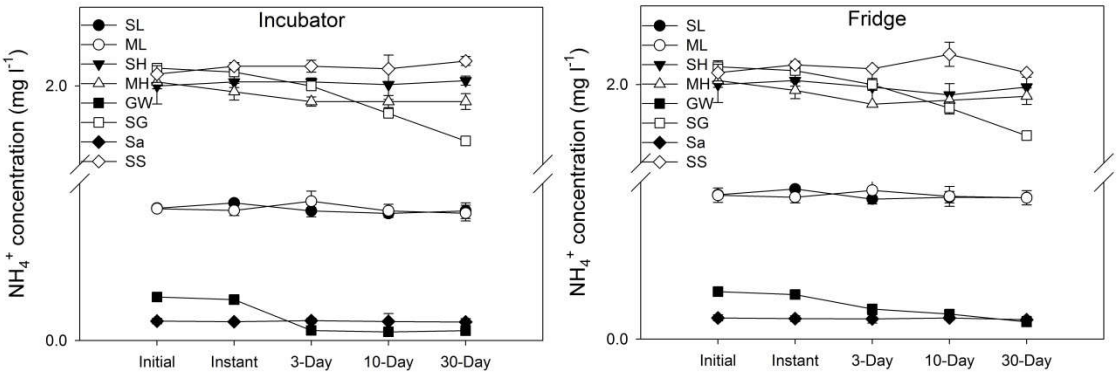

Figure IV. 5 Temporal change of NH_4^+ in different water samples at two temperature environments, 4°C and 20°C. Data are means ± standard deviations of three replicates. The abbreviations in the figures are identical with descriptions in Figure IV.4

The behaviour of NH_4^+ in single-compound standards was proved to be stable in the two concentration levels, while a significant decrease in NH_4^+ concentration was observed in when the fresh water samples and spiked freshwater samples were tested. This suggests that concentration of NH_4^+ is not the key factor for sorption to occur. Furthermore, all groups with significant adsorption of NH_4^+ showed substantial organic matter (DOC: 9 to 19 mg l^{-1}). Hence, it can be inferred that the decrease of NH_4^+ concentration in stored samples might result from attraction of NH_4^+ onto organic

molecules in water samples (Mackin and Aller 1984). In terms of temperature effect that determined in groundwater samples, molecular movement, e.g. Brownian movement, could play a part. High temperature activates movement and increases the possibility that NH_4^+ is trapped by carbon colloids (Levenspiel 1972). Alternatively, the higher temperature may also promote chemical transformation between NH_4^+ and organic compounds.

Table IV.2 Dynamic constants and concentration reductions in determined water samples, the values are calculated on the basis of Eq. (5). The F/I in the table indicates insignificant differences between two temperature treatments; hence we only calculated dynamic factors for the incubator temperature (20°C). Groups with brackets in the table indicate significant differences in solute concentrations between vacutainers and glass vials. NO in the table represents not observed. C_{ins} is decline due to instant adsorption, *k* is the rate constant, and C_e is estimated final concentration

Solutions	Analyte	Condition	C_{ins} (mg l^{-1})	*k*(day^{-1})	C_e (mg l^{-1})
Low-Single	SRP	F/I	NO	0.11	4.1×10^{-2}
	[DOC]	Fridge	0.22	0.05	0.85
	[DOC]	Incubator	0.22	0.03	1.0
Low-Multi	SRP	F/I	NO	0.10	4.1×10^{-2}
High-Single	SRP	F/I	NO	0.05	0.18
High-Multi	SRP	F/I	NO	0.05	0.18
	[NH_4^+]	Fridge	NO	0.19	1.2×10^{-2}
	[NH_4^+]	Incubator	NO	>1.0	7.5×10^{-3}
Groundwater	[SRP]	Fridge	NO	0.55	6.0×10^{-3}
	[SRP]	Incubator	NO	>1.0	6.0×10^{-3}
	[DOC]	Fridge	0.51	0.08	7.1
	[DOC]	Incubator	0.51	0.05	7.5
	[NH_4^+]	F/I	NO	0.08	1.86
Spiked-GW	[SRP]	F/I	NO	0.21	0.17
	[DOC]	Fridge	0.94	0.07	16.2
	DOC	Incubator	0.94	0.04	16.9
Saline	SRP	F/I	NO	0.10	1.0×10^{-2}
Spiked-Saline	SRP	F/I	NO	0.05	0.18

IV.4.4 Adsorption of SRP

A significant decrease in SRP concentrations was observed amongst all the groups

(Fig.IV.6). In low concentration standard solutions, the reduction was approximately 0.01 mg l^{-1} after 30 days in both temperature conditions. At the higher SRP concentration level, the adsorption amount increased to 0.03 mg l^{-1} (single-compound solution). Compared to standard solutions, natural water samples showed a stronger adsorption trend, especially in groundwater samples. Specifically, 83% of SRP in groundwater samples was adsorbed on the surface after 30 days at 20°C. Temperature influence was insignificant in all groups except fresh groundwater (t=3.22, P=0.05). It showed active SRP adsorption (large *k* value) at the high temperature condition.

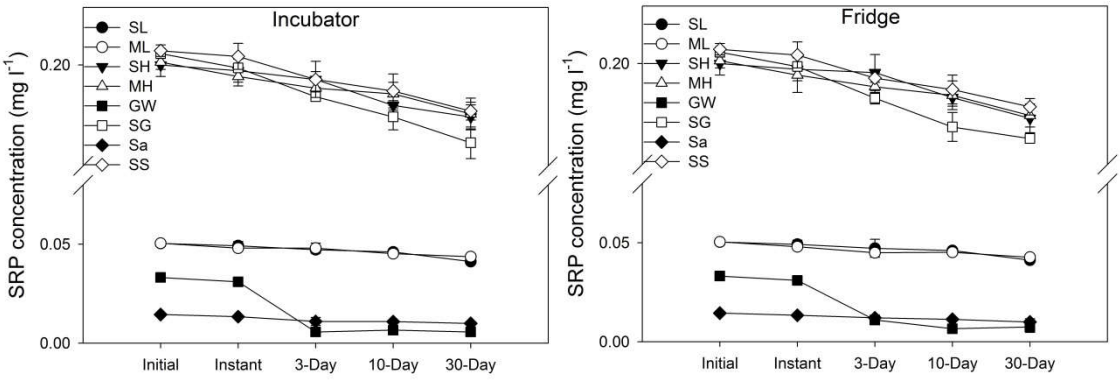

Figure IV.6 Temporal change of SRP in different water samples at two temperature environments, 4 °C and 20°C. Data are means ± standard deviations of three replicates.

SRP can be adsorbed by a spectrum of materials, including mineral particles (Goldberg and Sposito 1985), natural organic matter in sediments (Davis 1982), and adsorbents in aqueous environments (Dai et al. 2011). Correspondingly, SRP sorption occurred in all the groups in the vacutainer tests. For the standard solutions, the sorption amounts were identical when results from the experimental runs with single-compound and multi-compound tests solutions were compared. This trend suggests sorption of SRP is independent of the presence of other solutes, maybe directly attracted to the inner surface of the vacutainers. Increasing SRP concentration in the standard test solution can boost the amount of adsorbed, whereas, decreasing the dynamic constant. The reason may be found in sorption mechanisms. Adsorption procedures are usually described as single layer coatings (e.g. Langmuir model). However, the real connection between solute and surface may be complex, containing

several layers and chemical bonds with different strengths (Brunauer et al. 1938). Generally, the first layer that is closely attached to the surface has the highest dynamic factor and the strongest chemical connection. When the first layer is saturated, the second layer may be developed, and this tends to be weak in attraction and slow in sorption rate. With an increasing amount of layers, the total dynamic factor drops, though the total adsorption amount increases. However, the tests involving natural groundwater samples showed that the decrease in concentration was best described by a significantly larger dynamic constant than that of saline water, though SRP concentration in groundwater samples was comparatively high. In addition, the spiked groundwater samples also showed more active SRP adsorption than that of spiked saline water samples. This difference may be explained by two reasons. The first is the impact of ionic strength of the solution on adsorption mechanisms. In particular, saline samples with high ionic strength may decrease the adsorption of SRP onto the inner surface of vacutainers by introducing solute competition for adsorption sites. On the other hand, organic matter in solution may play an important role in SRP adsorption. In particular, the groundwater samples employed in the tests contain high concentrations of terrestrial organic matter, including humic and fulvic acids (Kelly and Rocha 2014), which have complex molecular structures (Cheng et al. 2005). This structure strengthens the chemical connection between SRP and carbon particles and traps additional SRP (Borggaard et al. 1990). Therefore, the reduction of SRP possibility contains direct and indirect pathways. The direct decrease in solute concentrations in the test solution may be due to chemical adsorption onto surface sites on vacutainers. The indirect sorption effect (or sequestration form solution) might instead result from the immobilisation of SRP by complex carbon molecules. It is worthy of note that the temperature effect is not significant among all water samples, except for fresh samples. It may indicate that dynamics of indirect sorption may be an endothermal reaction.

IV.4.5 Adsorption of DOC

The DOC concentration in standard solutions and saline samples increased after 30 days storage for both temperature treatments, while small concentration decreases were observed in spiked groundwater samples at the same time point (Fig.IV.7). However, DOC release from the vacutainer surface was significant (Fig.IV.3). Consequently, the desorbed amounts were not the declines from the direct measurement. Under the assumption that desorption and adsorption are independent reactions (IV.3.6), the effective concentration at each time point is equal to difference between observed concentrations and level of carbon release from vacutainers (Fig.IV.3). Subsequently, ANOVA suggested that DOC adsorption may have occurred in treatments of low concentration standard (single), groundwater and spiked groundwater samples. Their rate constants range from 0.03 day^{-1} to 0.08 day^{-1}. DOC adsorption tended to be active at 4°C.

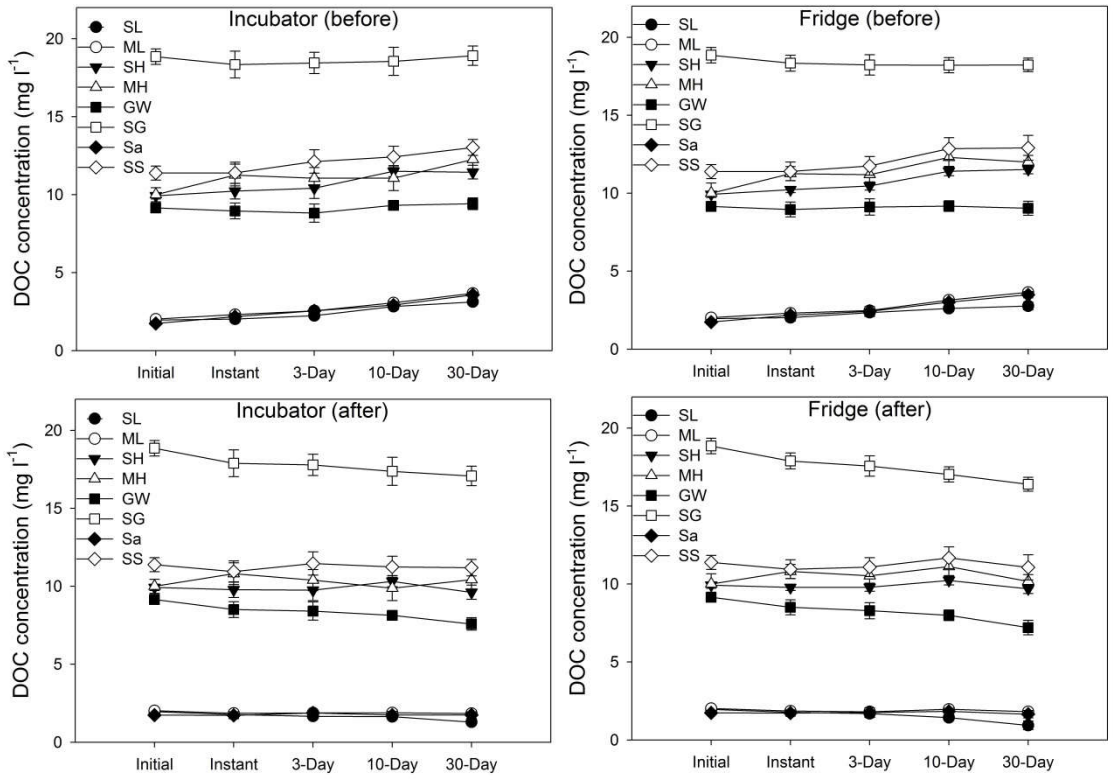

Figure IV.7 Temporal changes of DOC concentration (before correction and after correction) in different water samples at two temperature conditions, the upper is original determination values and the bottom is effective concentrations. Data are means ± standard deviations of three replicates.

Organic carbon adsorption is complex. It can be influenced by several factors including carbon concentration, temperature and ionic strength (Gu et al. 1994). In this study, after correction from blank contamination, adsorption for low concentration standards tended to be active. Apart from bias generated from our calculation approach, solution concentration and ionic strength may explain this. Specifically, comparatively high concentrations of carbon may increase the molecular attraction between carbon solutes (Yadav et al. 2011) which potentially decrease the adsorption amount on the surface in high concentration standard solution. On the other hand, higher concentration indicates stronger ionic strength, which may influence carbon adsorption. However, in natural water samples, DOC sorption showed a more complex pattern. In groundwater samples, the original concentration of DOC was approximately 9 mg l^{-1}, which is similar with DOC level in the high concentration standard solutions. However, adsorption was an important process for groundwater. The difference may be due to the presence of terrestrial organic compounds. Organic matter with a complex structure possibly offers more adsorption sites, increasing the molecular attraction to other carbon matter (Yan et al. 2013), such as vacutainer surface material. Therefore, the chemical connection between organic matter in groundwater samples and the vacutainer surface is prone to be established. Moreover, complicated organic matters could immobilise other organic solutes, e.g. free small molecular carbon (Schreiber et al. 2005), which indicates the organic matter adsorbed on the surface of vacutainer may trap additional carbon solutes and increase the adsorption amount. Therefore, the sorption of DOC in groundwater was significant ($F_{2,12}$=6.08, P=0.015). In terms of standard solution, the occurrence of sorption may be due to low ionic strength (Hayes and Leckie 1987). In the test, DOC adsorption was active at low temperatures since carbon adsorption is an exothermal reaction (Al-Degs et al. 2008).

IV.4.6 Comparison test

Results of comparison test are displayed in Fig.IV.8. After 30 days incubation,

concentrations of NO_3^- in all the solution stored in vacutainers and glass vials tend to be stable. Paired t-test confirmed an insignificant difference between two storage approaches (8 different solutions, df=7, t=0.86, P=0.42). It suggests that vacutainers are suitable storage vessels for the determination of NO_3^- concentrations. Similar conclusions can be made on the performance of vacutainers for NH_4^+ analysis for those batches where adsorption was not observed. In addition, for spiked groundwater samples, although adsorption was significant in vacutainers; whereas student t-tests exhibited an insignificant trend between two storage approaches, indicating that vacutainers may be a reliable storage method for this solution within 30 days storage time length. However, for groundwater samples (Fig.IV.8), there is clear advantage in preserving/storing samples in glass vials as higher concentrations of NH_4^+ were determined. Therefore, the application of vacutainers in water samples with substantial terrestrial DOM may lead to storage artefacts.

After 30 days, concentration of SRP in all test liquids stored in vacutainers was lower than that in solution preserved in glass vials (Fig.IV.8). Student t-tests suggested that statistical differences were determined in groundwater and spiked groundwater. For the remaining samples, vacutainers might be as suitable as glass containers for 30 days preservation since the minimum P value derived from t-test was 0.12. In DOC test, the effective DOC concentration was employed. It is the difference between the concentration determined in incubation test and release amount from process blank in section VI.4.1. For those groups without significant adsorption, after correction, the concentration difference in solutions between glass vials and vacutainers was statistically insignificant. On the contrary, significant difference in concentrations was observed in groups where a strong adsorption effect was determined, like groundwater and spiked groundwater samples. Preservation in glass vials showed higher DOC concentration remains in the solution after storage.

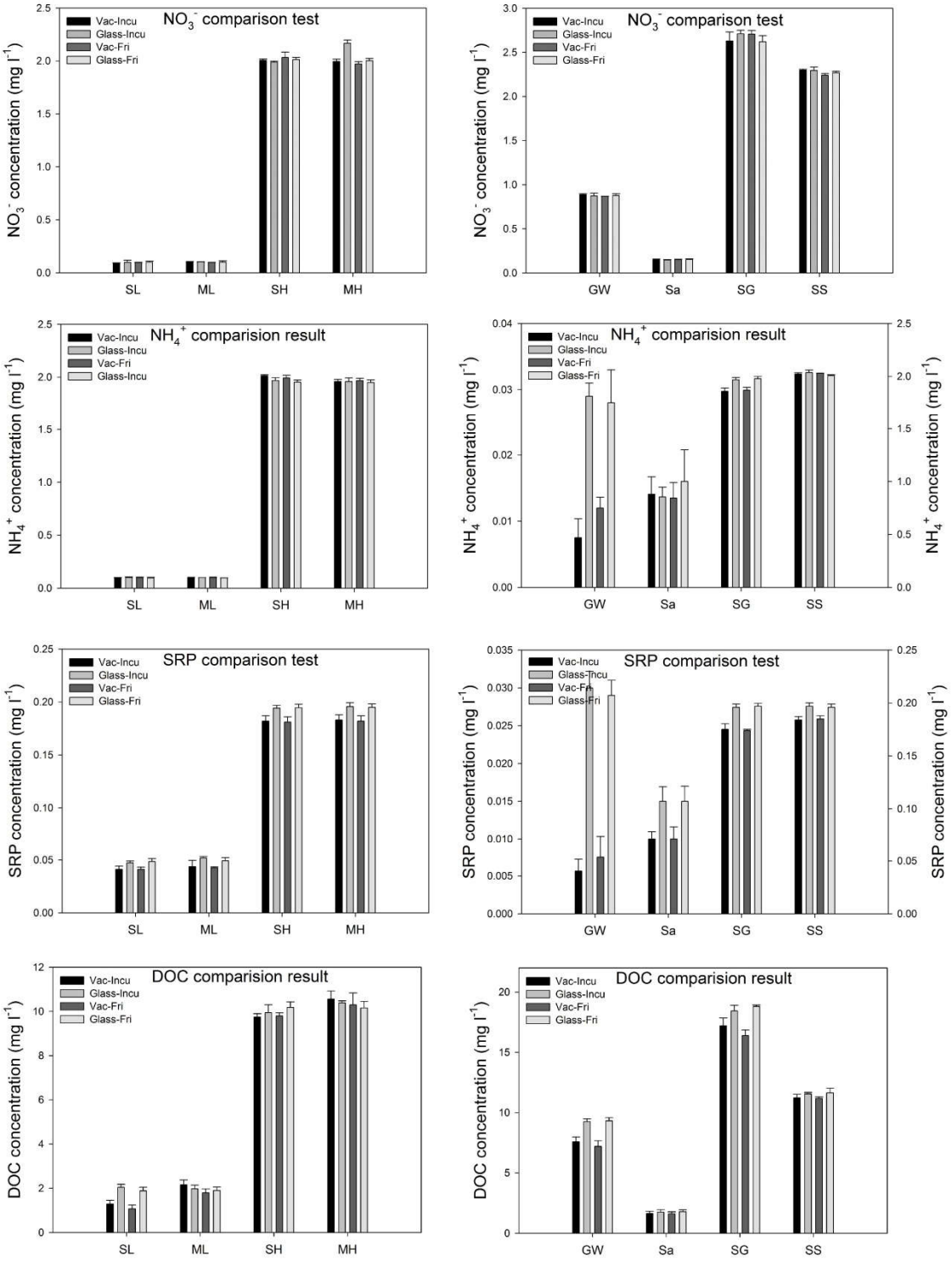

Figure IV. 8 Results of comparison test. In the figure, treatment conditions comprise vacutainers in incubator (Vac-Incu), glass vails in incubator (Glass-Incu), vacutainers in fridge (Vac-Fri) and glass in fridge (Glass-Fri). Data are means ± standard deviations of three replicates. The abbreviations in the figure are same with description in Figure IV.4.

IV.4.7 Uncertainties

Adsorption dynamics of DOC is complex. In this study, I assumed that desorption and adsorption are independent and desorption dynamics were derived from incubations of DOC-free water. However, the organic matter solutes in the remaining test liquid may influence the desorbed DOC amount from the vacutainer surface via solute interaction. As a consequence, the adsorption amount in Section IV.4.6 might not be precise. In addition, other factors not considered here would also influence the adsorption in vacutainers, such as pH. It may affect amounts of NH_4^+ adsorbed onto the surface by influencing potential formation of new sorption sites or by changing the ionic competition for these sites. Thus, some of the differences in the measured sorption dynamics might be attributed to the different pH environment of the solutions.

IV.5 Implications

Rocha and Woodward (2011) suggested proper storage for survey samples is one of the key processes for reproducibility of nutrient analyses results and accuracy with regard to the original concentrations found on the sampled waters. Potential interference from storage may significantly impact the determined concentration. Therefore, a comprehensive examination on the sample storage processes is necessary with a view to determine effects of storage on target solutes. In this study, the suitability of vacutainers in four conventional natural nutrient analytes was examined. Results indicated that vacutainers are an appropriate storage container for NO_3^-. With suitable filtering to eliminate bacteria, for instance, Rhizon membrane filter, samples stored in vacutainers can reflect concentration of NO_3^- at sampling site at least 30 days. Comparisons of concentrations between glass vials and vacutainers confirm this suitability. This result is significantly important for coastal water surveys and surface water monitoring since the concentration of NO_3^- is an important determinant in

defining eutrophication status of water bodies. The result is also important for the biogeochemical research of porewater in coastal beaches, where high concentrations of NO_3^- are frequently reported

The vacutainer is also a suitable storage vessel for determination of NH_4^+ concentration in water samples. Firstly, vacutainers do not introduce NH_4^+ into water samples. In addition, the NH_4^+ level in the majority of water samples preserved in vacutainers was stable during the storage time period (30 days). This has been confirmed by a series of comparison tests. For water samples where the decline of NH_4^+ concentration in vacutainers tended to be significantly larger than that in glass vials, such as groundwater (probably due to high level of terrestrial DOM), application of vacutainer in sample collection should be avoided. If alternative storage is unavailable, the optimised sample storage time to guide the application of vacutainers is displayed in Table IV.3 on the basis of the reduction ratio, i.e. a quotient between calculated concentration declines and initial concentrations. It can be seen that one-day storage time may be the appropriate period allowed before analysis to prevent any significant artefacts. To minimise NH_4^+ loss from adsorption, low temperature environment, for instance, cooler boxes with ice packs, would decrease the adsorption of NH_4^+ on the surface of vacutainers.

Table IV. 3 The preservation time length for NH_4^+, SRP, and DOC and corresponding concentration reduction percentage. Instant represents reduction occurs immediately when water samples are injected into the vacutainer. SG indicates spiked groundwater in fridge condition and GW is groundwater in fridge environment.

Solutes	Reduction level				
	2%	5%	10%	20%	30%
NH_4^+ (GW)	1 day				2 days
SRP(SG)	1-3 days	10 days	------	------	
SRP (GW)	1 day				2 days
DOC (SG)	Instant	1 day	5-10 days	------	------
DOC (GW)	Instant		5-10 days	20 days	------

The suitability of vacutainers for preservation of SRP depends on concentration levels of SRP and whether terrestrial organic compounds are present in the sample, as well as its ionic strength. Vacutainers can be suitable in the determination of water samples with high concentration of SRP and low terrestrial organic matters, for instance, brackish porewater from a coastal beach. For those samples with high concentrations of both terrestrial organic matter and SRP, for instance, spiked groundwater, after 3 days, the reduction percentage of SRP concentration may only reach 5% on the basis of dynamic parameters extracted from modelling the adsorption process. Nevertheless, for groundwater samples, the typical example of low in SRP level and ionic strength and high in terrestrial DOM, rapid analysis is recommended if vacutainers are applied in surveys. If samples have to be stored for a longer period, a cooler environment should be taken into consideration.

Vacutainers also can be conditionally applied for the determination of DOC concentrations if alternative borosilicate glass vials are not available. Firstly, due to leakage from the surface of vacutainers, process blank samples, i.e. deionised water stored in a vacutainer, needed to be prepared during field campaigns. It could provide the desorption level for correction the concentration of DOC in collected water samples, as the process in section VI.4.5. Organic carbon adsorption is influenced by ionic strength, carbon concentration, structure of the carbon compounds, and temperature. For brackish and saline water samples, application of vacutainers may be feasible. In addition, vacutainers may be used for the collection of freshwater samples with less complicated organic matter. For terrestrial groundwater, DOC tended to be actively attracted to the vacutainer surface (after accounting for the increase due to desorption contamination). Based on the dynamic constant from groundwater, a 10% reduction of DOC concentration might be observed within 5 days. It suggests survey for terrestrial DOC concentration should be compacted on temporal scale in order to avoid large analytical uncertainties if no other options than vacutainers are available.

IV.6 Comments and recommendations

The results showed the possible interference of vacutainers to different nutrient analytes, which were not identified in previous applications of vacutainers. Based on release/sorption results, vacutainers have been proved to be suitable for the preservation of NO_3^- in different kind of filtrate. Vacutainers also can be conditionally applied for the determination of NH_4^+, SRP and DOC. Generally, brackish and saline water are suitable liquid for storage due to their higher ionic strength and lower concentrations of complex organic matter. With process blanks, proper sample preservation temperature and optimised storage time, analytical uncertainties introduced from vacutainers can be minimised.

Chapter V

Seasonal variation of nitrogen transformations in a subterranean estuary on the Ria Formosa lagoon barrier

V.1 Abstract

The barrier islands of the Ria Formosa lagoon frequently host substantial seepage of terrestrial groundwater-borne nitrogen (N) into the system. As the subterranean estuary, the permeable beach in the barrier islands may modulate the magnitude of N fluxes derived from Submarine Groundwater Discharge (SGD). To understand the temporal dynamics of benthic N reactivity of the lagoon beach, a seven-month field survey on the barrier island was conducted. The concentrations of N solute in porewater were analysed. Subsequently, the reaction rates of N were determined by a combination of hydraulic modelling and non-steady state mass balance. Results showed that the subterranean estuary can be an important N reactor and influence on the magnitude of N fluxes associated with SGD. It shifted seasonally between acting as a source and a sink for nitrate (NO_3^-) and total dissolved nitrogen (TDN). In particular, biogeochemical processes within the sandy sediment that removed reactive N from porewater followed either the canonical denitrification or the oxygen-limited autotrophic nitrification/denitrification (OLAND) pathway. The maximum net removal rates for NO_3^- and TDN were observed in May and February, reaching 0.67 and 13.11 mmol m^{-3} bulk of sediment h^{-1}, respectively. On the other hand, the subterranean estuary could increase concentrations of NO_3^- and TDN in seepage fluids via remineralisation and nitrification. The maximum net production rate for NO_3^- reached 2.44 mmol m^{-3} h^{-1}, while the net TDN addition rate was 21. 49 mmol m^{-3} h^{-1}. Compared to the estimated N concentrations in the fresh groundwater endmember, the subterranean estuary from December to February may lead to an increase of 152% in the magnitude of NO_3^- fluxes. In contrast, from March to June, the subterranean estuary may foster a decrease of 22% for NO_3^- flux into the lagoon. These observations suggest that the subterranean estuary regulates N fluxes and is an important reaction node within the lagoon system.

V.2 Introduction

SGD is 'any and all flow of water on continental margins from the seabed to the coastal ocean, regardless of the fluid composition or driving forces' (Burnett et al. 2003). It generally occurs as diffusive flow into the coast wherever a costal aquifer is connected to the sea with a positive head relative to sea level (Johannes 1980). SGD comprises two components: fresh groundwater and recycled saline water (Taniguchi et al. 2002). Global estimations suggest that SGD could represent 5% to 10% of the total fresh water discharge to the coast (Zektser and Loaiciga 1993). Prior to entering coastal ecosystems, terrestrial groundwater first travels across a subterranean estuary (Moore 1999), i.e. a mixing zone between fresh and saline waters in coastal aquifers.

Coastal regions are a focus of human activity. They are often adjacent to large human populations and support a number of recreational and commercial uses. These can include but are not limited to: maritime transportation, tourism, and intensive agriculture (Windom and Niencheski 2003). Due to, and concurrent with, these increased human activities, a significant increase in N (mainly as NO_3^-) concentrations in terrestrial groundwater in coastal aquifers across the globe has occurred (Moore 1999; Moore 2010; Beusen et al. 2013). Other sources such as sewage and mains leakage, septic tanks, industrial spillages and/or the use of manure and sewage sludge inland can also contribute to the high concentration of N in coastal aquifers (Wakida and Lerner 2005). As a consequence, SGD can be an important delivery pathway for N to coastal zones, has been shown for more than 40 research locations (Zhang and Mandal 2012), including: America, Europe, Asia and Australia.

Currently, the magnitude of N fluxes associated with SGD has been estimated by a variety of methodologies, in particular direct measurement (e.g. Leote et al. 2008; Loveless and Oldham 2010), and radiogenic tracer studies, specifically, determination of activities of radon (e.g. Santos et al. 2008) and radium (e.g. Kim et al. 2005; Paytan et al. 2006). Direct measurements usually offer limited spatial coverage and are labour

intensive and may largely fail to provide reliable estimation on a system scale. Consequently, the majority of scientific workers employed radioactive tracers in their research (e.g. Garrison et al. 2003; Charette and Buesseler 2004; Kim et al. 2005; Paytan et al. 2006; Shellenbarger et al. 2006; Kroeger et al. 2007; Knee et al. 2008; Hwang et al. 2010; Waska and Kim 2011; Tait et al. 2014). The main advantage of natural tracer studies is that they produce spatially integrated estimates of flux (Cable et al. 1996) while simultaneously decreasing the errors from short term variability (Burnett et al. 2001). The integrated activity of radioactive tracers can offer information on the rates of SGD. Subsequently, combining with N concentrations in each end-member, N fluxes delivered by SGD can be quantified. However, application of this approach usually includes considerable uncertainties. In particular, a great number of researchers assume the magnitude of N fluxes, especially those comprising terrestrial groundwater-borne N, is conservative during the mixing procedure in subterranean estuaries (e.g. Senal et al. 2011; Lee et al. 2012; Tse and Jiao 2012).

However, sea water infiltration can transport oxygen and labile organic matter into subterranean estuaries (Slomp and Van Cappellen 2004; Santos et al. 2009), which in turn might enhance local microbial remineralisation processes (Aller 1994; Sun et al. 2002). Moreover, interactions with sediment particles, presence of physical and chemical gradients in subterranean estuaries between different end-members and/or ion activity modulation by shifting ionic strength can change the N content of SGD (Moore 1999; Moore 2010). Therefore, subterranean estuaries are not passive conductors of N fluxes in coastal zones. Instead, they act as biogeochemical reactors that may influence the magnitude of N fluxes on whole system scale in a significant way.

This study was conducted in the Ria Formosa, a coastal lagoon surrounded by highly urbanised and intensively farmed aquifers, where SGD has been shown to carry substantial loads of N into the system (Leote et al. 2008). In this study, a seasonal

survey that covered winter, spring and summer was conducted. The temporal and spatial changes of dissolved inorganic nitrogen (NH_4^+, NO_2^-, and NO_3^-) and TDN concentrations in beach porewater were measured at a single site. The main hypothesis in this research is that the subterranean estuary is an active N reactor in coastal zones. I further hypothesised that the role the subterranean estuary played may shift between acting as a sink or source of N to the lagoon, potentially due to concentration variation in reactants in benthic environment, such as NO_3^- and reactive organic matter. Our objective in the current evaluation was to explore these hypotheses and identify effective N concentration in the fresh groundwater endmember for an understanding of possible N modulation ability in the subterranean estuary.

V.3 Study site

V.3.1 Geological background

The site for this study, Ria Formosa lagoon, is located in southern Portugal, extending from 36°58'N 8°20'W to 37°30'N 7°32'W, and covering the majority of the Algarve coastal area (Fig.V.1). North of the lagoon is Campina de Faro, a coastal plain site with intensive agricultural activities. Since the early 1980s, the original land cover has been gradually replaced by olive and citrus trees to boost the local economy. Due to limited annual precipitation (Stigter et al. 1998; Salles 2001), irrigation has been introduced to meet the needs of agriculture. After the rise in irrigation system use, an overabundance of fertiliser crossed the aquifer surface by infiltration, and contaminated groundwater in Plio-Quaternary sand aquifer and sub-horizontal Miocene sandy layers beneath Campina de Faro (Rocha et al. 2009). Along with the hydraulic gradient, the resultant NO_3^- plumes in groundwater flow towards the Ria Formosa lagoon (Stigter et al. 2006a).

When the NO_3^- plume reaches the coastal region, it seeps into a highly permeable layer, consisting of Quaternary gravels and sands (Arnaud-Fassetta et al. 2006). At the

bottom of the permeable layer, it is an infilling sequence. In the Ria Formosa lagoon, the infilling sequence is muddy sediment, 0.60 to 1.3 m thick (Bettencourt 1994). In addition, finer sediments beneath the marshes act as an impermeable layer for subsurface flow, in a geomorphological context to support typical saltmarsh ecosystems. Terrestrial groundwater may flow below this confining layer, seeping to the coarse sandy beaches in the barrier island (Johannes 1980; Corbett et al. 1999).

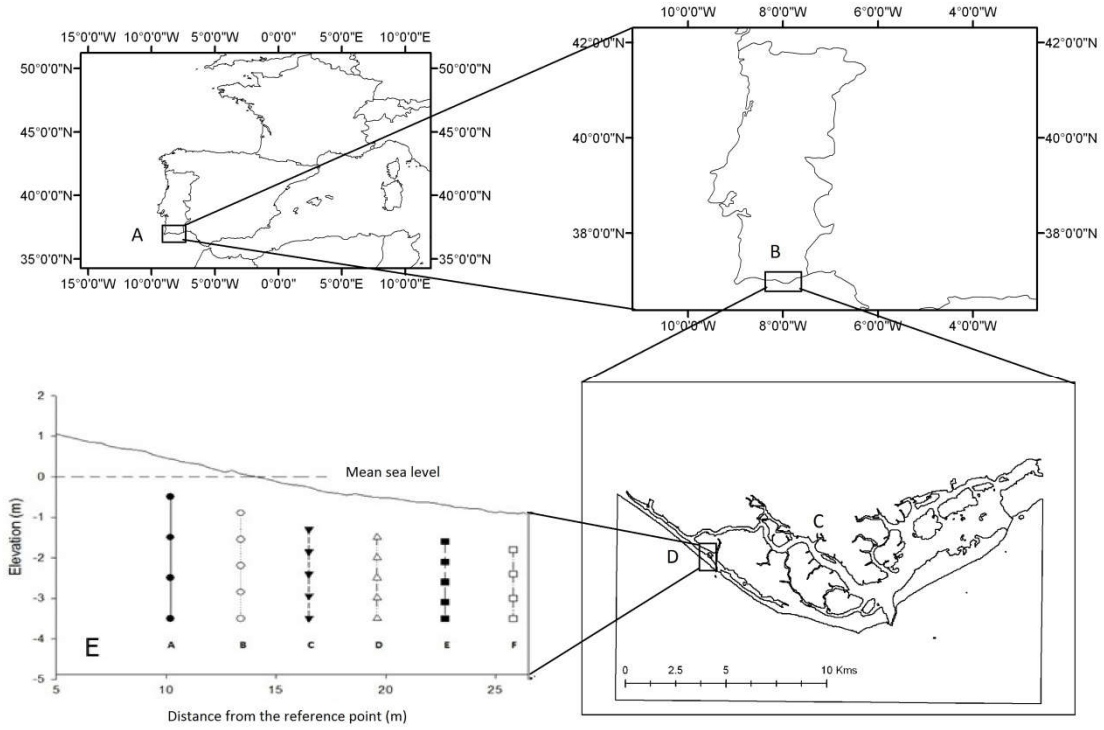

Figure V.1 Location for Portuguese beach face field site; A. – Portugal; B. –Algarve ; C. – region of the Ria Formosa lagoon; D. – Study site, Praia de Faro beach; E.- Location of piezometer sets, the definition of reference point can be seen in Figure V.2.

V.3.2 Hydraulic setting

The climate in the region of the Ria Formosa is Mediterranean. Average temperatures range between 11°C during the winter and 24°C during the summer. Annual precipitation is 480 mm in the city of Faro (West) and 580 mm in Tavira city (East) (Salles 2001). The adjacent coastal ocean has a semidiurnal, mesotidal regime. Tidal amplitude varies from 1.3 m during neap tides to 2.8 m during spring tides, with the extreme amplitude of 3.5 m (Vila-Concejo et al. 2004). The extensive intertidal

region developed by the shallow water depth (2 m, Andrade et al. 2004) hosts substantial SGD.

V.3.3 Sampling site and sample collection

The field survey presented in this chapter was part of NITROLINK project (2009 to 2011), which was assisted by our research group member, Liliana Carvalho. She also facilitated a part of N analysis in this chapter.

The sampling site for this study is located on the beach of the Ancão peninsula, approximately 1.5 km southeast from the access bridge to the ‘‘ilha de Faro’’. Andrade et al. (2004) found the presence of assemblages of freshwater tolerant diatoms which suggests the injection of groundwater into the lagoon. A field survey in 2006 showed a typical mixing process between terrestrial groundwater and saline water beneath the beach face via measurement of salinity and determination of DIN (Leote et al. 2008).

To collect porewater samples from the subterranean estuary, six sets (4 to 5 piezometers in each set) of piezometers (e.g. Beck et al. 2007b) were ordered from A to F and planted into the deep area of the site, following the beach slope (E in Fig.V.1). In each set, the depths of sampling piezometers ranged from 0.5 m to 3.5 m beneath the sand surface. Sampling project took place between December 2010 and June 2011. It covered both high tide and low tide in these seven neap tide periods (seven surveys in total). During each survey, water samples from 14 piezometers, from A to E piezometer sets, were gathered. In particular, the beach porewater was extracted via a peristaltic pump into HDPE sampling bottles. In order to avoid influences from dead-end water in tubes that connect a piezometer outlet and the peristaltic pump, the first 2 litres of water sample gathered from each piezometer were discarded prior to collection. The sampling interval between two piezometers was approximately 5 minutes. The water was filtered with ultra-filtration membrane samplers (Rhizon SMS, e.g. Ibánhez and Rocha. 2014b) with a mean pore diameter of 0.1 µm, into non-additive vacutainers (Chapter IV) for posterior laboratory determination.

From December 2010 to April 2011, collected samples were analysed for NO_2^-, NH_4^+ and NO_3^- using a FOSS Flow Injection Analyser (FIAstar 5000). Nitrite determination was colorimetric, based on the development of red azo dye with a method detection limit (MDL) of 0.2 μg N l^{-1}. Concentration of NO_3^- determination was based on prior reduction of nitrate using cadmium–copper reduction (MDL: 0.7 μg N l^{-1}). NH_4^+ was quantified following the spectrophotometric methods described in Grasshoff et al. (2009) with a detection limit of 0.4 μg N l^{-1}. These analyses were conducted by Liliana Carvalho in University do Algarve.

In June, concentrations of NO_3^-, NO_2^- and NH_4^+ for water samples were analysed in Ireland with LACHAT Quickchem 8500 Flow Injection Analysis system following standard colorimetric methods (Grasshoff et al. 2009) as adapted for automated sequential analysis by the manufacture. In addition, concentrations of TDN for all the water samples from December to June were determined in an Elementar Vario TOC Cube at 680°C. The MDL for each analyte determination was calculated (NO_3^- 1.2 μg N l^{-1}, NO_2^- 0.9 μg N l^{-1}, NH_4^+ 1.2 μg N l^{-1}, and TDN 32 μg N l^{-1}) on the basis of US EPA recommendations. The salinity for all the water samples was determined by WTW Tetracon 325 probe. These analyses were conducted by the author in Centre for the Environment, Trinity College Dublin.

V.4 Modelling approach

V.4.1 Aims of modelling

As an effective approach to sediment reactivity, advection-reaction modelling has been widely applied in coastal environment (e.g. Santos et al. 2009; Ibánhez et al. 2011; Chassagne et al. 2012). In practice, the calculating process consists of two steps: determining advection rate of porewater via hydraulic modelling and estimating benthic reactivity via mass balance calculations. As the key procedure, hydraulic modelling may determine the magnitude of reaction rate. Classical studies on porewater advection mainly focused on analytical solutions (e.g. Nielsen 1990; Teo et

al. 2003; King et al. 2010). However, all analytical approaches assume the presence of limited tidal amplitude and a vertical beach profile. These hypotheses are inconsistent with the environmental setting in the study site. As a consequence, in this study, the advection rate of porewater was simulated by numerical modelling.

V.4.2 Hydraulic model

In subterranean estuaries of barrier islands, porewater circulation is influenced by tidal pressure from both sides (Santos et al. 2012a). The bottom region of the barrier island is hydraulically connected with the terrestrial aquifer (Rocha et al. 2009). Generally, the pressure gradient of terrestrial groundwater is smaller than that of seawater due to the long distance between barrier islands and terrestrial groundwater source at on the continent; therefore, the barrier island can be treated as a tide-dominated system (Rocha et al. 2009). Our approach considers an idealised cross section of the barrier island lying between ocean gulf and lagoon tidal creek and resting on an impermeable bottom layer, as seen in Fig.V.2. Entire sections of the barrier island can be divided into two distinct domains; ocean domain on Faro beach, and lagoon domain on Ria Formosa beach (Andrade et al., 2004). In the model, it was assumed that the lagoon deposition extends to the connection point between the lagoon beach slope and the horizontal surface of barrier island, which is in line with field surveys of Bettencourt (1994) near Ancão inlet. A free exchange boundary was established between these two regions, which guarantees flux balance and avoids an unrealistic beach groundwater table during simulation.

The Faro beach is adjacent to the Atlantic Ocean, filling with coarse sandy particles (Cascalho and Taborda 2004; Vousdoukas et al. 2012). It has a gentle slope, gradually extending to the bottom of the Atlantic Ocean (Ciavola et al. 1997; Almeida et al. 2012). The lagoon beach region consists of medium-grain size sand particles (Ibánhez et al. 2011). In the simulation, the domain thickness was assumed to be 6 meters, which is accordance with determinations from Bettencourt (1994) and Andrade et al. (2004). Small fluctuations on the beach surface profile are neglected. These two simulation

regions in the barrier island are presumed to be homogeneous, isotropic and consist of a non-deformable solid through which exchanges between porewater and lagoon water occurs. Between two beaches, the surface of the barrier island was treated as an impermeable boundary. External hydrodynamic forcing is represented in the tidal oscillation, while high frequency water mass transfer due to waves was not taken into account (Chassagne et al. 2012).

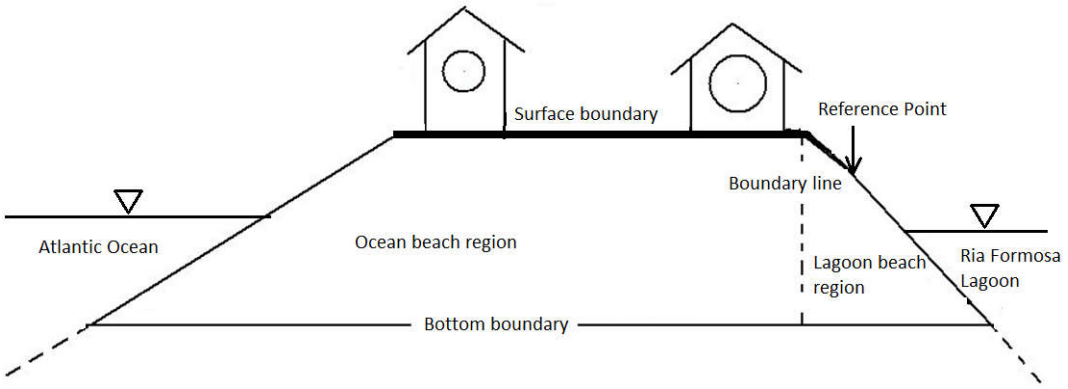

Figure V.2 Conceptual model of the barrier island in the Ria Formosa lagoon. The dash line represents the boundary between ocean and lagoon regions. The reference point is taken as the starting point in the field survey.

In a variably saturated porous medium, the flow velocity v (m s^{-1}) through permeable sediment can be deduced from the hydraulic conditions by the equation described by Chassagne et al. (2012):

$$v(h) = -K(h)\nabla.(h + z) \quad (1)$$

where *h* is the water pressure (m), *z* is the vertical coordinate and *K* is the relative hydraulic conductivity (m s^{-1}), which is related to the effective hydraulic conductivity at saturation k_s (m s^{-1}) (Li et al., 2008). I assume the relative hydraulic conductivity is identical in both the horizontal (x-axis) and vertical directions (z-axis). The saturated hydraulic conductivity k_s depends on the character of geologic medium, symbolising the capacity of fluid conductivity in the beach. The flow of water inside the sediment is governed by the Richards equation (Richards, 1931):

$$\frac{\partial\theta(h)}{\partial t} + \nabla.v(h) = 0 \quad (2)$$

where $\theta(\mathrm{h})$ is the volumetric water content (dimensionless) and the two dimensional divergence operator $\nabla . = \left(\frac{\partial}{\partial x}\right) + (\frac{\partial}{\partial z})$ is adopted for clarity. As Chassagne et al. (2012) shown, Eq. (1) and Eq. (2) can be combined together to form:

$$\frac{\partial \theta(h)}{\partial t} - \nabla(K(h)\nabla(h) + K(h)ez) = 0 \quad (3)$$

where *ez* is the upward unit vector. The main unknown in Eq. (3) is *h*, the height of the local groundwater table. Resolution of Eq. (3) requires information of the porewater retention curve $\theta(h)$ and the relative hydraulic conductivity function $k(h)$ in permeable sandy regions. There are different empirical equations that describe the relations between porewater content, pressure head and hydraulic conductivity I required (Brooks and Corey 1964; Mualem 1976; Van Genuchten 1980). In this study, the Van Genuchten model modified by Vogel et al. (2000) was utilised for this study.

Table V.1 Model parameters (lagoon beach region and ocean beach region), figures in the table: (1)-Field survey (2013), (2)-Ibánhez et al. (2011), (3)-Ramos et al. (2013), (4)-Almeida et al. (2012). (5)-Masselink et al. (2013), (6)-Balouin et al. (2005), and (7) - Rocha et al. (2009).

Parameters	Lagoon	Ocean
Beach slope, tan(β)	$0.11^{(1)}$	$0.07^{(4)}$
Saturated hydraulic conductivity, k_s(m s^{-1})	$3.19\times10^{-5(2)}$	$5\times10^{-4(5)}$
Tidal frequency (s^{-1})	$1.39\times10^{-4(1)}$	$1.39\times10^{-4(1)}$
Tidal Delay (s^{-1})	$2700^{(1)}$	$0^{(1)}$
Capillary fit parameter, α(m^{-1})	$1.8^{(3)}$	$2.4^{(3)}$
van Genuchten fitting parameter, n	$2.6^{(3)}$	$1.8^{(3)}$
Saturated water content, θ_s	$0.35^{(7)}$	$0.4^{(6)}$
Residual water content, θ_r	$0.02^{(3)}$	$0.02^{(3)}$

The solution of this formalism depends on a range of parameters related the sand hydraulic properties: the hydraulic conductivity at saturation (k_s), the capillary parameter α (m^{-1}), the dimensionless fitting parameter *n*, as well as the porewater

content at saturation and the residual porewater content (Van Genuchten 1980). All parameters are listed in Table V.1. Subsequently, the volumetric water content function of the water pressure head and relative hydraulic conductivity from the two beach domains can be seen in Fig.V.3. Eq. (3) predicts the pressure head distribution and allows us to compute the level of groundwater and the velocity field of porewater within the barrier island at each time step.

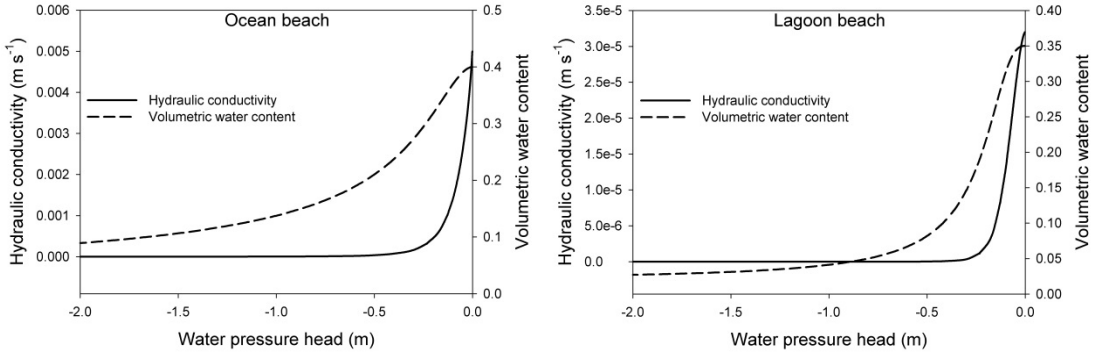

Figure V.3 Volumetric water content function of the water pressure head and relative hydraulic conductivity from the two beach domains

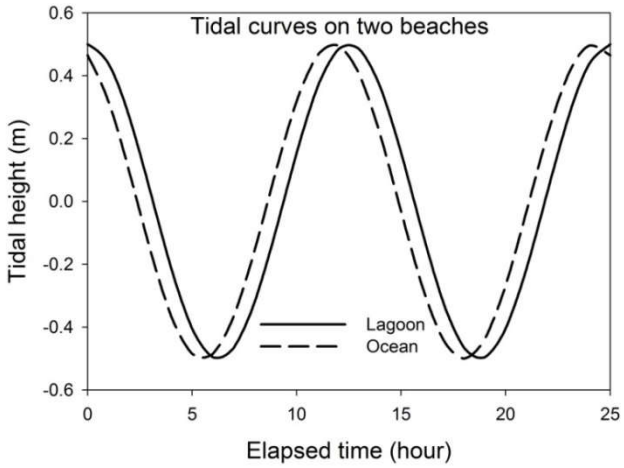

Figure V.4 Fluctuation of tidal height at the lagoon beach and ocean beach, a delay in phase is 45 minutes. The tidal amplitude is assumed to be 0.5 m for neap tide, and the tidal cycle is approximately 12.5 hours.

To solve Eq. (3) also requires appropriate boundary conditions. On both beach faces, a fluctuating boundary condition is imposed to describe pressure head derived from sinusoidal tidal height (Fig.V.4), which is given by

$$h_{tide} = M + A \times cos\ (\omega \times\ t + D) \quad (4)$$

where h_{tide} is tidal height, *M* is elevation of MSL, *A* is tidal amplitude, ω is tidal frequency, *t* is the time point, and *D* is the delay in tidal phase that is only applied on the lagoon boundary due to the slow propagation of water in lagoon channel system (Pacheco et al. 2007). In light of the impermeable layer on this barrier island, a Newman boundary $Q = 0$ (Darcy flow is zero) is applied.

V.4.3 Division of sampling region

To facilitate mass balance calculation, benthic regions need to be divided. In this study, four sub-sampling piezometers were combined into one grid, which was used as the basic unit for subsequent modelling. Hence the sampling site was divided into 8 grids. The corner of each gird represents a sampling point (Fig.V.5). However, in piezometer set A and B, due to blockage by sandy particles, I artificially generated two corner points (A 1,4 and B 2,5 in the figure) in a central location by averaging values from the top and bottom piezometers.

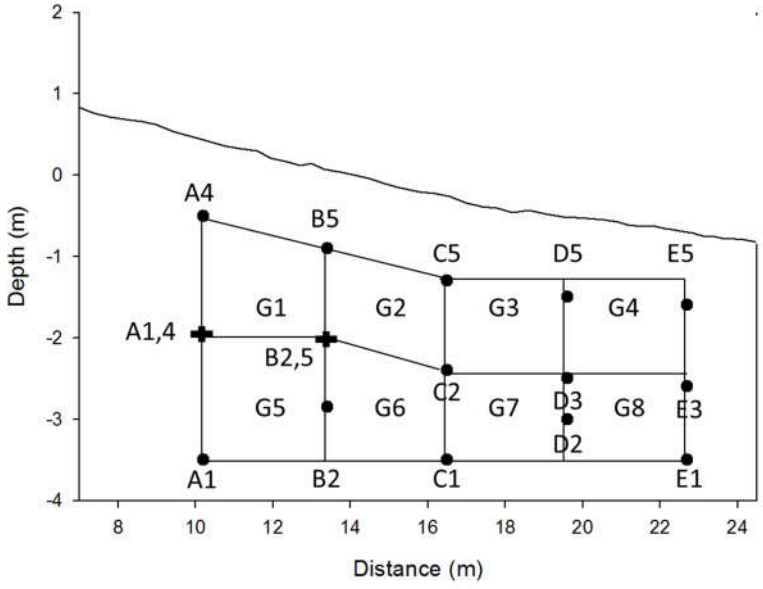

Figure V.5 Grid division and each piezometer in the sampling location; the distance counts from reference point. Each corner of a gird is one sampling site, the zero level in depth indicates mean sea level (MSL). The distance indicates the measured distance from the reference point in Figure V.2

V.4.4 Benthic mass balance

Hydraulic circulation in the subterranean estuary is highly dynamic due to changes in the terrestrial pressure head and fluctuation of tidal height, as well as other influencing factors, such as density flow due to temperature and salinity. In this study, based on advection rates calculated from the hydraulic model, a two-dimensional advection–diffusion-reaction model was invoked to calculate the N reaction rate within specific divided box and provide detailed information into the N circulation in beach porewater:

$$\frac{\partial C}{\partial t} = D_s \frac{\partial^2 C}{\partial x^2} + D_s \frac{\partial^2 C}{\partial y^2} + v_x \frac{\partial C}{\partial x} + v_y \frac{\partial C}{\partial y} + R \quad (5)$$

where $\frac{\partial C}{\partial t}$ is the temporal change of N concentration, D_s is the wet sediment diffusion coefficient, v is the advection rate in each grid derived from the hydraulic model, and R is the reaction rate. Because the advection rate in the permeable beach falls in an order of 10^{-6} m s^{-1}, and the diffusion coefficient is in the order of 10^{-9} m s^{-1} (Huysmans and Dassargues 2005), transport of the porewater is dominated by the advection and molecular diffusion in the permeable beach can be negligible (Santos et al. 2009). Based on the temporal change of N concentration in each small box within the determined subterranean estuary, Eq. (5) can be simplified as follows:

$$\frac{\Delta C}{\Delta t} = \left(v_{in}C_{in} - v_{out}C_{out} + v_{sw}C_{sw} - v_{sw}C_{out}\right) \Big/ V_{grid} + R \quad (6)$$

where $\frac{\Delta C}{\Delta t}$ is the rate of change of the N concentrations, $v_{in}C_{in}$ is the N input flux from upstream (it can be adjacent a grid or a boundary if the grid is located at the margin, for instance, A4 to B5 is the upper boundary for G1 on the vertical direction), $v_{out}C_{out}$ is the advective output downstream, and $v_{sw}C_{sw}$ is the input from seawater recharge to balance the salinity budget and the $v_{sw}C_{out}$ is outflow due to salinity balance, V_{grid} is the volume of the grid. The sketch for this calculation can be

seen in Fig.V.6.

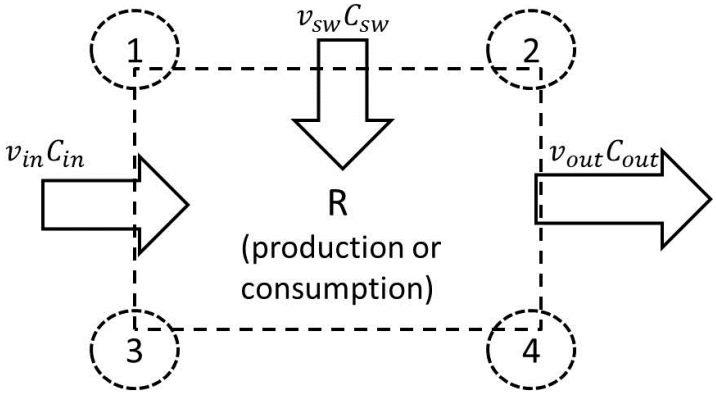

Figure V.6 Schematic illustrating the models applied for estimating reaction rate for an individual grid on the basis of Eq. (6). The number at each corner stands for one piezometer.

V.5 Results

V.5.1 Hydraulic circulation

The numerical model reproduces the general hydraulic circulation in the subterranean estuary under the stated assumptions. This model depicts three zones in the subterranean estuary: the permanently saturated zone without variation in porewater content, the transient zone in which the porewater content varies during the tidal cycle, and the permanently unsaturated zone: located away from the point of tidal forcing. The piezometers are located in the permanently saturated zone, as seen in Fig.V.7. During flood tide, seawater intrudes into the sandy beach via the upper region, which is identified as the recharge phase, while during ebb tide, beach groundwater seeps out of sediment from the lower limit of the beach domain, which is the discharge phase. The fluctuation of beach groundwater table derived from the modelling was consistent with field measurements conducted in 2013, which serves as the validation of the modelling (Two figures from the comparison are shown in Appendix B).

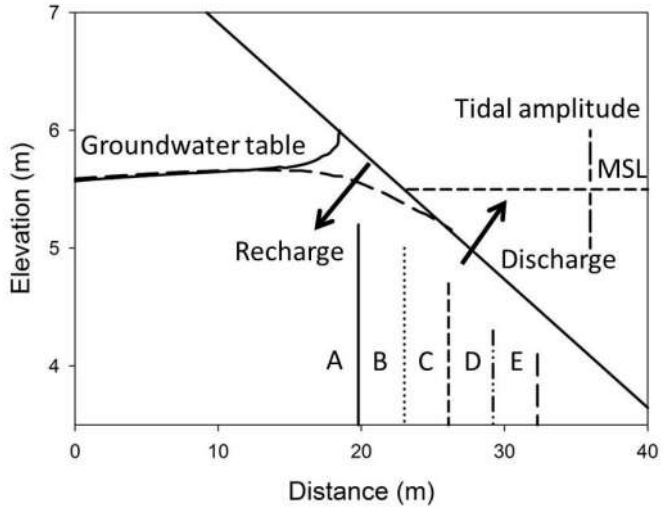

Figure V.7 Beach groundwater table at high and low tide during neap tide in the lagoon region. Also displayed are the locations of the piezometers (A-E) and the basic advection direction during recharge and discharge (arrows).

To apply the benthic reaction model in the sampling zone, the porewater advective fluxes for each grid during discharge and recharge was calculated (Fig.V.8). In particular, in low tide, the maximum magnitude of fluxes in horizontal direction can be seen at the upper limit of the beach domain, reaching 1.22×10^{-6} m^3 s^{-1}. Concurrently, the vertical advection velocity peaks at 2.85×10^{-6} m^3 s^{-1} in the same region. When tidal phase shifts to high tide, the maximum flux in the horizontal direction is 0.97×10^{-6} m^3 s^{-1}. Generally, they decrease in the lagoon direction. On the contrary, the magnitude of vertical flux generally increases in this direction, peaking at the third grid with a rate of 2.37×10^{-6} m^3 s^{-1}. The information for the remaining phases can be found in the attached supplemental material.

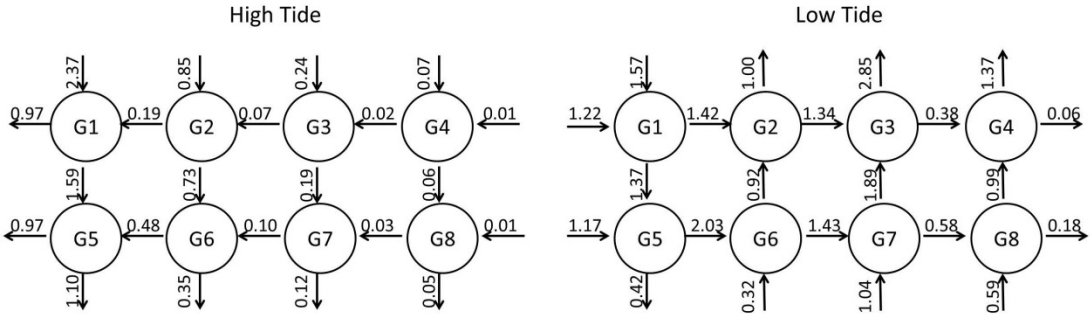

Figure V.8 Advection rate for each grid during high tide and low tide on the basis of hydraulic model calculation. The unit of velocity is 10^{-6} m^3 s^{-1}

V.5.2 Nitrogen variability

During the sampling period, NO_2^- and NH_4^+ were present at extremely low concentrations in porewater. In the majority of porewater samples, concentrations of both solutes were below 1 µM. The concentration range of these two N species from December to June (original data in appendix) is shown in Table V.2. The maximum concentrations for NH_4^+ and NO_2^- were only 3.60 µM and 3.25 µM, respectively. Therefore, the concentration variations of both NH_4^+ and NO_2^- in the subterranean estuaries were limited.

Table V.2 NO_2^- and NH_4^+ concentration range during the sampling period. 0 means that determined concentration was below the detection limit.

Month	NH_4^+ (µM)	NO_2^- (µM)
December	0.17-1.21	0-1.21
January	0.29-2.01	0.15-0.80
February	0.25-1.91	0-1.38
March	0.12-1.23	0-3.25
April	0.11-3.60	0.04-0.63
May	0.12-1.83	0-0.81
June	0.34-2.84	0.26-1.96

In comparison, concentrations and variations of NO_3^- and TDN in porewater were significant. The peak concentrations of both analytes were approximately 250 µM and 800 µM, respectively and concentration change in NO_3^- and TDN reached 10^1 and 10^2 orders of magnitude between two successive tidal phases. To understand the seasonal fluctuation and variation in different tidal periods for these two solutes, results in January, April and June with respect to salinity, NO_3^- and TDN are displayed. The results for the remaining months are included in the Appendix.

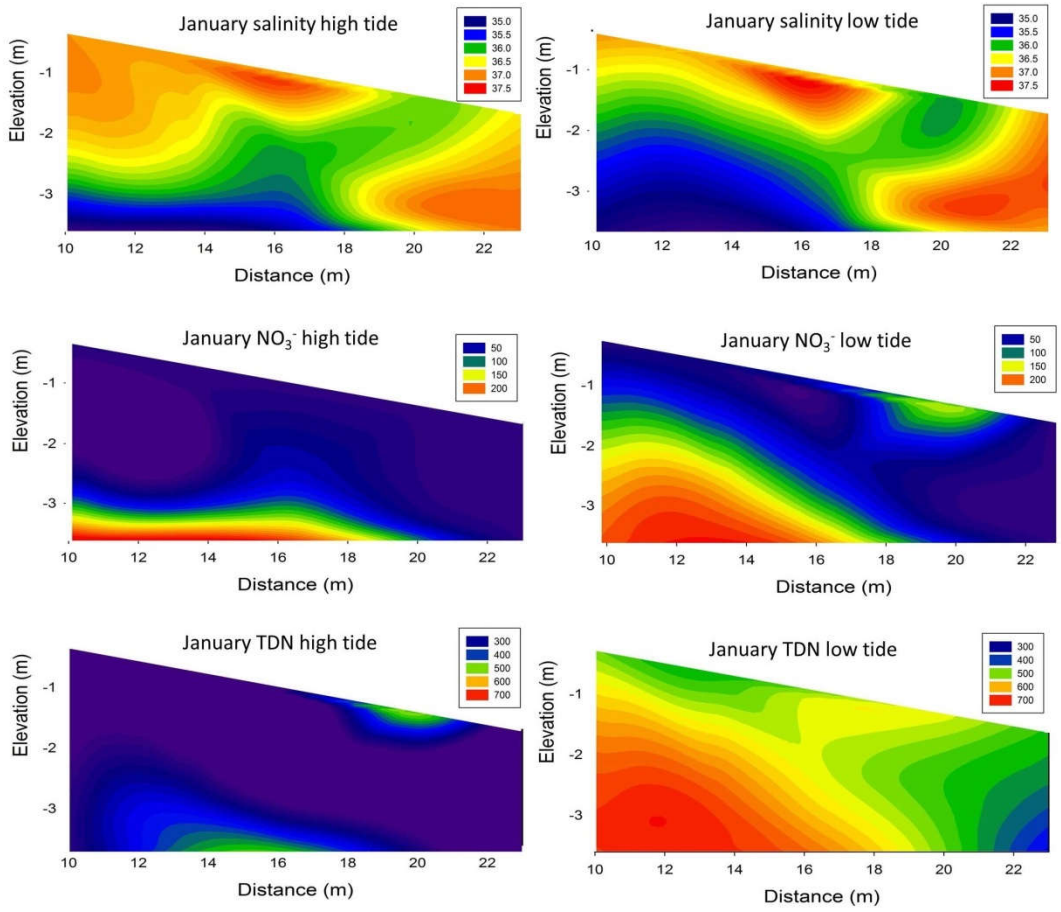

Figure V.9 Profiles of salinity, NO_3^- and TDN in the subterranean estuary for the 2011 January survey. The left panel shows distributions during high tide, while the right column exhibits distributions during low tide. The units for salinity and N are psu and µM, respectively. The scales among Figure V.9, Figure V.10, and Figure V.11 are different due to large variations of N concentration.

For the January high tide, low salinity porewater in the bottom region (represented by the blue contour in Fig.V.9) can be observed, suggesting the injection of terrestrial groundwater into the subterranean estuary. Correspondingly, concentration of NO_3^- in porewater reached 200 µM. For TDN at high tide, concentrations in sampling region varied from 300 µM to 500 µM. When the tide ebbed, amount of terrestrial groundwater in the subterranean estuary tended to rise so that it decreased salinity and increased NO_3^- concentration present within porewater. The increments of TDN concentration fall in the range from 150 µM to 200 µM in all grids.

Compared to January, porewater salinity in April decreased (Fig.V.10). In particular, the lowest salinity in the benthic region dropped to 32.9 psu, indicating the amount of terrestrial groundwater in the subterranean estuary had increased. However, the decline of salinity did not trigger an increase of TDN. Compared with observed TDN distribution in January, the maximum concentration of TDN in porewater was only 220 μM. In contrast, concentration of NO_3^- in porewater was sustained within the range of 8.9 μM and 183 μM due to injection of terrestrial groundwater.

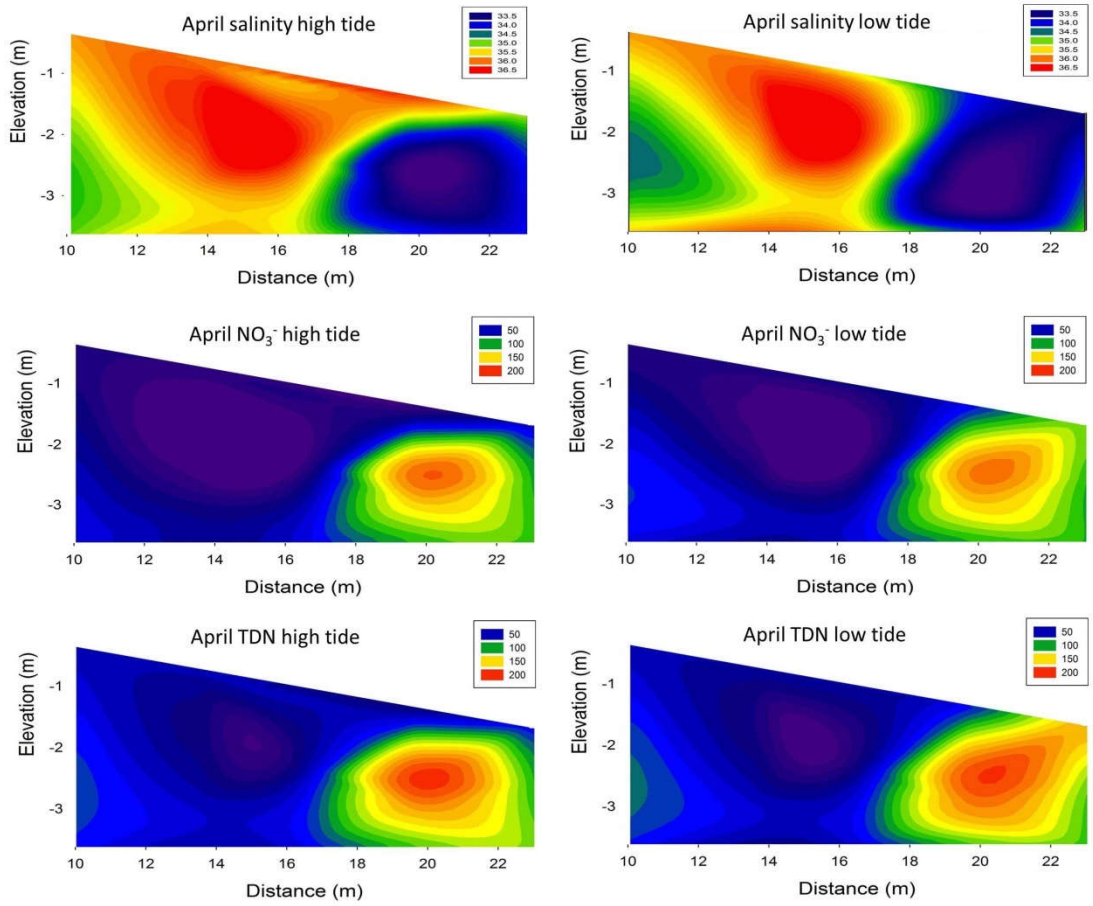

Figure V.10 Salinity, NO_3^- and TDN profiles at high tide and low tide in April, 2011.The units for salinity and N are psu and μM, respectively. The scales among Figure V.9, Figure V.10, and Figure V.11 are different due to large variation of N concentration.

In June (Fig.V.11), porewater salinity in the subterranean estuary was sustained at a level of 36 psu. This suggests that the fraction of terrestrial groundwater in the subterranean estuary had decreased when compared with April. During both high and low tide, salinity at the surface region was comparatively high. Due to the reduced influence of terrestrial groundwater, the concentration of NO_3^- in porewater had

declined. The maximum value was only 5.8 µM. Between high tide and low tide, a small but measurable increase in NO_3^- could be seen. For TDN, concentration fell in the range of 20 µM to 40 µM.

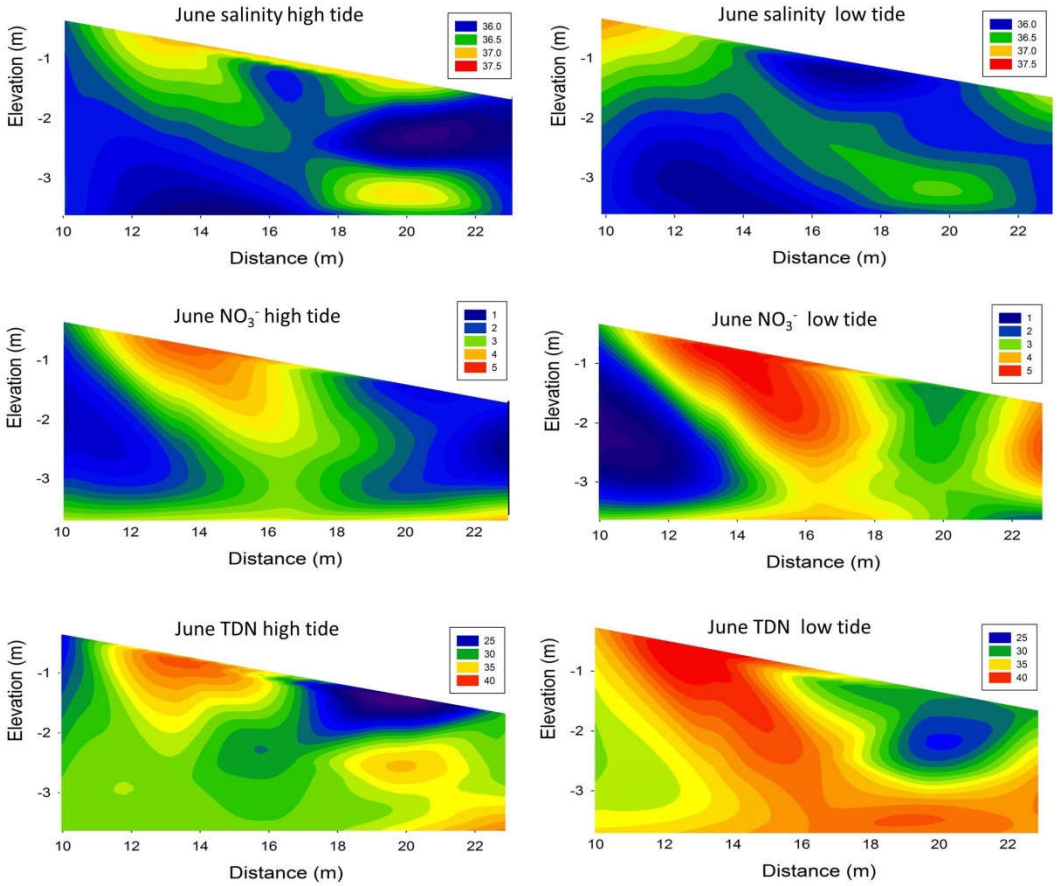

Figure V.11 Salinity, NO_3^- and TDN profiles at high tide and low tide in June, 2011.The units for salinity and N are psu and µM, respectively. The scales among Figure V.9, Figure V.10, and Figure V.11 are different due to large variation of N concentration.

V.5.3 N transformation rate in the subterranean estuary

Based on Eq. (6), N transformation rates within the benthic region were obtained. Due to the limited concentration variation in both NH_4^+ and NO_2^-, N transformation rates were calculated on the basis of change in NO_3^- and TDN levels in the subterranean estuary. Transformation rates derived from the model calculation varied significantly for different months. For simplicity, four typical N transformation patterns in this study site are shown (Fig.V.12). In December and January, the entire beach domain was dominated by the building-up of NO_3^- and TDN. Model-derived NO_3^-

production rates ranged from 0.77 mmol m^{-3} bulk sediment h^{-1} to 2.44 mmol m^{-3} bulk sediment h^{-1}. The accumulation rate for TDN was higher, ranging from 14.96 mmol m^{-3} h^{-1} to 21.49 mmol m^{-3} h^{-1}.

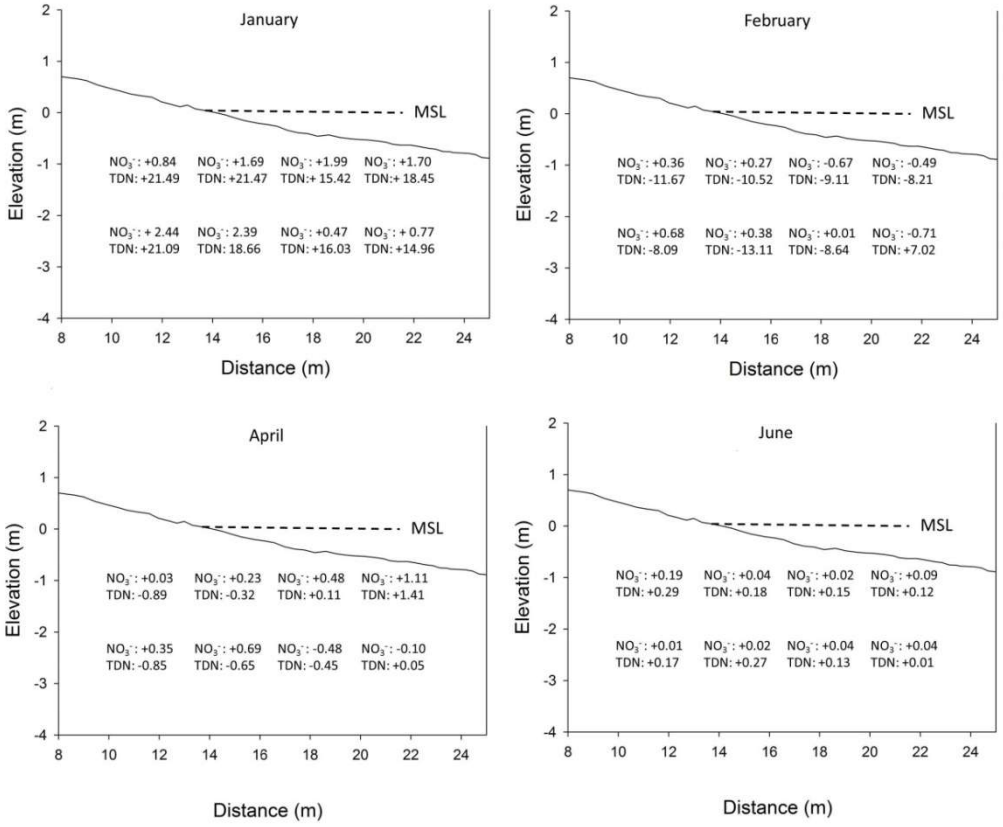

Figure V.12 NO_3^- and TDN reaction rates for each gird for selective months. Positive values represent net accumulation while negative values are net removal. The rate unit is mmol m^{-3} h^{-1}.

In February, transformation of TDN in the subterranean estuary shifted from a net accumulation to net removal. The higher reduction rate was found in the bottom layer, reaching 13.11 mmol m^{-3} h^{-1}, while the lowest removal rate was 7.02 mmol m^{-3} h^{-1}. In contrast, transformations occurring in the majority of benthic regions tended to increase NO_3^- in porewater. The accumulation rates ranged from 0.01 mmol m^{-3} h^{-1} to 0.71 mmol m^{-3} h^{-1}. From March to May, the transformations of NO_3^- and TDN in the benthic region where patchy, with both net increase and decrease trends observed. When compared with reactivity estimated from December to February, N transformations from March to May were depressed. For TDN, the peak reaction rate was only 1.41 mmol m^{-3} h^{-1}. Concurrently, for the reaction rate of NO_3^-, the highest additive rate was 1.11 mmol m^{-3} h^{-1}, while the maximum net removal rate was 0.48

mmol m^{-3} h^{-1}, at the lower limit of the sampling region. In June, the presence of terrestrial groundwater in the subterranean estuary declined sharply. In this scenario, transformation of NO_3^- and TDN was similar to the trends observed in January. The reaction rates in the benthic region reached 0.27 mmol m^{-3} h^{-1} for TDN and 0.19 mmol m^{-3} h^{-1} for NO_3^-.

V.5.4 Dominant N reaction pathway in the subterranean estuary

In Fig.V.13, the dominant reaction pathway in each month was displayed by plotting the production rate of NO_3^- relative to that of TDN, following the method outlined by Hays and Ullman (2007) and Santos et al. (2009). The plot was designed with five potential pathways which are frequently reported and reviewed in subterranean estuaries (Santoro, 2010), including anoxic remineralisation (Anox. Rem.), oxic remineralisation (Ox. Rem.), nitrification (nitrif.), OLAND, and denitrification (Deni).

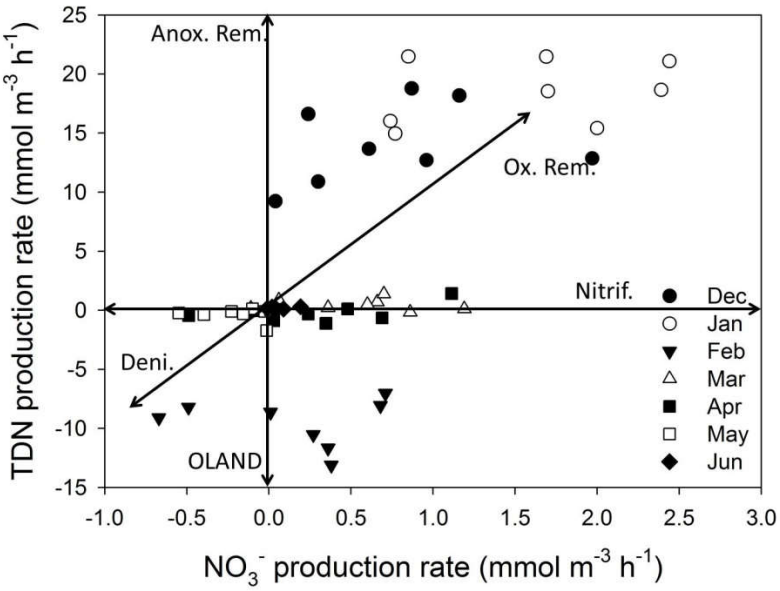

Figure V.13 Systematics of potential reaction pathways in the subterranean estuary on the basis of the systems developed by Hays and Ullman (2007) and Santos et al. (2009).

For December and January, intensive remineralisation and nitrification dominated N circulation in the subterranean estuary. In February, remineralisation was inactive,

the major pathways in the subterranean estuary shifted to OLAND and denitrification. Nitrification was still active in February. From March to May, the subterranean estuary is under balance between denitrification and nitrification. In June, the beach region was re-dominated by mineralisation of pelagic material and nitrification.

V.5.5 N mixing in the subterranean estuary

The distribution of NO_3^- and TDN along salinity gradient was displayed in Fig.V.13. During December to January, the R^2 for NO_3^- derived from regression is 0.83, while the constant dropped to 0.18 for the trend of TDN. From March to June, the regression trend for the NO_3^- mixing host a R^2 value of 0.89. The R^2 for TDN mixing is 0.90.

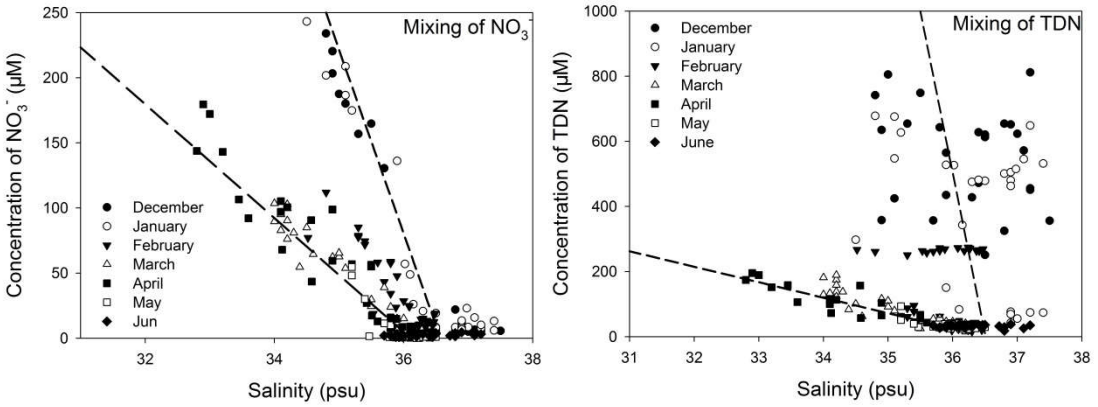

Figure V.14 Distribution of effective concentrations in NO_3^- and TDN along the salinity gradient.

V.6 Discussion

V.6.1 N transformation and controlling factors

The results show that the subterranean estuary is not a passive transport region for dissolved N between land and the sea. Model-derived reaction rates varied temporally. The maximum reaction rates extracted from the model reach the order of 10^1 mmol m^{-3} h^{-1}, suggesting a high reaction potential for this benthic environment. These results were in the order of published kinetics (c.f. Table V.3). In particular, the maximum NO_3^- reduction rate in the study site is consistent with reduction rates

reported by Rocha and Cabral (1998) in exposed intertidal sandy sediment using mass balance approach; nitrification rates are in line with the observation of Santos et al. (2009) in Mexico bay and those reported by Kuwae et al. (2003) for Tokyo bay.

Table V.3 Selected N transformation rates in subterranean estuaries collated from the literature

Site	Sediment	Rate (mmol m^{-3} h^{-1})	Reference
Muri Lagoon (Cook Islands)	Sand	-0.16 (NO_3^-)	Erler et al. 2014a
Gulf of Mexico (U.S.)	Sand	0.33 to 1.52 (NO_3^-) 0.23 to 2.34 (TDN)	Santos et al. 2009
Cape Cod (U.S.)	Sand	-0.09 (NO_3^-)	Kroeger and Chaette 2008
Tokyo Bay (Japan)	Sandflat	-6.6 to 4.8 (NO_3^-)	Kuwae et al. 2003
Key Colony Beach (U.S.)	Sand	-0.08 (NO_3^-)	Griggs et al. 2003
Sado Estuary (Portugal)	Sand	-2.16 (NO_3^-)	Rocha and Cabral 1998
Ria Formosa (Portugal)	Sand	-0.69 to 2.44 (NO_3^-) -13.11 to 21.49(TDN)	This study

Subterranean estuaries represent complex reaction environments for different bacteria. A number of biogeochemical reactions, such as denitrification, nitrification, anaerobic ammonium oxidation (anammox) and oxygen-limited autotrophic nitrification denitrification (OLAND), contribute to the temporary mobilisation/immobilisation and eventually to the permanent attenuation of N moving from land to sea in this permeable environment (Santoro 2010; Ibánhez et al. 2011). Prior studies usually assumed denitrification to be the dominant process contributing to the net attenuation of NO_3^- in these environments, thus benthic systems are widely expected to act as a net sink of reactive N (Herbert 1999; Erler et al. 2014a). Notably, the results presented here show N addition/reduction rates varying significantly on a temporal basis and the subterranean estuary shifting between being a sink and a source of reactive N, potentially indicating a frequent shift in dominance of any single reaction pathway to another in the subterranean estuary.

The variation of N reaction rate in subterranean estuaries usually combines with the shift of dominant reaction pathways. In natural sediment, there are a number of environmental conditions that might lead to the replacement of the dominant N-transformation pathway, including substrate concentrations, temperature and flow rate, among others (Rivett et al. 2008). Among all these factors, the concentration of

substrates is the most important one since each bacterial community only selects those that benefit its particular metabolism (Burgin and Hamilton 2007). Consequently, the observed shift of dominant pathway in the benthic environment reflects primarily a change of substrate input and availability.

At the land-ocean interface, reactants such as organic matter, NO_3^- and NH_4^+ fluctuate significantly due to a change of in the composition of the mixture of seawater and groundwater in porewater, but also in response to seasonal and event-triggered oscillations in the available organic matter in intruding seawater. From December to January, organic matter remineralisation increases the TDN pool in the benthic domain, indicating enhanced amounts of reactive particulate organic matter (POM) in the porewater. Santos et al. (2009) revealed similar trends in the Gulf of Mexico and suggested the increase of TDN results from intrusion of reactive organic particles into the benthos. In the Ria Formosa lagoon, these are mainly derived from algae debris or waste water discharge. On the one hand, these substantial reactive particles may be derived from waste water pipe due to operational mistakes by plant manager (personal communication with Prof. Nicholas Gray in TCD). Alternatively, POM might be the consequence of intensive resuspension of particles lining in the bottom of lagoon due to strong wind during winter season (Newton and Mudge 2003). The remineralisation of organic matter generated abundant NH_4^+ solutes in porewater. Subsequently, NH_4^+ was rapidly oxidised into NO_3^- due to the high concentration of dissolved oxygen (DO) delivered by seawater intrusion. In addition, high levels of the ferric ion (Caetano et al. 1997) in porewater may also act as a strong oxidant to produce NO_3^-. The extremely low concentration of NH_4^+ in porewater is also important evidence to support a drastic alternation from NH_4^+ to NO_3^-.

In February, a decrease of POM in the porewater due to decline of suspended particles in lagoon water led to a sharp decline in remineralisation rates. The subterranean estuary shifted into being a net sink for TDN. From March to May, the level of POM in porewater kept decreasing, and the TDN removal increased, overcoming the TDN production rate. In addition, the difference in concentration

between TDN and NO_3^- during this period decreased, especially in the bottom section of the sampling region, characterized by the presence of larger amounts of NO_3^-. This decrease suggests a decline in concentration of DON. In parallel, nitrification rates dropped since decomposition of DON generates NH_4^+ directly feeding nitrification. As a result, denitrification became the dominant reactive pathway affecting the benthic N pool.

In June, the proportion of terrestrial groundwater in the subterranean estuary decreased significantly. Salinity in the majority of the beach section was above 36 psu. The lack of NO_3^- inputs thereby conditioned the potential denitrification rate. Remineralisation of pelagic material and nitrification evolved into being the dominant reactive pathways affecting the benthic N pool, in similar fashion to the pattern observed in December and January. Notably, December and June were the coldest and hottest months in our survey, respectively; whereas dominant pathways in benthic zones were identical, hence supporting our contention that the supply of substrate is the most important factor influencing N transformation.

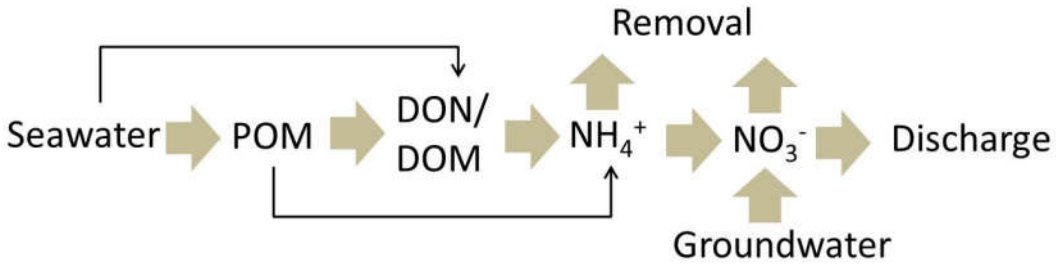

Figure V.15 Benthic reaction chain in the subterranean estuary

To conclude, on the basis of our results the dominant reactive pathway present *in-situ* conditioning the role the subterranean estuary played in N transformation was dependent on the delivery of marine derived POM, DOM and groundwater-borne NO_3^-, as illustrated conceptually in Fig.V.14. Generally, comparatively intensive input of POM leads to an increase in TDN and NO_3^-. Net removal of NO_3^- in the benthic region hence seems to hinge on low levels of POM and DOM and enrichment of NO_3^-.

V.6.2 N concentrations deduction and N modulation capability

Intensive transformation of N confirmed our suggestion that subterranean estuaries are not a 'silent partner' in the modulation of N transport from land to sea. Previously our discussion focused on the N transformation rate at beach scale. To understand the modulation capability for reactive N in the subterranean estuary and the way it might lead to shifts in the magnitude of land-sea N fluxes, I introduced a comparison between 'real' N concentrations and observed N concentrations in groundwater endmember. In particular, the 'real' concentrations are deduced from the regression curves displayed in Fig.V.14.

During December to January, because of intensive NO_3^- generation in porewater, the NO_3^- concentration derived from regression in the fresh endmember was 5.3 mM. Rocha et al. (in press) reported groundwater in the Campina de Faro aquifer system is the fresh source of SGD in this study site. Ferreira et al. (2007) calculated average NO_3^- concentration of 2.1 mM over the entire aquifer. Compared to calculated NO_3^- concentration in December to February, the increase of magnitude of NO_3^- in the subterranean estuary may reach 152%, which is consistent with the maximum addition ratio in Chapter III. It suggests the subterranean estuary will introduce additional NO_3^- into the receiving water. Although this increase trend may be occasional, future coastal management should pay more attention to monitor the reactive organic matter in lagoon water since it links to injection of high concentrations of NO_3^-. Subsequently, it may trigger harmful algae blooms (HABs) and/or 'fish kill' events. The TDN concentration in terrestrial groundwater endmember during this sampling period reached 36.5 mM, which is significantly larger than the maximum TDN concentration (20.3 mM) observed in the field survey from 2011 to 2013; consequently, confirming the strong N-accumulation ability of the subterranean estuary.

From March to June, the NO_3^- concentration in the terrestrial groundwater endmember dropped to 1.6 mM on the basis of regression trend which is in agreement with the relative active NO_3^- reduction determined in these grids with enrichment of

NO_3^-. Compared with the average concentration of fresh groundwater in the aquifer, the subterranean estuary effectively reduced 22% of groundwater-borne NO_3^-. This reduction capability is in line with the global reducing range of NO_3^- reduction in subterranean estuaries outlined in Chapter III, as well as the assumption (20% to 40%) made by Beusen et al. (2013). In this circumstance, the subterranean estuary served as important barrier to protect nutrient balance in the receiving water. In light of the reaction capability for TDN, the TDN concentration in the terrestrial groundwater endmember decreased to 1.8 mM, which is only 5% (1.8/36.5) of TDN solute observed during December to January.

V.7 Concluding remarks

The intensive and spatially distributed measurements in the subterranean estuary conducted on a barrier island of the Ria Formosa lagoon revealed sediment activity in processing N. Different injection scenarios of labile organic matter and NO_3^- may create significant variations in N transformation rates and pathways. Generally, the coexistence of nitrification and remineralisation significantly increase concentrations of NO_3^- and TDN in porewater, which defines the subterranean estuary as a source of reactive N. In contrast, denitrification and OLAND pathways continuously removed N from sediment which prevent the accumulation of N in lagoon waters. These observations validated that the subterranean estuary is highly active in N processing. For the N budget estimation, influence from subterranean estuaries is highly necessary to be considered in coastal management strategies.

Chapter VI

Influence of labile dissolved organic matter (DOM) on nitrate reduction in aerobic subterranean estuaries

VI.1 Abstract

The lack of significant amount of labile dissolved organic matter (DOM) is usually assumed to be a major factor constraining NO_3^- removal in coastal sediments. To determine the influence of DOM on benthic nitrate (NO_3^-) reduction in aerobic subterranean estuaries, a series of Flow-Through Reactor (FTR) experiments were conducted under controlled environmental conditions. Experimental results revealed that the addition of labile DOM to porewater does not trigger significant enhancement in NO_3^- reduction capability. Alternatively, the intensity of aerobic respiration was boosted from 50 μmol dm^{-3} h^{-1} to 90 μmol dm^{-3} h^{-1} under glucose amendments, accounting for approximately 70% consumption of the labile DOM pool in porewater. This rapid consumption may hamper the combination of NO_3^- reducing capability of the sediment. Combined with analysis of Chromophoric Dissolved Organic Matter (CDOM), it can be inferred that NO_3^- reducers tended to utilise sediment organic matter as a supplier of reactive carbon. As a result, enrichment of DOM in oxic subterranean estuaries may only benefit aerobic remineralisation and potentially subsequent nitrification, thus promoting the increase of ensuing NO_3^- fluxes to adjacent coastal areas.

List of abbreviations

K_{red1}	Maxmium NO_3^- reduction rate (µmol h^{-1})
$K_{halfnitrite}$	Half − saturation NO_3^- reduction constant (µmol)
K_{red2}	Maxmium NO_2^- reduction rate (µmol h^{-1})
$K_{halfnitrite}$	Half − saturation NO_2^- reduction constant (µmol)
K_{com}	Maxmium DOC consumation rate (µmol h^{-1})
$K_{halfDOC}$	Half − saturation DOC consumtion constant (µmol)
K_{ads}	Rate constant of first order glucose adsorption (h^{-1})
$[Glu]_{eq}$	Total glucose adsobed at the equilibrium in the reactor (µmol)
$[Glu]_{ads}$	Total glucose adsobed in the reactor (µmol)

VI.2 Introduction

Human activities have significantly increased NO_3^- concentration in coastal waters (Slomp and Van Cappellen 2004; Beusen et al. 2013), promoting eutrophication, harmful algal blooms (HABs), the accumulation of organic matter, and subsequent enhancement of oxygen consumption. As a consequence, a progressive reduction in water quality coupled with loss of biodiversity has been observed worldwide (Falkowski 1997; Rabouille et al. 2001; Smith 2003; Rabalais et al. 2009).

Globally, NO_3^- loading into coastal waters was thought to occur mainly through terrestrial surface runoff and atmospheric deposition (Smith and Atkinson 1994). Following extensive investigations, evidence now suggests Submarine Groundwater Discharge (SGD) can be another important source of NO_3^- input to coastal zones, especially when originating from NO_3^- contaminated continental aquifers (Cable et al. 1997; Ullman et al. 2003; Leote et al. 2008; Santos et al. 2011; Tait et al. 2014; Rocha et

al. 2015). On a global scale, SGD pathway is deemed to be responsible for 33.5 Tg NO_3^--N per year (Chapter III). To prevent further deterioration of coastal ecosystems and in anticipation of the negative effects of global climate change on the N cascade, control over the magnitude of NO_3^- fluxes derived from SGD pathway is an important focus activity of the scientific community (Slomp and Van Cappellen 2004)

SGD is 'any and all flow of water on continental margins from the seabed to the coastal ocean, regardless of the fluid composition or driving force'. It includes distinct processes, one recycling seawater mainly through tidal pumping (Li et al. 1999) and the other introducing fresh groundwater (Taniguchi and Iwakawa 2004). Generally, the NO_3^- concentration in seepage originating from these two processes is significantly different. Due to the percolation of chemical fertilisers and leakage from poorly insulated septic tanks (Chapter I), the level of NO_3^- in groundwater can be several orders of magnitude higher than that of seawater (Moore 1999). Consequently, understanding the processes that are conducive to mitigation of terrestrial groundwater-borne NO_3^- before it discharges into the sea becomes an important research objective in understanding processes that regulate of SGD-borne NO_3^- fluxes into coastal areas.

Prior to discharge, terrestrial groundwater enriched with NO_3^- is intercepted by a mixing region at the littoral zone, dubbed the subterranean estuary (Moore, 1999). Here, the salinity gradient established within the aquifer significantly influences the distribution of important physical and chemical properties, such as redox potential or pH, the concentrations of reactive solutes like dissolved oxygen (DO) and DOM, and strongly determines the activity coefficients of solutes driven by ionic strength gradients (Charette and Sholkovitz 2006). As a result, subterranean estuaries are an active natural bioreactor hosting a wide spectrum of biogeochemical transformations (Rocha 2008; Erler et al. 2014a).

Previous studies assumed the lack of significant labile DOM to be a major limiting factor of NO_3^- reduction in aquifers (Bradley et al. 1992; Rivett et al. 2008). In subterranean estuaries, seawater penetrates into the sediment during flooding and pore water drains out during ebbing (Wilson and Gardner 2006). Hence, there is a continuous supply of reactive organic substrates, such as pelagic DOM, to the sediment (Santos et al. 2009). Benthic microorganisms degrade DOM and this process is coupled with the reduction of electron acceptors. In particular, the possible combination between DOM and terraneous NO_3^- in this benthic environment may effectively reduce the concentration of NO_3^- in SGD. In the intertidal zone, wave set-up and tide-driven advective pore water circulation also results in the infiltration of oxygenated seawater into sediment and the replacement of oxygen depleted pore water (Charbonnier et al. 2012; Reckhard et al. 2015). Therefore, oxygen is frequently replenished in the sediment (Anschutz et al. 2009). As a strong oxidiser (Rivett et al., 2008), DO may preferentially be consumed in the mineralisation of DOM via aerobic respiration, suggesting that the enrichment of DOM in porewater cannot benefit NO_3^- reduction. However, prior studies in NO_3^- circulation and turnover in subterranean estuaries mainly focused on the determination of transformation rates and pathways (e.g. Santoro et al. 2006; Rocha et al. 2009; Ibánhez et al. 2011; Erler et al. 2014b; Reckhard et al. 2015). Much less attention has been paid to determining whether and to what extent DOM in subterranean estuaries might be involved into NO_3^- reduction, though it can be a key process to regulate SGD-borne NO_3^-.

In the current study, the temporal change of NO_3^- concentrations in permeable sandy sediment from the Ria Formosa lagoon, with different level labile DOM availability (controlled by glucose amendments) was studied. To investigate this, Flow-Through Reactor (FTR) experiments and kinetic modelling of the resulting distribution of NO_3^-, DOM and DO in porewater were carried out. The main objective was to evaluate links between the availability of labile DOM and the magnitude of NO_3^- reduction in aerobic subterranean estuaries and to elaborate on possible explanations

for this linkage. The knowledge gained in this research helps to improve the understanding of NO_3^- removal and the nature of NO_3^- balance in subterranean estuaries, which facilitate coastal management in constraining SGD derived NO_3^- fluxes.

VI.3 Study site

The Ria Formosa lagoon is located in the south of Portugal (Fig.VI.1), extending from 36°58'N 8°20'W to 37°30'N 7°32'W, covering the majority of the Algarve coastal area (Andrade et al. 2004). It is a shallow coastal system separated from the Atlantic Ocean by a chain of five barrier islands and two peninsulas with six inlets for the sea water and lagoon water exchange (Salles 2001; Pacheco et al. 2007). It has approximately 170 km^2 coastal area with 55 km length and 2 m average depth (Andrade et al. 2004; Ibánhez et al. 2011).

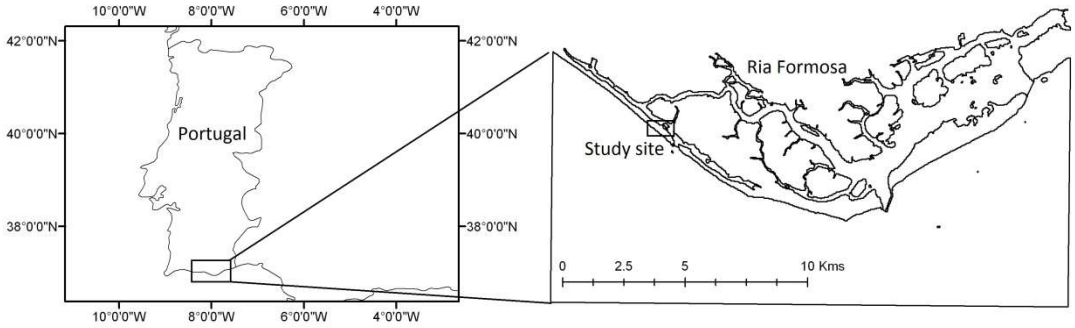

Figure VI.1 Map of sediment collection location, at the Ancão Peninsula (Ria Formosa coastal lagoon, SW Iberian peninsula).

The sampling site is located at beach on the Ancão peninsula, with a distance of 1.5 km (southeast) to the bridge of 'ilha de Faro'. The collection point was located on the inner side of the peninsula, facing towards the major water channel leading to Faro. The sandy beach comprises median size quartz particles (d_{50}: 0.44 mm) and hydraulic conductivity can reach 5.5×10^{-3} cm s^{-1} (Rocha et al. 2009). NO_3^- in the study site is derived from terrestrial groundwater at adjacent coastal aquifers (Rocha et al. 2009). The study site hosted substantial groundwater-borne NO_3^-. The maximum

concentration of NO_3^- in porewater at the sampling site between 2010 and 2013 was approximately 400 µM.

VI.4 Material and methods

V.4.1 FTR experiments

The FTR experiments were conducted on sediment collected from the permanently saturated beach which was influenced by periodic NO_3^--enriched SGD. The surface 5 cm of sediment was removed before collection due to enrichment of debris of shellfish. Undisturbed and saturated sediment cores (15 cm length, 6.6 cm inner diameter), near the maximum discharge line at the intertidal seepage face, were collected with polycarbonate sediment corers. The sediment was gathered manually. In practice, the core liners were pushed into the sediment at low tide. Subsequently, they were dug out and frozen in the laboratory immediately. An adapted core slicer (Renberg and Hansson 2008) was used to transfer selected sediment slices from sediment cores into Teflon FTR cells, which was designed by Ibánhez and Rocha (2014a). The components in each reactor are displayed in Fig.VI.2. To guarantee minimum build-up of preferential flow paths in the sediment cells, a collimator system (collimator and GF/F filter, Whatman®) was designed, which covers the cross-section of reactors at input and output endmembers. The GF/F filter papers in the collimator system also reduced bacteria amounts in the reaction solution preserved in the flasks. All the FTR cells with test sediment were translocated into an incubator at a constant temperature of 20°C. Before each experiment, the sediment inside the reactors was flushed with filtered seawater for 24 hours to acclimatise the saline environment. During the incubation, both the flow-reaction solutions and the reactor itself were covered with tin-foil to reproduce the absence of light in subterranean estuaries.

A sequence of different experiments, carried out in triplicate (Table VI.1), was

performed with different concentrations of NO_3^- and labile DOM (glucose in this case due to lability in biogeochemical reaction). In order to guarantee reliability of incubation experiment, three times experimental runs were performed for each group, which generated nine replicates of results per treatment in total.

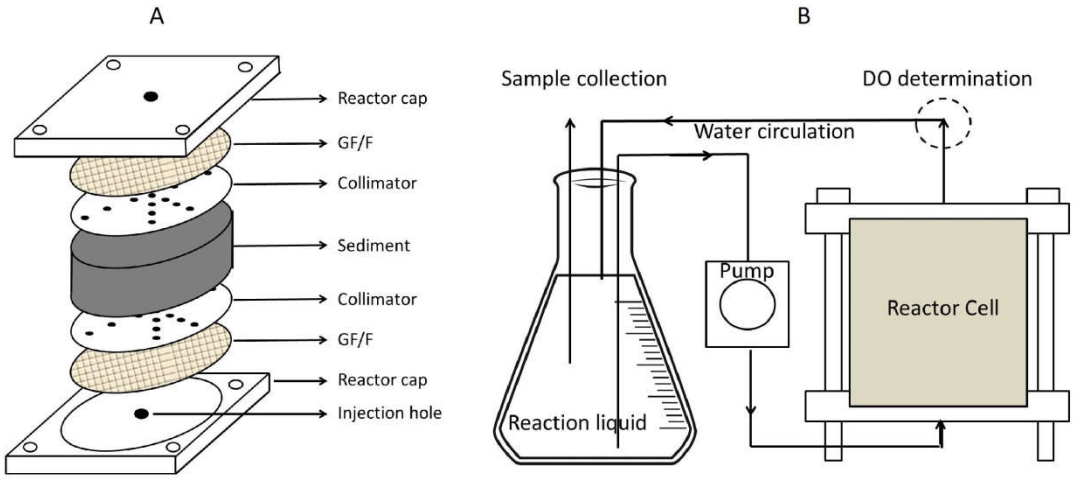

Figure VI.2 Schematic view of the experimental set-up: A. Detailed reactor design. B. Flow-Through Reactor experimental setup. Figure is based on Ibánhez and Rocha (2014a)

Subterranean estuaries are considered, at their outer rim, generally aerobic environments since infiltration of seawater promoted by tidal oscillation introduces high concentrations of DO (Santos et al. 2009). Furthermore, solute exchange between the sediment and atmosphere (Whalen 2005) also imports oxygen into subterranean estuaries. Therefore, experimental reaction solutions were kept saturated in DO to reproduce aerobic environments in subterranean estuaries while running the FTR experiments. DO concentration in the effluent (Fig.VI.2) was measured by with an OxiCal® probe under the salinity calibration module. A single run for FTR experiments was performed for a period of 48 hours. Samples (20 ml) were taken from the reservoir into pre-combusted glass bottles at constant time intervals and stored at −20°C until analysis. To keep the volume constant during incubation, identical volumes of the original solution were added to the reservoir after each collection.

Table VI.1 List of relevant environmental and porewater conditions characterising each of the FTR experiments discussed in this study. The abbreviation Exp. indicates experiment. This was used for the following figures and tables.

Experiment	NH_4^+ (µM)	NO_3^- (µM)	DOC (µM)	Treatment
Exp.1	2.1±0.2	2.5±0.2	218.1±5.4	Control
Exp.2	1.9±0.1	15.1±0.2	213.4±4.3	Low N, low DOM
Exp.3	2.2±0.1	15.1±0.2	990.1±9.7	Low N, high DOM
Exp.4	1.7±0.2	75.2±1.2	217.2±3.9	High N, low DOM
Exp.5	1.8±0.1	75.8±1.3	995.1±8.9	High N, high DOM

Filtered seawater was used as a carrier during all the experiments. The background concentrations of NH_4^+ and NO_3^- in seawater were 2.1±0.2 µM and 2.5±0.2 µM, respectively. Salinity was 36.2 psu. For different treatments, the seawater was amended with AccuStandard® NO_3^- standard stock and Anala R® glucose. The maximum NO_3^- concentration was 75.8 µM. DOC concentration after amendment by glucose reached 995.1±8.9 µM, i.e., an enhancement of 780 µM.

The reaction solution was pumped from the bottom of the reactor cell toward the top (arrow in Fig.VI.2), thus simulating the approximate one-dimensional advection flow in seepage faces, the region with the most active biogeochemical reactions in subterranean estuaries (Ibánhez et al. 2013; Ibánhez and Rocha 2014). The selected porewater velocity in my stimulation experiments was 10.5±0.5 cm h^{-1}, which fell in the range of the local advective porewater flow rate measured during active seepage at the study site (Rocha et al. 2009). Porewater flow rate and temperature were kept stable during both the acclimation period and the experimental runs.

VI.4.2 Determination of sediment parameters

The collected sediment was composed mainly of medium-coarse sand. Sediment was dried in an oven at 105°C until reaching a constant weight. The water content was then calculated as a ratio between the weight loss and original weight (Ibánhez and Rocha 2014b). Since the sediment was saturated, porosity can be estimated using the

following equation:

$$\theta = \frac{V_{pw}}{V_{sand}+V_{pw}} \quad (1)$$

where V_{pw} is the volume of porewater, V_{sand} is the volume of sediment, and V_{pw} is calculated on the basis of mass difference between the wet and dry sediment divided by the density of freshwater.

Total organic matter was determined by the loss on ignition method in a muffle furnace at 450°C for 4 hours, and subsequently the temperature was elevated to 1000°C for determination of the total carbonate content (Dean Jr 1974). The total organic carbon (TOC) content and total organic nitrogen (TON) for each sediment sample were analysed by combustion in a Vario EL® Cube elemental analyser after removal of inorganic component from sediment samples by acid (36.5% HCl) fumigation (Harris et al. 2001).

VI.4.3 Porewater analysis

The concentration of NO_3^-, NO_2^- and NH_4^+ in all water samples was determined with a Lachat Quickchem 8500 Flow Injection Analysis system following standard colorimetric methods (Grasshoff et al. 2009). The concentration of DOC was determined with a Vario TOC Cube elemental analyser, after acidification (2 M HCl) and purging (carbon free gas) to remove the dissolved inorganic components.

VI.4.4 Excitation-emission-matrix (EEM) fluorescence and parallel factor (PARAFAC) analysis

Three-dimensional EEM spectra of CDOM in samples derived from the FTR experiments were measured on a Cary Varian Eclipse® spectrofluorometer. Prior to

scanning, all the tested samples were immerged in a water bath at 20°C to avoid fluctuations in spectral intensities resulting from temperature variations. Bandwidths I selected in the process were constant, 10 nm for emission and 5 nm for excitation. Emission and excitation wavelengths fell in the range of 280 to 560 nm (2-nm interval) and 220 to 440 nm (5-nm interval), respectively. To avoid inner filter effects in the determinations, samples with absorbance higher than 0.08 measured at 350 nm were diluted accordingly (Guo et al. 2010). Millipore water was used as blanks. The values derived from blanks were subtracted from the sample spectra to remove influences from Raman scatter peaks (Ibánhez and Rocha 2014a). The area of Millipore water of Raman peaks was integrated together in the method in order to calibrate method for eventual instrument-dependent random errors (Lawaetz and Stedmon 2009). Subsequently, the first and second order Rayleigh scatter peaks was corrected and the PARAFAC analysis of samples was completed using the DOM Fluor Toolbox in MATLAB (Stedmon and Bro 2008).

This procedure decomposed the complex determined spectra from EEM scanning into several fluorescence fluorophores. It also permits quantification of scores established in the calculation process for each fluorophore present in the database. The signal intensity for each component is directly proportional to the concentration (Ibánhez and Rocha 2014a). Additionally, in my experiment, the PARAFAC analysis was conducted over all water samples from the entire incubation experiment to guarantee a large database. Split-half validation was used to check the correctness.

VI.4.5 Glucose adsorption

In order to minimise the influence of adsorption of glucose onto sediment (Henrichs and Sugai 1993) on the apparent total consumption rates observed during the experimental runs, sediment incubations in filtered seawater amended with different glucose concentrations were performed. Due to the influence of

mineralisation in sediment to determination of adsorption amount, test sediment and seawater were autoclaved for 30 minutes at 120°C to repress bacterial activity (Jiang et al. 2008). Subsequently, known quantities of sediment (4-5 g) were incubated for 4 hours at 20°C with 15 ml different level glucose solutions. On completion of the 4-hour period, seawater solution solutions were filtered and glucose adsorbed onto the sediment surface was then extracted with 20 ml 2M KCl solution (Corre et al. 2002). The entire procedure was performed in triplicate.

The amount of extracted DOC from KCl solution and weights of sediment represent original sorption amount (in Fig.VI.3). The results in Fig.VI.3 suggest a clear increasing trend of original sorption amount when glucose concentration ranges from 0 to 750 µM. For the solution with 1000 µM glucose, adsorption amount on surface of sediment became stable, which indicates adsorption reached a state of equilibrium. Since KCl solution can extract all loosely bonded organic matter from sediment surfaces (Erler et al. 2014b), sorption dynamics of glucose on sediment needed to be adjusted by subtracting amount at glucose free solution. Afterwards, the adsorbed glucose amount in different concentrations was linked by an exponential curve (Fig.VI.3). To include the heterogeneous equilibrium between the glucose in solution and that adsorbed onto the sediment surface in the modelling procedure, adsorption amount was scaled to the reactor size. For this purpose, it was corrected by:

$$[Glu]_{eq} = S\ \rho\ V_{reactor} \tag{7}$$

where S is the sediment adsorption amount, ρ is the sediment density (2.65 g L^{-1}), $V_{reactor}$ is the volume of the reactor, and $[Glu]_{eq}$ is total adsorbed glucose on sediment. In the simulation of adsorption, we assumed the decrease of DOC concentration in the first 4 hours is mainly the consumption of glucose due to high reactivity for benthic bacterial community.

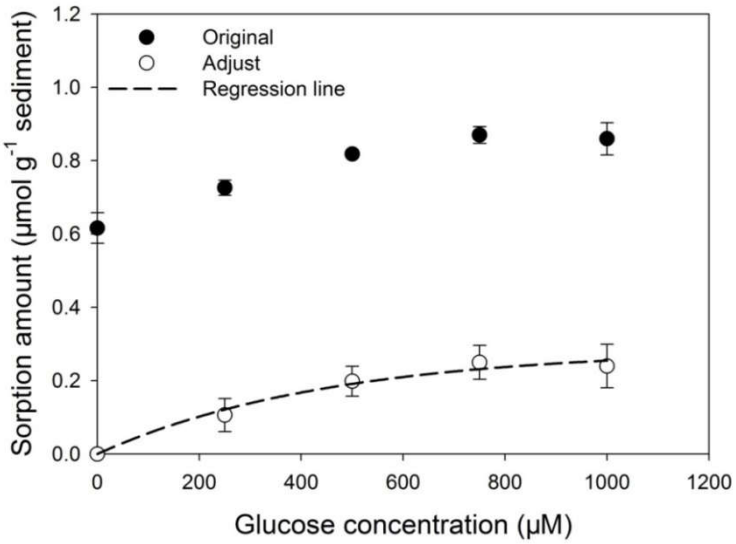

Figure VI.3 Glucose adsorption isotherm at 20°C characteristic of the sediment. The concentration range for underpinning the curve is 0 to 1000 µM. The regression expression is $\mathbf{y = 0.29 \times (1 - e^{-2.20 \times 10^{-3} x})}$, where y is sorption amount and x is glucose concentration. Data are means ± standard deviations of three replicates.

VI.4.6 Kinetics modelling

The sediment FTR experiments were highly depending on the biogeochemical reactivity of certain solute and the circulation rate of the fluid in FTR cells (e.g. Ibánhez and Rocha 2014a). The fluid residence time is a product of reactor volume and the fluid velocity. It is needed to large enough to distinguish the difference of the reactant in the solution between the input and the output endmembers within the FTR. Previous research evidenced rapid changes of DO concentration within permeable sediments. For instance, Erler et al. (2014b) showed a significant decrease of DO within the upper 10 cm of sediment during an incubation experiment. Therefore, in this study, the consumption rate of DO can be determined by the concentration difference between reactor input and output from the reactor (Fig.VI.2). The acquired rate is assumed to be the intensity of aerobic respiration in the tested sediment. However, in highly permeable sediment, it is difficult to conduct an identical measurement to quantify the change of NO_3^- concentration, because the residence time is short for advection and the reaction potential of N is relatively low (Ibánhez 2012). Furthermore,

there are several N reaction pathways in the sediment, which may largely influence the NO_3^- processing within the sediment, especially in the steady state due to the rapid increase of biomass. As a consequence, I used a recirculation mode to determine NO_3^- reaction rate within the sediment cell (Fig.VI.2). In particular, the outflow stream flowed back to the 1 litre container after passing through the reactors. Sediment reactivity was defined by calculating the temporal change of N concentration in the plastic container.

Assuming that microbial biomass or solute were distributed evenly in the reaction cell, FTR experiments embodied in the research under the porewater recirculation can be treated as a well-mixed reactor (Levenspiel 1999). As a direct result, the potential of microbe-mediated process under the stable state can be calculated as the difference of the solute concentration between the input and the output:

$$R = \frac{\Delta C \times Q}{V} \quad (2)$$

where R is the reaction rate, ΔC is the change in the concentration of the solute between the input and the output endmembers, Q is the flow rate and V is the reactor volume. Compared with sediment, the reactivity in the solution is limited due to fewer microbial amounts. Consequently, the time to reach a steady state in the reactor should be smaller than the temporal scale of changes within the reservoir. In addition, the water volume in the reservoir was constant by adding solutions. As a result, reaction rates derived from the concentrations changes can be assumed to be products of the sediment reactivity.

To understand the NO_3^- behaviour within the cells and to determine detailed reaction rate for difference pathways, kinetic models are necessary. They were computed on the basis of the non-linear Monod equation (Monod, 2012). The NO_3^- reduction was simulated by a two-step process, including the NO_3^- reduction to NO_2^-

and subsequent NO_2^- reduction. Considering the variations of DOC concentration, first order DOC consumption kinetics was designed to describe decreasing trend in DOC concentration. For adsorption of glucose, it can be described by the Langmuir pseudo first order rate equation. The adsorption equilibrium was believed to be a period of 2 hours (K_{ads}=0.5 h^{-1}), which is consistent with the adsorption dynamics of NH_4^+ (Ibánhez 2012) and soluble phosphate (Jiang et al. 2008).

(3) NO_3^- reduction to NO_2^- $$\frac{d[NO_3^-]}{dt} = -K_{red1}\frac{[NO_3^-]}{K_{half} + [NO_3^-]}$$

(4) NO_2^- reduciotn N_2 $$\frac{d[NO_2^-]}{dt} = -K_{red2}\frac{[NO_2^-]}{K_{halfnitrite} + [NO_2^-]}$$

(5) Comsumation of DOC $$\frac{d[DOC]}{dt} = -K_{com}\frac{[DOC]}{K_{halfDOC} + [DOC]}$$

(6) Adsorption of glucose $$\frac{d[Glu]}{dt} = -K_{ads}([Glu]_{eq} - [Glu]_{ads})$$

This system of first-order ordinary differential equations was solved numerically using MATLAB®. The time step in the simulation was set to be 20 minutes. A fitting procedure was performed on the basis of minimising the total standard deviation (e.g. Ibánhez et al. 2011).

VI.5 Results

VI.5.1 Ancillary parameters

The highly permeable sediment at the sampling site was composed mainly of medium-coarse sand (average grain size 0.5 mm; silt + clay $<$ 1.7% weight; Rocha et al. 2009). Porosity of the collected sediment was 0.35±0.02. The relative percentage of organic matter in sediment fell into the range between 0.38% and 0.41% by weight, whereas the TOC content was approximately 0.038%. The inorganic content of

sediment was 11.2% in total weight of sediment. The results confirmed that standing stocks of organic matter were low within the sediment at the subterranean estuary. The mean residence of porewater in the reactor was 21 minutes.

VI.5.2 Variations of N concentrations and DO

Variations of N solutes and DO concentrations show distinct trends in different experiments (Table VI. 1), as illustrated in Fig.VI.4. In Exp.1, the level of NO_3^- slightly increased at the beginning of stage of incubation, reaching approximately 5 μM. Afterwards, it declined to the background level found in seawater, approximately 2 μM. In Exp.2 and Exp.3, concentration of NO_3^- was elevated to 15 μM. Circulation within sediment produced exponential decline in concentrations of NO_3^- in water samples. After 12 hours reaction, all additive NO_3^- was reduced, and the concentration of NO_3^- in the solution dropped back to 2 μM. In the high level NO_3^- experiments, a similar decreasing trend was observed, whereas the total reduction procedure in sediment was prolonged to more than 36 hours. Modelled temporal distribution of the NO_3^- suggests reduction rates obtained from experiments varied from 1.8±0.2 μmol dm^{-3} sediment h^{-1} to 3.5±0.2 μmol dm^{-3} h^{-1} among Exp.2 and Exp.3 within first 8 hours (Table VI.2). In the high level NO_3^- treatments, reduction rates significantly increased, peaking at 7.1±0.3 μmol dm^{-3} h^{-1}.

In the low concentration NO_3^- treatment, amended groups showed increased mean sediment reduction rates from 3.5 μmol dm^{-3} h^{-1} to 3.6 μmol dm^{-3} h^{-1}; however, student t-test suggests this difference in reduction ability during this time period between two treatments is not significant. Moreover, from 4 hours to 8 hours, mean reaction rates between the two treatments dropped to similar levels, which confirms that the trend observed in the first 4 hours was insignificant. When NO_3^- concentration in porewater was elevated to approximately 80 μM (Exp.4 and Exp.5), the stimulation effect from glucose was still weak. In particular, the maximum difference in reduction

rate only reached 0.4 μmol dm^{-3} h^{-1} (4-hour time point), an approximately 6% increase in activity. T-test analysis suggests insignificant difference of NO_3^- reduction (4-hour). For the period between 4-hour to 8-hour and 8-hour to 12-hour, t-test also confirms insignificant difference between glucose treatment group and non-additive group. Therefore, enhancement of DOM in porewater, even glucose, one of the most labile DOM, cannot significantly enhance NO_3^- reduction capability in subterranean estuaries.

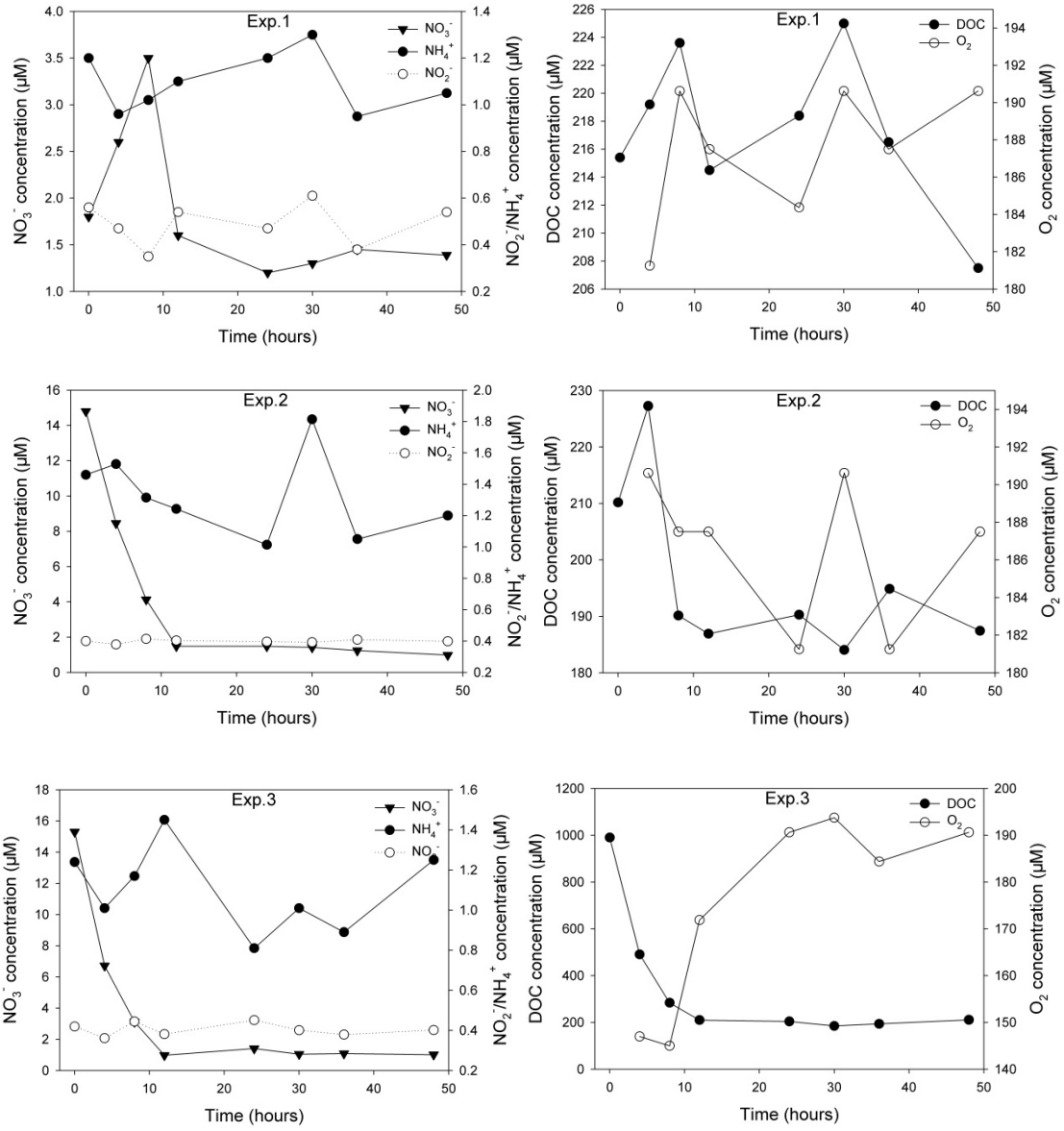

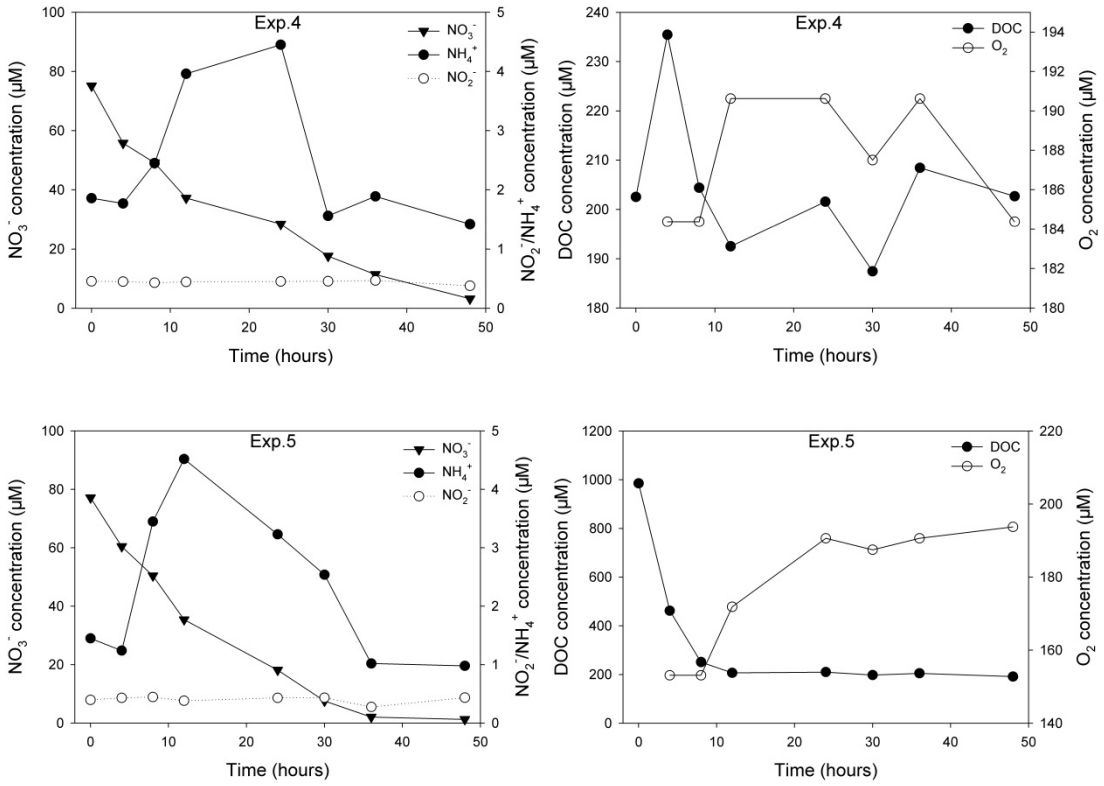

Figure VI.4 Time series of concentrations for different N species (NO_3^-, NO_2^- and NH_4^+), DOC in water samples, and concentration of DO in effluent. In the figure, Exp. stands for experiment, as described in Table VI.1

In light of concentration variations for NH_4^+ and NO_2^-, NH_4^+ concentrations exhibited a small increase at the beginning of incubation for NO_3^- addition experiment, as Fig.VI.4 shows. The peak values varied from 3.7 μM to 6.2 μM. For concentration of NO_2^-, a random fluctuation trend was observed during 48 hours incubation, varying from 0.28 μM to 0.48 μM. This is probably a manifestation of the instant nature of the reduction of NO_2^- to N_2 and hence that the transformation of NO_3^- to NO_2^- is the rate-limiting step (Wada et al. 1975).

Concentrations of DO in effluent were stable in Exp.1, Exp.2 and Exp.4, randomly fluctuating between 180 uM and 192 uM (Fig.VI.4). On the basis of Eq. (1), DO consumption rates (in Table VI.2) in glucose free treatments fell in to the range from 42.7±2.2 to 52.6±2.7 μmol dm^{-3} bulk sediment h^{-1}. In Exp.3 and Exp.5, the addition of glucose significantly decreased concentration of DO in the effluent. Specifically, at the

4 and 8-hour time points, DO concentrations were determined in the range between 140 to 160 µM. Correspondingly, a high consumption rate of 90.7 µmol dm^{-3} h^{-1} was reached. After 12 hours, DO concentration increased to the original level of 180 µM.

Table VI.2 Results obtained from the model calculation of FTR Exp.2 to Exp.5, including consummation rates of O_2 and DOC, as well as NO_3^- reduction rate in distinct time points along incubation time line. The DOC consumption rates were determined in glucose addition groups (Exp.3 and Exp.5). The unit for all the rates in table is µmol dm^{-3} sediment h^{-1}. Detailed test information can be seen in Table VI.1

Time	Exp.2 & Exp.3			Exp.4 & Exp.5		
	R_{O2}	R_{NO3-}	R_{DOC}	R_{O2}	R_{NO3-}	R_{DOC}
4 h	47.1±2.2/88.6±2.2	3.5±0.2/3.6±0.2	132.5±6.4	48.2±2.9/82.2±2.6	6.8±0.3/7.1±0.3	138.7±6.6
8 h	50.4±2.8/90.7±2.5	1.8±0.2/1.8±0.2	113.6±5.2	43.8±2.1/84.4±2.8	6.4±0.3/6.6±0.3	114.0±5.9
12 h	50.4±2.6/62.5±2.7	--------	---------	48.7±2.6/70.1±2.2	6.0±0.3/6.2±0.3	--------
24 h	52.6±2.7/49.3±2.7	--------	---------	47.7±2.8/44.9±2.8	4.0±0.3/3.9±0.2	--------
30 h	49.3±1.6/46.1±2.4	--------	---------	44.9±2.0/48.2±2.8	2.8±0.2/2.5±0.2	--------
36 h	51.5±2.3/50.4±1.9	--------	---------	46.1±2.3/47.1±2.1	1.5±0.2/1.3±0.2	--------
48 h	49.3±2.7/47.2±1.6	--------	---------	44.9±2.8/47.1±2.3	--------	--------

VI.5.3 Change of organic matter in porewater

Concentrations of DOC in experiments run without the addition of glucose (Exp.1, Exp.2 and Exp.4) tended to randomly oscillate around 200 µM during the observation period. For glucose addition treatments, concentrations of DOC in water samples exhibited a significantly decline, from 1000 uM to 200 µM. The associated DOC consumption rate at the 4-hour time point was 132.5±6.4 µmol dm^{-3} h^{-1} in Exp.3. In Exp.5, consumption rate slightly increased, reaching 138.7±6.6 µmol dm^{-3} h^{-1}. As time increased, consumption of labile organic carbon sharply declined. After 12 hours, concentration of DOC decreased to the background level; subsequently the net consumption rate of DOC in the tested solution was negligible.

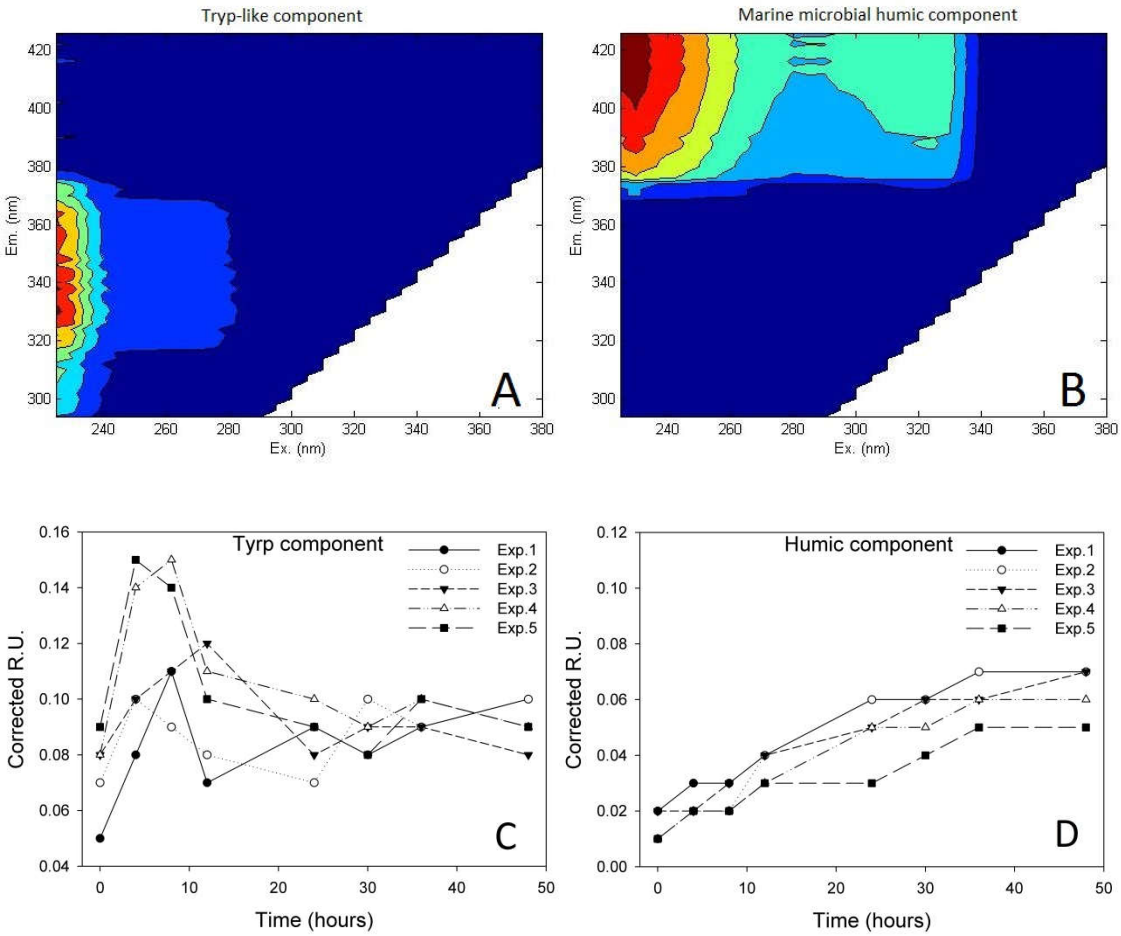

Figure VI.5 Figure A is the Tryp-like component, while figure B is Marine microbial humic component. The C and D exhibit time series of change of two components in water samples during different incubation experiments.

For components of CDOM in water samples, two determinable CDOM components were identified from PARAFAC analysis. The first is Tryptophane-like (Amino acid free or bound in proteins, Coble 1996). It shows Ex/Em peak at approximately 230 nm and 340 nm, respectively. The other is marine microbial humic-like material with approximately 235 nm/420 nm characteristic peaks (Ibánhez and Rocha 2014b). In all the FTR experiments, the relative concentrations of Tryptophane-like organic matter showed a comparatively stable trend during 48-hour incubation. It fluctuated between 0.05 R.U. to 0.15 R.U. For marine humic matter, a distinctive increase was witnessed in all treatments. Specifically, the relative concentration of humic material at initial seawater was 0.01 R.U. At the end of experiment, it increased to a range between 0.04 R.U. and 0.07 R.U. as shown in

Fig.VI.5. Similar with glucose, relative concentration of Tryptophane in porewater showed similar fluctuations between experiments with different treatment of NO_3^-, suggesting activity of NO_3^- reducers is also irrelevant with natural labile DOM in porewater. Even in high concentration experiments NO_3^- reduction was active and organic matter was highly demanded.

VI.6 Discussion

VI.6.1 Response of NO_3^- reduction to labile DOM

Lack of significant amounts of labile organic matter is usually considered to be the major factor limiting the NO_3^- removal rates in coastal sediment (Cornwell et al. 1999; Ibánhez et al. 2011; Ibánhez et al. 2013). However, results from our experiments revealed that reduction of NO_3^- in subterranean estuaries can be independent of the availability of labile DOM. This contradiction may be explained by mechanics of NO_3^- removal in aerobic sediments. Specifically, in permeable sediments subject to porewater advection, heterogeneity creates flow divergence on the surfaces thus establishing a variable fluid field when compared with the macroscopic advective transport. As a direct result, the transport of nutrients in a dynamic flow field together with molecular diffusion is named mechanical dispersion (Bijeljic and Blunt 2006). On a micro scale, the successful establishment of these microenvironments subject to the advective flow field could create a numbers of sub-oxic or anoxic microniches within the porous medium. The production of microniches with anoxic environments possibly facilitates NO_3^- reducing potential in the aerobic sandy sediments (Gao et al. 2010). Although this special environment may support NO_3^- reduction activity in an aerobic environment, it also suggests that the chemical connection between DO and labile DOM in porewater occurs before DOM is utilised by NO_3^- reducers. In oxic sediment, aerobic respiration can be intensive because O_2 is a preferential electron acceptor in the oxidation of DOM (Charbonnier et al. 2012; Huettel et al. 2014). In this experiment,

respiration rates without glucose amendments fluctuated around 45 µmol dm^{-3} h^{-1}. Injection of glucose enhanced the activity to a level of 90.7 µmol dm^{-3} h^{-1} at its maximum point. Compared with the DOM utilisation rate at same time point, aerobic respiration by DO consumes more than 70% of labile DOM. Less than 30% of labile DOM may therefore be attributed to the remaining pathways. In sediment, other oxidisers, such as Fe^{3+} and MnO_2, are also potential labile DOM competitors (Canfield et al., 1993). Hence, the portion of labile DOM that is left available to NO_3^- reducers may be limited. This explains why NO_3^- reducers might not have responded to the addition of glucose in the tested sediment. In terms of the positive relationship between labile DOM availability and NO_3^- reduction found in previous studies (e.g. Hill and Sanmugadas 1985; Pfenning and McMahon 1997; Starr and Gillham 1993), the sediment tested in their experiments was cohesive (muddy) and allows DO to be rapidly consumed within the surface layer. In deeper regions, under anoxic conditions, NO_3^- reducers could then oxidize DOM in porewater.

VI.6.2 Alternative organic matter source for NO_3^- reducers

In aerobic sediment, due to the presence of DO, labile DOM was largely consumed in porewater (Fig.VI.6). In addition, compared with DO, the dispersion rate of DOM from porewater to microniches is slow because of large molecular weight. Consequently, NO_3^- reducers in sediment microniches barely obtain enough labile DOM; whereas, to avoid the inhibition by DO, NO_3^- reducing activity is constrained to this microniche. To support metabolism, this nitrate reducing population would have to choose alternative organic matter. In this regard, Addy et al. (2005) reported an insignificant response of the denitrification rate in salt marsh sediments when acetate was injected into benthic regions. Therefore, they suggested sediment organic matter (SOM) might meet the need for electron donors by denitrifiers. Generally, SOM comprises polysaccharides, aryl and alkyl, amongst others (Dodla et al. 2008). Labile components in SOM are also biochemically active, which could act as potential carbon

source to support benthic biogeochemical transformations.

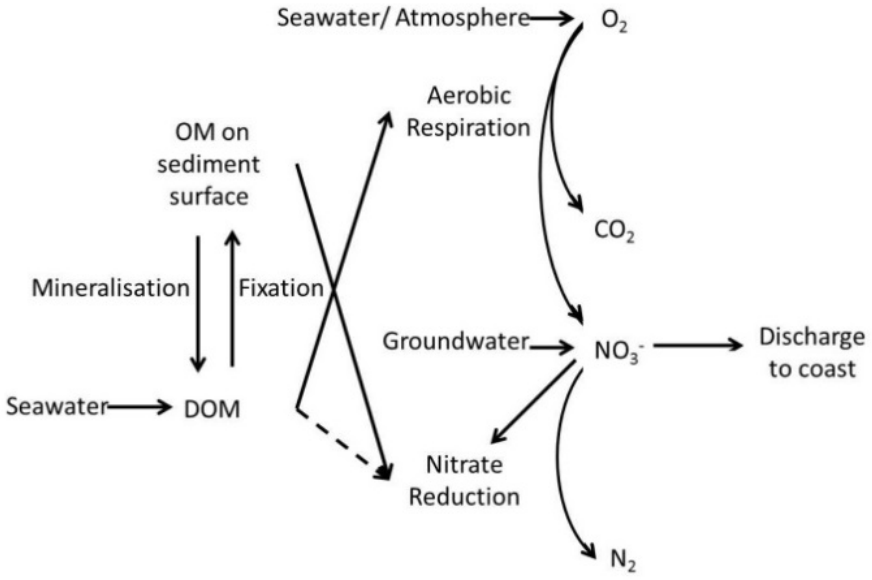

Figure VI.6 Sketch of DOM and SOM distribution in subterranean estuaries. The dash line indicates weak linkage between source of DOM and biogeochemical process.

Though a part of aerobic respiration may build on the mineralization of SOM (Grundmanis and Murray 1982), competition between reduction and respiration in assimilation of SOM may be limited due to spatial isolation of bacterial communities on particle surfaces. As a metabolite of aerobic respiration (Ibánhez and Rocha 2014b), marine humic material gradually enriched in porewater in all the treatments, possibly indicating that degradation of SOM is also linked to respiration. In benthic environments, NO_3^- reducers barely produce humic material (Ibánhez and Rocha 2014b). The gradual increase confirms that competition between NO_3^- reduction and respiration in utilisation SOM can be moderate. As a result, after long-term evolution, the function of DOM assimilation in reducers may be less sensitive since SOM is a stable source of labile carbon to reducing activity. This also explains why both glucose and tryptamine have not involved in NO_3^- turnover in our experiment. Furthermore, Ibánhez and Rocha (2014b) reported that high NO_3^- concentration in porewater can shift seepage faces from a sink of dissolved organic carbon (DOC) to a source, which also suggests NO_3^- reducers in sediment are using SOM as carbon source, instead of

DOM.

V.6.3 Implications for the magnitude of SGD-borne NO_3^- fluxes

Subterranean estuaries can be a highly aerobic environment due to periodical tidal pumping and ensuing solute exchange (Fig.VI.6). Intensive respiration in this environment acts as efficient decomposer of organic matter, potentially releasing NH_4^+ into porewater via remineralisation (Burgin and Hamilton, 2007). Subsequently, DO and other oxidative solutes, like Fe^{3+}, MnO_2, transform NH_4^+ into NO_3^- via the nitrification pathway (Santoro 2010). On the other hand, NO_3^- reducers continuously remove NO_3^- in porewater. Hence, the magnitude of outgoing NO_3^- fluxes depends on activity of reduction and addition. Compared with a highly variable DOM component (Chapter VI), SOM inventories in marine environments may be stable (e.g. Canuel and Martens 1993; Pusceddu et al. 1999), which results in a steady NO_3^- reduction potential. This may benefit continuous removal of NO_3^-, especially land-borne NO_3^- since terrestrial groundwater is low in reactive DOM (Shaw, 2003). Alternatively, in those regions where DOM accumulates, such as upper limit of subterranean estuaries due to seawater intrusion (Ibánhez et al. 2011; Chapter VI), aerobic respiration strength may significantly increase, releasing substantial NO_3^- into porewater. Subsequently, NO_3^- fluxes from SGD may be enhanced. More importantly, when coastal water is polluted by waste water particles or algae debris, organic matter concentration dramatically increases. Intrusion of excessive organic compound results in intensive respiration, potentially triggering high NO_3^- production. Concurrently, if terrestrial groundwater also adds NO_3^- in subterranean estuaries, magnitude of NO_3^- fluxes can be extremely large in effluent (Fig.VI.6), stimulating growth of algae, and then providing an additional source of DOM leachate in waters. Such positive feedback may eventually lead to eutrophication and subsequent harmful algae blooms in coastal zones.

VI.6.4 Final considerations and future directions

In my experiment, the maximum DOC concentration was 1000 μM due to addition of glucose. As a result, there might be a difference when treatment conditions change. In particular, if extremely high level of glucose was added into sediment, high level respiration may decrease the DO immediately and potentially create an anaerobic environment, indirectly increasing NO_3^- reduction capability. However, in subterranean estuaries, concentration of pelagic DOC barely reaches a level of 1000 μM. Increasing concentration to a higher level only generates a meaningless result, which rarely occurs in natural environments.

Compared to natural substances, glucose only contains C. The introduction of glucose may shift the C:N ratio in the tested sediment, subsequently influencing the activity of bacterial community. However, due to relatively low concentration of glucose in solution, the shift of C:N in SOM triggered by addition of glucose was less than 1%, suggesting a small impact to benthic bacterial community.

The study examined influence of labile organic matter in porewater to NO_3^- removal capability via laboratory stimulation. Comparing with spatially and temporally variable porewater in natural porous media, my experiments represent a 1-dimensional, steady state, and unidirectional system. Hence, there is a strong need to assess this determined relationship in future fieldwork. There is also a need to understand variation of stable isotope abundance to refine the distribution of labile organic matter to different pathways, facilitating understanding of NO_3^- recirculation and balance in subterranean estuaries.

VI.7 Conclusions

Labile organic matter in sediment is an important electron provider to

heterotrophic reactions. However, experimental results suggest addition of reactive DOM into porewater does not significantly improve removal efficiency of NO_3^-. More than 70% of dissolved DOM is consumed by DO-related aerobic respiration. Consequently, NO_3^- reducers in aerobic sediments may tend to utilise sediment organic pool instead, which indicates reduction of NO_3^- capability in sediment is relatively stable. As a consequence, increasing labile organic matter in subterranean estuaries may primarily strengthen intensity of aerobic respiration, likely resulting in an accumulation of NO_3^- via nitrification. Subsequently, enhanced NO_3^- fluxes from SGD are likely. To prevent deterioration of coastal systems, reactive organic matter in seawater needs to be reduced, which requires better management of sewage and waste water discharge.

Chapter VII

Quantification of nitrogen (N) loading from Submarine Groundwater Discharge (SGD) and subsequent transformation in Ria Formosa lagoon

VII.1 Abstract

The magnitude of Submarine Groundwater Discharge (SGD) and its contribution to nitrogen (N) biogeochemistry in a lagoon in Southern Ria Formosa were investigated in a summer on the basis of excessive radon inventory and propered defined endmember concentrations. Results suggested that the SGD pathway delivered 1.3(±1.0)×10^3 kg day^{-1} NO_3^- and 220.3±163.3 (mean ± stand deviation) kg day^{-1} DON to the lagoon, even though substantial N was reduced in the subterranean estuary prior to discharge. Compared to the entire N inputs to the lagoon, magnitude of fluxes from SGD accounted for 89% and 37% of NO_3^- and DON, respectively. Furthermore, in total SGD, approximately 98% NO_3^- was derived from fresh groundwater, which also contributed 76% DON. A combination of lagoon regional surveys and time series (48 h) monitoring at the inlet and the end of the lagoon channel suggest the exogenous NO_3^- associated with SGD was rapidly removed in the lagoon system. In particular, the reduction rate reached 69.9±68.5 μmol N-NO_3^- m^2 h^{-1}. Although denitrification in lagoon water transforms NO_3^- to N_2, dissimilatory nitrate reduction to ammonium (DNRA) and subsequent biological assimilation may also contribute to this high removal rate. As a result, substantial NO_3^- associated with SGD poses a serious risk to ecological balance in the lagoon, and likely trigger algal blooms and seasonal hypoxia. The monitoring results also revealed a net production of DON, at a rate of 36.3±35.4 μmol N-DON m^2 h^{-1}, which indicates an increase in biomass, possibly resulting from intensive assimilation of terraneous NO_3^-. As a consequence, future monitoring and potential control over N derived from SGD is highly necessary in the lagoon.

VII.2 Introduction

Exponential increases of N inputs to the coastal zone have been reported worldwide (Mackenzie et al. 2002; Smith et al. 2003). Since N is often the limiting factor that constrains biomass increase of algae in coastal environments (Howarth and Marino 2006), increasing N fluxes to coastal waters enhances the likelihood of eutrophication events, raising the frequency of harmful algal blooms (HABs) occurrence, leading to the local accumulation of organic matter and the increase of oxygen consumption; consequently, a reduction in water quality and economic loss is likely to be observed (Falkowski 1997; Rabouille et al. 2001). To prevent further deterioration of coastal ecosystems and in anticipation of the negative effects of global change, the scientific community has promoted the control over the introduction of reactive N (e.g. Galloway et al. 1995; Camargo and Alonso 2006; Howarth and Paerl 2008; Rabalais et al. 2009).

Atmospheric deposition is one of the main sources that transfer anthropogenic N to the oceans (Smith and Atkinson 1994). Indeed, it has been estimated to account for 30% of the external N input to the ocean (Duce et al. 2008). The remaining 70% of the external N inputs enters the oceans through surface loading and sub-surface pathway. Compared with well-documented surface runoff via estuarine outflows, the diffuse sources arising from subsurface transport (groundwater discharge) have only recently been explored (Moore 1999; Taniguchi et al. 2002; Burnett et al. 2003). However, it is deemed to be responsible for 52% of the total dissolved solids transferred across the land-ocean interface via submarine groundwater discharge (SGD, Zektser and Loaiciga 1993). i.e. ‘any flow of water across the sea floor, regardless of fluid composition or driving force’ (Burnett et al. 2003). Accordingly, SGD is not limited to fresh groundwater discharge but also includes seawater recirculation (Taniguchi et al. 2002). On the system scale, influences from these two compartments on the local nutrient inventory in the receiving water are significantly different (Chapter I). In particular,

nutrient derived fresh groundwater in SGD is allochthonous (Howarth and Marino 2006), which directly enlarges the reactive nutrient inventory in the coastal ocean. In contrast, recirculation of seawater is identified as an internal process in the system, which barely perturbs nutrient stability (Chapter I).

Literally, SGD has the potential to occur in any permeable layer of the coastal zone (Burnett et al. 2001; Santos et al. 2012). It may happen at the fringe of the open ocean, directly diluted by seawater. Alternatively, it may flow into coastal semi-enclosed systems, such as bays and lagoons, where in transit to the adjacent ocean, the residence time of inputs from land increases due to restrictions imposed by tidal circulation and winds (Ridderinkhof et al. 1990). Usually, coastal semi-enclosed systems are the focus of human activities. They are often adjacent to large human populations and support a number of recreational and commercial uses of the coastal environment such as maritime transportation, tourism and intensive mariculture (Windom and Niencheski 2003). Good ecological and environmental status of coastal systems is important to sustain human development. Substantial allochthonous nutrient fluxes delivered via the SGD pathway into coastal semi-enclosed systems may lead to eutrophication and subsequent algae blooms which threaten the stability of the entire ecosystem (Young et al. 2008; El-Gamal et al. 2012; Kharroubi et al. 2012; Bernard et al. 2014). However, SGD is ‘‘invisible’’ (Finkl and Krupa 2003) and hard to predict in both time and space (Leote et al. 2008), resulting in difficulty in quantification of its actual dimension and intensity. Therefore, nutrient fluxes from SGD have been frequently ignored in local nutrient mass balances (Burnett et al. 2003), and subsequent regulation and management of nutrient fluxes in the coastal zone (Windom and Niencheski 2003; Tait et al. 2014). As a consequence, quantifying nutrient fluxes from SGD in coastal semi-enclosed systems and separating contributions from the two sources, namely, freshwater and recycled seawater in total SGD, are important tasks in current environmental research.

This study was conducted in the Ria Formosa lagoon, a coastal lagoon surrounded by a highly urbanised and intensive farmed area. The lagoon sustains high primary productivity during the entire year, but evidence of changes in its trophic status has surfaced in the literature, such as decreasing bivalve harvests (Dinis 1992), an increase in the occurrence of algal blooms (Baptista 1993), the replacement of typical salt marsh vegetation by macro algae (Padinha et al. 2000) and increasing incidences of 'fish kills' during winter-spring seasons (Newton et al. 2003). These changes may arguably be linked to nutrient enrichment, especially N, which is frequently excessive in the lagoon (Ferreira et al., 2003; Newton et al., 2003, Newton and Mudge 2005). Nevertheless, until now, the major exogenous N source to the lagoon was still highly debated (Ferreira et al. 2003).

In this study, a quantitative investigation of NO_3^- and DON fluxes from SGD was conducted in May 2010. The main hypothesis in this research was that SGD delivers substantially extraneous NO_3^- and DON to the receiving water. I further hypothesised that SGD is the main stressor to the lagoon's dissolved inorganic nitrogen (DIN) balance since magnitude of NO_3^- fluxes from fresh groundwater overwhelms that of any other contributing pathways. The objectives in the current evaluation were to explore these hypotheses to identify the biogeochemical response of lagoon water to NO_3^- and DON. The results from this research will benefit future lagoon management with respect to regulation of N fluxes via SGD.

VII.3 Material and methods

VII.3.1 System definition

Ria Formosa is located in the Algarve, south Portugal (36°58'N 8°20'W to 37°30'N 7°32'W, Fig.VII.1). It is a semi-enclosed system, separated from the Atlantic by a multi-inlet barrier island and two peninsulas. The lagoon has a surface area up to 111

km^2 and shows an average depth of 2 m (Andrade et al. 2004). The tide is semi-diurnal with mean level ranges between 1.3 and 2.8 m (Chapter I). The maximum average tidal volume in the lagoon is measured to be approximately 140×10^6 m^3 using the GPS techniques (Rocha et al. in press). Lagoon water is frequently exchanged with the Atlantic Ocean through six tidal inlets, and the average tidal flux is 8×10^6 m^3 (Balouin et al. 2001). The lagoon contains large salt marsh area, complex network of tidal beach and natural channels. The submerged area reaches 55 km^2 at high spring tide and varies of 14 to 22 km^2 at low spring tide (Tett et al. 2003). From west to east, inlets are defined as Ancão, Faro-Olhão, Armona, and Fuzeta, Tavira and Lacem. The 90% of the tidal exchange occurred within the major three inlets Ancão, Faro-Olhão, Armona (Fig.VII.1). In particular, they contribute to 61%, 23% and 8% of the tidal flow during spring tides and 45%, 40% and 5% during neap tides, respectively (Pacheco et al. 2010).

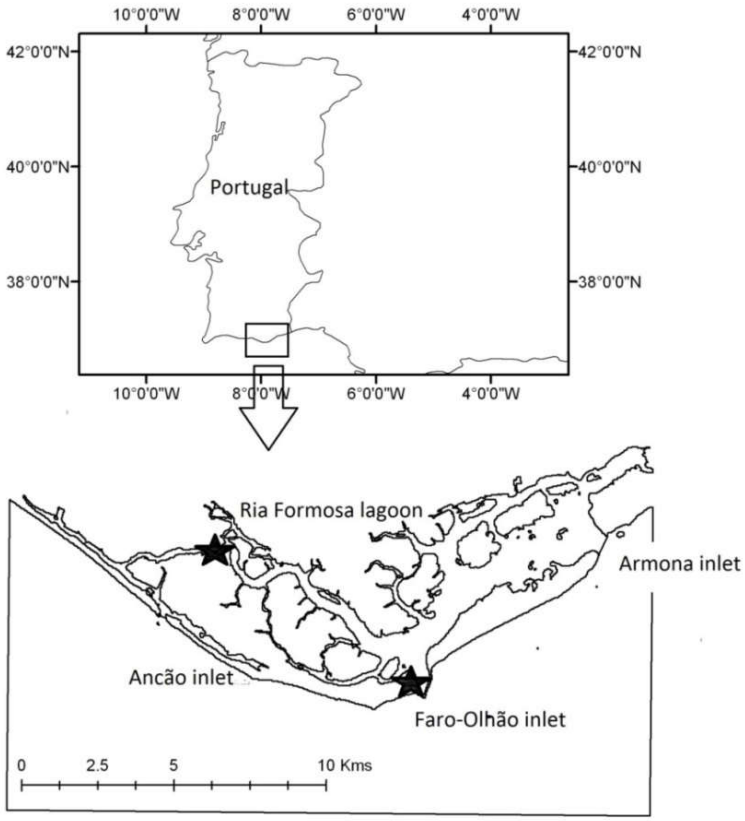

Figure VII.1 Map of Ria Formosa lagoon, selectively showing three main inlets in Ria Formosa lagoon system. The two stars represent the locations of the fixed sampling sites.

The regional climate shows typical characters of Mediterranean weather. The average annual temperature is 17°C in the air, with averages of 11°C in winter and 24°C in summer, respectively. Annual precipitation is 480 mm in the Faro (West Boundary), and it increases to 580 mm in the East Limit and effective precipitation is 151 mm (Salles 2001). Surface loadings, such as rivers and streams are usually seasonal and limited, except the River Gilão, which discharges directly into the adjacent coastal ocean through the Tavira inlet at the eastern boundary of the lagoon (Rocha et al. in press).

VII.3.2 SGD and N fluxes

The Ria Formosa supports local economy based on tourism through natural resource harvesting and is therefore strongly affected by human activities on the surrounding watershed. Campina de Faro, in the northern section of the lagoon, is a coastal plain site of intensive agricultural activities. Since the early 1980's, the original land cover has been gradually replaced by olive and citrus trees to boost local economy. Due to limited annual precipitation (Stigter et al. 1998; Salles 2001), irrigation has been introduced to meet the need of this increasing agriculture. Subsequently, over-amount N fertiliser directly seeps into the Plio-Quaternary sand aquifer and the sub-horizontal Miocene sandy layers beneath Campina de Faro. Due to the hydraulic gradient, seriously NO_3^--polluted groundwater flows towards the Ria Formosa lagoon (Stigter et al. 2006a). When the NO_3^- plume reaches the coastal region, it seeps into a highly permeable layer, consisting of Quaternary gravels and sands (Arnaud-Fassetta et al. 2006). At the bottom of the permeable layer, it is an infilling sequence. In the Ria Formosa lagoon, the infilling sequence is muddy sediment, 0.60 to 1.3 m in thickness (Bettencourt 1994). In addition, finer sediments sustaining the marshland were assumed to be impermeable for subsurface flow. The polluted groundwater flows below this confining layer and seeps to the lagoon as SGD. In some highly permeable beach with presence of the coarse sediments, the recorded SGD rate could be

substantial if local hydraulic pressure overwhelms the sea level (Corbett et al. 1999; Rocha et al. 2009).

Leote et al. (2008) first discovered the existence of SGD in the Ria Formosa lagoon. They performed a series of sampling campaigns in the intertidal area of Ancão peninsula. Brackish porewater associated with high NO_3^- content seeped through the beach face and discharged to the lagoon. They also found that NO_3^- content in the seeped water was inversely correlated with salinity (Leote et al. 2008), suggesting that the source of the fresh component in SGD was inland. Furthermore, Rocha et al. (in press) revealed high excessive fluxes of ^{222}Rn (4.14×10^8 Bq day^{-1}) in the lagoon, possibly due to the existence of SGD, which is a milestone in the quantitation of SGD rate in this lagoon, as well as acting as important theoretical support for this research.

VII.3.3 Regional survey of N distribution

The field survey presented in this chapter was part of NITROLINK project (2009 to 2011), which was conducted by other members in my research group. The salinity data and a part of N results in this chapter are contributed by other members.

Lagoon water samples were continuously collected during a boat survey in May (due to less tourists) 2010 at a depth of 20 cm below the surface into a HDPE sampling bottle, and then filtered into non-addition vacutainers via pre-cleaned Rhizon membrane filters (0.1 μm pore size). Salinity was continuously recorded by a CTD diver (Schlumberger™). During the survey, the coordinates of each sampling location were recorded using a Garmin ® handheld GPS. Sampling campaigns lasted for approximately 24 hours. The route and sampling locations included the majority of navigable parts of the lagoon during both ebbing and flooding tides at two complete tidal cycles. Samples gathered on board were kept in cooler boxes until subsequent analysis. N concentrations (DIN, in the form of NH_4^+, NO_2^-, NO_3^- and TDN) were then

determined for all water samples.

VII.3.4 Tidal variability of N concentration at fixed locations

Measurements of N were also carried out at two fixed locations over three full tidal cycles (stars in Fig.VII.1 display the locations). The locations of these measurements were located in the largest inlet, Faro-Olhão inlet. These locations guarantee the maximum understanding of tidal circulation within the system and could offer reliable knowledge on the exchange of N fluxes between the lagoon and the adjacent ocean. Water samples were collected synchronously at two locations for consecutive tidal cycles with 20 minute sampling intervals. Concurrently, salinity was determined by YSI 600 probes (Yellowstone instrument).

The tidal amplitude data at Faro-Olhão inlet was applied to calculate the net exchange of N for the sampling cross section (http://tides.mobilegeographics.com). In practice, if a vertically sufficient mixed water column was assumed, N fluxes exchange across a fixed boundary can be determined by the oscillating tidal flow. Firstly, the instantaneous directional flux ($F_N\Delta_t$) was calculated, where Δ_t is the counting interval (20 minutes), $C_N\Delta_t$ is the concentration of any N species integrated over the time interval and $\frac{dh}{dt}$ is the change in tidal height, relative to mean sea level (MSL), occurring over that interval:

$$F_N\Delta_t = (\frac{dh}{dt}) \times C_N\Delta_t \quad (1)$$

$F_N\Delta_t$ is then plotted against time, and the total N flux in each direction can be calculated by integrating the instantaneous directional flux over time (the area beneath each curve), for flood and ebb periods. The total outflow (negative) and inflow (positive) of N through the channel is then calculated for each determined

semi-tidal period. Difference between two complete outflow and inflow periods is the net flux that transfers across selected section during each tidal cycle. In my survey, data for three successive complete tidal cycles showed different values for net transfer. The mean value from three cycles was used to reach the final net exchange flux across each sampling site.

VII.3.5 Mass balance approach

To determine N transformation within the lagoon, a mass balance approach was designed (Fig.VII.2). The cross-channel tidal measurement at two fixed locations within the Faro Channel was defined as two endmembers for the estimation of N reaction rate. During the lagoon water transport, SGD, atmospheric deposition and sediment diffusion are defined as input pathways that increase the N concentration in the sampling water. Hence, the mass balance equation can be expressed as:

$$N_{reaction} = N_{out} - N_{in} - N_{SGD} - N_{air} - N_{diff} \quad (2)$$

where $N_{reaction}$ is the N reaction in the Ria Formosa lagoon, N_{SGD} is SGD-borne N, N_{diff} is N inputs due to sediment diffusion, N_{air} is N from air deposition, N_{out} and N_{in} are N output and input, respectively.

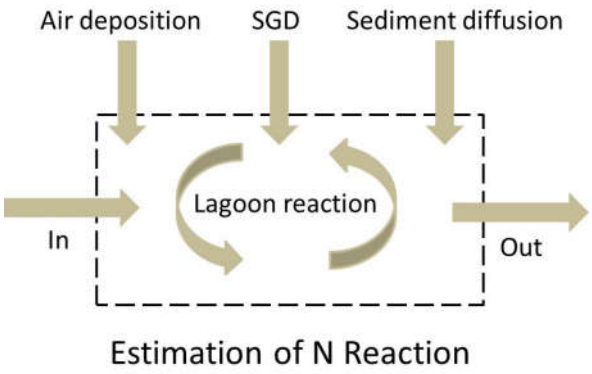

Figure VII.2 A conceptual diagram of N mass balance models to determine N reaction in the Ria Formosa Lagoon, including distinct input and output pathways, modified from Tait et al. (2014).

VII.3.6 Laboratory analysis

Collected samples were analysed for nitrite (NO_2^-) and ammonium (NH_4^+) in a FOSS Flow Injection Analyser (FIAstar 5000). Nitrite determination was colorimetric, based on the development of red azo dye with a method detection limit (MDL) of 0.2 μg N l^{-1} (Carvalho et al. 2013). NH_4^+ was quantified following the spectrophotometric methods described in Grasshoff et al. (2009) with a detection limit of 0.4 μg N l^{-1}. Both analyses were conducted by Liliana Carvalho in University do Algarve. Concentrations of NO_3^- for all water samples were determined using a LACHAT Quickchem 8500 Flow Injection Analysis was performed following standard colorimetric methods (Grasshoff et al. 2009) as adapted for automated sequential analysis by the manufacturer. Concentrations of total dissolved nitrogen (TDN) were determined using an Elementar Vario TOC Cube at 680°C. These analyses were conducted in the Centre for the Environment (TCD) by the author. MDL for these two analytes was were found to be NO_3^- (1.2 μg N l^{-1}) and TDN (32 μg N l^{-1}). The subtraction of the three inorganic N components from concentrations of TDN represents the level of dissolved organic nitrogen (DON) in the water samples.

VII.3.7 Propagation of uncertainty

Uncertainty analysis was calculated following the description of Taylor and Cohen (1998). In particular, they used relative proportions to determine the uncertainty of an unknown term. For instance, if R is the result of I want to calculate, such as nitrogen reaction rate in the lagoon (Eq.4), and there are three independent contributors, X (SGD), Y (Sewage) and Z (Stream), where the standard deviations are $\pm 1\sigma x$, $\pm 1\sigma y$, and $\pm 1\sigma z$, respectively. The relative uncertainty of each term is $\frac{\sigma x}{X}$, $\frac{\sigma y}{Y}$, and $\frac{\sigma z}{Z}$, which contains information of the magnitude of the uncertainty associated with each contributor. For the statistical uncertainty for the final result of R, it can be calculated as:

$$\sigma R = (R \times \sqrt{\left[\left(\frac{\sigma x}{X}\right)^2 + \left(\frac{\sigma y}{Y}\right)^2 + \left(\frac{\sigma z}{Z}\right)^2\right]}) \quad (4)$$

Due to large differences between distinct terms in the mass balance approach, the direct sum rule to determine the absolute uncertainties can yield very large deviation that might be meaningless. In contrast, the application of Eq.(4) could provide an estimation that guarantees realistic figures through subtraction between several contributors, which may help define the realistic fluctuations of the required term in a complex natural system.

VII.4 Results

VII.4.1 Regional distribution of N

Regional scale surveys have shown uniform distribution of N in the lagoon water (Fig.VII.3), expect for accumulation of NH_4^+ and NO_3^- at the at the northwest (dark colour in the maps), where solutes reached 8 µM in concentration. For the remaining sites, concentration of NH_4^+ fluctuated between 0.3 to 2.1 µM. Likewise, concentration of NO_3^- also ranged between 0.1 to 2.2 µM. The low concentration range of DIN is in agreement with previous research (Newton et al. 2003; Synthesis report 2003). In comparison, concentrations of DON were significantly high. The peak value was 61.7 µM while the minimum fell only to 45.2 µM. This comparatively uniform distribution on spatial and temporal scale confirmed the well-mixed status of the lagoon water, which guarantees the accuracy of mass balance calculations on a regional scale.

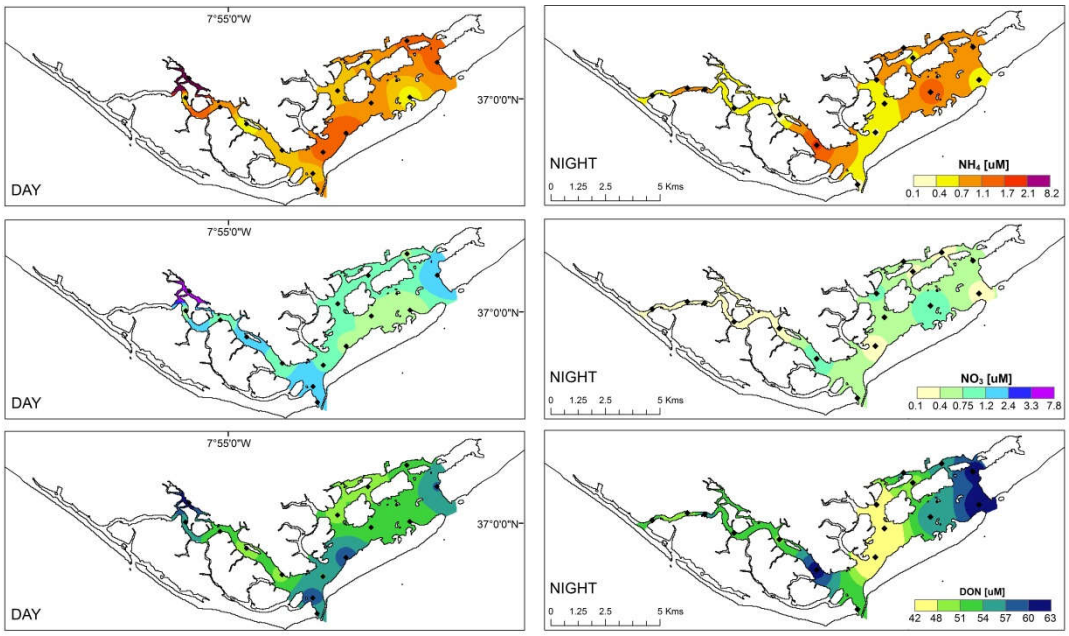

Figure VII.3 Distribution of NH_4^+, NO_3^-, DON in lagoon waters during day time (mainly low tide) and night time (mainly high tide).

VII.4.2 N inputs from SGD pathway

Both steady state (fixed sampling) and tidal variation (cruise) models revealed the excess ^{222}Rn flux in the lagoon water during our sampling period was 4.14×10^8 Bq day^{-1} (Rocha et al. in press; this submitted article mainly focused on determination of excess radon flux during same sampling period and origination of fresh groundwater in the lagoon; more information in Appendix D). During the fixed location survey, fluctuation of salinity was observed in both sectors. For channel inlet, there was 0.3 psu difference in salinity between peak and trough (Fig.VII.4). At the channel end, minimum salinity was 35.6 psu, approximately 0.6 psu lower than the maximum salinity observed in the next tidal phase. In addition, the decrease in salinity between the two fixed locations was observed during both day and night, which indicates that salinity oscillation in lagoon water may not be only driven by difference of evaporation between day and night. Injection of fresh terrestrial groundwater may also contribute to the decline of salinity. Consequently, the excessive radon budget is likely to be the contribution from SGD, in particular, a combination between freshwater component and recirculated

seawater (Mulligan and Charette 2006).

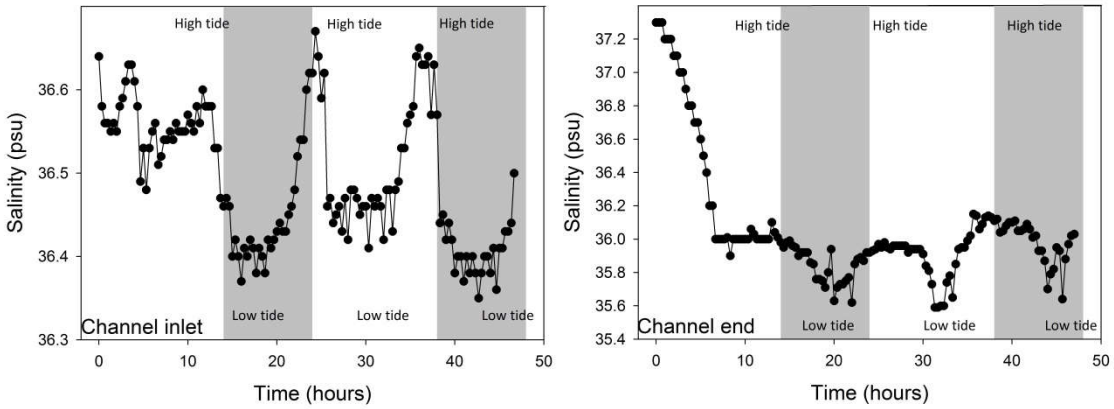

Figure VII.4 Time series monitoring of salinity, the dark region indicates night time. High tide and low tide points are also included in the figure.

In order to distinguish contributions from two independent sources, radon activity for each endmember needs to be defined. For terrestrial groundwater endmember, there are three aquifer systems around the lagoon, Campina de Faro, Quinta João de Ourém, and São João da Venda (Stigter et al. 2006a; Ferreira and Leitão 2014). Due to difference in bedrock, groundwater radon concentration may vary significantly between aquifers. In order to define the correct endmember value for terrestrial groundwater, relative abundance of hydrological stable isotopes (^{2}H and ^{18}O) in the lagoon water was determined (Rocha et al. in press, Appendix D). Given the enrichment of light isotopes determined in the beach and a good correlation in isotope concentration between lagoon water and terrestrial groundwater from Campina de Faro (Rocha et al. in press), radon activity (6625 Bq m^{-3}) in groundwater endmember was defined as the measurement in the Ramalhete borehole, i.e. the boundary between Campina de Faro and the lagoon (Table VII.1). For recycled seawater, radon activity was defined as 305 Bq m^{-3} using the porewater associated with the highest salinity (more than 36 psu).

Compared to conservative propagation of radon in permeable sediment, concentrations of NO_3^- and DON in fresh groundwater can be significantly altered in

the subterranean estuary (Slomp and Van Cappellen 2004; Spiteri et al. 2008; Chapter V), i.e., the typical mixing zone between meteoric water and saline water in coastal aquifers (Moore 1999). The subterranean estuary in Ria Formosa lagoon has been proven to be an active reactor for groundwater-borne N (Chapter V; Chapter VI). As a result, concentrations of NO_3^- and DON (difference in concentration between TDN and NO_3^-) in the terrestrial groundwater endmember on the basis of regression should be practiced, instead of using the original concentration in fresh water (Beck et al. 2007; Santos et al. 2009). In the Ria Formosa, the concentration of N at terrestrial endmember may increase drastically between different seasons (e.g., December to January in Chapter V). In this study, we focused on the conservative and the most general condition in the estimation of N fluxes. Therefore, the concentrations for NO_3^- and DON at terrestrial groundwater endmember were 22.4 mg l^{-1} and 2.9 mg l^{-1}, respectively (Table VII.1) on the basis of field observation from March to May 2011 (Chapter V). Concurrently, the concentration of NO_3^- and DON for recycled seawater was defined as 0.2 mg l^{-1} and 0.5 mg l^{-1}.

Table VII.1 Endmember values and individual contribution of NO_3^- and DON in fresh SGD and recycled saline SGD, SW is seawater, GW is groundwater.

	[^{222}Rn] Bq m^{-3}	[NO_3^-] mg l^{-1}	[DON] mg l^{-1}	Ratio %	Rate (10^4 m^3 day^{-1})	NO_3^- kg day^{-1}	DON kg day^{-1}
Recycle SW	305	0.2	0.5	64.2%	10.4±7.7	20.8±15.4	52.1±38.6
Fresh GW	6625	22.4	2.9	35.8%	5.8±4.3	1.3(±1.0)×10^3	168.2±124.7
Total	—	—	—	100%	16.2±11.9	1.3(±1.0)×10^3	220.3±163.3

Because excessive radon inventory represents the contribution of total SGD (Chapter I), the composition of fresh water and recycled seawater in total SGD is required before quantification of N fluxes derived from each endmember can progress. Based on Darcy's law (Darcy 1856), discharge rate of groundwater from is positively related with hydraulic gradient. It is assumed that the discharge rate of total SGD is relatively stable; hence, the composition of fresh groundwater in total SGD is likely dependent on the hydraulic pressure head in the aquifers. Here, the record of fresh

composition (January to July) in total SGD measured by seepage meters, conducted in 2006 by the BGR research group (Leote et al. 2008), was invoked. In addition, groundwater piezometric head records from different boreholes (in Campina de Faro, data from http://www.snirh.pt) were used to match the composition of the fresh compartment in SGD, as can be seen in Fig.VII.5 (A). Clearly, the fluctuation of the fresh composition in total SGD parallels with the oscillating groundwater pressure head. By this line of reasoning, linear regressions were conducted to link pressure head in different boreholes with fresh composition data, e.g., C and D in Fig.VII.5. The values of R^2 derived from these regressions range from 0.66 (Quinta) to 0.86 (Gambelas).

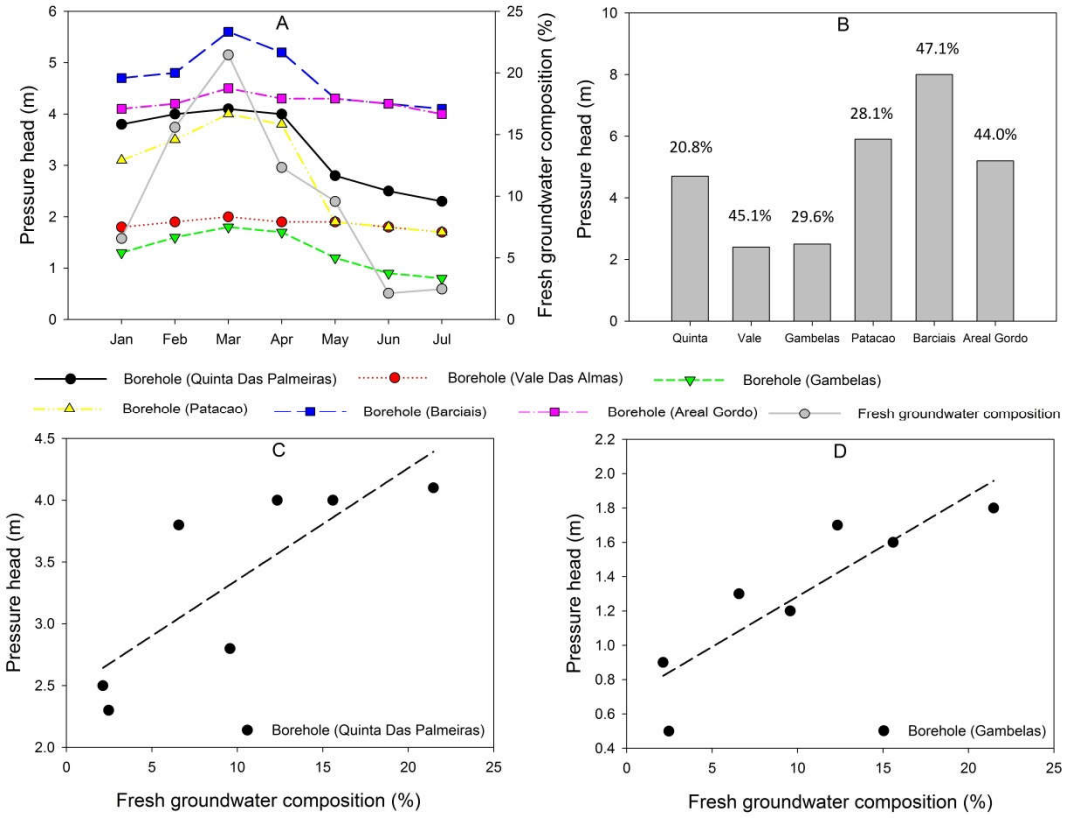

Figure VII.5 (A) Piezometric pressure head in adjacent boreholes and fresh groundwater composition in total SGD during January to July in 2006; (B) pressure head measurements in different boreholes and prediction of the fresh composition in total SGD in each borehole in May, 2010; Regression trends between fresh groundwater composition and pressure head in Quinta Das Palmeiras (C) and Gambelas (D).

In May 2010, the groundwater table in the aquifer was significantly elevated, ranging between 2.2 m and 8.3 m in different boreholes (B in Fig.VII.5). The high pressure head also suggests the presence of terrestrial groundwater in total SGD.

Given the relationship described in the regression curves, the ratios of fresh SGD in May 2010 fall into the range between 20.8% (Quinta) and 47.1% (Barciais). Notably, in Ria Formosa, the possible recharge of seawater into aquifers during spring tide leads to an increase in the local groundwater table and subsequently influences data accuracy. In addition, irrigation and groundwater extraction from local agriculture activities also add uncertainties in the predication. In order to minimise the indeterminacy in the following quantification, mean fresh composition (35.8%) derived from all six borehole results was employed. Combined with relative contribution of fresh and saline water to total SGD, the discharge rate for each type of water was estimated. In particular, the discharge rate of fresh SGD was $5.8(\pm4.3)\times10^4$ m^3 day^{-1}, while the recycled saline SGD was $10.4(\pm7.7)\times10^4$ m^3 day^{-1}. After amendment from transformations in the subterranean estuary, magnitude of NO_3^- fluxes from fresh SGD was estimated to be $1.3(\pm1.0)\times10^3$ kg day^{-1} and the DON fluxes were 168.2(±124.7) kg day^{-1}. In comparison, seawater recirculation only introduced 20.8±15.4 kg NO_3^- and 52.1±38.6 DON every day in to the lagoon.

VII.4.3 Tidal N fluxes and lagoon reaction

Time series of N concentrations were obtained at two end-locations within the Faro channel, one at the inner and one at the inlet (Fig.VII.1). Sampling occurred continuously over 48 hours at both sites simultaneously. Amongst three inorganic N species, NH_4^+ was the dominant inorganic N species in the lagoon water. From the distribution of input/out fluxes shown in Fig.VII.6, there is a clear variation of NH_4^+ fluxes between different tidal cycles. Additionally, magnitudes of DON fluxes were significantly larger than that of any inorganic compartment. In line with the regional survey, monitoring at fixed sites showed concentrations of DON fluctuated between 40 µM and 70 µM, generating a flux range of 4.2×10^4 µmol m^{-2} h^{-1} to -4.1×10^4 µmol m^{-2} h^{-1}. In contrast, NO_3^- solutes were comparatively depleted in the lagoon water. As a consequence, the fluctuation of NO_3^- fluxes only manifested small amplitude during

the tidal survey. Concentrations of NO_2^- in the majority of water samples were below MDL and the highest level only reached 0.17 µM.

The hydraulic circulation in the Ria Formosa is complex. Flood begins at the inlet while ebbing is usually occurring among all the other inlets, creating a tidal circulation towards the eastward through the Olhão channel and westward through the Faro Channel (Rocha et al., in press). Hence, N import (landward) overwhelms export (seaward), which generates significant residual fluxes in our two fixed locations. In particular, the residual fluxes of NH_4^+ were $0.2(\pm0.02)\times10^3$ µmol m^{-2} h^{-1} at the channel end and $0.3(\pm0.04)\times10^3$ µmol m^{-2} h^{-1} at the inlet, as can be seen in Table VII.2. Residual fluxes for NO_3^- were smaller, only $0.6(\pm0.06)\times10^2$ µmol m^{-2} h^{-1} (end) and $0.5(\pm0.06)\times10^2$ µmol m^{-2} h^{-1} (inlet). The residuals of DON fluxes were $0.8(\pm0.02)\times10^3$ µmol m^{-2} h^{-1} and $0.7(\pm0.09)\times10^3$ µmol m^{-2} h^{-1} (Table VII.2).

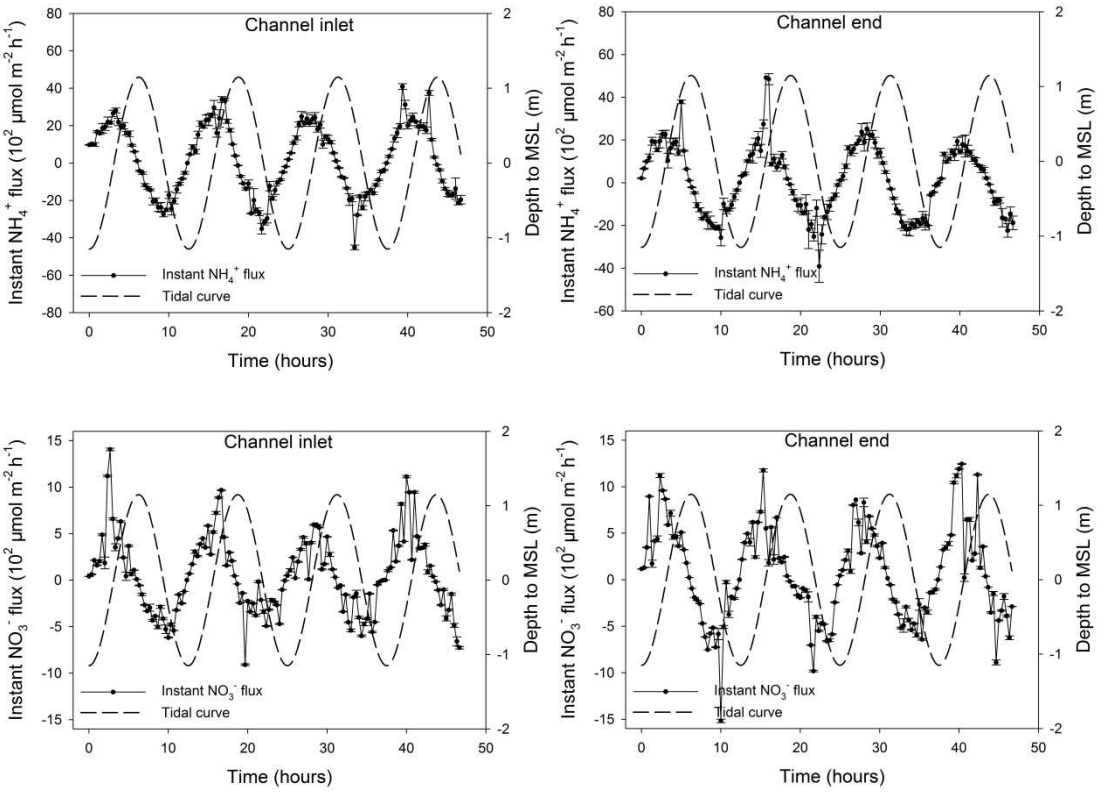

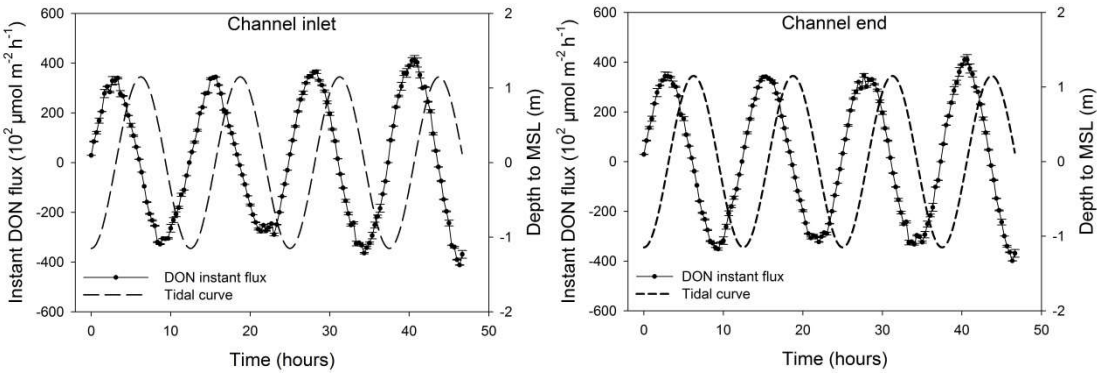

Figure VII.6 Time series analysis of NH_4^+, NO_3^- and DON fluxes at channel inlet and channel end

VII.4.4 N transformation rate in the lagoon

To understand N transformation rates in the lagoon, definition of N inputs from diffusion and atmospheric deposition are required. The diffusion of NO_3^- and DON in this work was quoted from benthic measurements made by Falcão et al. (2009). Their work determined fluxes of inorganic and organic portions in a sampling site near the Ancão inlet. Diffusion of NH_4^+ is invoked from measurements undertaken for the Synthesis Report, (2003). Inorganic N fluxes via atmospheric deposition for the Ria Formosa lagoon were taken from Flechard et al. (2011), who determined this at the monitoring site of the NitroEurope network in Espirra, Portugal. For organic N deposition, the ratio of inorganic N composition in atmospheric inventory from Cornell et al. (2001) was applied to estimate DON fluxes. Both N fluxes from SGD and deposition were then transformed according to the average submerged area of the lagoon (Tett et al. 2003). The residual fluxes, determined at two survey locations, were defined as input and output endmembers in the mass balance estimation.

Table VII.2 N exchange due to tidal fluxes and residues between flood tide and ebb tide in two study sites, as well as N inputs and transformation rates in the lagoon, the unit is µmol N m^{-2} h^{-1}. The dash line represents not 'a source' for this species.

	NH_4^+	NO_3^-	DON
Residual calculation			
Channel end			
Export	1.3(±0.07)×10^3	4.2(±0.1)×10^2	20.6(±0.5)×10^3
Import	1.5(±0.1)×10^3	3.6(±0.1)×10^2	21.4(±0.4)×10^3
Residual	0.2(±0.02)×10^3	0.6(±0.06)×10^2	0.8(±0.02)×10^3
Faro-Olhão inlet			
Export	1.5(±0.07)×10^3	3.5(±0.3)×10^2	19.7(±1.9)×10^3
Import	1.8(±0.3)×10^3	3.0(±0.2)×10^2	20.4(±2.0)×10^3
Residual	0.3(±0.04)×10^3	0.5(±0.06)×10^2	0.7(±0.09)×10^3
Inputs			
SGD	—	71.1±65.9	8.4±7.8
Diffusion	16.2±1.0	5.2±1.3	0.3±0.08
Deposition	6.6	3.6	19.5
Reactions			
Transformation	-62.8±15.0	-69.9±68.5	16.8±15.7

Combining all endmembers, N processing abilities in the lagoon are shown in Table VII.2. The data is processed on the basis of propagation of uncertainties. In particular, the system manifested intensive reduction for NO_3^-, reaching 69.9±68.5 µmol m^2 h^{-1}, while the transformation of NH_4^+ was 62.8±15.0 µmol m^2 h^{-1}. Notably, saline water in total SGD is a product of system circulation. In the Ria Formosa, the subterranean estuary acts as a reactor for NO_3^- and DON. Consequently, both NO_3^- and DON fluxes from SGD should be net fluxes. As a result, the contribution from recycled saline water is given as the difference between discharge fluxes and recharge fluxes in the subterranean estuary. However, for NO_3^-, seawater recirculation contributed an insignificant portion, only 2% in total SGD, which barely influences the transformation rate calculation. In contrast, DON fluxes from saline endmember accounts for 32% in total SGD-borne DON, indicating the necessity of amendment. Combined with mean DON concentration in lagoon water during our survey (0.7 mg l^{-1}), the net flux of DON from SGD was 8.4±7.8 µmol N m^{-2} h^{-1}. Therefore, the lagoon produced DON at a rate of 36.3±35.4 µmol m^{-2} h^{-1}.

VII.4.5 Comparison between intrinsic pathways

A comprehensive comparison between different N sources was made (Fig.VII.7). The surface drainage from seasonal streams and rivers was invoked from the Synthesis Report (2003) and the contribution from the waste water outlet was based on the field survey result in 2013 (Appendix D). The total NO_3^- injection was 1486 kg day^{-1}. Daily contribution from SGD was 1320 kg, accounting for 88.8% in total. The addition of all other pathways only represented 160.9 kg NO_3^- day^{-1}. SGD contributed to 68.7% of total DIN inputs due to the high concentration of NO_3^-. Besides inorganic N fluxes, SGD is also an important contributor of DON. Though the subterranean estuary around the lagoon reduced a substantial portion of DON from porewater due to remineralisation, SGD was still also an important input source for DON, which exports 220.3 kg N-DON day^{-1}. Similar to inorganic N composition of SGD, the fresh compartment is the dominant source of SGD-borne DON, accounting for 28.4% of total DON input in the lagoon.

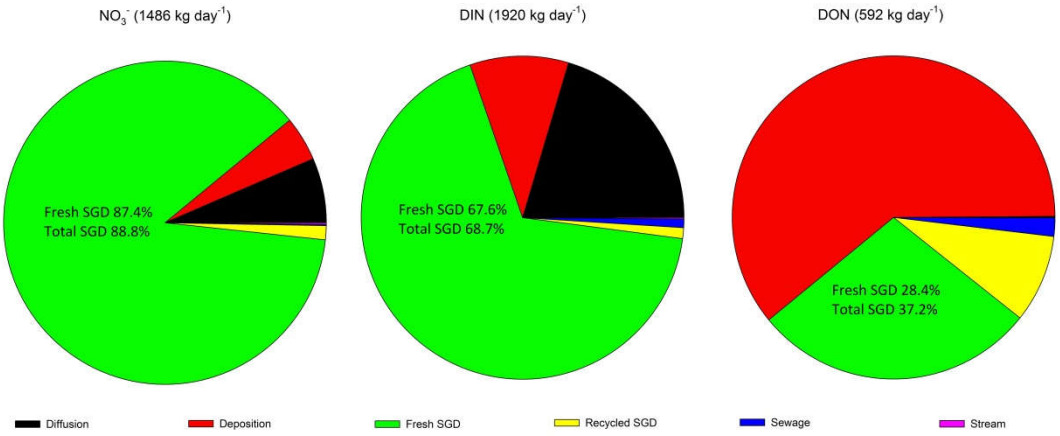

Figure VII.7 Contributions and comparison of NO_3^-, DIN and DON from distinct sources to the Ria Formosa lagoon

VII.5 Discussion

VII.5.1 N contributions via SGD

The Ria Formosa lagoon has been diagnosed as eutrophic due to inorganic N contamination (Newton et al. 2003; Newton and Mudge 2005), which is related with exogenous N input (Paytan et al. 2006). Previous studies examined a number of possible N input pathways to the lagoon, including sewage, stream flow and atmospheric deposition, etc. (Wayland et al. 2008; Gari et al. 2014). However, the main stressor that disturbed N inventory in the lagoon had not been ascertained.

In this study, substantial inorganic N fluxes via the SGD pathway have been observed (Fig.VII.7). Though N concentrations and discharge volume at the waste water outlet and streams may fluctuate seasonally, their contributions to the lagoon NO_3^- inventory will still be limited due to their small injection volumes and endmember concentration compared to SGD. Ferreira et al. (2003) estimated diffusive DIN injection to the lagoon (1600 kg day^{-1}) via a mass balance approach. In this study, the diffusive source (SGD and sediment diffusion) contributed 1690 kg day^{-1}, showing the consistency between this research and previous observations. As a result, SGD in the Ria Formosa lagoon can be evaluated as the main stressor for DIN balance in the lagoon (Newton et al. 2003). Geographic distribution also supports this conclusion. In particular, Newton et al. (2003) revealed occurrences of lagoon scale eutrophication due to enrichment of DIN. Sewage and stream inputs are typical point pollutant sources that usually influences adjacent lagoon channels (Duarte et al. 2005); hence, their impacts barely extend to the lagoon scale. Ria Formosa has geological suitability to host substantial SGD since the coastal line on the edge of the lagoon is highly permeable (Leote et al. 2008; Rocha et al. 2009). Consequently, the hydraulic gradient established between land and ocean (Stigter et al. 2013), means SGD-borne NO_3^- can influence the entire system.

Quantitative studies on SGD-borne NO_3^- and DIN inputs to the coastal zone have been carried out in a small number of regions only. Though limited, the importance of SGD delivering substantial N to coastal semi-enclosed systems can be witnessed (Table

VII.3), since N concentration, especially NO_3^- in coastal groundwater is several orders of magnitude greater than that of seawater (Moore 1999; Moore 2010). Our results are compared to these literature values (Table VII.3). On a global scale, the contribution of NO_3^- fluxes via the SGD pathway ranges from 38% of total exogenous inputs (Florida Bay) to nearly 100% (Tolo harbour and Kinvarra bay). Our result (89%) is located within this range. For coastal systems with limited surface runoff, the ratio of NO_3^- in SGD published by Tait et al. (2014) is also comparable. DIN ratio at our study site is 69%, which is also consistent with observations in other coastal systems (Table VII.3). From these comparisons, previous definition in this section that SGD in the Ria Formosa can be confidently confirmed as the main stressor that leads to enrichment of NO_3^- or DIN in the system.

Table VII.3 Comparison of global N budgets in coastal semi-enclosed systems (bay and lagoon), in the table, F. indicates the abbreviation of flux, the unit for all fluxes is kg d^{-1}. Ratio indicates the portion between flux from SGD and total input sources.

Site	F. NO_3^-	Ratio	F. DIN	Ratio	F. DON	Ratio	Reference
Masan Bay			4.4×10^3	43%			Lee et al. 2009
Jeju Island			4.1×10^3	92%	1.8×10^3	98%	Kim et al. 2013
Patos lagoon	9.4×10^3	41%	3.4×10^4	55%			Niencheski et al. 2007
Wenchang lagoon	1.5×10^2	51%	1.6×10^2	37%	145.7	9 %	Liu et al. 2011
Hanalei Bay	12.4	73%	13.9	60%			Knee et al. 2008
Florida Bay	4.3×10^3	38%	2.0×10^4		8.1×10^3		Santos et al. 2008
Muri lagoon	27.4	87%	30.7	81%	12.7	13%	Tait et al. 2014
Tolo Harbour	1.0×10^4	99%	1.6×10^4	98%			Lee et al. 2012
Manila Bay			2.0×10^3	23%			Taniguchi et al. 2008
Kinvarra Bay	2.7×10^2	99%	2.7×10^2	95%	8.2	62%	Rocha et al. 2015
Ria Formosa	1.3×10^3	89%	1.3×10^3	69%	220	37%	This study

On a global scale, only a handful of research has been conducted on DON budgets in coastal semi-enclosed systems. However, research still evidenced SGD can be an important contributor to DON inventory in the receiving water with a maximum ratio of 98 % in Hwasun Bay (Kim et al. 2013). In the Ria Formosa, though SGD is not the

dominant source of DON, it still accounts for 37% of total DON input, which is parallel with global ranges.

VII.5.2 N circulation and turnover in the lagoon

Though SGD contributes large amounts of NO_3^-, results from the regional survey (Fig.VII.3) and fixed sites monitoring (Fig.VII.5) suggest concentrations of NO_3^- in lagoon water were relatively low. The difference between substantial NO_3^- input from SGD and limited enrichment in lagoon water indicates a rapid turnover of NO_3^- in the lagoon system. Based on a mass balance approach, capability of NO_3^- reduction in the lagoon was 69.9±68.5 μmol m^2 h^{-1}. In coastal systems, sediment is usually considered as an important reactor to process NO_3^- in the system via denitrification (Herbert 1999) and/or DNRA (Gardner et al. 2006; Rocha et al. 2015). However, previous studies evidenced that sediment from both intertidal and benthic regions in the Ria Formosa lagoon releases NO_3^- in to the overlaying water (Falcão and Vale 1990; Murray et al. 2006; Serpa et al. 2007; Falcão et al. 2009). It indicates that NO_3^- reducers in the sediment may not be active to create a net sink for NO_3^-. In addition, sediment lining the bottom of the lagoon also manifests relatively low diffusion rate of NH_4^+ (16.2 μmol m^{-2} h^{-1}, Synthesis report 2003), when compared to other coastal systems influenced by substantial SGD associated NO_3^-, e.g., NH_4^+ diffusion rate in the subtidal sediment in Kinvarra bay reached more than 400 μmol m^{-2} h^{-1} (Rocha et al. 2015). As the final product of DNRA, the diffusion rate of NH_4^+ represents the intensity of DNRA in the sediment (An and Gardner 2002). Consequently, contribution from the lagoon sediment to NO_3^- removal may be limited in the Ria Formosa. The factor that constrains NO_3^- removal in sediment may be low availability of NO_3^- in the sediment. In particular, owing to intensive mixing processes in the nearshore region (Uchiyama et al. 2000), substantial NO_3^- solutes from SGD is rapidly attenuated in lagoon water. It hampers the establishment of NO_3^- concentration gradient between lagoon water and porewater. In the benthic sediment, diffusion is the crucial pathway that transports

solute into sediment (Rocha 2008), and the concentration gradient is the only driving force in diffusion. As a result, SGD associated NO_3^- hardly intrudes into the sediment, which leads to a NO_3^- 'starving' status for reducers in the sediment.

Without active participation from sediment, the biogeochemical reactions in lagoon water are the only explanation for the intensive NO_3^- reduction. There are a number of distinct pathways in saline water that decrease NO_3^- concentration (Francis et al. 2007), including denitrification, anaerobic ammonium oxidation (Anammox) and DNRA. Denitrification and Anammox effectively reduce NO_3^- to N_2 while DNRA transforms NO_3^- to NH_4^+ (Fig.VII.8). Compared with NO_3^-, NH_4^+ is more prone to be consumed into biomass in the aquatic environment (Rice and Tiedje 1989). It can be assumed by diatom (Lomas and Glibert 1999) as well as blue-green and green algae (Rocha et al. 2002). Abundant seagrasses in Ria Formosa are also sensitive to change in NH_4^+ and capability to digest NH_4^+ rapidly (Wayland et al. 2008). In this study, NH_4^+ in the lagoon was rapidly removed at a rate of 62.8±15.0 μmol m^{-2} h^{-1}, which represents hydrophyte in the lagoon acting as an efficient NH_4^+ filter. By this line of reasoning, DNRA pathway in the lagoon does not decrease the risk from intensive NO_3^- input. Recent research has revealed high activity of DNRA in the oceanic environment (Lam et al. 2009; Jensen et al. 2011), ranging from 8.3 μmol m^{-2} h^{-1} to 175 μmol m^{-2} h^{-1} (Jensen et al. 2011). It suggests that a substantial portion of exogenous NO_3^- delivered from SGD may transfer into biomass in the Ria Formosa, indicating the lagoon faces the risks of algal blooms and subsequent hypoxia.

The circulation and turnover of DON in Ria Formosa lagoon differed from DIN. Generally, the DON concentration in the lagoon water is low. For instance, in the Great Barrier Reef, DON was the largest N species, with mean concentration ranging between 4 and 8 μM (Furnas et al. 2011). In Muri lagoon, another tropical lagoon, concentration of DON fell in the range of 0.1 to 20 μM (Tait et al. 2014). In comparison, concentrations of DON in Ria Formosa was in the range of 40 μM to 70 μM. In addition,

the mass balance showed a net increase of DON in lagoon water at a rate of 36.3±35.4 μmol m^2 h^{-1}. On the one hand, it suggests inactive consumption of DON in lagoon water. SGD is an important source of DON to the lagoon (Fig.VII.8). A portion of DON is marked as labile, in particular, amino acids (Ibánhez and Rocha 2014a), which can be used by heterotrophic bacteria (Ferguson et al. 2007). However, this easily utilised DON may be consumed in the subterranean estuary prior to discharge. Consequently, Tait et al. (2014) assumed DON from SGD is refractory. For the DON delivered by atmospheric deposition, Gari et al. (2014) suggests it is derived from particles emitted from the adjacent aquifer, which may also be refractory. As a result, DON in the lagoon may not be active in biogeochemical reactions. More importantly, the net increase of DON in the lagoon confirms the rapid procession of NH_4^+ into biomass since active production of DON may be linked to decomposition of organic debris in waters (Reckhardt et al. 2015). Recent studies of total dissolved nitrogen stable isotopes (^{15}N) over a coral reef by Thibodeau et al. (2013) indicated that there was higher DON concentration at low tides from the release of DON by organisms, which is in line with our observation. As a result, the net production of DON due to biomass increase confirms the presence of algal blooms triggered by NO_3^- injection from SGD.

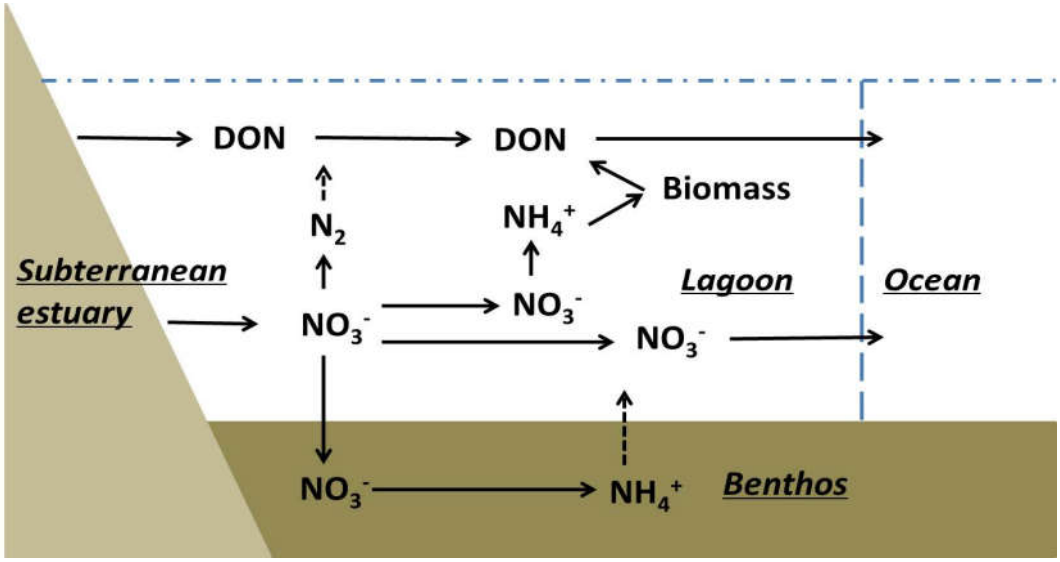

Figure VII.8 Conceptual representation of terrestrial groundwater-borne N cycling within Ria Formosa lagoon

As the connection zone between land and ocean, lagoons modulate influences of different terraneous impacts (Barnes 1980). In the Ria Formosa, due to active NO_3^- reduction in the lagoon, only 190 kg N-NO_3^- day^{-1} was delivered into ocean via tidal exchange, significantly reducing the likelihood of DIN enrichment in the adjacent ocean. In comparison, the lagoon is an intensive source of DON during summer though the subterranean estuary can effectively reduce DON from entering the lagoon. Approximately 526 kg N-DON day^{-1} was delivered to the adjacent ocean. Currently, the research of the concentrations and impacts of DON in coastal water is limited. It is difficult to deduce the actual bioavailability of DON in biogeochemical circulation since it is a continuum with different molecular weights. This labile part can be rapidly circulated, possibly consumed within hours (Carlson and Ducklow 1995). The remaining fraction of DON, especially DON from terrestrial groundwater, is largely recalcitrant, which may be buried in the sediment.

VII.5.3 Further consideration of N fluxes from SGD between distinct methods

In the section VII.4.2, the N fluxes on the basis of the ratio of fresh groundwater and recycled seawater in total SGD were reached. These compositions are derived from linear regression curves between piezometric head and hydraulic composition data obtained from the field survey in 2006. However, the survey result from 2010 to 2011 (Chapter V) displayed that the salinity of beach porewater was constantly higher than 32 psu. It suggests a relatively less fresh compartment in total SGD. Here, we introduce another scenario of hydraulic composition in SGD. The pressure head in the boreholes was also treated as a reference to deduce the portion of fresh groundwater in SGD. In particular, in December 2010, measurements of piezometric head in different boreholes were similar to those recorded in May 2010 (Fig.VII.9). Furthermore, paired t-test analysis confirms an insignificant difference in pressure head between these two months for all six boreholes (P=0.75). In December 2010, the salinity in the subterranean estuary at the lagoon barrier was, in fact, approximately

34.7 psu, indicating only 5% of fresh compartment in the total SGD, as shown in Table VII.4.

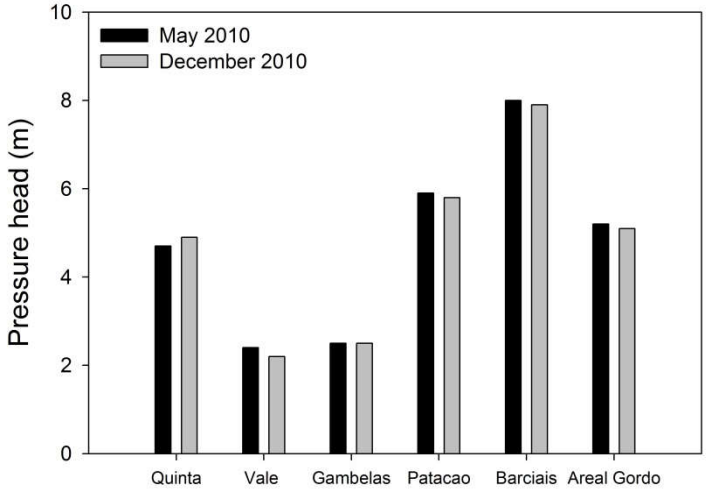

Figure VII.9 Pressure head in sampled boreholes in May 2010 and December 2010

Based on this deduction, the magnitude of extraneous NO_3^- fluxes from SGD significantly decreases (3rd scenario in Table VII.4), dropping to 181.6 kg day^{-1}. Accordingly, the magnitude of DON fluxes declined to 23.5 kg day^{-1}. This substantial difference in magnitude of N fluxes between two estimations suggests the importance in establishing the correct definition of hydraulic composition in SGD, which was largely ignored in previous studies. In this study, it is difficult to unilaterally quantify this on the basis of current data. However, it is important to show the coexistence of different probabilities in the current quantification approach, which would be an important research subject for future studies. In addition, this difference also provides important information for coastal management by indicating the risk in regional quantification of nutrient fluxes on the basis of simple hydraulic deduction. Particularly problematic is the calculation on the basis of hydraulic measurement over different years, which requires an identical environmental setting in the survey region over the years being studied. However, any changes in land-use may alter the sub-surface flow path and subsequently influence the discharge rate of fresh groundwater in the coastal line. In this study, the difference in hydraulic composition may result from excavation

of additional boreholes in Faro airport. The groundwater extraction from these boreholes possibly decreased hydraulic pressure that controls seepage of fresh groundwater in permeable beaches.

Table VII.4 Comparison between different scenarios of N fluxes delivered from fresh SGD

Scenario	Fresh %	$[NO_3^-]$ mg l^{-1}	$F.NO_3^-$ kg day^{-1}	[DON] mg l^{-1}	F.DON kg day^{-1}
1st	35.8	22.4	1.3×10^3	2.9	168.2
2nd	35.8	74.2	4.3×10^3	436.8	2.5×10^4
3rd	5	22.4	181.6	2.9	23.5
4th	5	74.2	600.7	436.8	3.5×10^3

In section VII.4.2, the quantification of SGD was based on the conservative N concentrations from the groundwater endmember. In Table VII.4, we also included N concentration values for the terrestrial groundwater endmember on the basis of regression results from December 2010 and January 2011. Briefly, during these two months, due to intensive mineralisation and nitrification in the subterranean estuary (Chapter V), both NO_3^- and DON concentrations in the terrestrial groundwater endmember significantly increased, reaching 74.2 mg l^{-1} and 436.8 mg l^{-1}. Accordingly, potential fluxes of NO_3^- and DON from fresh SGD drastically increased (2nd scenario), reaching 4.3×10^3 kg day^{-1} and 2.5×10^4 kg day^{-1}, respectively. Even in the scenario (4) with 5% fresh composition, the magnitude of NO_3^- fluxes may be 600.7 kg day^{-1}. This comparison suggests the importance of the subterranean estuary in the modulation of N fluxes from SGD. Currently, the mediation role played by subterranean estuaries are seldom considered in quantification works for SGD-borne nutrient. The significant difference presented in this section highlights the necessity to include the influences of subterranean estuaries in nutrient mass balance estimations.

VII.5.4 Limitation in N transformation rate

As a classical approach, mass balance could reveal nutrient budget and nutrient transformation rates within a system. One of the most important assumptions in the mass balance approach is the conservative propagation between two end-locations. However, the Ria Formosa lagoon is a multi-inlet, complex hydraulic system (Cravo et al. 2013). As Fig.VII.1 shows, there are several branches along the channel between the two survey locations. Consequently, there are frequent water exchanges between the main channel and branches. In addition, lagoon water flows freely over the flats, i.e., the bank of the channel, and transports into other regions during flood tides. The channel also receives waters from other channels at ebb tide. As a result, there is a miscalculation of the material balance between the two end-locations that are derived from other parts of the lagoon, without passing through the two end sectors. These environmental settings are contrary to the requirement of mass balance approach. However, in this research, due to the insufficiency of field researchers, the fixed location survey was only conducted at two ends of the channel. As a result, it might introduce uncertainties in the estimation of the N reaction rate, as well as the result of salinity in lagoon water.

VII.6 Conclusions

This study shows that high N fluxes discharge via the SGD pathway into the Ria Formosa lagoon. Due to high concentration of NO_3^- in continental groundwater, SGD is the dominant contributor of allochthonous NO_3^- fluxes to the lagoon. In addition, SGD also contributes 168.2 kg day^{-1} exogenous DON to the lagoon. Even though the SGD-borne NO_3^- can be rapidly removed in the lagoon water via denitrification, the intrusion of NO_3^- enriched terrestrial groundwater was still a risk to the lagoon system, which likely triggers algae blooms and leads to seasonal hypoxia. In comparison, the majority of DON in SGD is recalcitrant, which is difficult to be evolved in N circulation.

Hence, approximately 582 kg N-DON day^{-1} was delivered to the adjacent ocean every day. Based on current results, in order to reduce environmental risk of excess N, proper management of N inputs from fresh SGD is urgently needed. However, these N fluxes discharged into the lagoon can be traced back to historical pollution several decades ago. Hence, long term regulation and research monitoring are necessary.

Chapter VIII

The variation of nutrient ratios and limiting nutrients in Submarine Groundwater Discharge

VIII.1 Abstract

SGD has been recognised as an important nutrient deliverer in coastal regions. Nutrient structure, namely, nutrient ratios and limiting nutrients, in SGD may significantly influence nutrient equilibrium in the receiving water, subsequently disturbing ecological structures. Because SGD usually consists of fresh groundwater and recycled saline water, nutrient ratios and limiting nutrient in SGD may vary significantly in different mixing ratios. To understand variations of nutrient structure in SGD, an annual field survey in the barrier island at the Ria Formosa lagoon was conducted. The limiting nutrient along the salinity gradient was examined via a combination of frequency analysis and Dirichlet regression. Results indicate that the limiting nutrient in SGD can vary between N and P in both spring and autumn. Furthermore, in autumn, the occurrence of Si-limitation in SGD was observed, which may result from the increase of nitrate (NO_3^-) concentration in terrestrial groundwater and the presence of a spectrum of biogeochemical reactions in the subterranean estuary, especially at the seepage face. Since SGD is the dominant nutrient input source in the Ria Formosa, the shift of limiting nutrient in SGD might be the major reason for spring green algae blooms in the lagoon. To constrain the impact from SGD to ecological structures in the lagoon, two possible regulation methods, reduction of the NO_3^- concentration in terrestrial groundwater and proper management on groundwater source, need to be included into future regulation.

VIII.2 Introduction

SGD is 'any and all flow of water on continental margins from the seabed to the coastal ocean, regardless of the fluid composition or driving forces' (Burnett et al. 2003). It usually consists of meteoric water and recycled saline water (Taniguchi et al. 2002). Different from riverine injection, SGD occurs as diffusive flows, and injects to the coast wherever a coastal permeable aquifer is connected to the sea with a positive head relative to the sea level (Johannes 1980; Burnett et al. 2001). Previous research frequently ignored nutrient delivery capability of SGD (Burnett et al. 2003) since SGD only represents 5% to 10% (2400 km^3 yr^{-1}) of the total fresh water discharge to the ocean (Zektser and Loaiciga 1993). However, growing evidence suggests that SGD acts as an important nutrient deliverer, particularly when originating from contaminated continental aquifers (Lee and Olsen 1985; Cable et al. 1997; Valiela et al. 1999; Ullman et al. 2003; Leote et al. 2008; Santos et al. 2008; Rocha et al. 2015). Recent studies based on radium isotope suggested that SGD is deemed to be responsible for more than 50% of the total dissolved salts crossing the land-ocean interface (Moore 2010).

Despite that the elevated magnitude of nutrient fluxes associated with SGD in more than 40 study sites has been evaluated on a global scale (Zhang and Mandal 2012), our understanding of nutrient structure, namely, ratios between different nutrient elements and limiting nutrient, in SGD remains incomplete. In ocean research, limiting nutrient can be defined as the nutrient in shortest supply relative to average composition of nutrients assimilated in algae with the so-called Redfield ratio (Redfield 1958), which reflects the general nutrient need from algae in seawater (Hodgkiss and Ho 1997; Chen et al. 2013). Currently, the existing research with regard to the nutrient structure in SGD mainly assumed that the limiting nutrient in SGD is consistent with that in the terrestrial endmember (e.g. Lee and Kim 2007; Taniguchi et al. 2008; Wu et al. 2013). Indeed, nutrient concentration in the terrestrial groundwater significantly influences the nutrient structure in SGD. However, SGD usually is a mixture between

freshwater and recycled seawater; consequently, the nutrient structure in SGD is depending on contributions from both endmembers. In particular, the composition between recycled seawater and fresh groundwater varies significantly on spatial and temporal scales (Johannes and Hearn 1985; Burnett et al. 2003; Leote et al. 2008; Weinstein et al. 2011). In field measurements, these different mixing ratios usually can be witnessed as a spectrum of salinity values (e.g. Swarzenski et al. 2007; Leote et al. 2008). More importantly, terrestrial groundwater and recycled saline water intensively mix in subterranean estuaries, i.e. the mixing zone between fresh groundwater and recycled seawater in coastal aquifers (Moore 1999). Recent research has identified subterranean estuaries as an active nutrient reactor (Nowicki et al. 1999; Ueda et al. 2003; Kroeger and Charette 2008; Spiteri et al. 2008; Rocha et al. 2009; Erler et al. 2014a) because of interactions between porewater and sediment particles, microbial activity, physical and chemical gradients during mixing process and ion activity modulation by changing ionic strength (Moore 1999; Moore 2010). Consequently, nutrient concentration ratio among different elements and limiting nutrient in SGD may be highly dynamic.

As an important nutrient vector (Moore 2010)**,** the nutrient structure in SGD can significantly influence the nutrient equilibrium in the receiving water. Research has shown that the temporal alternation of limiting nutrient due to shift of nutrient equilibrium usually combines with biomass increase of opportunistic species (Justić et al. 1995a). The long term replacement can shift ecological structures in coastal waters, varying from seasonal (Lopes et al. 2007) to permanent (Rabalais et al. 1996). This is often associated with harmful algae blooms (HABs) and hypoxia (Rabalais et al. 1996; Zingone and Enevoldsen 2000), which threatens coastal fisheries and tourism development, subsequently causes great loss in economics (Chen et al. 2013).

Due to the widespread occurrence of nutrient delivery from SGD and its potential impact on the ecology of coastal zones, comprehensive research on nutrient ratios and

limiting nutrient in SGD is highly necessary. Here, an annual survey was conducted on one of the barrier islands surrounding the Ria Formosa lagoon. The distribution and variation of limiting nutrient among N, P, and Si along salinity gradient were temporally examined via a combination of frequency analysis and Dirichlet regression. The main objective of this study is to determine the temporal variation of nutrient ratios and limiting nutrient in SGD. The results from this research will benefit future management in regulating nutrient balance in SGD.

VIII.3 Material and methods

VIII.3.1 Study site

Ria Formosa lagoon is located in the south of Portugal (Fig.VIII.1), extending from 36°58'N 8°20'W to 37°30'N 7°32'W, covering a large proportion of the Algarve coastal area (Andrade et al. 2004). It is a shallow coastal lagoon separated from the Atlantic Ocean by a chain of five barrier islands and two peninsulas with six inlets for the sea water and lagoon water exchange (Salles 2001; Pacheco et al. 2007). It has an area of approximately 170 km^2, with 55 km length and 2 m average depth (Andrade et al. 2004).

The Campina de Faro, a coastal plain, site of intensive agricultural activities lies directly north of the Ria Formosa's western sector. The Campina de Faro presents two main aquifers. The deeper aquifer is formed by Cretaceous limestone and the surficial formed by sands and gravels from Pilo-Quaternary. Both aquifers are connected through sub-horizontal Miocene sandy layers (Almeida et al. 2000). Since the early 1980s, the original vegetation cover in this coastal plain has been progressively replaced by farmlands of tomato, olive, and citrus trees. To meet the agricultural demands, intensive chemical fertiliser has been applied. Afterwards, heavy nitrate (NO_3^-) pollution in the surficial aquifer system was identified and then percolated into

the deeper region (Almeida and Silva 1987). Ferreira et al. (2007) suggested that the average NO_3^- concentration in groundwater was 2.1 mM over the entire aquifer systems with some samples containing in excess of 28.6 mM. Dissolved silicate (DSi, chemical formula: $Si(OH)_4$) in groundwater varied from 56 µM to 112 µM (Field survey in 2013). In contrast, P is easy to be adsorbed by iron oxidates and calcium carbonates (House and Donaldson 1986; Borggaard et al. 1990; Isenbeck-Schröter et al. 1993) and it is therefore unsurprising to observe low concentrations of P in groundwater. In particular, the concentrations of reactive soluble phosphate (SRP), total dissolved phosphate (TDP) and total phosphate (TP) in the sub-surface were below 0.3 µM (Field survey in 2013). As a result, the nutrient ratio of N:Si:P in fresh groundwater endmember highly deviates from the Redfield ratios (16:15:1, Leote and Epping 2015), the standard to distinguish limiting nutrients.

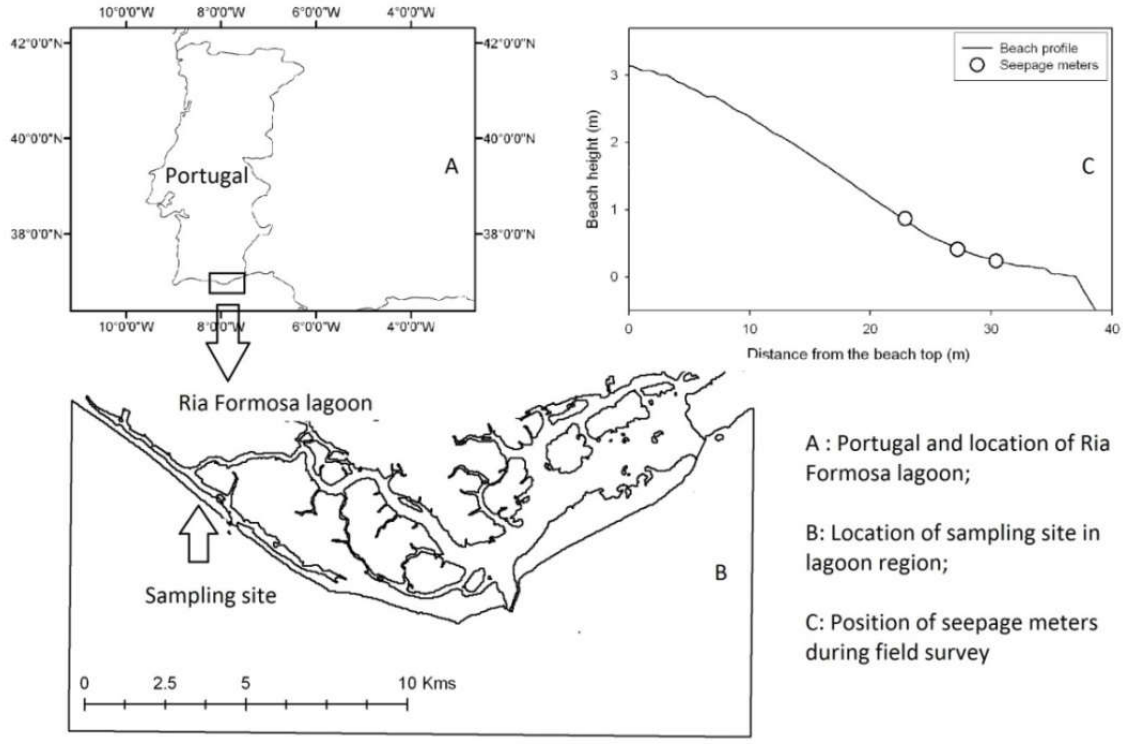

Figure VIII.1 Map of the study site, modified from Leote et al., (2008).

VIII.3.2 Sampling location

Field campaigns were conducted on a beach at the inner side of the Ancão peninsula, facing towards the major water channel leading to Faro—''Esteiro do Ramalhete'' (Fig.1). The sediment at the research site is medium sand with a median grain-size (d50) of 0.44 mm. The content of clay+silt ranged from 0.8% to 1.6%. The mean sediment porosity is 0.35, with hydraulic conductivity of 5.5×10^{-3} cm s^{-1} (Rocha et al. 2009).

The discharge rate measured by seepage meter in the study site showed an intrinsic relationship with tidal cycles. It usually peaked at low tide and decreased significantly during the high tide. (Leote et al. 2008). The maximum discharge rate was 190.6 cm day^{-1}, while the lowest value was only 1.7 cm day^{-1} (Rocha et al. 2009). The water temperature in the beach porewater ranged from 10.3°C in December to 26.1°C in July. The salinity in collected water samples fell in the range between 16.2 psu to 38.3 psu.

VIII.3.3 Sampling strategy

The field survey presented in this chapter is part of O-DOIS project (2005-2007). The original data used in this chapter was published by Leote et al. (2008). This chapter focused on data reanalysis for the new research question, i.e. the nutrient structure and limiting nutrients in SGD.

In the beach surveys, four to six Lee-type (Lee 1977) seepage meters connected to collecting bags were deployed along the beach profile (C in Fig.VIII.1). The seepage meters were deployed at a low tide and stabilised for 24 hours prior to water collections. The monthly field trips lasted from January to December in 2006. Field campaigns were conducted during each spring tide and the collection work covered

two successive tidal cycles. The water gathered in seepage collecting bags was analysed *in-situ* with an YSI 600 multi-parameter probe (Yellowspring Instruments®) for salinity. Hereafter, water samples were filtered with ultra-filtration membrane samplers (Rhizon SMS, Eijkelkamp Agriresearch Equipment®) with a pore diameter of 0.1 µm, into non-additive vacutainers for dissolved nutrient analysis. The samplers were flushed with sample water three times prior to the collection of filtrate to avoid interferences of the solute adsorption on the membranes (Ibánhez and Rocha 2014b).

VIII.3.4 Nutrient determination

SGD is a nutrient source for both inorganic and organic components. Compared with organic nutrients, inorganic compounds are prone to be assimilated by algae and seagrass (Furnas et al. 2005; Tait et al. 2014). Hence, inorganic nutrient composition and relative ratios play more important role to influence trophic structures. By this line of reasoning, this study focused on the nutrient structure of inorganic composition in SGD.

Concentrations of nitrite (NO_2^-), ammonium (NH_4^+) and DSi were determined following the spectrophotometric methods described by Grasshoff et al. (2009). Concentration of NO_3^- was quantified by cadmium reduction approach described by Jones (1984). The determination method for SRP is based on the colorimetric methodology (Eisenreich et al. 1975). Although SRP includes a portion of organic P (Tarapchak and Rubitschun 1981), it is still identified as one of the most bioactive P species in natural water (Nürnberg and Peters 1984; Haygarth and Sharpley 2000; Takano and Hino 2000), which can be assimilated into biomass as rapid as inorganic N and DSi. The method detection limit (MDL) for each analyte determination was calculated (NO_3^- 0.08 µM, NO_2^- 0.06 µM, NH_4^+ 0.09 µM, DSi 0.05 µM, SRP: 0.09 µM) on the basis of US EPA recommendations (e.g. Clayton et al. 1987).

VIII.3.5 Frequency calculation and Dirichlet regression

In this study, the distribution of limiting nutrient along salinity gradient was first analysed by the frequency calculation. In particular, the salinity range derived from entire water samples was divided into a number of compartments on the basis of total sample size. In each compartment, the frequency for an individual element that acts as the limiting nutrient on the basis of Redfield ratio was calculated by:

$$F_N = \frac{N_N}{N_N + N_{Si} + N_P} \quad (1)$$

where F_N is frequency of N-limitation scenario in a salinity compartment, N_N, N_{Si} and N_P are numbers of N-limitation, Si-limitation and P-limitation scenario in one salinity compartment. The same processing approach was applied on Si and P. Subsequently, the discrete frequencies from different intervals were simulated by Dirichlet regression (Aitchison 1986) to reveal the variation of limiting nutrient in entire salinity continuum. Here, a quadratic regression system was designed, which was expressed as following:

$$F_N^S = A_1 S^2 + B_1 S + C_1 \quad (2)$$

$$F_{DSi}^S = A_2 S^2 + B_2 S + C_2 \quad (3)$$

$$F_P^S = A_3 S^2 + B_3 S + C_3 \quad (4)$$

$$1 = F_N + F_{Si} + F_P \quad (5)$$

where F_N^S, F_{DSi}^S, and F_P^S are simulated frequencies for N, Si and P on the basis of initial frequency results, S is salinity, and all the characters of A, B, and C are terms generated in the quadratic regression system. Eq. (2), (3) and (4) were regression

equations to stimulate distribution of individual frequency along salinity gradient. Eq. (5) was designed to constrain the total frequency during the calculation. Ideally, total frequency is 1. This regression system was solved on the basis of minimising standard error approach (e.g. Ibánhez et al. 2011) in MATLAB®. In order to testify the reliability of the regression system, the correlation coefficient (R^2) from each polynomial curve was examined (Mullins 2003) according to:

$$\mathrm{R}_N^2 = 1 - \frac{\sum_{i=1}^{n}(F_{Ni} - F_{Ni}^S)}{\sum_{i=1}^{n}(F_{Ni} - F_{Ni}^a)} \quad (6)$$

where R_N^2 is correlation coefficient in N frequency regression, n is number of salinity intervals, F_{Ni} is frequency of N to be limitation in SGD within each salinity compartment on the basis of frequency transformation via Eq.(2), F_{Ni}^S is the frequency of N-limiting calculated from Dirichlet regression, and F_{Ni}^a is the mean frequency. The same procedure was applied for Si and P.

VIII.4 Results

VIII.4.1 Nutrients mixing

During the annual survey at the study site, concentration of NO_3^- in the seeping water varied significantly (Fig.VIII.2). The maximum concentration of NO_3^- in seeped water samples was 180.3 µM. The mixing conditions showed that concentrations of NO_3^- were related to salinity, suggesting the existence of a freshwater NO_3^- source. The mixing plots also showed a seasonal difference of the freshwater NO_3^- source, with a lower level of contamination from January to July and a higher pollution level from August to December. Consequently, the annual survey was divided into two terms: the spring term (January to July) and the autumn term (August to December). Compared with NO_3^-, concentrations of NH_4^+ and NO_2^- in the seeped beach water were limited. The maximum concentrations were only 17.2 µM (NH_4^+) and 7.1 µM (NO_2^-) and these

solutes were below 2 µM in more than 70% of the seepage meter samples. The dissolved inorganic nitrogen (DIN; NO_3^-+NO_2^-+NH_4^+) ranged from 1.7 µM to 184.3 µM, mainly depending on concentration of NO_3^-.

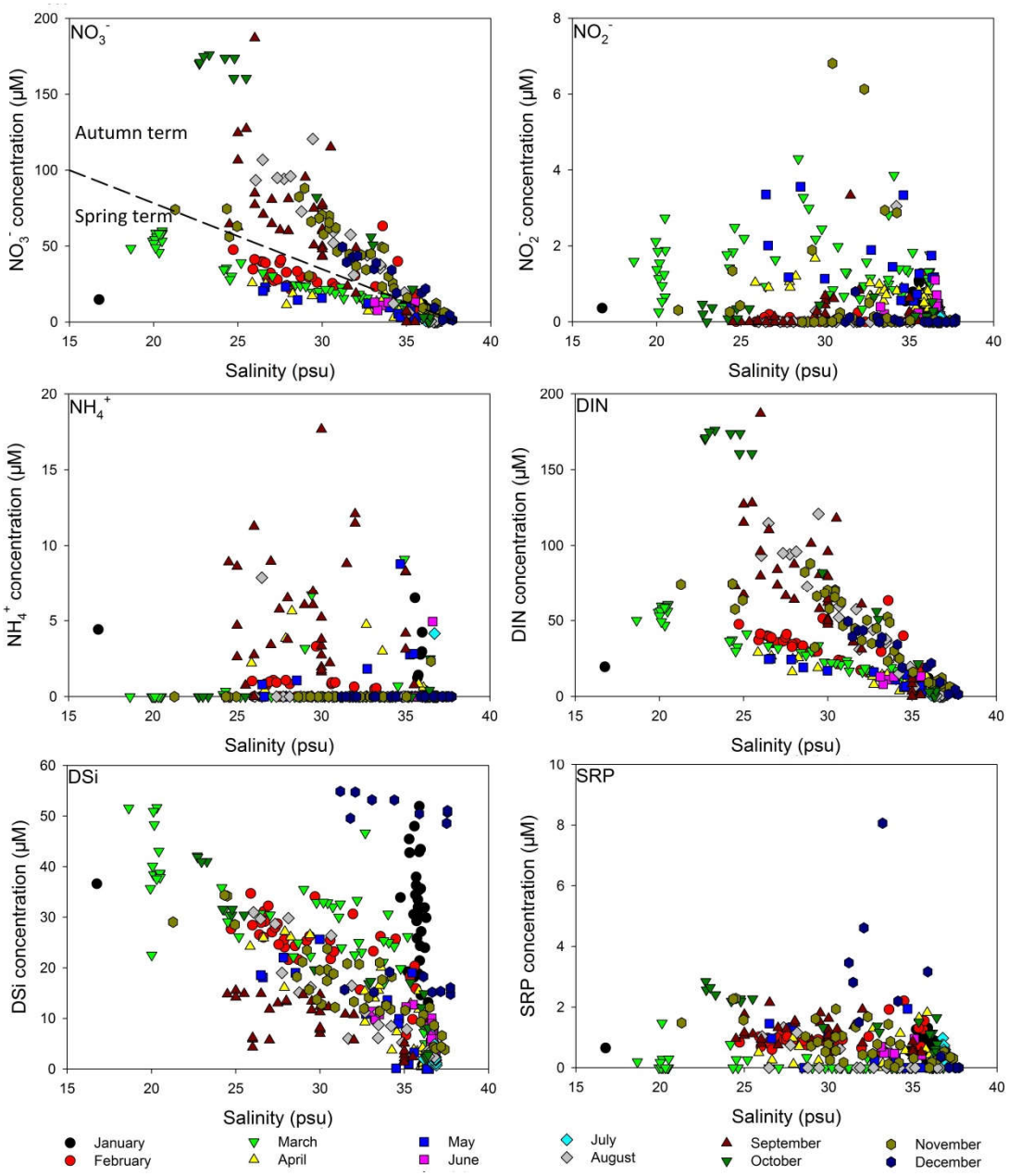

Figure VIII.2 Distribution of concentrations of different nutrient species along salinity gradient, including NO_3^-, NO_2^-, NH_4^+, DIN, DSi and SRP.

DSi concentrations in the SGD fell in the range from 0.3 µM to 55.3 µM. Different to NO_3^-, the maximum concentration of DSi in two terms can be witnessed in both saline water endmember (>36 psu) and brackish water endmember (<20 psu).

However, the minimum of DSi concentration in the saline water endmember was 0.3 μM, while it increased to 22.1 μM in brackish water endmember. This distribution pattern suggested the DSi concentration may depend on fresh input and generation in the permeable beach (Anschutz et al. 2009). Concentrations of SRP in more than 40 water samples were below MDL. The maximum concentration in remaining water samples was approximately 8 μM. It is worth noticing that seasonal variation pattern was not observed in distribution of NH_4^+, NO_2^-, DSi, and SRP.

VIII.4.2 Nutrient ratio in SGD

Nutrient ratios amongst N, P, and Si in the seeped water along the salinity gradient are shown in Fig.VIII.3. In some cases, the low level of SRP results in an extremely large ratio. Therefore, the maximum nutrient ratio in the plot was arbitrarily defined as 100. Compared to the Redfield threshold (dash line in the figure, i.e. N:Si:P is 16:15:1, Leote and Epping 2015), in the spring term, when salinity was below 32 psu, the ratio between N and P in all the water samples exceeded 16:1, indicating abundant N in the SGD. As salinity increased in the seeped water, the ratio in a number of samples dropped below the Redfield threshold. In the seawater endmember, the minimum ratio N:P (0.4) was observed. Similarly, the ratio between Si and P in the spring survey fluctuated around the Redfield threshold along the mixing gradient. In the plot, water samples with low salinity concentrated in the region with high S:P ratio and vice versa. In comparison, the pattern of N:Si ratio is different. When the salinity was below 30, the ratio between N:Si fell in the range, from 0.5 to 2. Whereas, the sample near seawater endmember hosted higher ratio in N:Si, reaching a level of 18.5.

In the autumn term, NO_3^- level at terrestrial groundwater endmember significantly increased (Fig.VIII.2). Correspondingly, ratio of N:P in more than 70% samples was above the Redfield boundary. With an increase of salinity, the ratio started declining, falling to 0.8 (Fig.VIII.3). Compared to the spring survey, water samples with high

terrestrial groundwater composition in the autumn frequently presented low Si:P ratio. For instance, the water sample in a salinity of 25 psu, the ratio was only 8. For the ratio of N:Si, the maximum value was 16.2, which was observed in a salinity value of 26. When salinity was above 31.2 psu, ratio of N:Si declined to a level below the Redfield ratio.

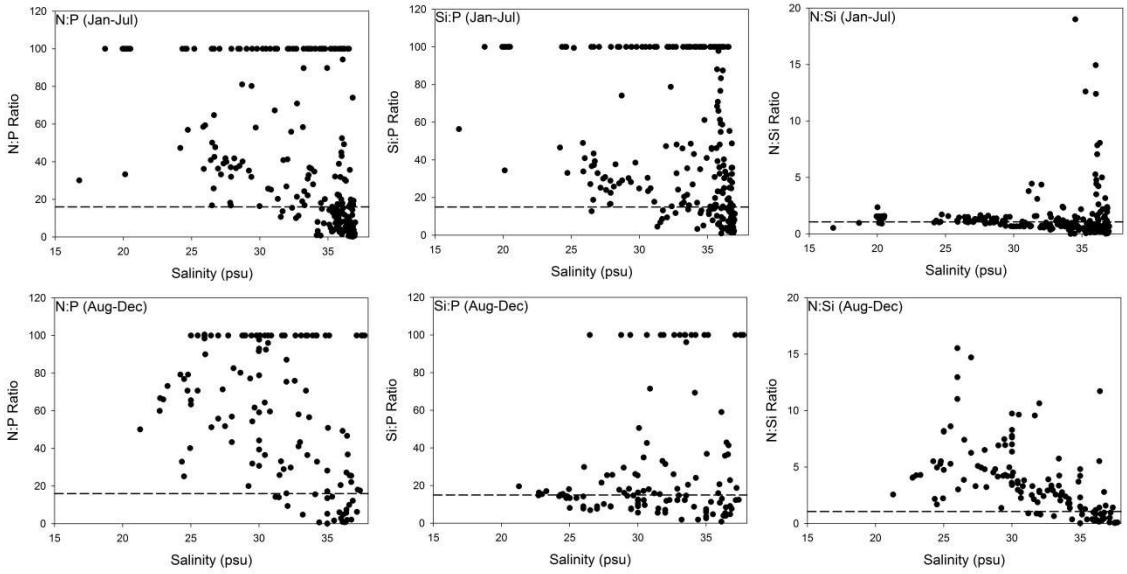

Figure VIII.3 Nutrient ratio in water samples, those theoretical thresholds (dash line) were calculated on the basis of nutrient composition in Redfield ratio (I also changed the salinity axis).

VIII.4.3 Limiting nutrient in SGD

For limiting nutrient in SGD, in Fig.VIII.4 (A), molar quotients between the in situ concentrations of potentially limiting nutrients are delimited by the N:P = 16, N:Si = 1.06, and Si:P = 15 lines (method derived from Rocha et al. 2002). These define 6 different areas within the figure, with each characterised by the potentially limiting nutrients in the order of priority (see B in Fig.VIII.4).

In the figure (A), it can be seen that limiting nutrient in SGD fluctuated between N, Si and P, instead of a constant element. In addition, variation of terrestrial inputs influenced the distribution pattern in the coordinate system. Specifically, from January to July (open circle), water samples tended to be N-limitation or P-limitation. From

August to December, P was also scarcity in the seeped water, the ratio between N:P reached 100 in more than 10 water samples, whereas, the occurrence of Si-limitation was frequent observed when compared to the spring term. In particular, approximately half samples can be identified as Si-limitation during the autumn survey. In contrast, less than 30% of water samples showed a lack of DSi in the spring.

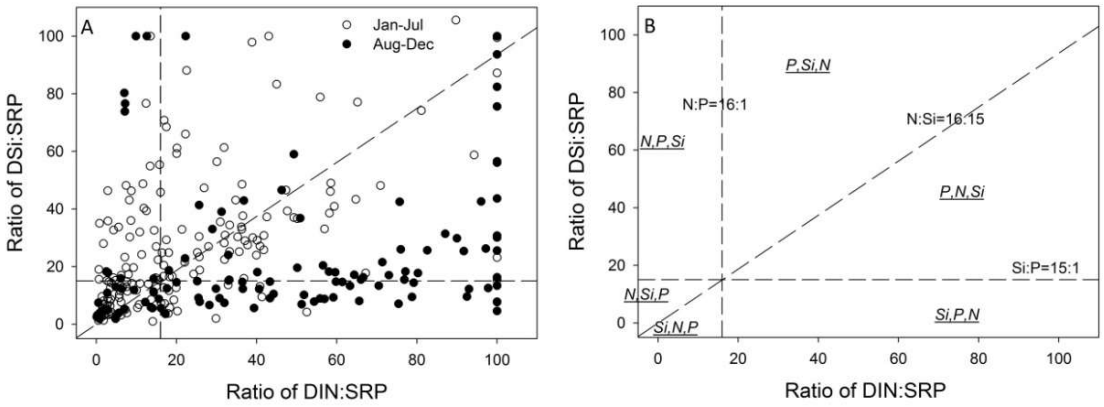

Figure VIII.4 The plot (A) shows distribution of limiting nutrient. The graph (B) displays the order nutrient limitation, the first nutrient is limiting nutrient in this compartment.

VIII.4.4 Frequency analysis and Dirichlet regression

To reach a better understanding of the variation of limiting nutrient in different mixing degrees, the distribution of limiting nutrient along salinity gradient was examined by the frequency analysis (Fig.VIII.5). From January to July, the entire salinity range was divided into seven intervals. The frequency in each limitation scenario is the quotient of number of occurrence to sample size. For instance, in the low salinity interval (below 25 psu), P-limitation frequency was 100%, which indicates all water samples were scarcity of P. In the range from 25 psu to 28 psu, Si started to be a limiting factor in SGD, accounting for 4% in total frequency. In the fourth interval (31 psu to 33 psu), approximately 14% water samples were lack of N. With further increase of salinity, frequency of N-limitation enlarges and finally overwhelms other frequencies in the salinity range of 35 psu to 36 psu. At the highest salinity range, frequency of N-limitation reached 56.6%, while P-limitation and Si-limitation shrank to 32.5% and 10.9%, respectively.

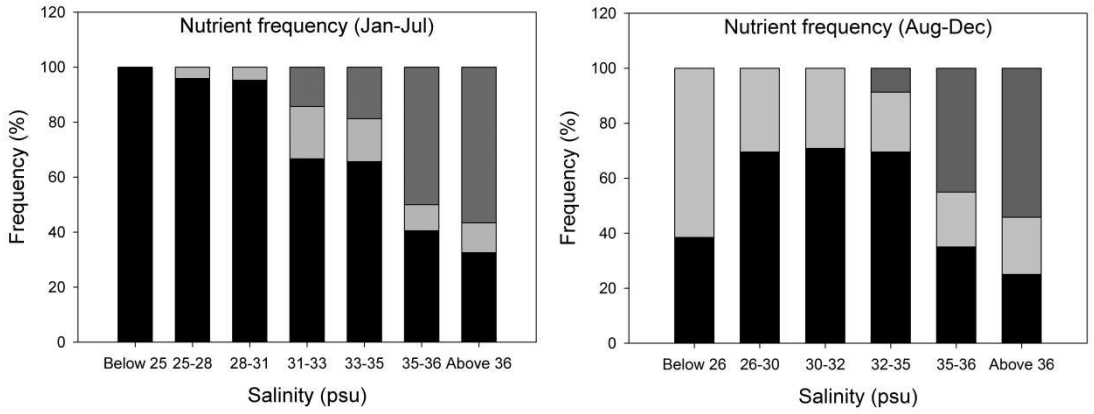

Figure VIII.5 The frequency distribution in two different kinds of water samples in two sampling periods, the black bar indicates frequency of P that acts as limiting nutrient element, the light grey bar is frequency of Si as limiting nutrient in water samples, and the dark grey bar is frequency of N scarcity in water samples

From August to December, six salinity intervals were designed due to less water samples were collected. In the lowest salinity range, frequency of Si-limitation accounted for 62.5% in total possibilities, indicating the majority of water samples were scarcity of DSi. Concomitantly, the likelihood of P-limitation was 38%. At higher salinity, the occurrence of Si-limitation decreased. In contrast, the possibility of P-limitation increased as salinity rose. In the interval of 32 psu to 35 psu, N started to be limiting factor in the seeped water and the frequency was 8%. Afterwards, it rose to 44% and peaks with a frequency of 54%. Concurrently, frequencies of P-limitation and Si-limitation dropped to 25.1% and 21.2%, respectively.

Based on the frequency analysis, the Dirichlet regression system was practiced and the best fitted curves were displayed in Fig.VIII.6. The regression system smooths small fluctuations in frequency and transforms the distribution into a continuum, which facilitates observation of dynamic variation of limiting nutrient along the salinity gradient. The total simulated frequencies in the two periods considered fluctuated between 94.5% and 105.3%, approximately 5% statistical error. The correlation coefficient (R^2) for each regression was calculated on the basis of Eq. (8). During the spring survey, the values of R^2 ranged from 0.85 to 0.94. In the autumn term, the

coefficients of N and P dropped. The reason for the decrease can be explained by the reduction of the salinity intervals. However, the minimum R^2 is 0.82, which suggests that our regression is still highly reliable (Mullins 2003).

Table VIII.1 R^2 for individual element from regression trend in two survey terms

Term	Jan-Jul	Aug-Dec
R^2 (N)	0.94	0.91
R^2 (Si)	0.85	0.90
R^2 (P)	0.93	0.82

In the spring term, the dominant trend varied between P-limitation and N-limitation along the entire mixing gradient and the shift occurs at the 35.4 psu salinity threshold (vertical line Figure VIII.6). During this term, the likelihood of Si-limitation never overwhelmed the others, which indicated limiting nutrient was either N or P in the SGD during that period. In contrast, in the autumn term, the dominant position shifted among all three elements, which suggested SGD is also possible to be Si-limitation. In particular, below the level of 26.8 psu, SGD can be identified as Si-limitation. In the interval from 26.8 psu to 35.5 psu, dominance of P-limitation can be witnessed in SGD. N-limitation can be the most frequent observed in SGD when the salinity was above 35.5 psu.

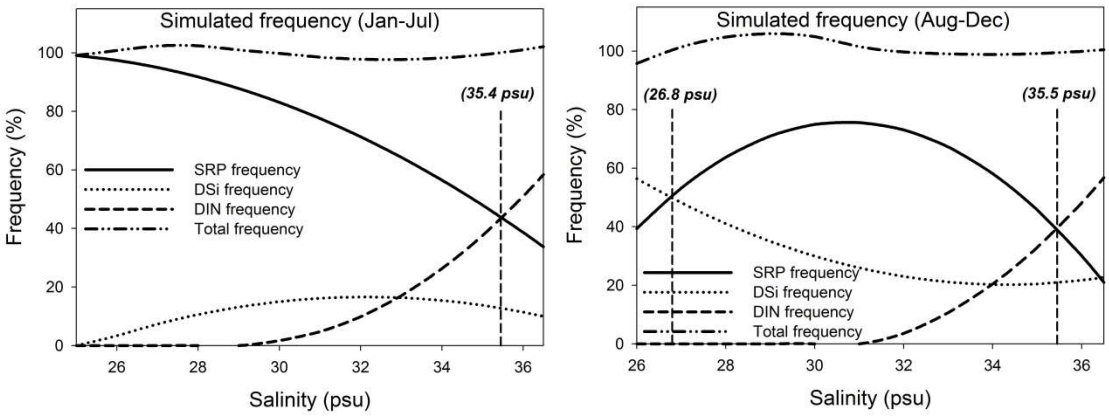

Figure VIII.6 Simulated result for the possibility of a given nutrient element as limiting factor along salinity gradient, the vertical line indicates the critical value in the shift of dominant limitation trend.

VIII.5 Discussion

VIII.5.1 Importance of frequency analysis in nutrient structure study

Previous studies in nutrient ratios and limiting nutrient associated with SGD focused on nutrient composition in terrestrial groundwater endmember (Lee and Kim 2007; Taniguchi et al. 2008; Wu et al. 2013) and assumed that the nutrient composition along mixing gradient can be determined as the linear mixing, like the trend displayed in estuaries (Neill 2005). However, the results in this study suggest that nutrient ratios (Fig.VIII.4) and the limiting factor (Fig.VIII.5) in SGD are variable. For instance, the water samples with identical salinity can be characterised with different nutrient ratios and limiting nutrient. The variability can be explained by a spectrum of modulating pathways in subterranean estuaries (Santoro 2010), especially in the seepage face, where has been highlighted as an active reactor for nutrients and other solutes (Ibánhez et al. 2011; Ibánhez et al. 2013, Ibánhez and Rocha 2014a). The possible pathways with regard to nutrient mediation in subterranean estuaries are displayed in Fig.VIII.7. For DIN, subterranean estuaries can decrease DIN concentration via canonical denitrification or anaerobic ammonium oxidation (Burgin and Hamilton 2007). Alternatively, enhancement of DIN fluxes was also witnessed in the permeable sediment, resulting from remineralisation of pelagic particles (Ibánhez et al. 2013) and/or N fixation (Santoro 2010). Apart from the decomposition of organic matter (Santos et al. 2009), the SRP concentration in subterranean estuaries can be mediated by the adsorption-desorption balance (Fig.VIII.7). The redox potential (Slomp and Van Cappellen 2004) and pH (Spiteri et al. 2006) are important factors that determine the behaviour of redox sensitive P and iron bounded P in sediments. The variation of dissolved oxygen in benthic environment due to porewater circulation and benthic reactivity (Ibánhez and Rocha in press) also impacts the sorption dynamic of SRP (Hupfer and Lewandowski 2008). Furthermore, the sediment organic matter is assumed to be the major carbon source for NO_3^- reducers in aerobic sediments

(Chapter VI; Addy et al. 2005), indicating that NO_3^- reduction may result to releasing of organic bounded P from the sediment surface into porewater. The permeable beach is also active in Si generation due to continuous decomposition of quartz (Anschutz et al. 2009; Chassagne et al. 2012). As a consequence, the possible coexistence of different reactive pathways raises uncertainness in nutrient ratios and limitation factor in SGD. In addition, coastal sediment is heterogeneous in hydraulic conductivity and porosity (Holland and Elmore 2008; Rocha et al. 2009), which leads to different reaction time length of porewater (Santos et al. 2012b), subsequently introducing additional uncertainties in nutrient structure in SGD. The gradient of bacterial biomass (Parkes et al. 2000) and preferential assimilation in bacteria community (Tobias et al. 2003) are also important reasons to explain the variability.

The high fluctuation of nutrient composition introduces difficulties to predict the nutrient structure in SGD. The classical approach, such as the scatter plot in Fig.VIII.4 and Fig.VIII.5, only provides the chance to observe the general trend between nutrient limitation and composition of terrestrial groundwater in SGD, whereas it is difficult to deduce a formulistic relationship. In addition, the approach that is used in estuary (Neill 2005) needs a relative homogeneous environment during mixing, which conflicts with the environmental setting in coastal permeable sediments. Therefore, it is necessary to introduce new methods into the limiting nutrient study in SGD. As an effective method that could smooth the uncertainty and highlights the dominant trend among all the possibilities, the frequency analysis have been used in determination of seasonal variation of limiting nutrient in surface runoff and estuary (e.g. Justić et al. 1995b). Compared with the traditional viewpoint that emphasised the certainty of limiting nutrient in SGD (e.g. Slomp and Van Cappellen 2004), frequency represents the possibility of occurrence, which is consistent with the heterogeneous setting in the coast line. In addition, combined with Dirichlet regression, the discrete data generated from frequency analysis can be transformed to a continuum, which successfully reveals variations of limiting nutrient in different mixing ratios. Compared to previous

approach, the new approach could predict the transition of limiting nutrient along mixing gradient and the regression formula may support coastal management, especially in the evaluation of cost performance.

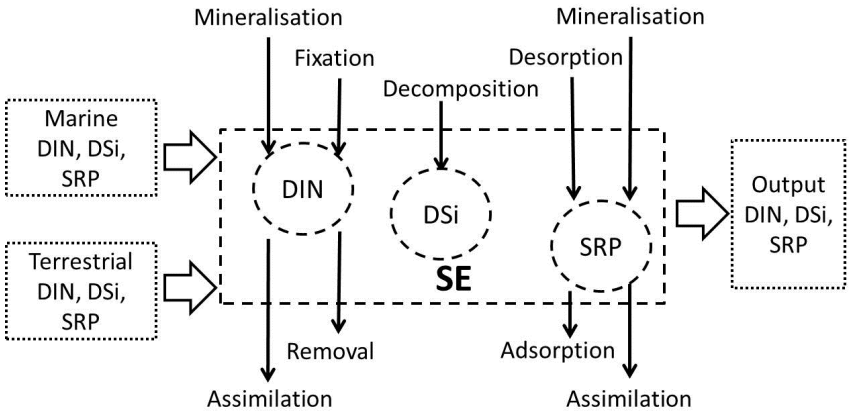

Figure VIII.7 Possible modulation pathways for DIN, DSi and SRP in subterranean estuaries (SE)

VIII.5.2 P-limitation, N-limitation and linkage to algae transition in the lagoon

In coastal research, SGD is reported as fluid with enrichment of terrigenous N and scarcity of P. As a consequence, Slomp and Van Cappellen (2004) suggested P is constant limitation in SGD, predicating coastal zones may face the ineluctably destiny of P-limitation, especially in the region that SGD has been defined as the major nutrient source. In the results, a shift between N-limitation and P-limitation as the dominant likelihood in SGD was evidenced. The transition is related with composition of terrestrial groundwater. In both spring and autumn terms, the transition occurred at a specific salinity boundary, approximately 35.5 psu, i.e. 2.7% of terrestrial groundwater in total SGD. The existence of this boundary can be explained by seawater dilution and biogeochemical modulation in the subterranean estuary. Compared to the mediation from the subterranean estuary, the dilution effect was limited since nutrient ratios in terrestrial groundwater are highly deviated from the Redfield ratios (concentration values in section VIII.3.2). Once the composition of terrestrial groundwater surpasses the boundary, the frequency of N-limitation shrank and P-limitation developed to be the dominance.

The oscillation between N-limitation and P-limitation is an important factor in the succession of flagellate communities. Previous study evidenced that blue-green and green algae only requires lower amount of P, and green algae are poor N competitors (Sommer 1989). Therefore, they have an ecological advantage in ecosystems with high N:P accessibility ratios (Rocha et al. 2002). The Ria Formosa is controlled by Mediterranean weather, and therefore rainfall concentrates in winter and spring seasons (Newton and Mudge 2003). Accordingly, the terrestrial groundwater pressure head in spring term is elevated, as can be seen in Fig.VIII.8 (A) (data from www.snrih.pt). It likely leads to an increase of fresh water component in SGD. Subsequently, P-limitation may become a major trend. As the dominant nutrient deliver in the lagoon system (Chapter VII), SGD in the spring term potentially results in a shortage of P and enrichment of N in lagoon water, which potentially stimulates the growth of green algae. During the summer season, the fresh compartment in SGD significantly decreases due to reductions of precipitation and increasing demand in irrigation. Consequently, the seeped beach water shifts to a dominance of N-limitation, which may accelerate the collapse of green algae community as discussed by Rocha et al. (2002).

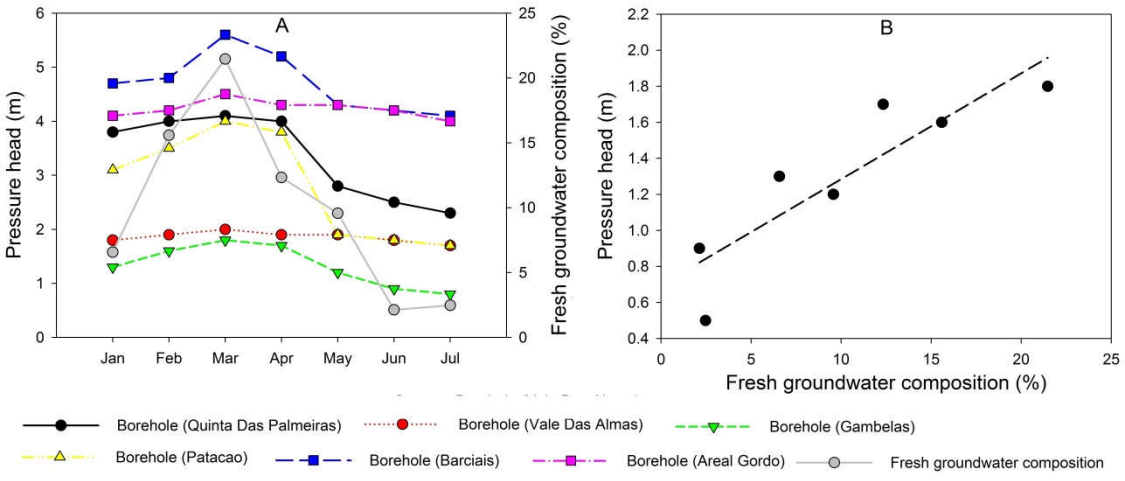

Figure VIII.8 (A) The groundwater pressure head in different borehole in Campina de Faro aquifer systems and fresh groundwater composition in SGD; (B) relationship between fresh composition and pressure head in borehole Gambelas.

This deduction is consistent with previous monitoring results in the lagoon. The

bloom of green algae is usually evidenced in the winter-spring seasons, which is often associated with hypoxia and 'fish kill' events (Padinha et al. 2000). From summer to autumn, the density of green algae decreased and the demand of algae to N decreased (Loureiro et al. 2005). The spring bloom of green algae has long been recognised as a conundrum for lagoon management. Previous studies mainly emphasised the influence of sewage input and surface runoff to the algae transition (Newton et al. 2003; Duarte et al. 2008; Gari et al. 2014). However, annual monitoring result suggested the nutrient composition in these waters is close to Redfield ratio (Synthesis Report 2003). More importantly, nutrient inputs from waste flow from pipeline and surface loading is limited. For instance, the daily DIN input from these two pathways may be less than 0.36 mg m^{-2} (Chapter VII). In comparison, DIN plumes from SGD can be significantly larger, varying from 1.09 mg m^{-2} day^{-1} to 3.27 mg m^{-2} day^{-1} in 2006 (Leote et al. 2008). Based on the regional investigation, SGD may contribute 21.81 mg DIN m^{-2} day^{-1} in May 2010 (Chapter VII). Furthermore, nutrient fluxes from SGD can easily extend to the entire lagoon and influence the ecological stability on the lagoon scale (Leote et al. 2008; Rocha et al. 2009). As a result, future study in algae community structure and transition should take SGD into consideration. In addition, proper regulation on SGD should be highlighted in future.

VIII.5.3 Possibility of Si-limitation in SGD

Previous research in surface loading reported occurrences of Si-limitation due to relative enhancements in anthropogenic N and P fluxes (Turner and Rabalais 1991; Justić et al. 1995a; Justić et al. 1995b; Wu and Chou 2003). In natural environment, the production of Si is highly abiotic; therefore, the circulation and transport of Si from land to ocean is barely influenced by human activity. Compared with surface runoff, the DSi is enriched in terrestrial groundwater. It can be orders of magnitude higher than that of seawater (e.g. Ullman et al. 2003; Kim et al. 2005; Rocha et al. 2015). In addition, Si can be produced from the porewater circulation in subterranean estuaries

(Chassagne et al. 2012). Consequently, prior studies seldom observed the deficiency of Si in SGD. In this study, the Si scarcity occurred in a number of water samples in both spring and autumn terms (Fig.VIII.4). In terms of frequency, during the spring term, the maximum for Si-limitation in SGD was 21.2% (Fig.VIII.5), indicating Si in SGD was relatively sufficient. However, during the autumn term, ratio of Si:P and Si:N frequently dropped below the Redfield thresholds (Fig.VIII.3), and the likelihood of Si-limitation developed to be the dominance at the lower end of salinity (Fig.VIII.5), which suggested SGD in the Ria Formosa may be a nutrient source with relatively insufficient DSi.

The occurrence of Si-limitation in SGD may result from the increase of land derived NO_3^-. Compared with fresh groundwater source in spring season, there may be a three folds increase in NO_3^- concentration in terrestrial endmember in the autumn survey (Leote et al. 2008). This enhancement likely stimulated the activity of NO_3^- reducer in the sediment, subsequently accelerating the P releasing in to porewater. For instance, in those water samples that salinity was below 25 psu, the SRP concentration was fluctuated around 2 μM, significantly higher than that in seawater (0.3 μM) and meteoric water (0.3 μM). In comparison, the production rate of DSi in SGD is stable. Consequently, the lack of DSi in SGD was observed. Based on the potential linkage between composition of fresh groundwater in SGD and piezometric head (B in Fig.VIII.8), the mean fresh composition in SGD may locate within the range of Si-limitation. For instance, it may reach 35% in May 2010 (Chapter VII), i.e. 24.33 psu in salinity. In addition, there is an increasing NO_3^- concentration in terrestrial endmember in the study site on the basis of annual survey from 2010 to 2013. As a result, the Si-limitation in SGD may have occurred.

Compared with limitation in N and P, the scarcity of DSi may result in more serious ecological problems. Due to the sensitivity of diatom in nutrient shift (Loureiro et al. 2005) the scenario of Si-limitation may trigger the transition of ecosystems from

siliceous-based to non-siliceous-based phytoplanktonic communities (Rocha et al. 2002). Subsequently, total biomass of diatom in the system may decline since diatom is a comparatively poor nutrient competitor (Smayda 1997) and it can be possibly inhibited by secondary metabolites from green algae (Keating 1978). This causal chain has been confirmed by Sommer (1985). In particular, he has observed that diatom can be fully replaced by green algae in an ecosystem if the DSi in nutrient source is below the Redfield threshold. In marine system, diatom is the most important primary supplier in the food web (Paine 1966). They contribute directly to filter feeding fish and shellfish populations (Ryther and Officer 1981; Beukema and Cadée 1991). In comparison, cyanobacteria and blue algae are not direct food source for zooplankton due to nutrients and toxin defensiveness (DeMott and Muller-Navarra 1997, DeMott 1998). Therefore, the decrease of diatom biomass may result in a loss of function in coastal systems.

As one of the largest coastal lagoons in Europe, the Ria Formosa represents an important role in economics and ecology. It offers uncountable goods and services (Smith and Atkinson 1994; Verhoeven et al. 2006). More than 6000 fishermen directly rely on the natural resources of the lagoon (Oliveira et al. 2009). The Ria Formosa is an important ground for in fishery and marine culture (Aníbal et al. 2011), representing 27% of the total seafood cultured in Portugal (Ibánhez 2012). Currently, diatom is the dominant species in the lagoon (Pereira et al. 2007). The decline of diatom availability may endanger the production of seafood such as clams (Newton et al. 2003), consequently threaten the economical income. Furthermore, Ria Formosa is on the main route of several migratory bird species (Cunha et al. 2009). It also serves as breeding and nursing grounds for several mollusc and fish species (Cunha et al. 2009). As a result, the insufficiency of diatom may directly limit the food supple to consumer and the biodiversity in the system might be declined.

VIII.5.4 Advices to future SGD management

Previously, N-limitation was frequently observed in the lagoon water (Falcao and Vale 1990; Newton et al. 2003). However, the appearance of P-limitation, especially in the region where water exchange is constrained, started to be the dominant trend in the latter survey (Newton et al. 2003). As the major nutrient input pathway, SGD is deemed to be responsible for this transition and the subsequent seasonal succession of algae community. Hence, SGD should receive more attention from lagoon management.

Practically, the primary task in the regulation of nutrient balance in SGD is to increase the possibility of N-limitation and avoid the occurrence of Si-limitation. There are two potential approaches. The reduction of DIN level, especially NO_3^-, in the adjacent aquifers is the most effective strategy. By the year of 2002, two of the most intensely farmed aquifers systems, Campina de Faro and Campina da Luz have been classified as Nitrate Vulnerable Zones (NVZ) according to the EU's Nitrate Directive (Stigter et al. 2006a). Through reducing chemical fertiliser application (Goodchild 1998), decline of DIN in groundwater endmember can be expected, which can increase the possibility of N-limitation in SGD. However, from our annual monitoring, the NO_3^- concentration at terrestrial groundwater, derived from regression, stably increases in the sampling site. In particular, in 2006, it ranged between 120 µM to 400 µM. In the year of 2011, it rose to 1.6×10^3 µM. Consequently, modulation NO_3^- concentration in terrestrial groundwater endmember is a long term task. The application of NO_3^- remediation techniques (e.g. Robertson et al. 2000) to purge the groundwater with high level NO_3^- plume may be necessary.

Proper water management also can be included in regulation of nutrient balance in SGD. In particular, it is feasible to decrease composition of terrestrial groundwater in SGD via adjustment of in-land groundwater hydraulic pressure, like the modelling

result shown by Li et al. (2008). In the Ria Formosa, the positive trend between fresh groundwater composition and terrestrial groundwater pressure head in 2006 (B in Fig.VIII.8) was witnessed. Compared with regulation in NO_3^- concentration, decreasing piezometric head can obtain an immediate effect in modulation nutrient conditions in SGD. Although the over extraction of groundwater can promote salinization of the aquifer and endanger freshwater resources, combined with prospection the reserves of fresh water in the aquifer, temporal shift of municipal water supplement from river water to groundwater (Stigter et al. 2006b) in spring season may be feasible since the terrestrial groundwater source is abundant and algae (De Baar et al. 1995; Platt et al. 2003) is sensitive to nutrient limitation shift in the lagoon water. In addition, application of effective irrigation is also necessary since excess irrigating water seeps to the aquifer and mixes with water from the regional groundwater flow system (Stigter et al. 1998)

VIII.5.5 Limitations

The appropriate interval division in frequency analysis is always a focus since the accuracy of frequency analysis is highly related with quantity of interval and sample size in each interval. Ideally, both factors should be extremely large. However, it is difficult to practice in environmental study. Furthermore, there is no specific guideline with regard to frequency analysis in environmental research. In this study, the entire salinity range in two terms was divided into seven and six sections and each contains 20-21 samples, except the most saline interval in spring term. Indeed, this division and following regression analysis combine with statistical uncertainties. However, this division guaranteed the uniformity among the majority of salinity ranges. It also balanced the requirements from interval quantity and sample size in each range. Consequently, it can be identified as an appropriate division.

VIII.6 Concluding remarks

(1) Nutrient structure in SGD is highly dynamic along mixing gradient and a combination of frequency analysis and Dirichlet regression can reveal the shift of limiting nutrient along salinity in SGD. It can be identified as a powerful tool in future management and regulation;

(2) A shift between P-limitation and N-limitation can be evidenced in SGD, which depends on biogeochemical modulation in subterranean estuaries and meteoric input composition. In 2006, the boundary between P-limitation and N-limitation was approximately 35.5 psu in both spring term and autumn term;

(3) In the Ria Formosa, the observed transition of algae community and HABs is consistent with variation of limiting nutrient in SGD. It suggests the necessity of management and regulation for SGD;

(4) High concentration of NO_3^-, derived from terrestrial groundwater may lead to Si-limitation in SGD. The scarcity of Si in lagoon water likely results in a significantly decline of diatom biomass and then entire ecosystem may collapse;

(5) A combination between decrease of NO_3^- concentration in terrestrial groundwater and control over terrestrial groundwater pressure head is an effective method to regulate nutrient balance in SGD.

Chapter IX

Final considerations

IX.1 Reconsideration of N circulation in the subterranean estuary

IX.1.1 Technique concerns

To study porewater flow in sandy sediments, researchers need to consider the importance of hydrological conductivity and the disturbance in the porewater solute distribution and associated fluxes (Beck et al. 2007a). In my research, a combination of field campaign techniques and laboratory stimulations in controlled environments was applied to determine N biogeochemistry in the sampling site. The field sampling via piezometers enabled the acquisition of *in-situ* porewater N distribution without significant interference in conductivity. The Flow-Through Reactor (FTR) simulations under laboratory conditions successfully reproduced porewater circulation and N transformations in the sediment with different mixing scenarios between NO_3^- and labile dissolved organic matter (DOM). Finally, appropriate modelling procedures were practiced to describe the benthic reactivity and solute transport.

To ensure the reproducibility and reliability of the data from experiments, a series of tests were performed before the techniques used in this research. For instance, determination of dead volume embodied in sampling beach allows precise acquirement of porewater from benthic sediment (Chapter V). More importantly, the performed tests by vaccutainer incubation discovered previously undescribed interference of solute exchange between storage containers and water samples. In particular, non-additive vacutainers were employed as a major storage approach in this study. In order to ensure that samples taken from surveys were representative of *in-situ* chemical compositions, a series of tests were carried out (Chapter IV). Results suggested that vacutainers are an appropriate storage method for NO_3^- in any environmental conditions. Results also showed that adsorption of solute (NH_4^+, SRP and DOC) onto the surface of vacutainers depend on ionic strength, temperature, and the presence of terrestrial organic matter. Variations in these properties promoted a

change in the solute adsorption dynamics, therefore influencing the accuracy of reproducing nutrient distribution in sampling sites. In my studies, procedures and operational protocols were applied to minimise the possible influences, such as refrigeration and replacement by glass vials. If alternative storage approaches cannot be provided, process blank was introduced into analysis procedure to reduce interference from vacutainers.

IX.1.2 N processing in the subterranean estuary

The magnitude of N fluxes from SGD pathway can be significantly influenced by the presence of biogeochemical modulations in subterranean estuaries on a local/global scale (Chapter III). A two-pronged approach was developed in my research that combines the hydrological circulation model and mass balance. It successfully revealed the N distribution and transformation in the study site (Chapter V). Results showed that the subterranean estuary in the Ria Formosa lagoon was an active reactor for nitrate (NO_3^-) and total dissolved nitrogen (TDN)**.** Previous research assumed coastal sediments to be a net sink for reactive N (Herbert 1999), in this study, the subterranean estuary can also be a source of nitrate (NO_3^-) and total dissolved nitrogen (TDN). In particular, during December and January, intensive remineralisation and nitrification were observed in the benthic region. This might result from a substantial input of organic particles. The reactive particles seeped into the sediment and reacted with a high level of dissolved oxygen (Leote et al. 2008) and/or Fe^{3+} (Caetano et al. 1997), subsequently increasing NO_3^- concentration in SGD.

From February to June, reactive particles in lagoon water decreased. Accordingly, the remineralization rate sharply declined. Consequently, the reduction of TDN became the dominant trend in TDN circulation and turnover. However, transformations of NO_3^- in the subterranean estuary displayed a complex pattern. Both reduction and addition were frequently observed in the study site. In particular,

nitrification was the dominant pathway to increase NO_3^- concentration in porewater while removal of NO_3^- was possibly due to the presence of denitrification.

Compared with organic N, inorganic N is prone to be assimilated by algae and seagrass in coastal systems. The substantial NO_3^- introduced by SGD might trigger harmful algae blooms (HABs). Therefore, the transformation of NO_3^- in the subterranean estuary plays a key role in sustaining coastal ecological equilibrium. The field observation suggested that the balance between generation and reduction of NO_3^- is highly related to the concentration of reactive organic matter. In particular, reduction of NO_3^- in a sediment environment is a heterotrophic reaction that consumes labile organic matter (Burgin and Hamilton 2007). Hence, the introduction of reactive organic matter may enhance NO_3^- removal ability. On the other hand, dissolved oxygen (DO) in the sandy sediment can increase the concentration of NO_3^- via aerobic respiration and nitrification (Fig.IX.1). Therefore, in Chapter VI, a series of Flow-Through Reactor (FTR) experiments were conducted to determine the influence from labile DOM (glucose) to NO_3^- reduction in the subterranean estuary. Based on first-order kinetic modelling, it can be seen that the injection of glucose rapidly accelerated the rate of aerobic respiration. Approximately 70% of glucose in porewater was attributed to aerobic respiration. In comparison, NO_3^- reduction pathways were barely benefited from enhancement of DOM. T-test suggested that the NO_3^- reduction was insignificantly enhanced by the presence of glucose.

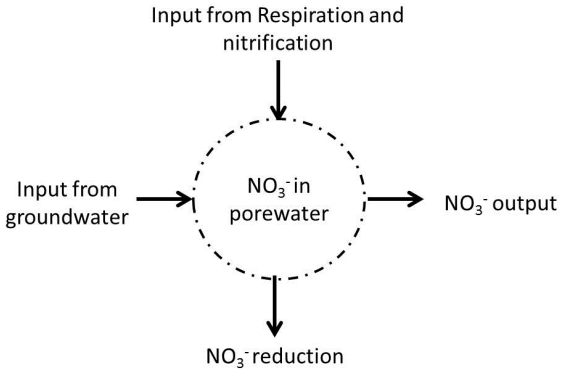

Figure IX.1 NO_3^- balance in the subterranean estuary

Previous research highlighted the importance of labile DOM in NO_3^- removal (Cornwell et al. 1999; Ibánhez et al. 2011; Ibánhez et al. 2013), which has not been observed in this study. The reason might link to the behaviour of the NO_3^- reduction bacteria community and the selection of organic matter supply. In particular, in the highly aerobic coastal zone, NO_3^- reducers may tend to concentrate in a microniche on the surface of the sediment. Though this special environment guarantees the activity of reducers in an aerobic environment, it also suggests the chemical connection between labile DOM and DO in porewater occurs before reducer activity. Consequently, the intrusion of DOM into the microniche can be difficult and NO_3^- reducers in the tested sediment cannot respond to the enhancement of glucose. To maintain the biogeochemical activity in processing NO_3^-, after long-term evolution, reducers may have developed the ability to decompose and utilise sediment organic matter (SOM).

In the coastal zone, inventory of SOM may be stable. In comparison, owing to the injection of sewage and debris from algae, concentrations of labile DOM in coastal waters fluctuate significantly. It suggests that NO_3^- reduction pathways may behave conservatively, while respiration intensity is likely dynamic. The active respiration may lead to an increase of NO_3^- due to the presence of nitrification. To conclude, the balance of NO_3^- in the subterranean estuary can be described in Fig.IX.1.

This research suggests the presence of high levels of DOM will potentially exacerbate NO_3^- pollution in lagoons. Previous studies assumed organic matter in lagoon water is low (Synthesis Report 2003). However, in this research, high concentrations of DOC and DON were witnessed, which may be derived from waste water due to operational mistakes (Mudge and Bebianno 1997) or suspended particles driven by strong winds during the winter season. Hence, monitoring reactive organic matter in lagoon water should receive more attention in the future in order to sustain the nutrient balance in the lagoon.

IX.2 SGD-borne N fluxes and nutrient structure in SGD

The Ria Formosa lagoon has been identified as having a eutrophication status due to the injection of substantial anthropogenic N (Newton and Mudge 2003). Previous research on exogenous N mainly focused on contributions from stream and waste water (Chapter VII). The results presented in Chapter VII revealed that NO_3^- input from SGD, mainly derived from terrestrial groundwater, accounted for more than 89% in total NO_3^- inputs. It can be identified as the major input to NO_3^- inventory. NO_3^- fluxes associated with SGD can be rapidly removed in the lagoon at a rate of 69.9±68.5 μmol m^{-2} h^{-1}. Though NO_3^- in saline water can be reduced to N_2 via denitrification (Francis et al. 2007), the possibility of dissimilatory nitrate reduction to ammonium (DNRA) may increase the ecological risk of SGD since NH_4^+ can easily be assimilated into biomass. Prior studies have proven the enrichment of ^{15}N in seagrass and algae (McClelland et al. 1997; McClelland and Valiela 1998). It suggests proper regulation in SGD is necessary in order to reduce the frequency of algae blooms. SGD is also a vector for dissolved organic nitrogen (DON). The DON injected into the lagoon may be recalcitrant. Therefore, the lagoon was a source for DON in summer. Approximately 586 kg N-DON day^{-1} was exported to the adjacent ocean.

An increase of the DIN concentrations in the lagoon is not the only consequence of the presence of SGD. The stoichiometric ratios of nutrients, Si:N, N:P and Si:P have also changed, which may lead to the alteration of the algae community structure. In Chapter VIII, nutrient ratios of Si:N, N:P and Si:P, and limiting nutrient in SGD were examined. Results suggested that the limiting nutrient in SGD can shift between P-limitation and N-limitation, which is dictated by the proportion of terrestrial groundwater and by the modulation ability in the subterranean estuary. In particular, when the composition of freshwater was below 2.7%, N-limitation can be expected in the SGD. In the Ria Formosa, the perception concentrated in winter and spring season subsequently elevated the piezometric pressure head of terrestrial groundwater.

Consequently, fresh groundwater in total SGD in spring may exceed the limit (2.7%) and shift SGD into P-limitation. As a poor competitor in N, growth of green algae can be significantly accelerated in this environmental condition. This prediction is consistent with previous observation on the bloom of green algae during spring. In addition, a high concentration of NO_3^- may shift the SGD into Si-limitation and subsequently lead to relative inefficiency of Si in the lagoon since SGD can be the dominated nutrient contributor in the lagoon system. Due to the sensitivity of diatoms to a nutrient shift (Loureiro et al. 2005) the scenario of Si-limitation may trigger the transition of ecosystems from siliceous-based to non-siliceous-based phytoplanktonic communities (Rocha et al., 2002). In the marine system, diatoms are the most important primary supplier in the food web (Paine 1966). Therefore, the alteration of community structure due to the scarcity of Si in SGD may result in deterioration and function loss in the coastal system. To reduce the ecological risk in SGD, two possible regulation methods, reducing the NO_3^- concentration in terrestrial groundwater and proper management on groundwater source, can be included in future regulation.

IX.3 Suggestions to coastal management

The primary task in the regulation of nutrient balance in SGD is to decrease reactive nitrogen loading via SGD pathway. There are two potential approaches. The reduction of DIN level, especially NO_3^-, in the adjacent aquifers is the most effective strategy. By the year of 2002, two of the most intensely farmed aquifers systems, Campina de Faro and Campina da Luz have been classified as Nitrate Vulnerable Zones (NVZ) according to the EU's Nitrate Directive (Stigter et al. 2006a). Through reducing chemical fertiliser application (Goodchild 1998), a decline of DIN in groundwater endmember can be expected. However, from our annual monitoring, the NO_3^- concentration at terrestrial groundwater, derived from the regression, stable increases in the sampling site. In particular, in 2006, it ranged between 120 µM to 400 µM. In the year of 2011, it rose to 1.6×10^3 µM. Consequently, modulation NO_3^- concentration in

terrestrial groundwater endmember is a long term task. The application of NO_3^- remediation techniques (e.g. Robertson et al. 2000) to purge the groundwater with high-level NO_3^- plume may be necessary.

Proper water management also can be included in the regulation of nutrient balance in SGD. In particular, it is feasible to decrease composition of terrestrial groundwater in SGD via adjustment of inland groundwater hydraulic pressure, like the modelling result shown by Li et al. (2008). In the Ria Formosa, the positive trend between fresh groundwater composition and terrestrial groundwater pressure head in 2006 was observed. Compared with regulation in NO_3^- concentration, decreasing piezometric head can lead to an immediate effect in modulation nutrient conditions in SGD. Although the over-extraction of groundwater can promote salinization of the aquifer and endanger freshwater resources, combined with prospection the reserves of fresh water in the aquifer, temporal shift of municipal water supplement from river water to groundwater (Stigter et al. 2006b) in spring season may be feasible since the terrestrial groundwater source is abundant and algae (De Baar et al. 1995; Platt et al. 2003) is sensitive to nutrient limitation shift in the lagoon water. In addition, application of effective irrigation is also necessary since excess irrigating water seeps to the aquifer and mixes with water from the regional groundwater flow system (Stigter et al. 1998).

IX.4 Future research

IX.4.1 Exploration of reaction pathways

Based the field survey and the subsequent modelling (Chapter V), the presence of different N transformation pathways in the subterranean estuary was observed. Furthermore, results derived from FTR experiments showed an intrinsic relationship between the consumption of organic matter and NO_3^- processing prior to discharge.

Consequently, additional research is highly necessary in order to understand the modulation effect and capability of the subterranean estuary in mediating SGD-borne NO_3^-. The use of labelled N compounds (e.g. $^{15}N\text{-}NO_3^-$) can help in tracking main processes involved in NO_3^- transformation within the sediment. This technique was previously used to examine the pathways involved in N attenuation within another benthic sediment system (e.g. Erler et al. 2014). Through applying this technique in the future, better acknowledge in the linkage between environmental conditions and an NO_3^- sink or source can be gained.

IX.4.2 Regional survey in winter

The regional survey showed the distribution of N in the lagoon in the summer. To completely understand the groundwater-borne NO_3^- behaver in lagoon water, a winter survey is necessary. However, during the winter survey, the weather was occasionally rainy, with frequent, intense gusts of wind. The working environment for the operation of the RAD7, equipment used to measure ^{222}Rn, was not ideal. Hence, the sampling procedure was cancelled. In future, these winter surveys may be attempted again. It may facilitate our understanding of NO_3^- circulation in the lagoon and improve local management of lagoon development.

IX.4.3 Construction of hydraulic model on regional scale

The regional survey revealed the terrestrial composition of the lagoon water on the basis of ^{222}Rn and mass balance. Furthermore, Leote et al. (2008) determined the SGD discharge rate and composition of terrestrial groundwater in SGD using seepage meters. One of the future research objectives is to construct a regional groundwater dynamics model, covering adjacent aquifers and entire lagoon (e.g. Scanlon et al. 2003; Oude et al. 2010). The database combining ^{222}Rn, mixing trend of ^{2}H and ^{18}O in the lagoon water and in-situ measurement of discharge rate can be used as an important

reference to validate the regional modelling. The regional modelling can predict discharge volumes of SGD, especially fresh SGD, for the entire lagoon system. Combining this with databases of NO_3^- concentration and the hydraulic pressure head of groundwater (SNIRH monitoring system, http://www.snirh.pt), NO_3^- fluxes from the SGD pathway can be predicated on a large temporal scale.

Appendix A

Support material for Chapter III and Chapter IV

Appendix A

Marmion Lagoon	
Salinity(psu)	$[NO_3^-]$ (µM)
4	365
6.5	350
11	270
14	240
17	220
21.5	170
24.6	120
30	80
32	60
34.2	10
Cape Henlopen	
Salinity(psu)	$[NO_3^-]$ (µM)
0	210
11	208
17	216
22	86
22.5	12
26.2	49
31.2	3.7
Huntington beach	
Salinity(psu)	$[NO_3^-]$ (µM)
33.6	0.5
33.7	8.7
34.5	270
21.3	337
8.7	203
Stinson beach	
Salinity(psu)	$[NO_3^-]$ (µM)
0.22	76
30.22	14
31.75	21
32.02	15
Puerto Morelos	
Salinity(psu)	$[NO_3^-]$ (µM)
1.64	268.6
9.69	8.3
25.79	0.16
33.75	0.15

Woods Hole	
Sub-location 1	
Salinity(psu)	$[NO_3^-]$ (µM)
32	0
30	10
25	80
4	400
Sub-location 2	
Salinit (psu)	$[NO_3^-]$ (µM)
31.8	0
29.8	0
20	55
5	120
Sub-location 3	
Salinity(psu)	$[NO_3^-]$ (µM)
3	285
7	140
26	60
26.5	10
27	2
32	0
Shelter Island	
10.7	110.2
22.9	80.8
32	20.7
3.5	254
17	167
30	0
Lynch Cove	
Salinity(psu)	$[NO_3^-]$ (µM)
14.5	21.1
14.6	19.8
14.7	20.5
15.5	23.7
16.8	27.1
17.1	25.5
17.3	28.9
17.6	19.2
18.1	30.2
25.9	0.8

Mariana Islands	
Sub-location 1	
Salinity(psu)	$[NO_3^-]$ (µM)
36.15	10
30.57	10
29.91	15
27.29	21
25.97	33
23.67	47
21.05	66
Sub-location 2	
Salinity(psu)	$[NO_3^-]$ (µM)
36.15	10
27.94	10
25.31	23
23.02	33
22.03	40
17.76	51
Concepcion bay	
Sub-location 1	
Salinity(psu)	$[NO_3^-]$ (µM)
2.6	315.2
10.7	110.2
22.9	80.8
32	20.7
Sub-location 2	
Salinity(psu)	$[NO_3^-]$ (µM)
0.6	745
5.3	513.7
25.3	24
Truc Vert beach	
Salinity(psu)	$[NO_3^-]$ (µM)
12	48
25.5	16
28	32
31	25
33	18
35	5

Ria Formosa lagoon		Dor Bay	
Sub-location 1		Sub-location 1	
Salinity (psu)	$[NO_3^-]$ (µM)	Salinity (psu)	$[NO_3^-]$ (µM)
23	170	2	330
27	85	5	210
30	80	12	225
33	61	38	5
36	11	Sub-location 2	
Sub-location 2		Salinity (psu)	$[NO_3^-]$ (µM)
Salinity (psu)	$[NO_3^-]$ (µM)	3.5	330
21	60	5	290
25	43	7	170
28	30	38	5
33	21	Sub-location 3	
37	8	Salinity (psu)	$[NO_3^-]$ (µM)
		25	100
		30	60
		32	35
		38	5

Table A.1 Concentrations of NO_3^- and salinity in different subterranean estuaries

Appendix A

Time	NO_3^-		NH_4^+		SRP	
	4℃	20℃	4℃	20℃	4℃	20℃
	1.0	-0.2	-0.2	-0.5	0	0
Instant	0.8	1.0	-0.1	-0.6	0	1.2
	0.9	0.8	-0.8	-0.3	0	0
	1.1	0.7	0.8	-0.5	0	0
3-Day	1.2	0.9	-0.6	-0.5	1.2	0
	0.9	0.7	0.2	0.7	0	0
	-0.1	0.7	1.0	-1.2	0	0
10-Day	0.4	0.6	1.1	0.7	0	0
	0.7	0.7	-0.5	0.6	1.5	0
	-0.2	-0.1	0.9	-1.1	1.2	0
30-Day	-0.3	0.2	0.7	-1.2	1.2	1.5
	0.5	0.5	0.8	0.8	1.5	0

Table A.2 Concentrations of NO_3^-, NH_4^+ and SRP in blank test, the unit in the table is 10^{-3} mg l^{-1}

Appendix B

N distribution in the subterranean estuary and benthic N transformation rates (Chapter V)

Appendix B

December				
Piezometer	NH_4^+ (µM)		NO_2^- (µM)	
	High tide	Low tide	High tide	Low tide
A1	0.32	1.05	0.25	0.32
C1	0.42	1.21	-0.2	0.20
E1	0.25	1.19	-0.12	0.48
E3	0.66	0.35	0.25	0.49
C3	0.21	0.51	0.25	0.45
A4	0.38	0.43	-0.33	0.39
C5	0.25	0.89	-0.25	0.28
E5	0.17	0.48	0.60	0.98
D2	0.23	0.47	0.57	0.36
B2	0.22	0.59	0.89	0.52
D3	0.45	1.02	0.37	0.43
D5	0.63	0.99	0.56	0.22
B5	0.27	0.87	0.45	0.68

Table B.1 Concentrations of NH_4^+ and NO_2^- in porewater samples during December

January				
Piezometer	NH_4^+ (µM)		NO_2^- (µM)	
	High tide	Low tide	High tide	Low tide
A1	1.32	1.58	0.17	0.37
C1	0.91	1.07	0.35	0.39
E1	0.99	1.21	0.25	0.28
E3	1.25	1.02	0.29	0.35
C3	1.05	1.00	0.34	0.51
A4	0.94	0.78	0.22	0.40
C5	0.82	0.26	0.47	0.39
E5	1.20	0.83	0.32	0.42
D2	2.01	0.64	0.80	0.58
B2	1.27	0.35	0.76	0.47
D3	0.63	0.32	0.75	0.32
D5	0.74	0.36	0.29	0.46
B5	0.83	0.79	0.29	0.15

Table B.2 Concentrations of NH_4^+ and NO_2^- in porewater samples during January

February				
Piezometer	NH_4^+ (µM)		NO_2^- (µM)	
	High tide	Low tide	High tide	Low tide
A1	1.67	1.35	0.12	0.17
C1	1.65	1.60	0.15	0.41
E1	0.42	1.88	0.14	0.52
E3	1.18	1.69	0.13	0.39
C3	1.48	0.46	0.17	0.47
A4	0.25	1.71	0.24	0.50
C5	0.36	1.69	0.25	0.26
E5	1.62	1.83	-0.16	0.45
D2	1.41	1.91	0.18	0.62
B2	1.72	0.68	0.20	0.37
D3	1.63	1.76	0.12	1.38
D5	1.42	1.52	0.29	0.63
B5	1.57	1.47	0.58	0.44

Table B.3 Concentrations of NH_4^+ and NO_2^- in porewater samples during February

March				
Piezometer	NH_4^+ (µM)		NO_2^- (µM)	
	High tide	Low tide	High tide	Low tide
A1	1.23	0.15	0.32	1.66
C1	1.02	0.22	0.21	0.22
E1	0.54	0.34	1.36	1.93
E3	0.14	0.28	0.26	0.17
C3	0.37	0.12	0.19	1.21
A4	0.45	0.43	0.20	1.15
C5	0.47	0.89	0.16	3.25
E5	0.81	0.23	-0.11	0.82
D2	0.15	0.17	0.21	0.25
B2	0.45	0.24	0.26	0.28
D3	0.65	0.23	0.15	1.23
D5	0.72	0.27	0.47	0.40
B5	0.28	1.01	0.12	0.15

Table B.4 Concentrations of NH_4^+ and NO_2^- in porewater samples during March

April				
Piezometer	NH_4^+ (µM)		NO_2^- (µM)	
	High tide	Low tide	High tide	Low tide
A1	3.60	0.33	0.08	0.25
C1	0.63	1.00	0.63	0.27
E1	0.76	0.59	0.22	0.18
E3	1.05	0.38	0.09	0.28
C3	0.78	0.11	0.10	0.32
A4	2.60	0.53	0.04	0.45
C5	2.40	0.69	0.15	0.48
E5	0.17	1.11	0.54	0.51
D2	3.46	1.44	0.82	0.14
B2	0.88	2.13	0.19	0.25
D3	0.75	0.59	0.88	0.17
D5	0.91	0.45	0.17	0.20
B5	0.72	2.34	0.12	0.28

Table B.5 Concentrations of NH_4^+ and NO_2^- in porewater samples during April

May				
Piezometer	NH_4^+ (µM)		NO_2^- (µM)	
	High tide	Low tide	High tide	Low tide
A1	0.58	0.54	0.28	0.33
C1	0.54	0.48	0.15	0.15
E1	0.77	0.12	0.28	0.25
E3	0.70	1.83	0.33	0.28
C3	0.39	0.56	0.19	0.37
A4	0.30	0.67	0.26	0.19
C5	0.70	0.38	0.15	0.06
E5	0.89	0.58	0.59	0.42
D2	1.06	1.02	0.37	0.81
B2	0.47	1.11	0.18	0.70
D3	0.82	0.28	0.68	0.17
D5	0.71	0.43	0.14	0.45
B5	0.63	0.65	0.62	0.17

Table B.6 Concentrations of NH_4^+ and NO_2^- in porewater samples during May

June				
Piezometer	NH_4^+ (µM)		NO_2^- (µM)	
	High tide	Low tide	High tide	Low tide
A1	2.45	0.53	1.76	1.18
C1	2.84	0.39	0.42	1.96
E1	1.11	1.45	1.73	1.63
E3	0.65	1.24	0.56	2.81
C3	0.96	2.47	0.26	0.50
A4	1.79	0.68	0.83	0.90
C5	1.47	0.39	1.30	1.19
E5	1.73	2.00	0.51	1.37
D2	1.08	1.34	0.82	1.01
B2	0.58	1.55	1.21	1.82
D3	1.83	0.34	0.79	1.00
D5	1.43	1.21	1.20	0.75
B5	2.18	1.37	1.11	0.73

Table B.7 Concentrations of NH_4^+ and NO_2^- in porewater samples during June

Month	NH_4^+(µM)	NO_2^-(µM)	NO_3^-(µM)	TDN (µM)
December	1.21	0.42	2.05	68.25
January	0.25	0.03	2.01	59.52
February	1.02	0.12	0.89	53.42
March	2.49	0.16	0.31	49.42
April	0.14	0.28	1.53	59.42
May	0.15	0.08	0.97	47.82
June	1.77	0.12	0.85	52.89

Table B.8 Chemical properties of lagoon water in different months, which were invoked in benthic modelling

Appendix B

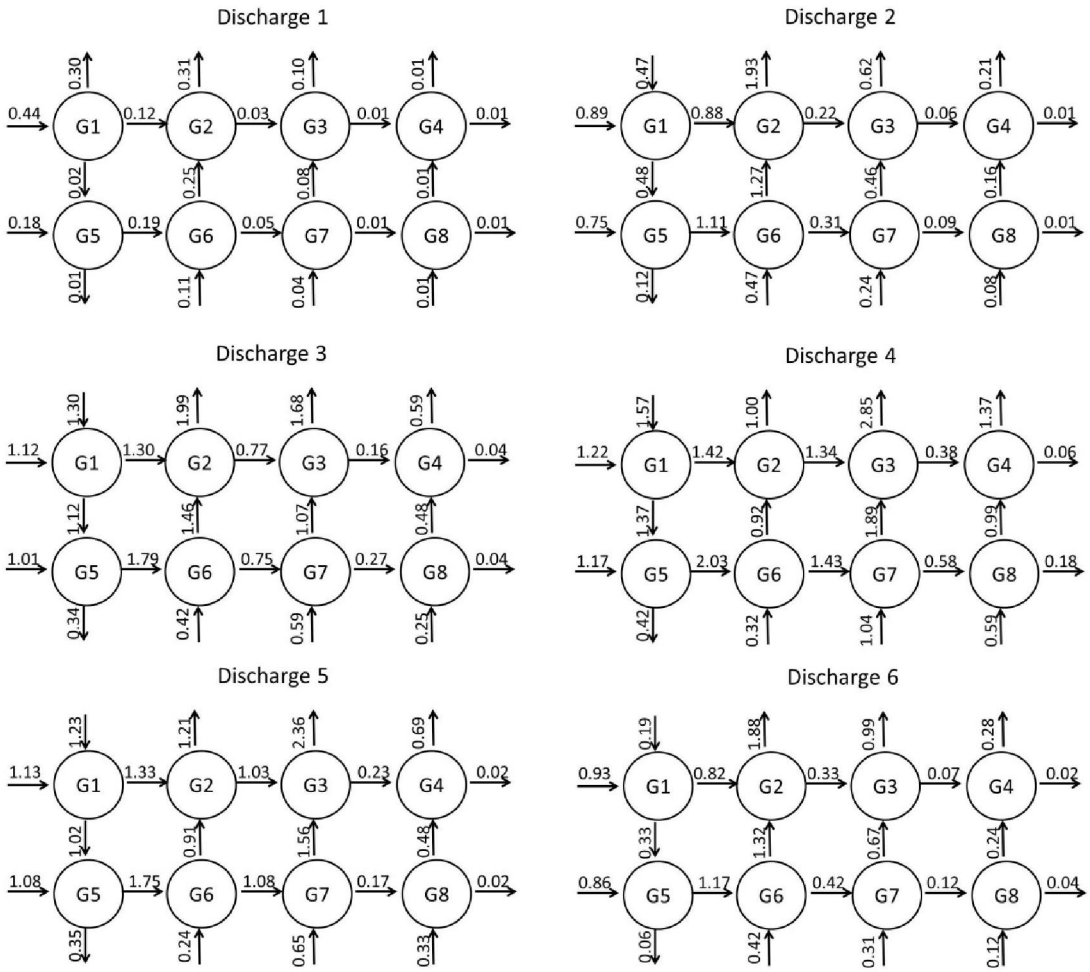

Figure B.1 Advection rate for each grid during ebbing tide on the basis of hydraulic model calculation. The unit of velocity is 10^{-6} m^3 s^{-1}

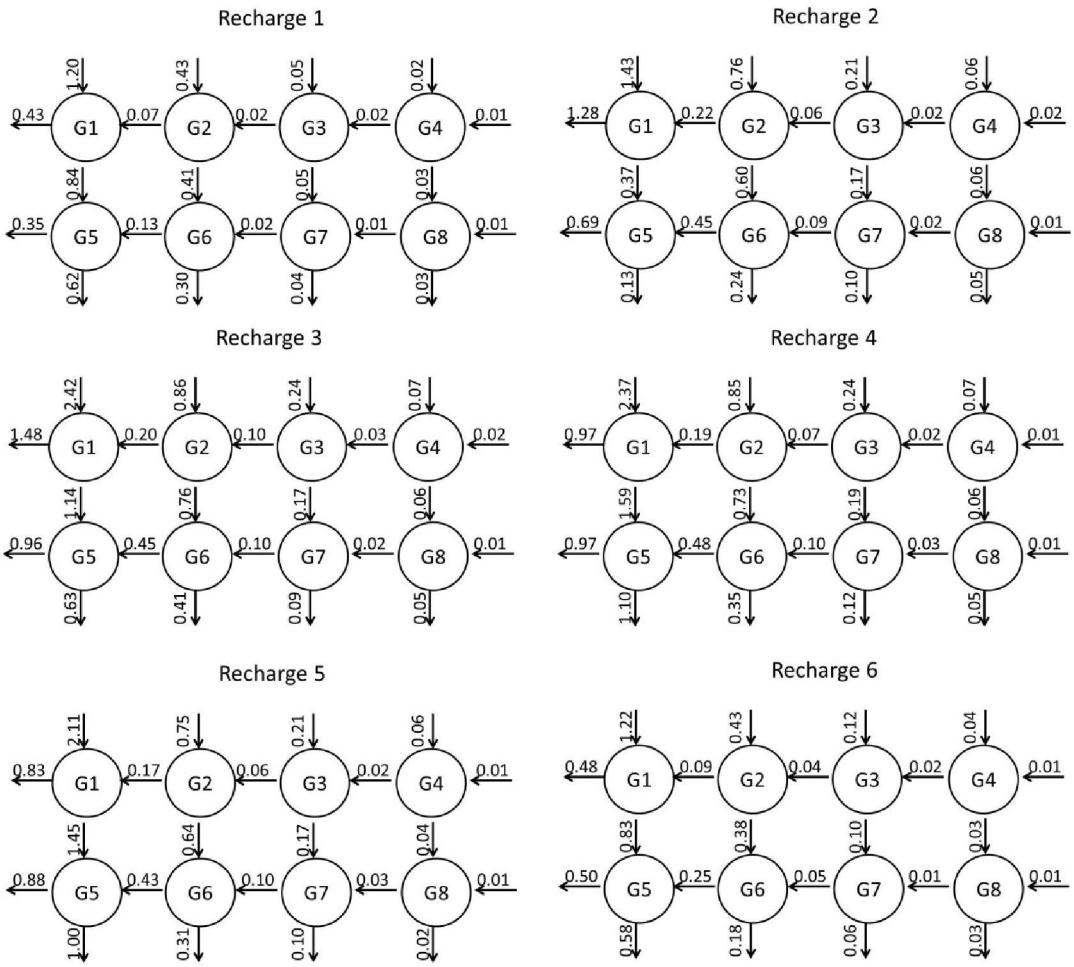

Figure B.2 Advection rate for each grid during flood tide on the basis of hydraulic model calculation. The unit of velocity is 10^{-6} m^3 s^{-1}

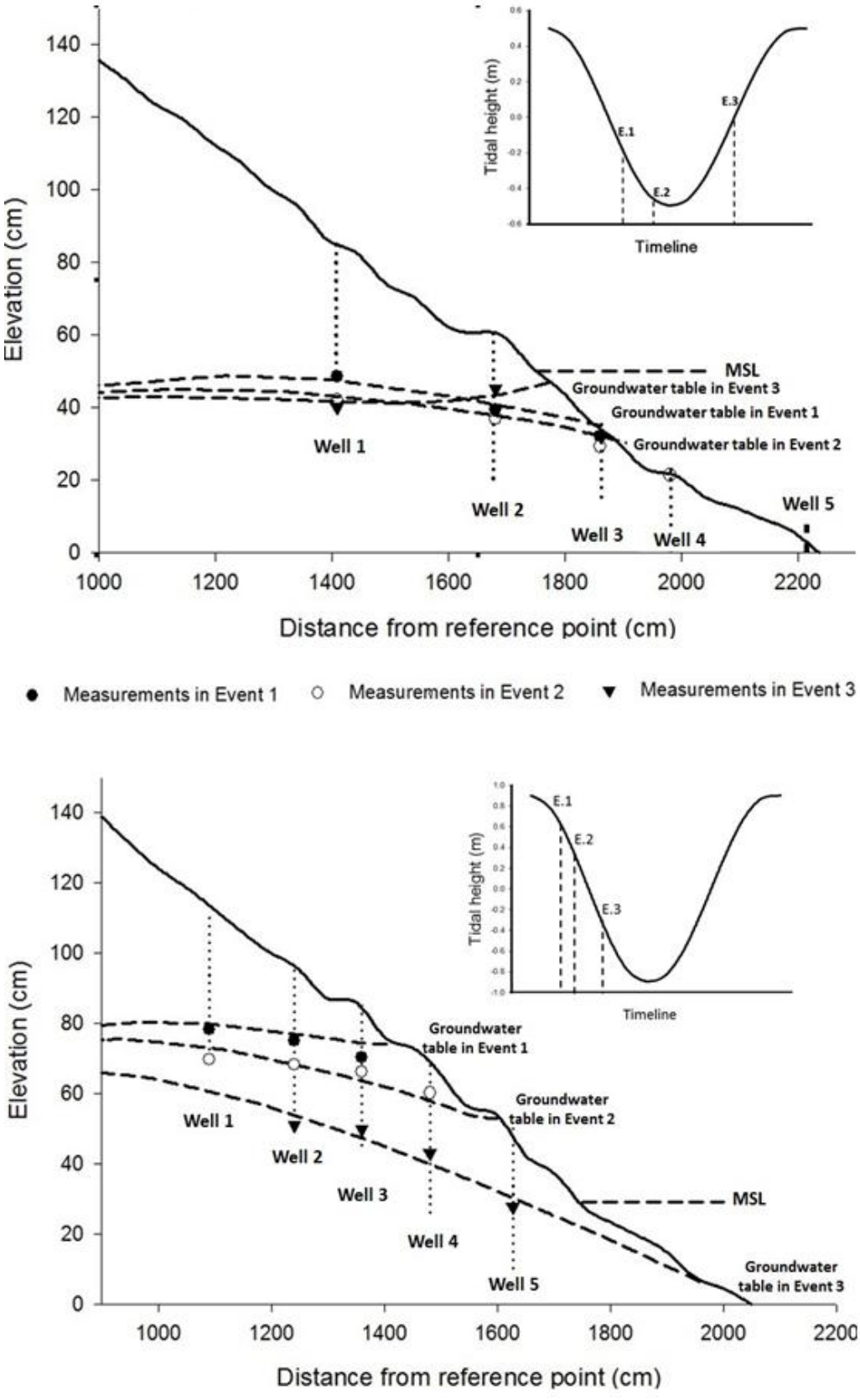

Figure B.3 Comparisons of the local water fluctuations from the field observations and predicted by the present model in 2013 (Two tidal cycles).

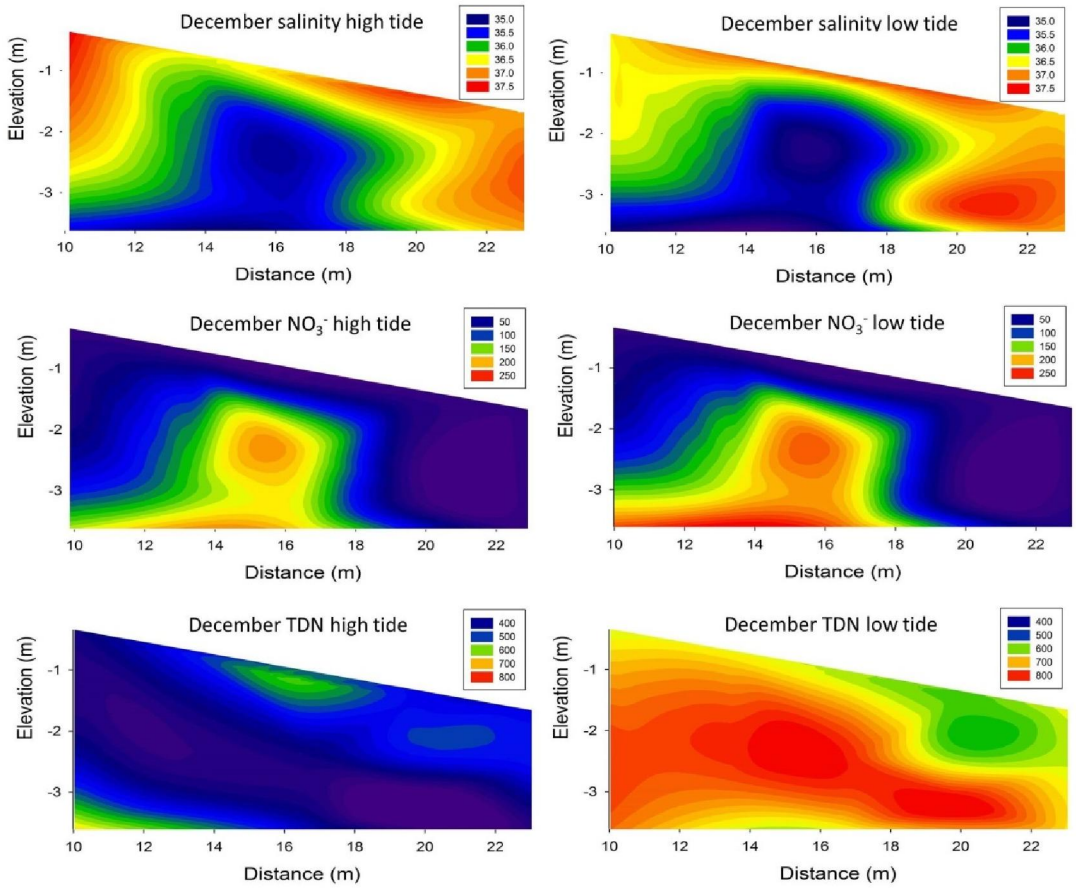

Figure B.4 Salinity, NO_3^- and TDN profilers at high tide and low tide in December, 2010. The units for salinity and N are psu and µM, respectively.

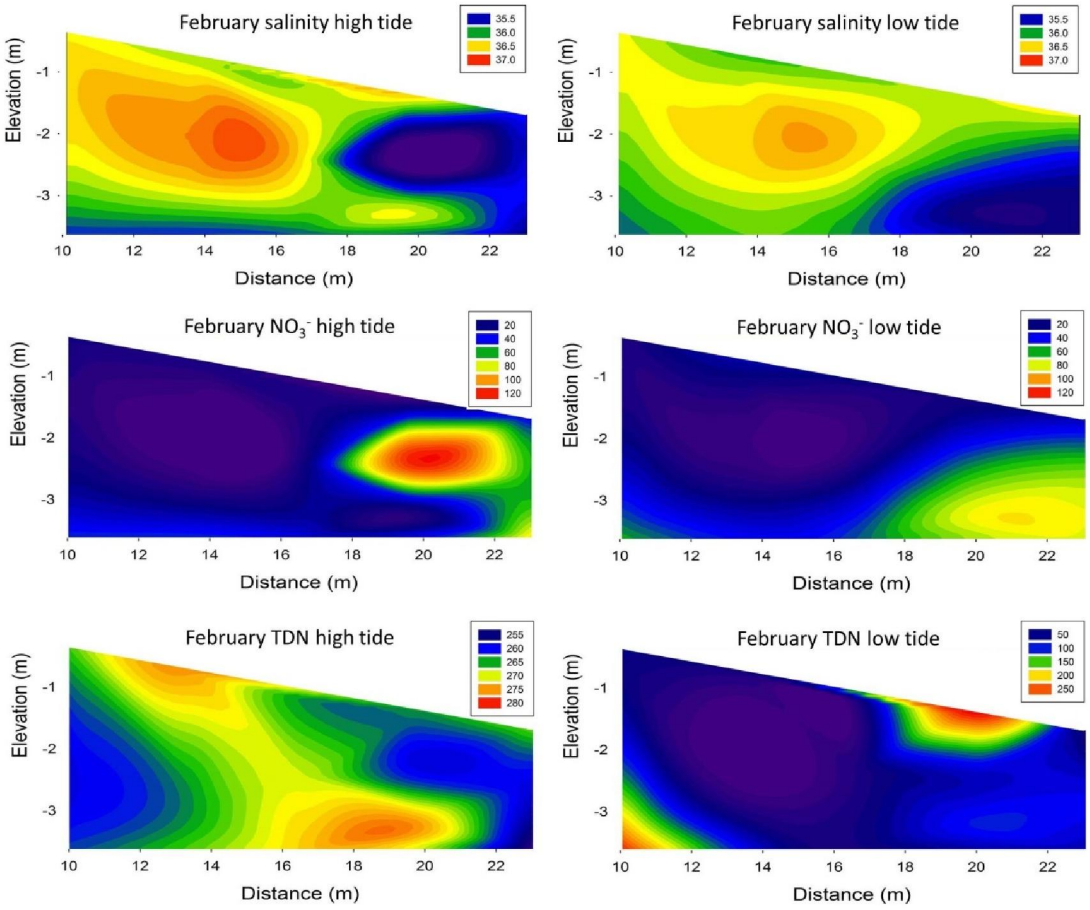

Figure B.5 Salinity, NO_3^- and TDN profilers at high tide and low tide in February, 2011.The units for salinity and N are psu and µM, respectively.

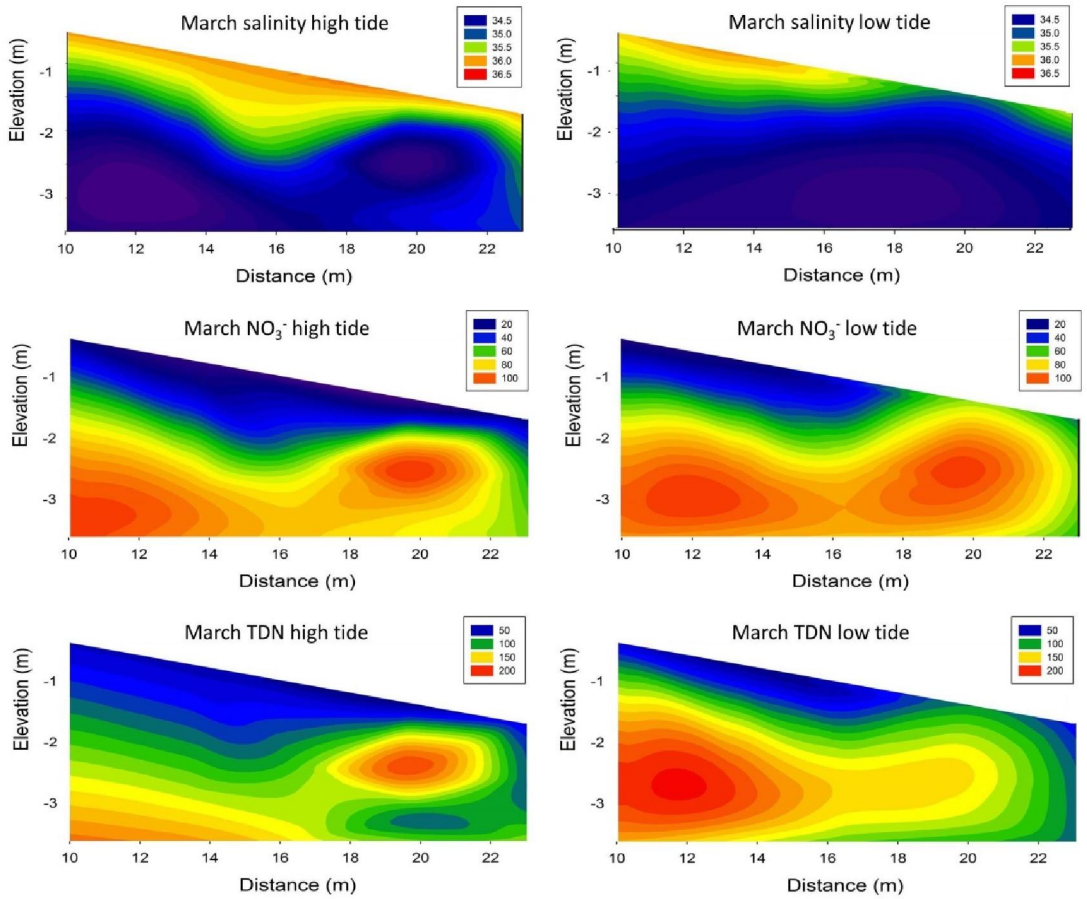

Figure B.6 Salinity, NO_3^- and TDN profilers at high tide and low tide in March, 2011.The units for salinity and N are psu and µM, respectively.

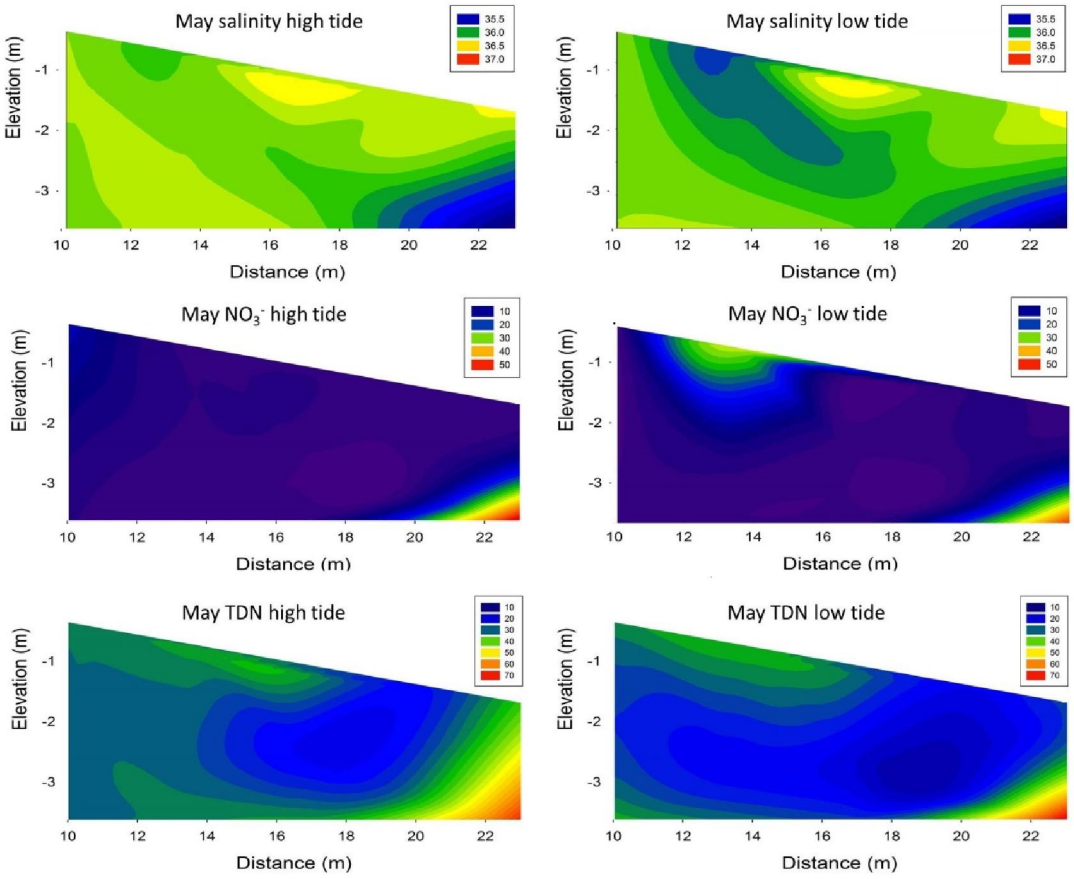

Figure B.7 Salinity, NO_3^- and TDN profilers at high tide and low tide in May, 2011.The units for salinity and N are psu and µM, respectively.

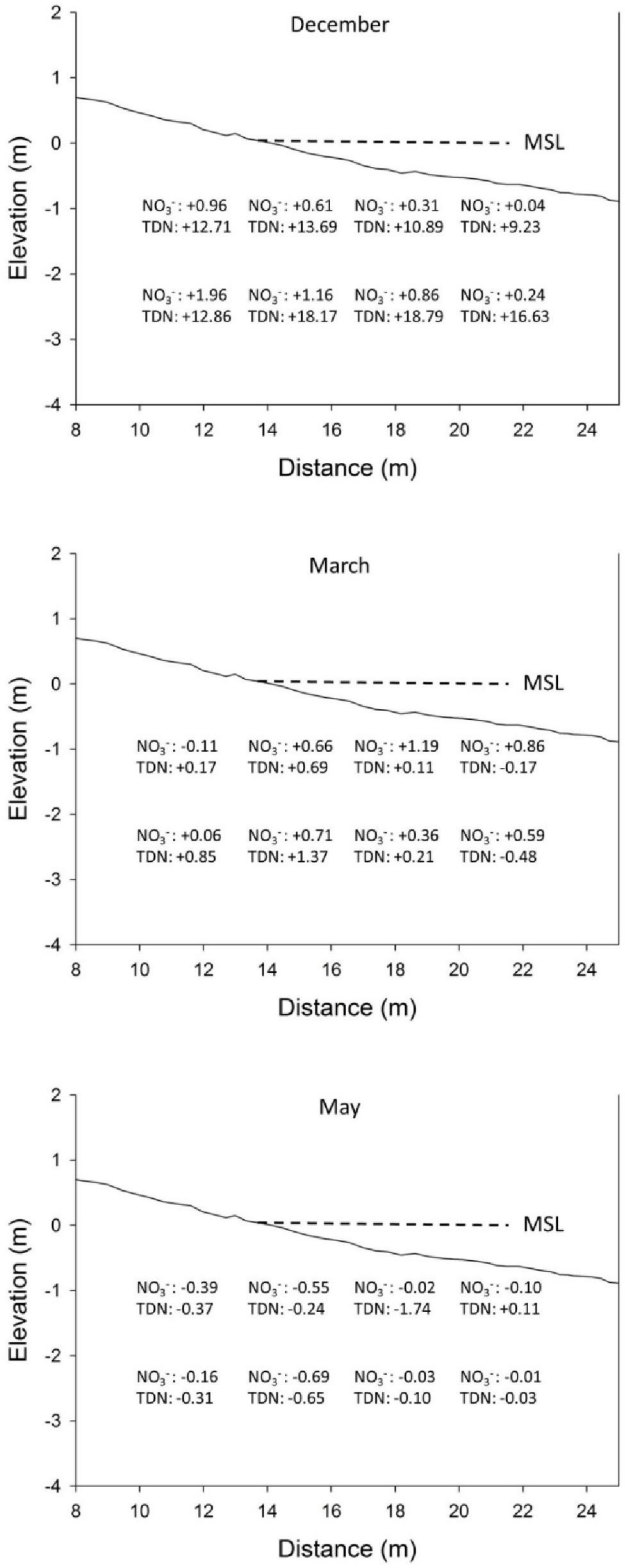

Figure B.8 Benthic reaction rates of NO_3^- and TDN for the remaining months, the unit is millimole (mmol) per cubic meter bulk sediment per hour.

Appendix C

Concentrations of N, DOC, DO and DOM in FTR tests (Chapter VI)

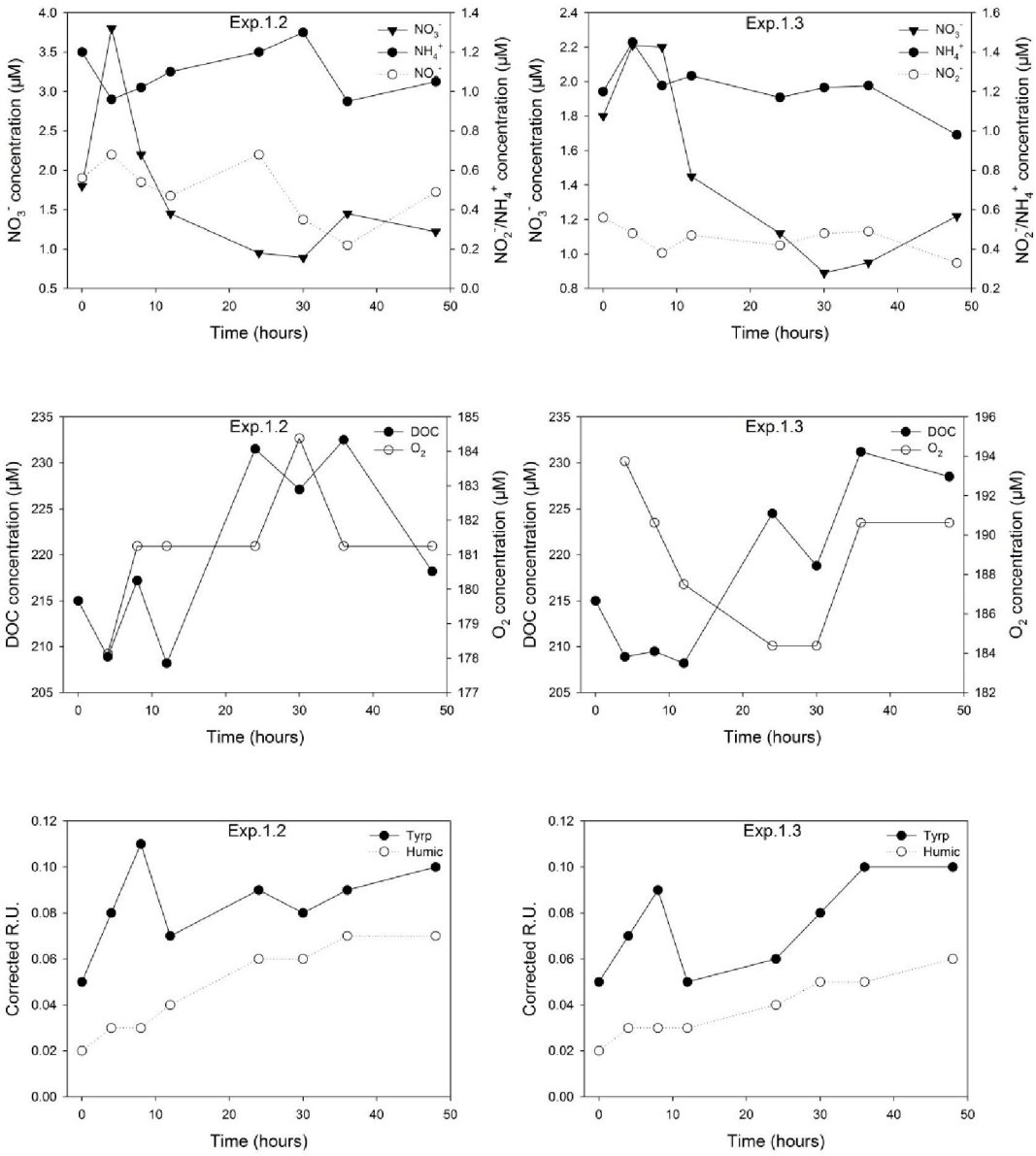

Figure C.1 Concentrations of NO_3^-, NH_4^+, NO_2^-, DOC and DO and relative concentrations of Tyrp-protein and humic material in repeated experiment of Exp.1.2 and Exp.1.3

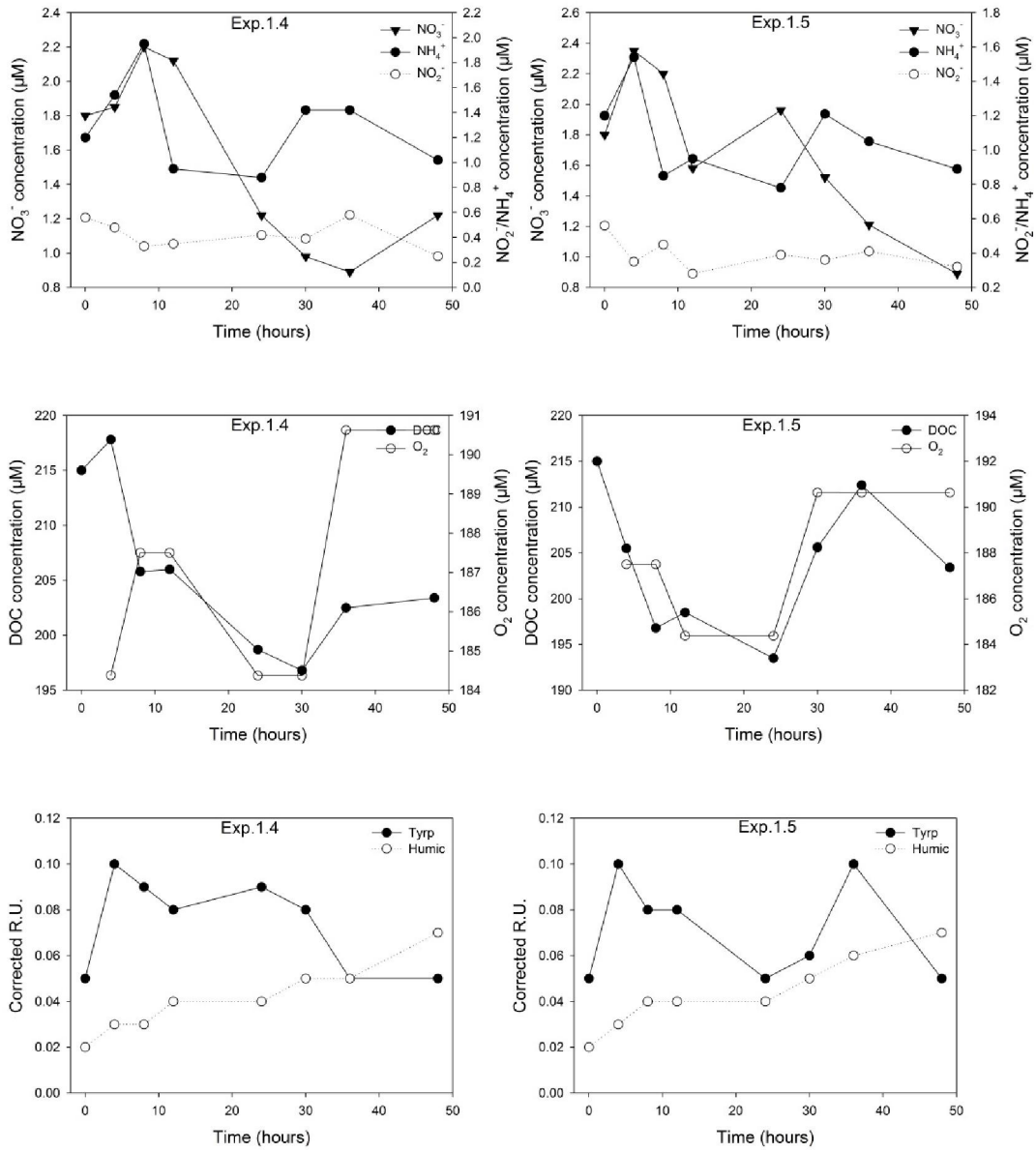

Figure C.2 Concentrations of NO_3^-, NH_4^+, NO_2^-, DOC and DO and relative concentrations of Tyrp-protein and humic material in repeated experiment of Exp.1.4 and Exp.1.5

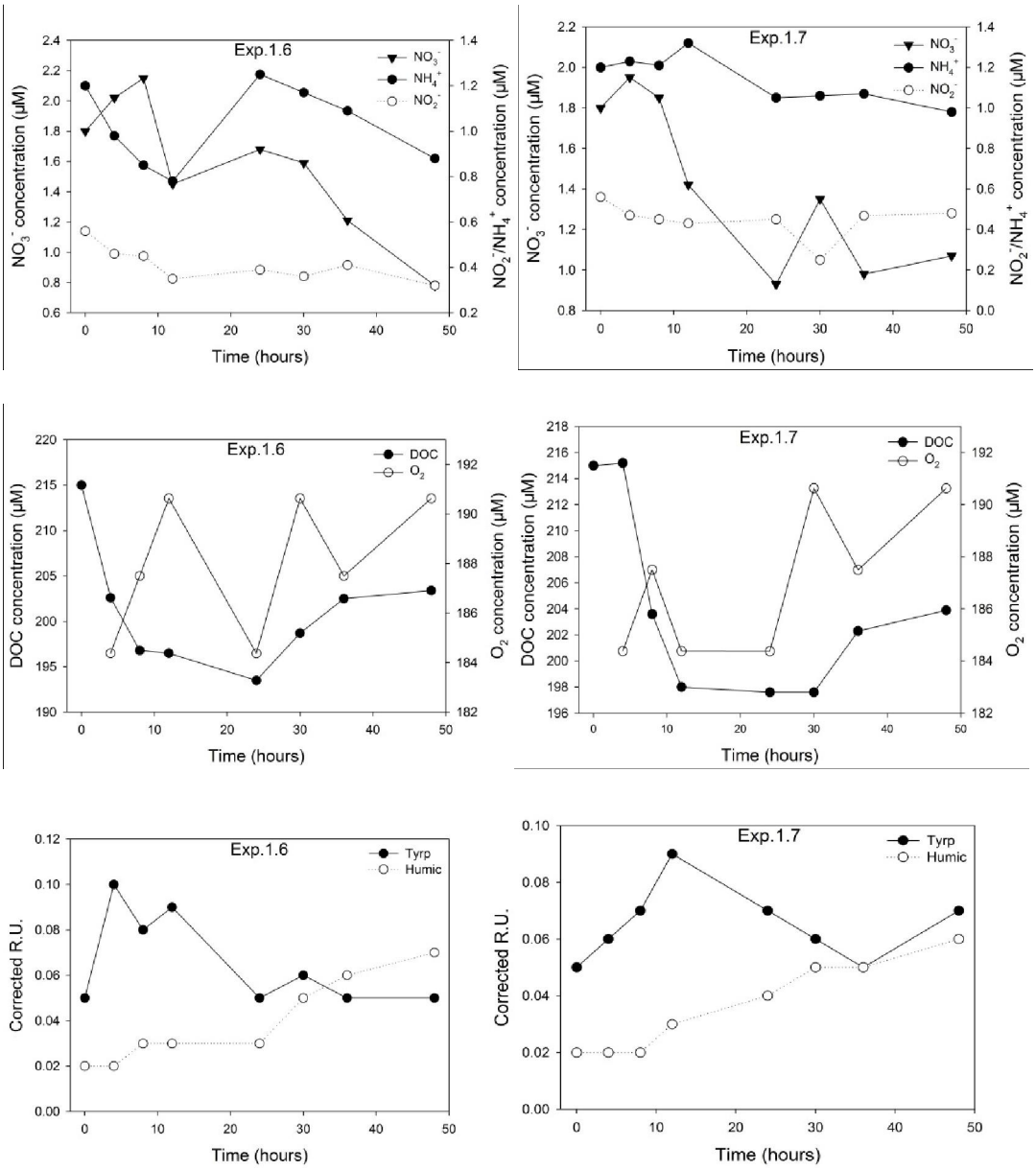

Figure C.3 Concentrations of NO_3^-, NH_4^+, NO_2^-, DOC and DO and relative concentrations of Tyrp-protein and humic material in repeated experiment of Exp.1.6 and Exp.1.7

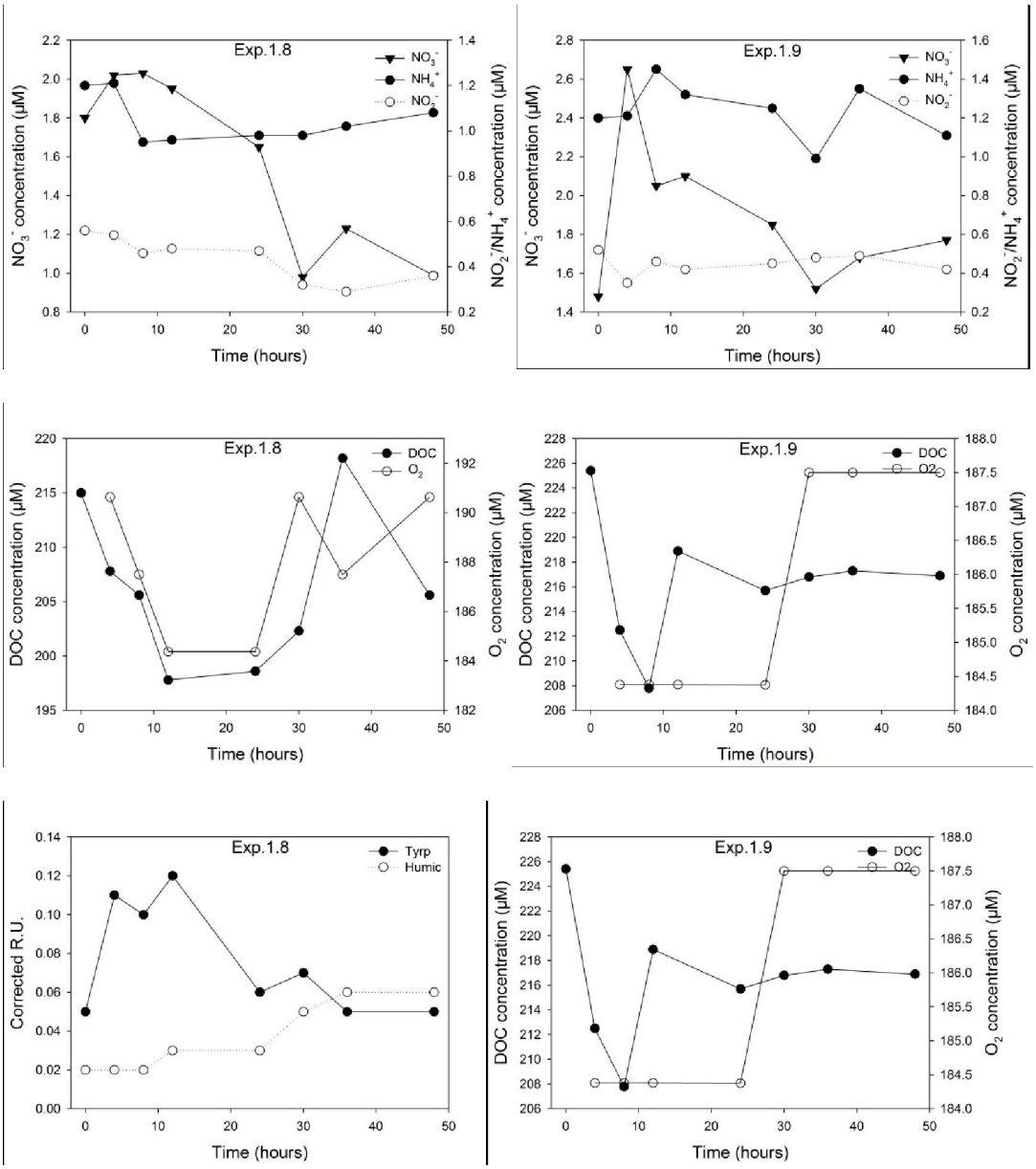

Figure C.4 Concentrations of NO_3^-, NH_4^+, NO_2^-, DOC and DO and relative concentrations of Tyrp-protein and humic material in repeated experiment of Exp.1.8 and Exp.1.9

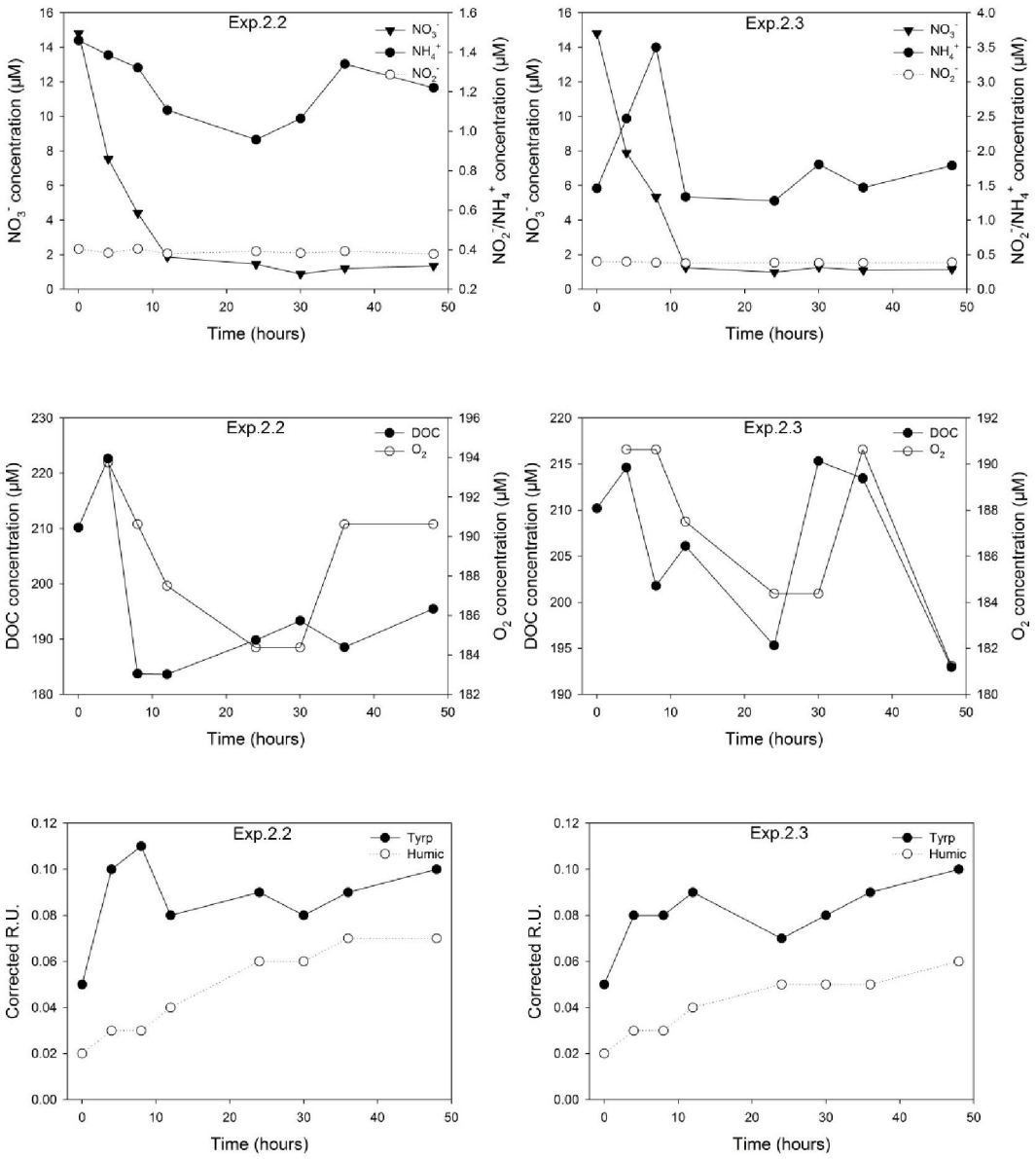

Figure C.5 Concentrations of NO_3^-, NH_4^+, NO_2^-, DOC and DO and relative concentrations of Tyrp-protein and humic material in repeated experiment of Exp.2.2 and Exp.2.3

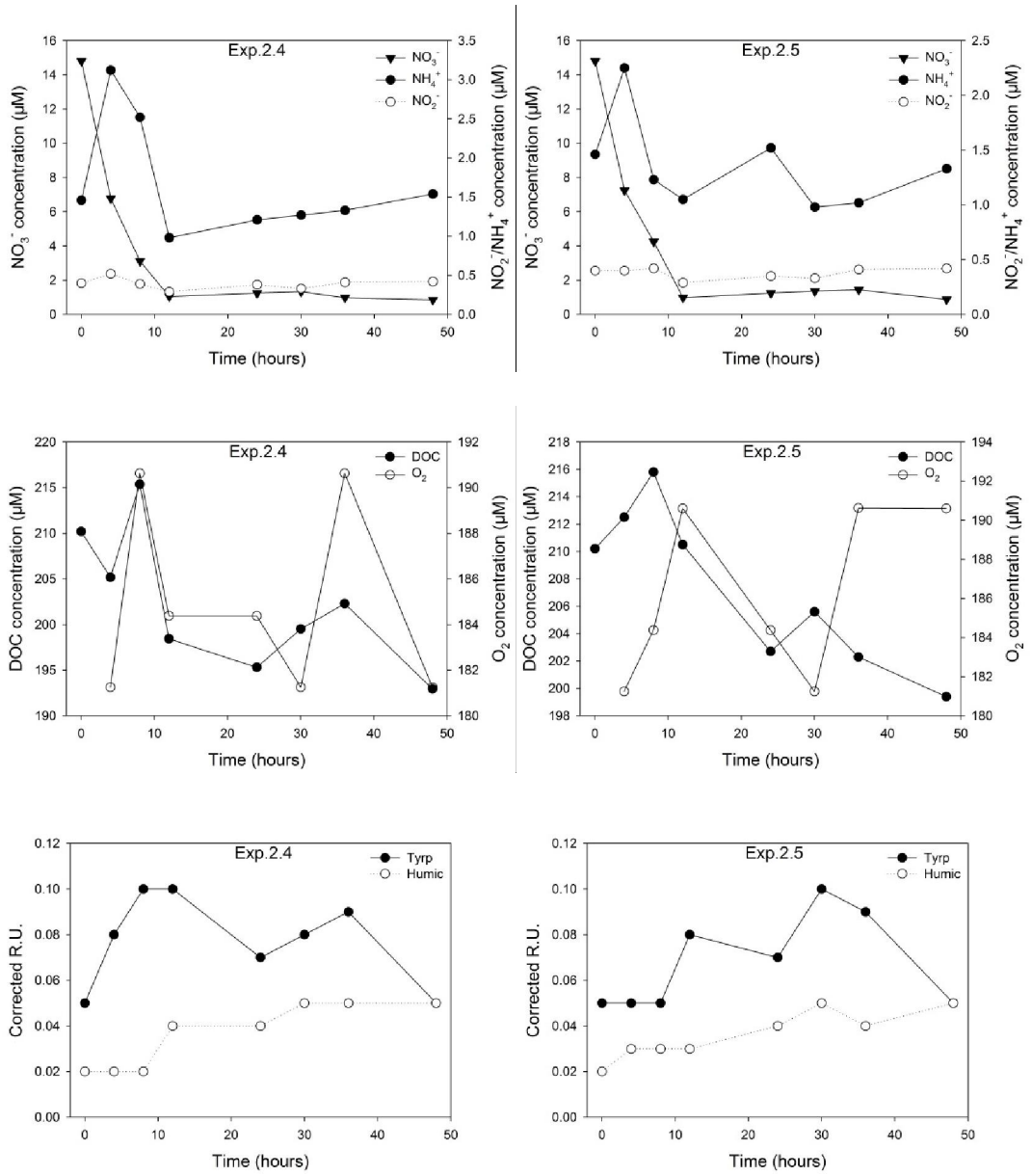

Figure C.6 Concentrations of NO_3^-, NH_4^+, NO_2^-, DOC and DO and relative concentrations of Tyrp-protein and humic material in repeated experiment of Exp.2.4 and Exp.2.5

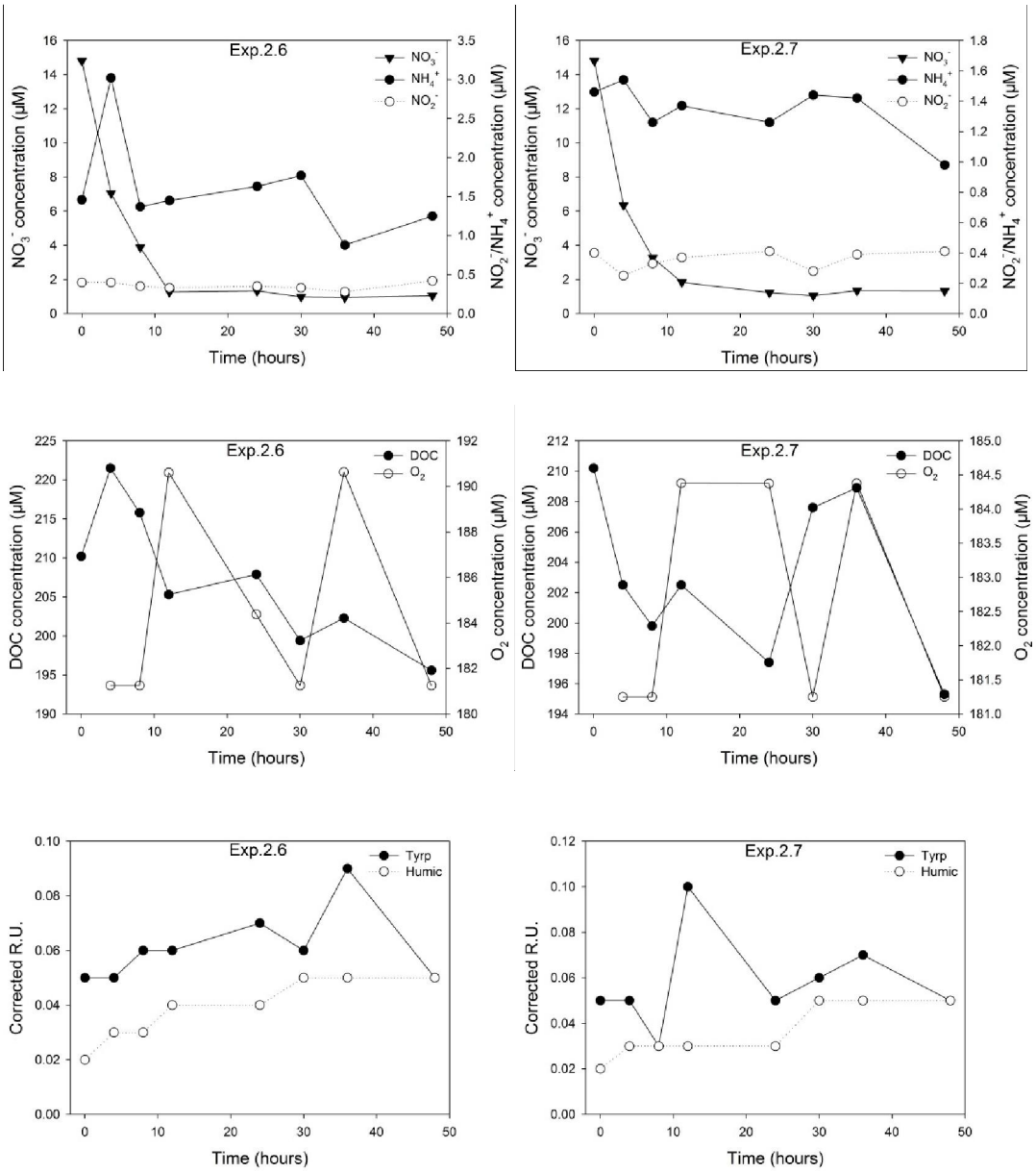

Figure C.7 Concentrations of NO_3^-, NH_4^+, NO_2^-, DOC and DO and relative concentrations of Tyrp-protein and humic material in repeated experiment of Exp.2.6 and Exp.2.7

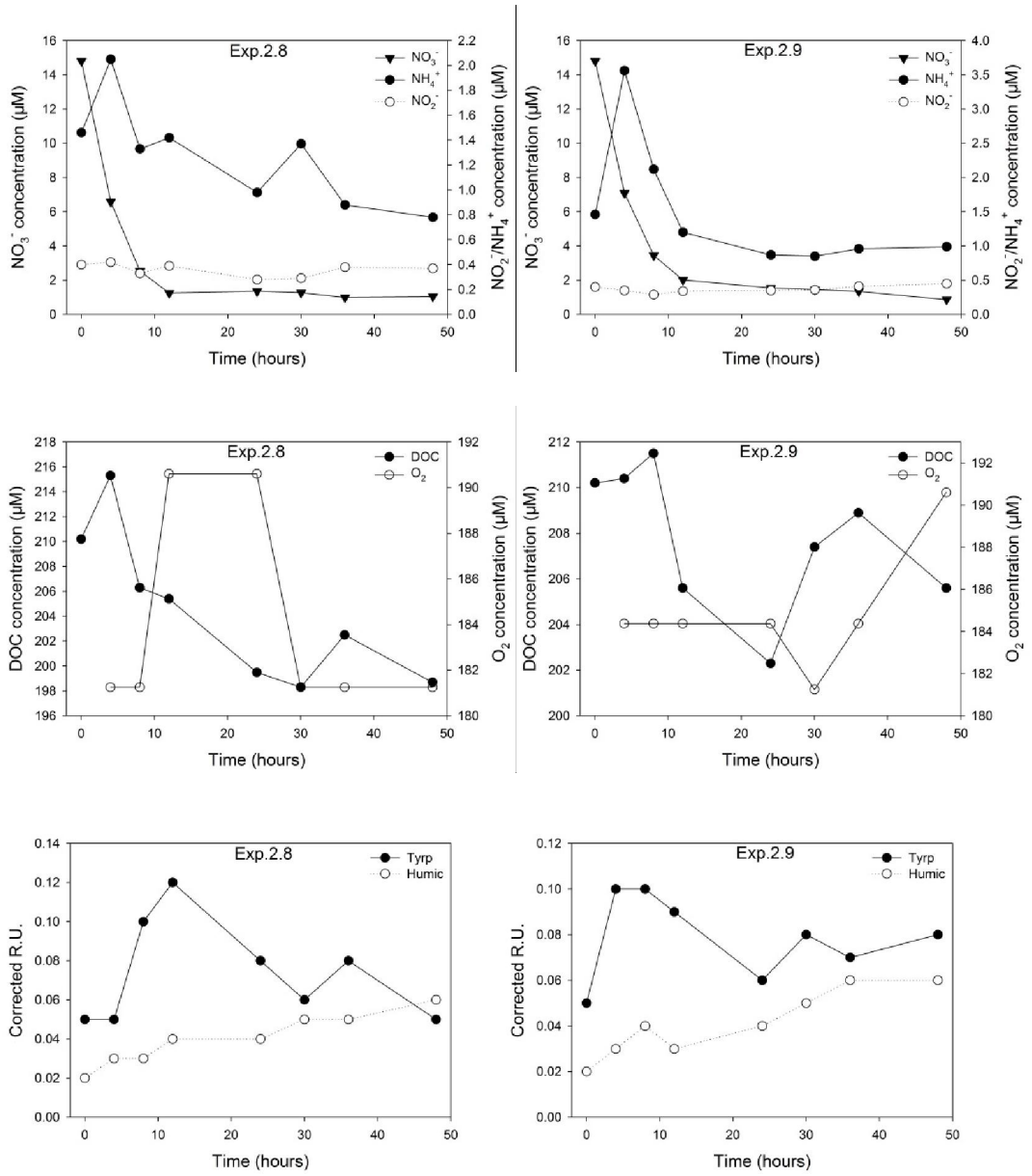

Figure C.8 Concentrations of NO_3^-, NH_4^+, NO_2^-, DOC and DO and relative concentrations of Tyrp-protein and humic material in repeated experiment of Exp.2.8 and Exp.2.9

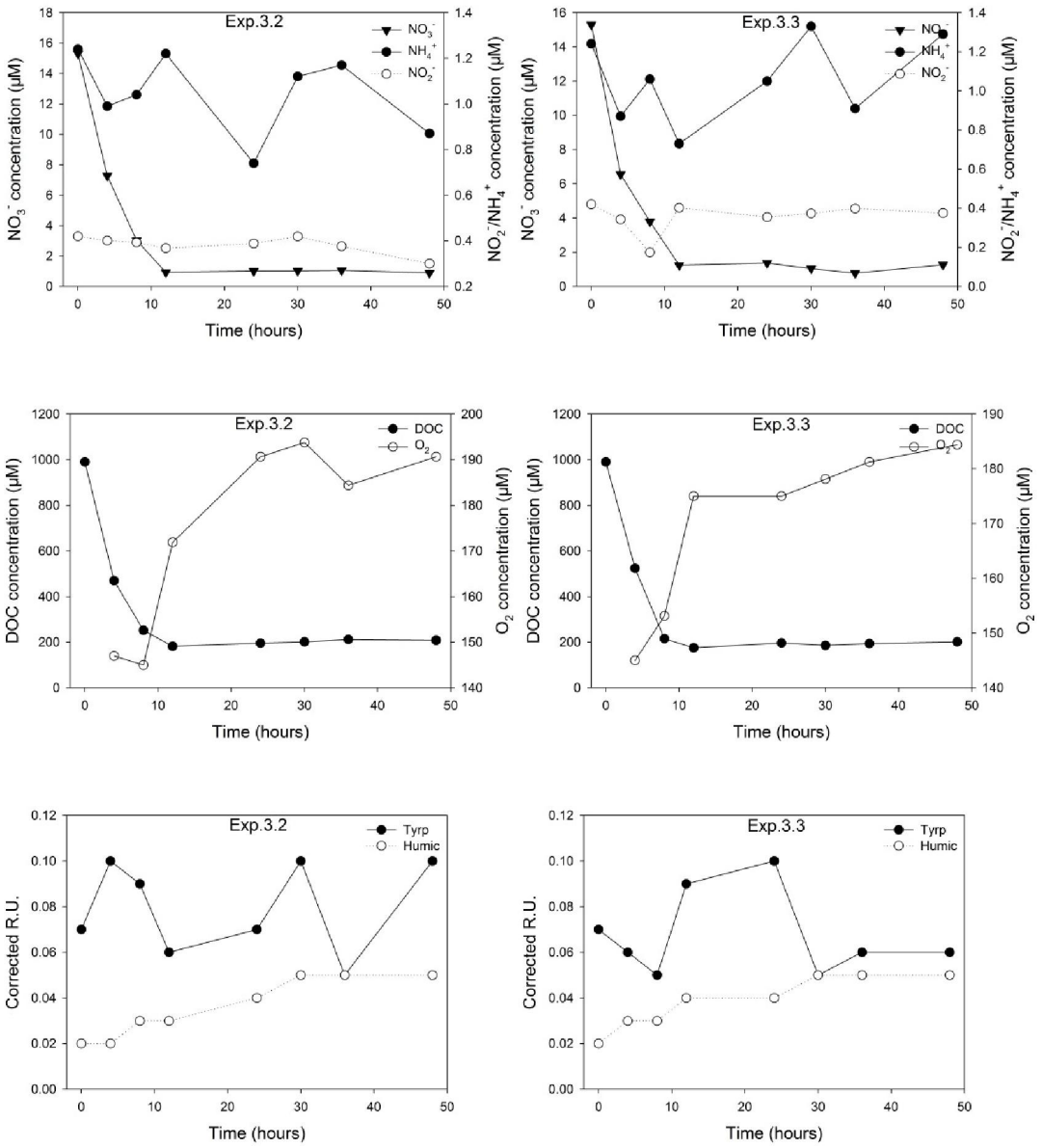

Figure C.9 Concentrations of NO_3^-, NH_4^+, NO_2^-, DOC and DO and relative concentrations of Tyrp-protein and humic material in repeated experiment of Exp.3.2 and Exp.3.3

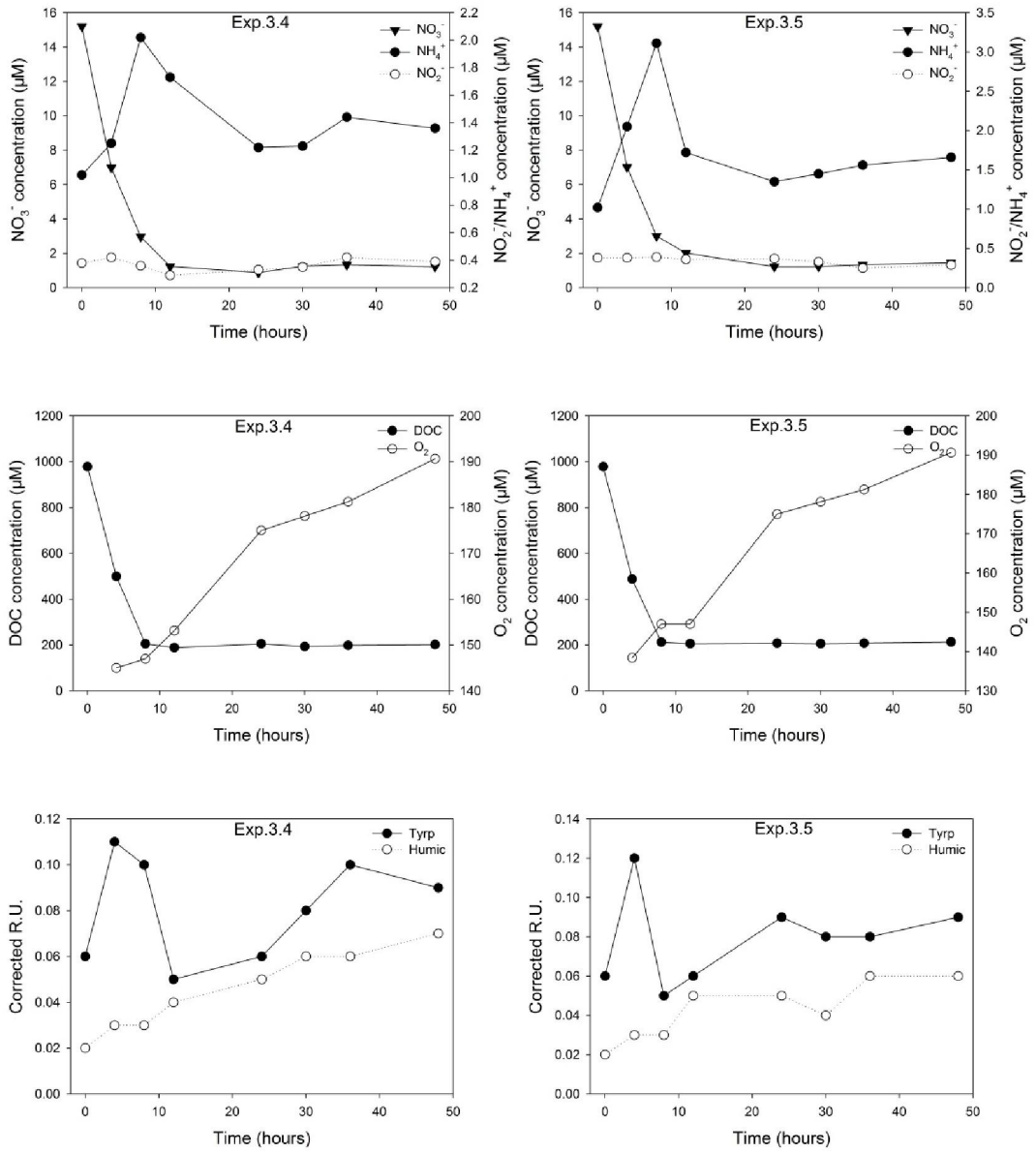

Figure C.10 Concentrations of NO_3^-, NH_4^+, NO_2^-, DOC and DO and relative concentrations of Tyrp-protein and humic material in repeated experiment of Exp.3.4 and Exp.3.5

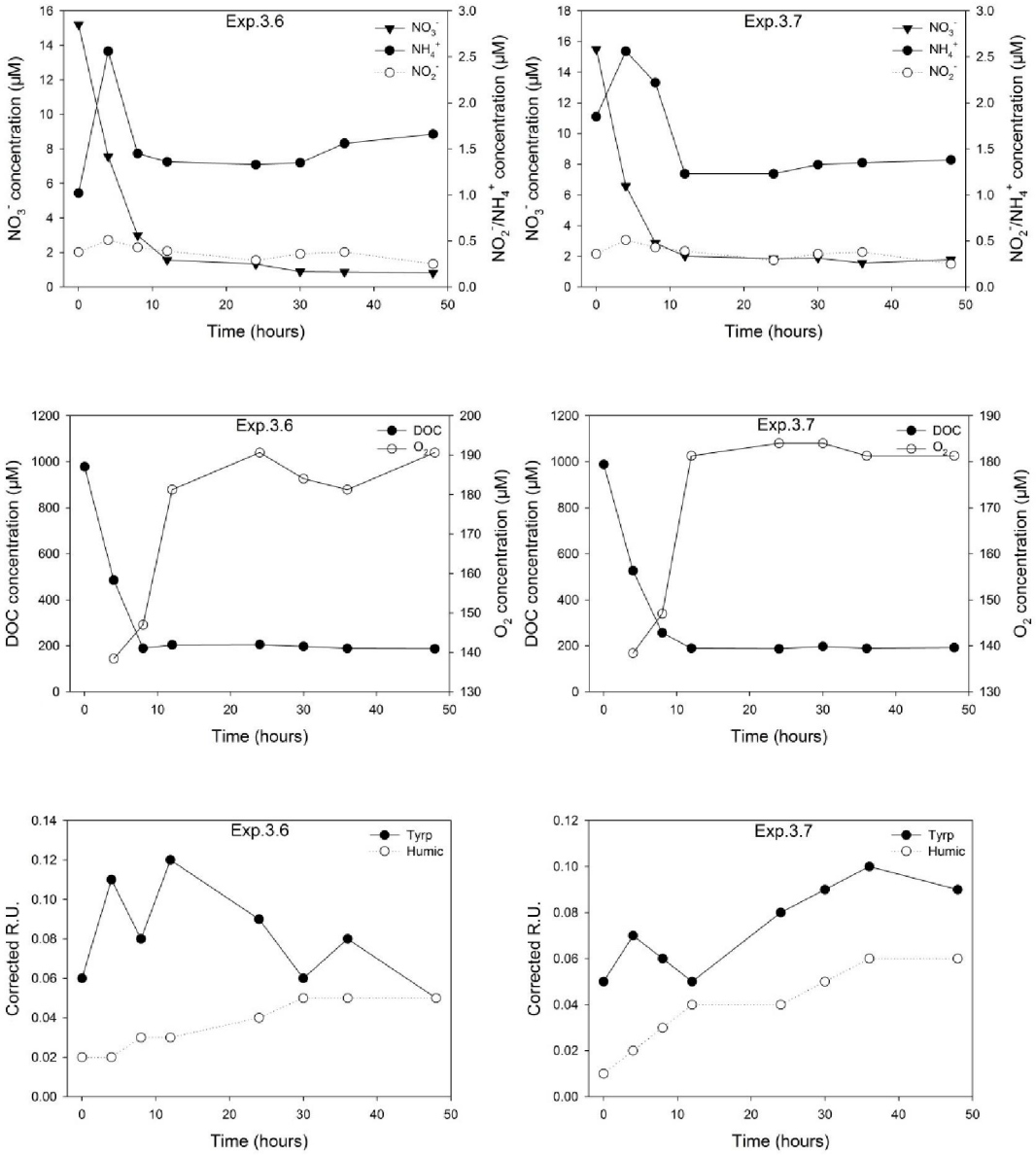

Figure C.11 Concentrations of NO_3^-, NH_4^+, NO_2^-, DOC and DO and relative concentrations of Tyrp-protein and humic material in repeated experiment of Exp.3.6 and Exp.3.7

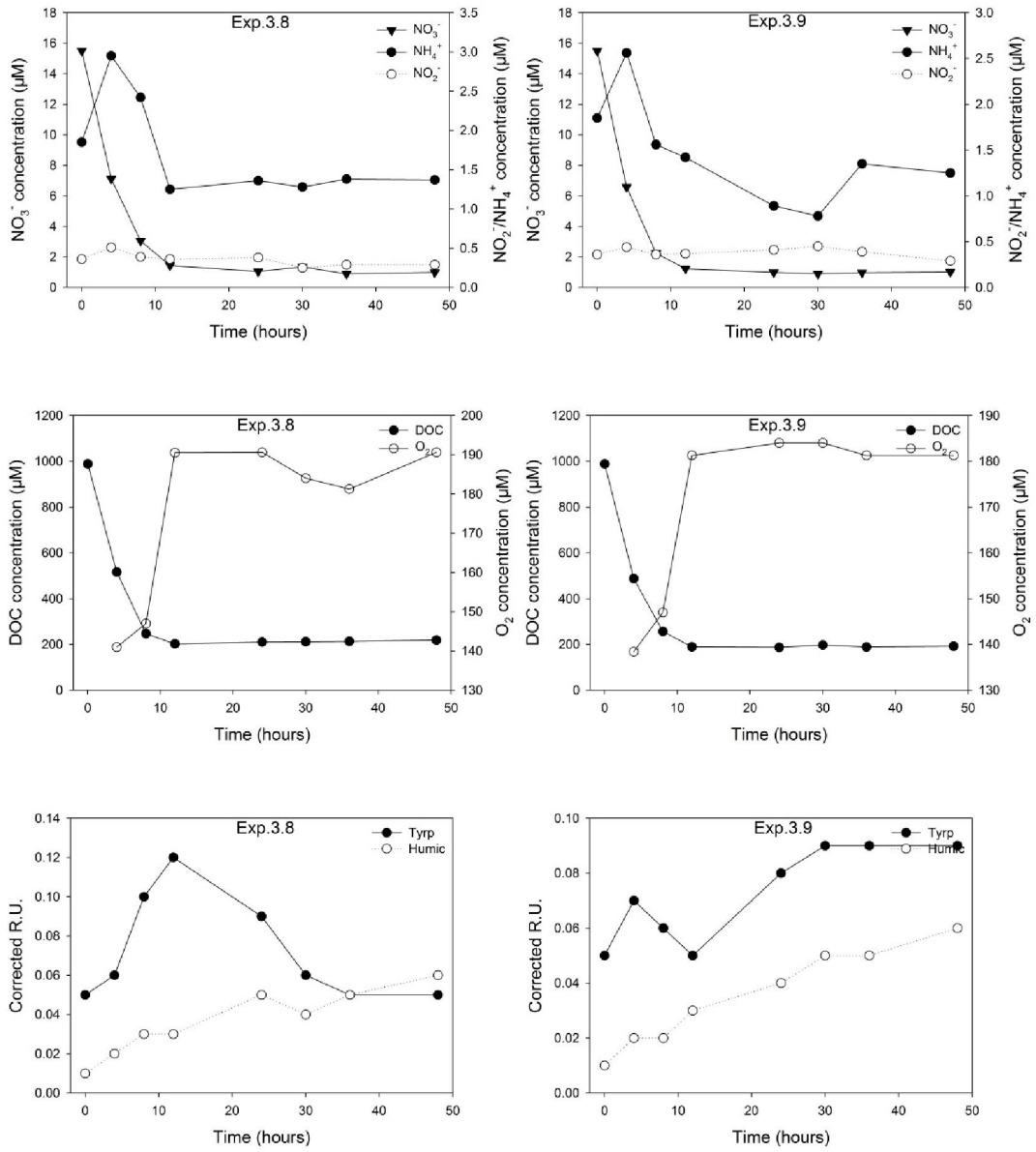

Figure C.12 Concentrations of NO_3^-, NH_4^+, NO_2^-, DOC and DO and relative concentrations of Tyrp-protein and humic material in repeated experiment of Exp.3.8 and Exp.3.9

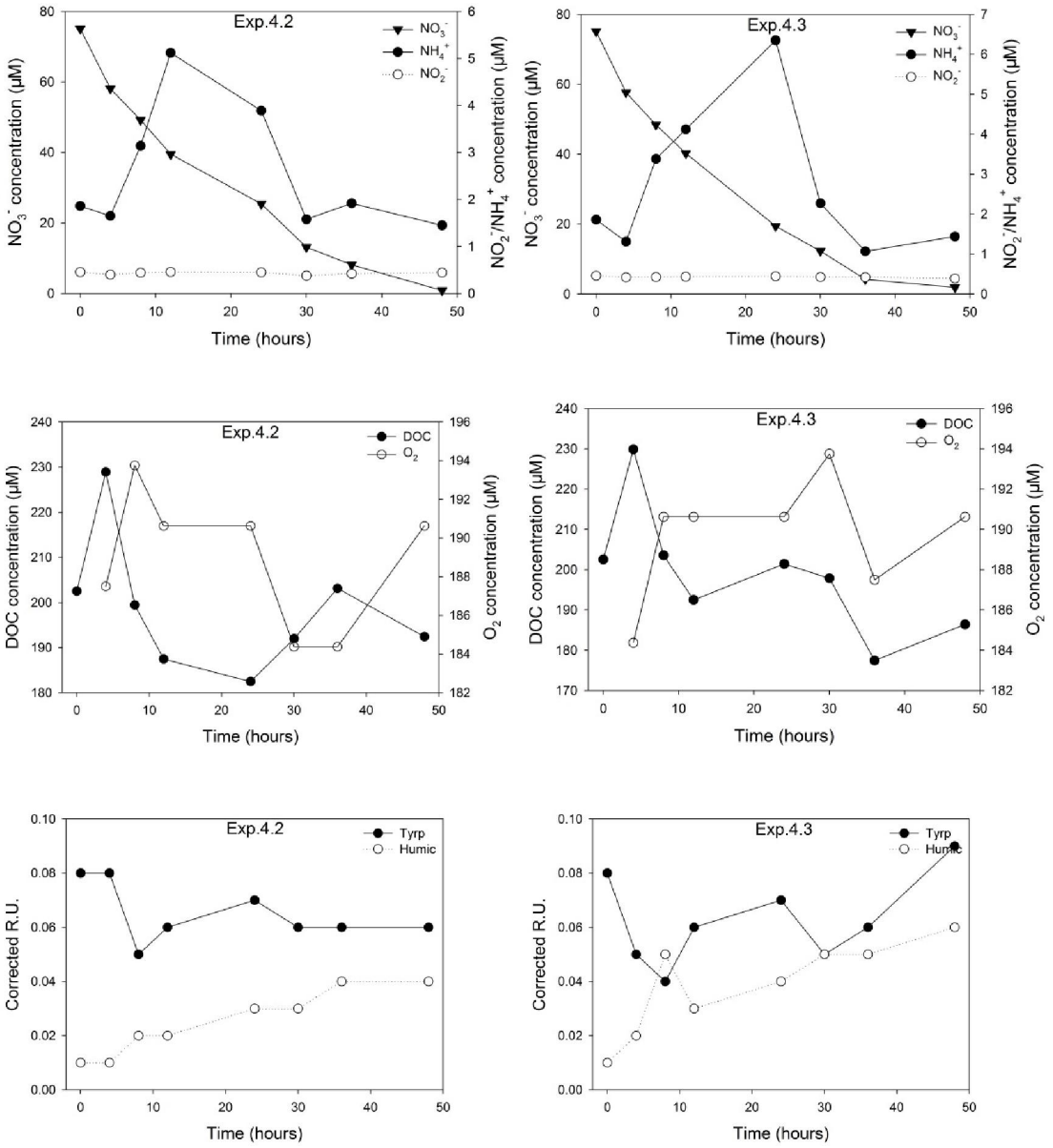

Figure C.13 Concentrations of NO_3^-, NH_4^+, NO_2^-, DOC and DO and relative concentrations of Tyrp-protein and humic material in repeated experiment of Exp.4.2 and Exp.4.3

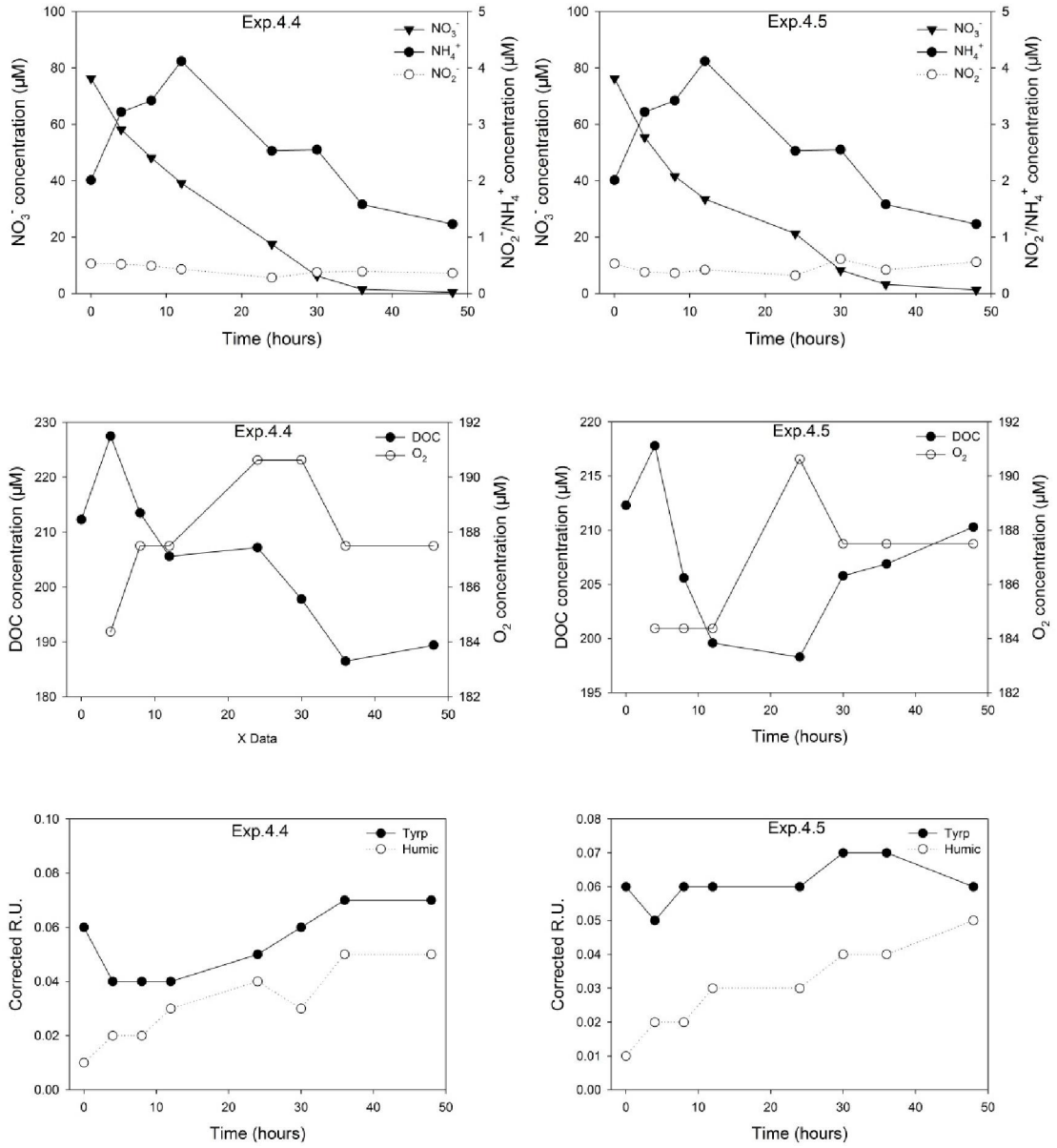

Figure C.14 Concentrations of NO_3^-, NH_4^+, NO_2^-, DOC and DO and relative concentrations of Tyrp-protein and humic material in repeated experiment of Exp.4.4 and Exp.4.5

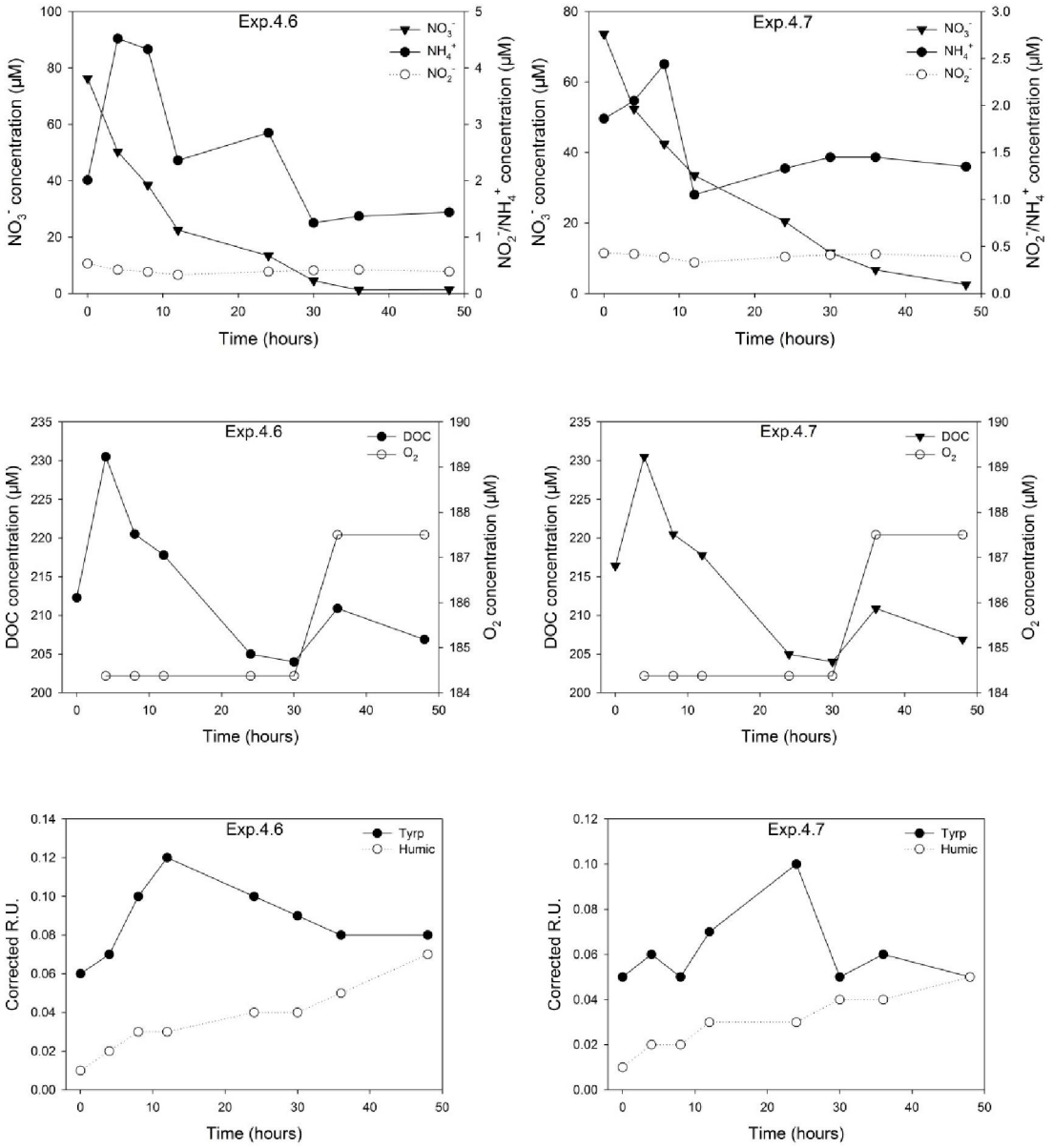

Figure C.15 Concentrations of NO_3^-, NH_4^+, NO_2^-, DOC and DO and relative concentrations of Tyrp-protein and humic material in repeated experiment of Exp.4.6 and Exp.4.7

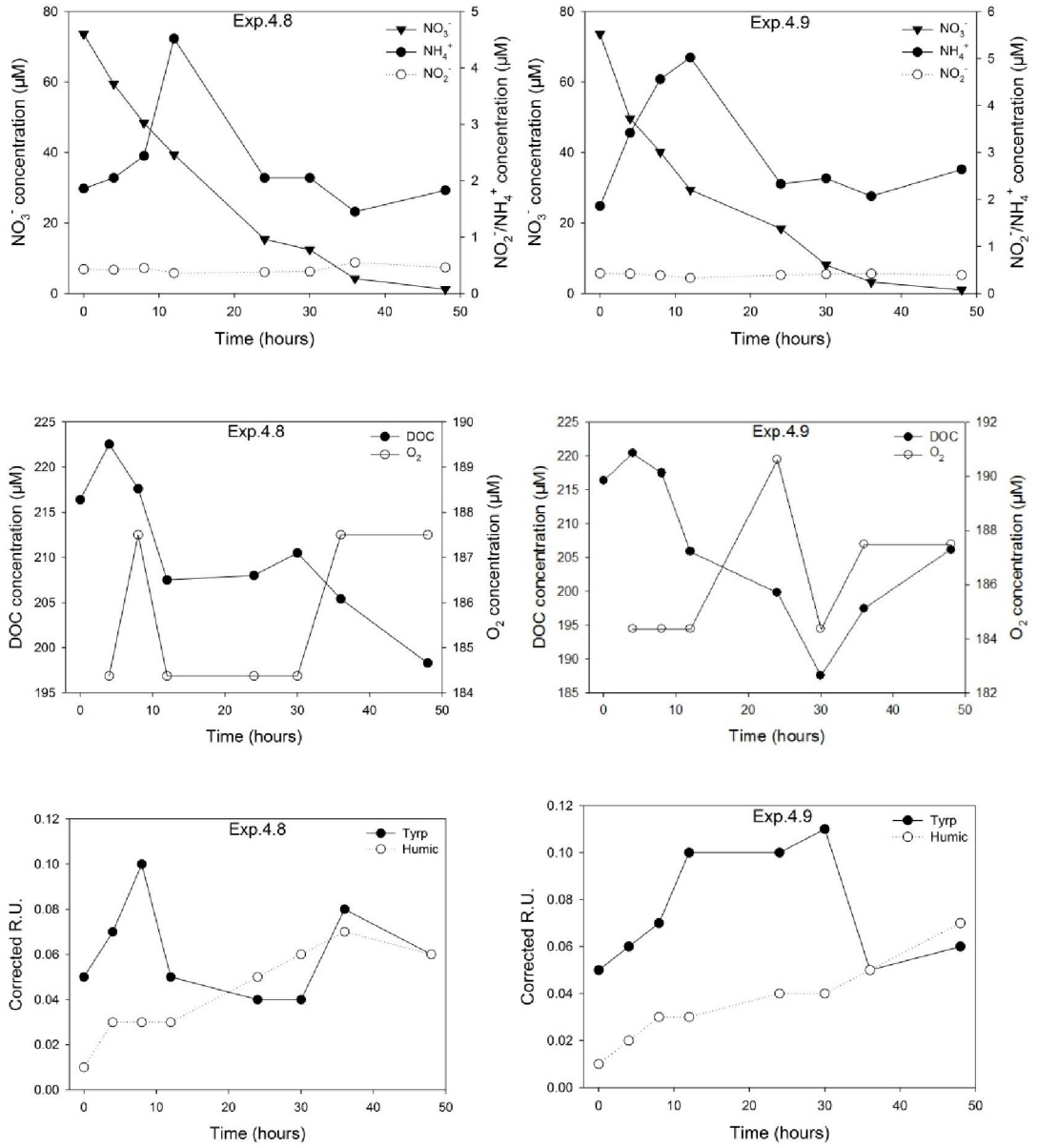

Figure C.16 Concentrations of NO_3^-, NH_4^+, NO_2^-, DOC and DO and relative concentrations of Tyrp-protein and humic material in repeated experiment of Exp.4.8 and Exp.4.9

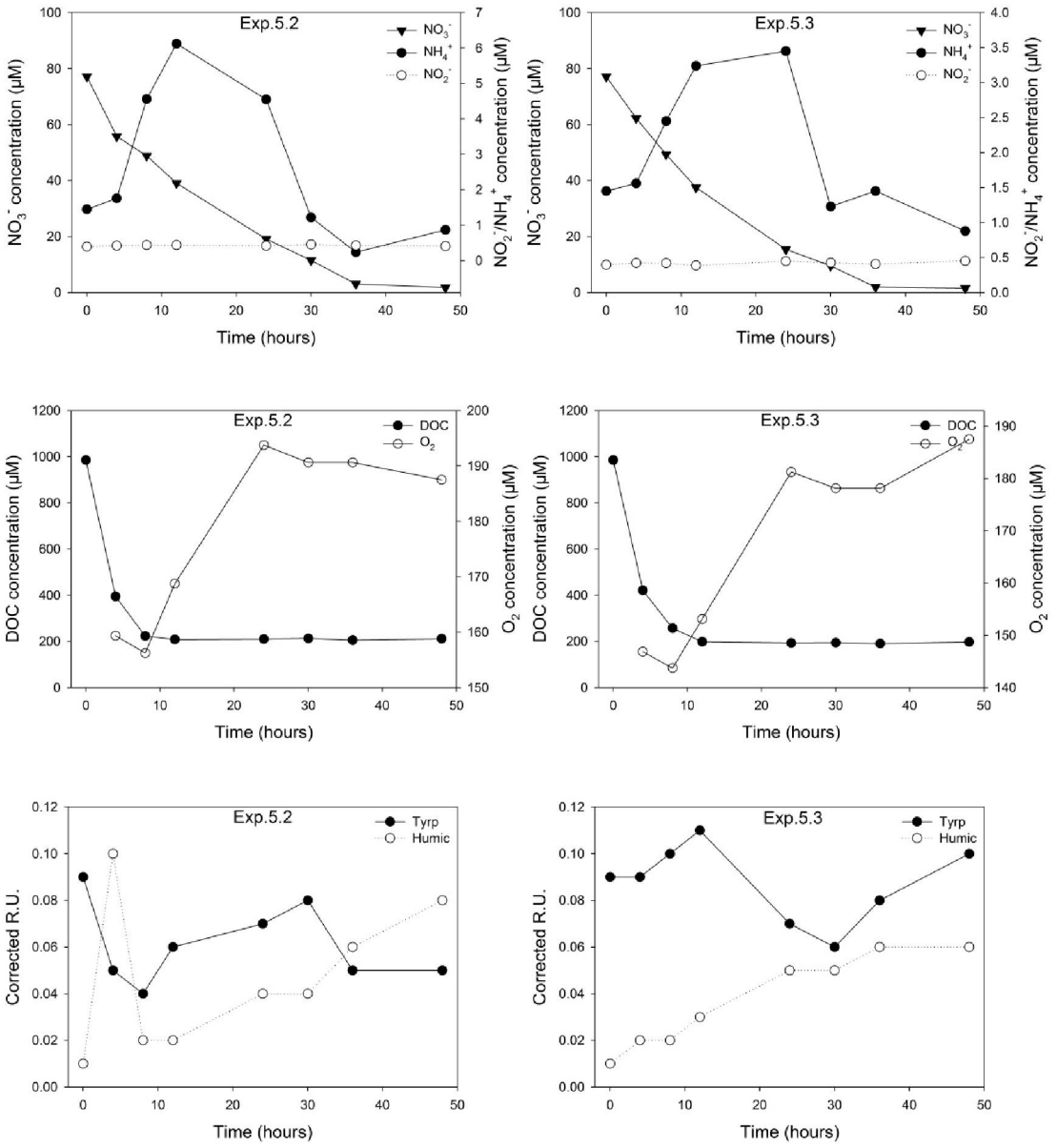

Figure C.17 Concentrations of NO_3^-, NH_4^+, NO_2^-, DOC and DO and relative concentrations of Tyrp-protein and humic material in repeated experiment of Exp.5.1 and Exp.5.2

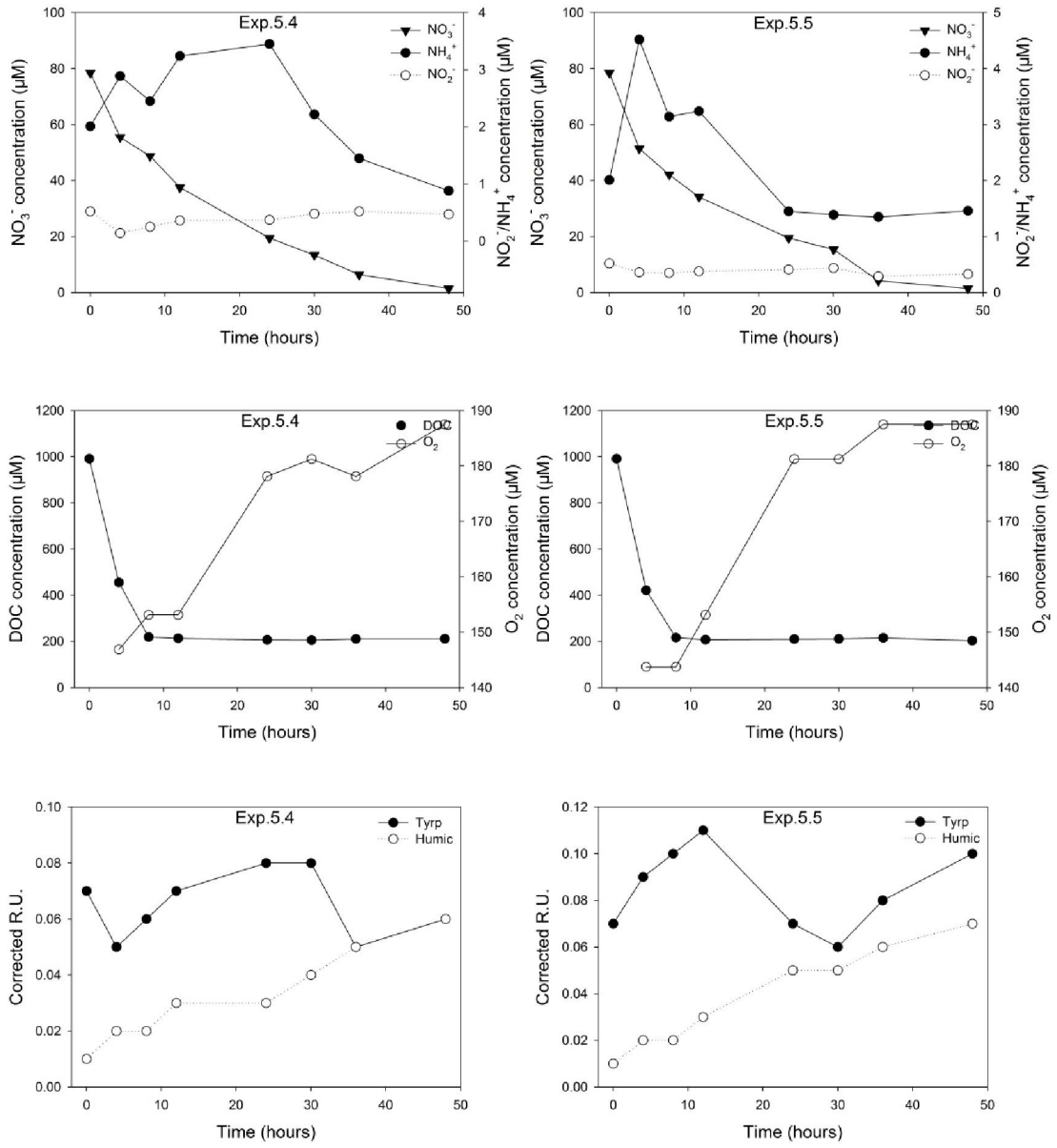

Figure C.18 Concentrations of NO_3^-, NH_4^+, NO_2^-, DOC and DO and relative concentrations of Tyrp-protein and humic material in repeated experiment of Exp.5.3 and Exp.5.4

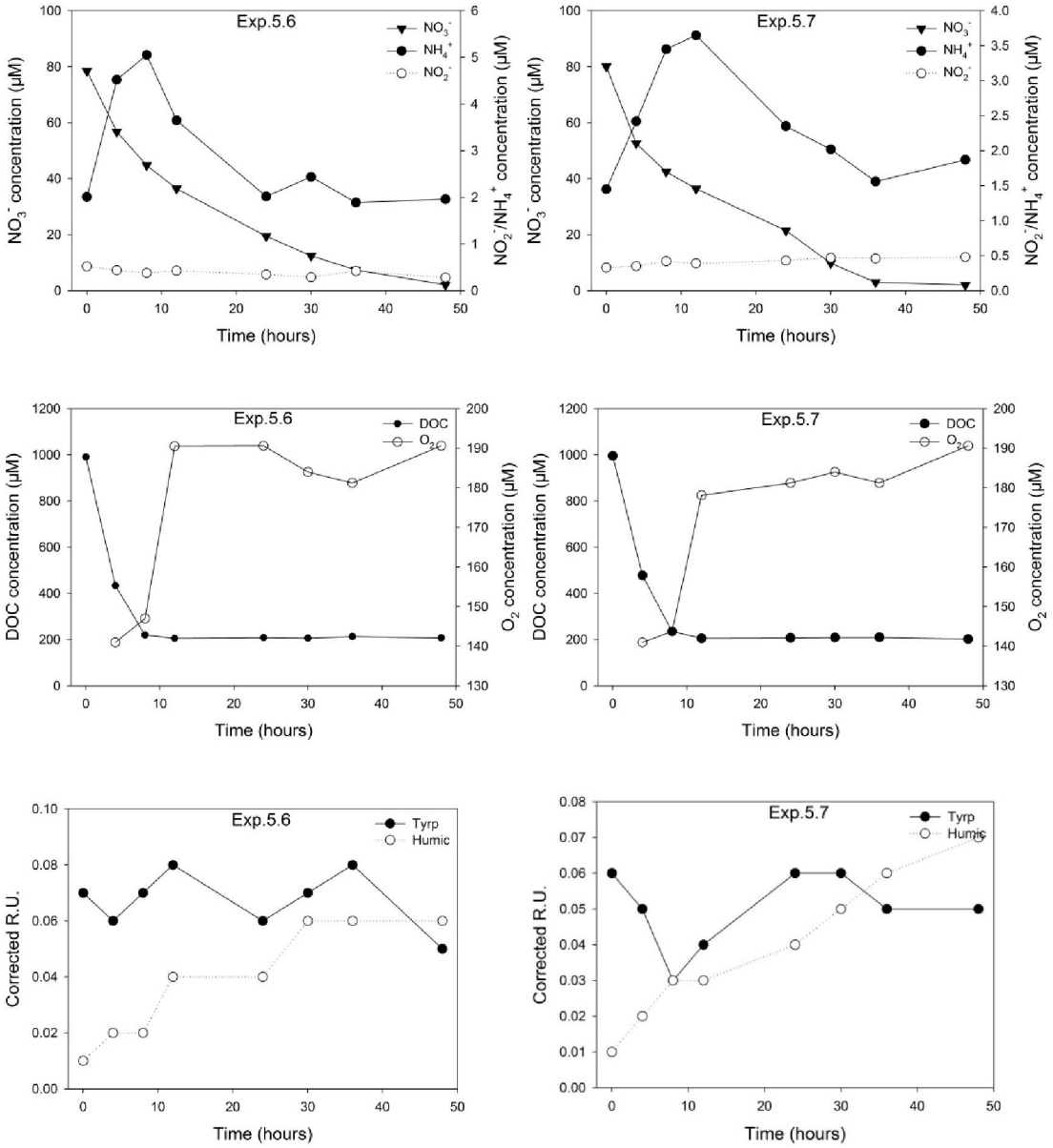

Figure C.19 Concentrations of NO_3^-, NH_4^+, NO_2^-, DOC and DO and relative concentrations of Tyrp-protein and humic material in repeated experiment of Exp.5.6 and Exp.5.7

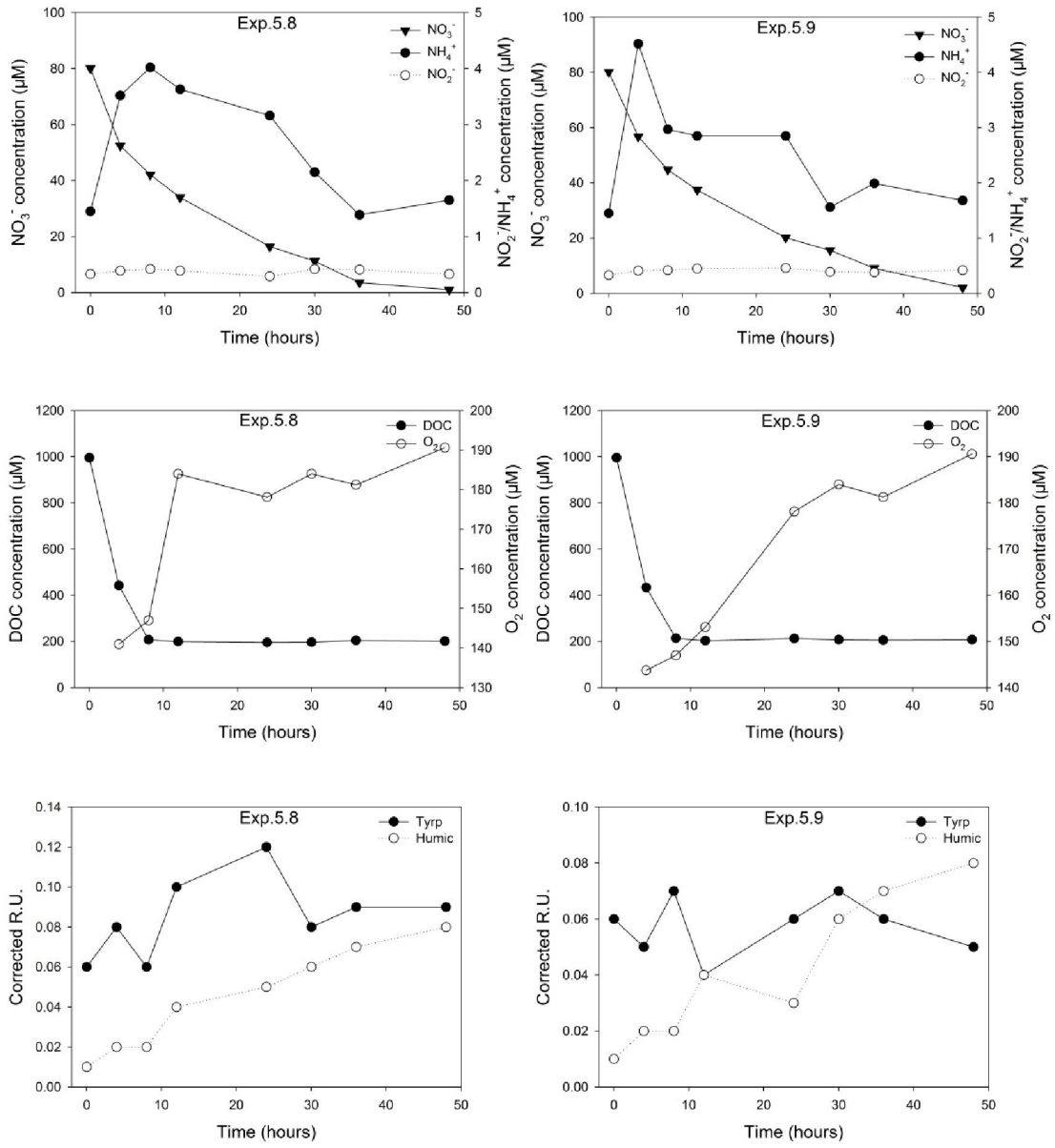

Figure C.20 Concentrations of NO_3^-, NH_4^+, NO_2^-, DOC and DO and relative concentrations of Tyrp-protein and humic material in repeated experiment of Exp.5.8 and Exp.5.9

Appendix D

Supplementary material for Chapter VII

Day		Night	
Site	**Concentration (µM)**	**Site**	**Concentration (µM)**
S1	0.18	S19	0.02
S2	0.02	S20	0.04
S3	0.03	S21	0.05
S4	-0.11	S22	0.04
S5	0.12	S23	0.03
S6	0.15	S24	0.02
S7	0.16	S25	-0.04
S8	0.19	S26	-0.08
S9	0.04	S27	0.11
S10	0.11	S28	0.04
S11	0.21	S29	0.05
S12	-0.04	S30	0.08
S13	0.05	S31	0.36
S14	0.17	S32	-0.12
S15	0.02	S33	-0.10
S16	0.08	S34	0.07

Table D.1 Concentration of NO_2^- in lagoon water during boat survey at May 2010

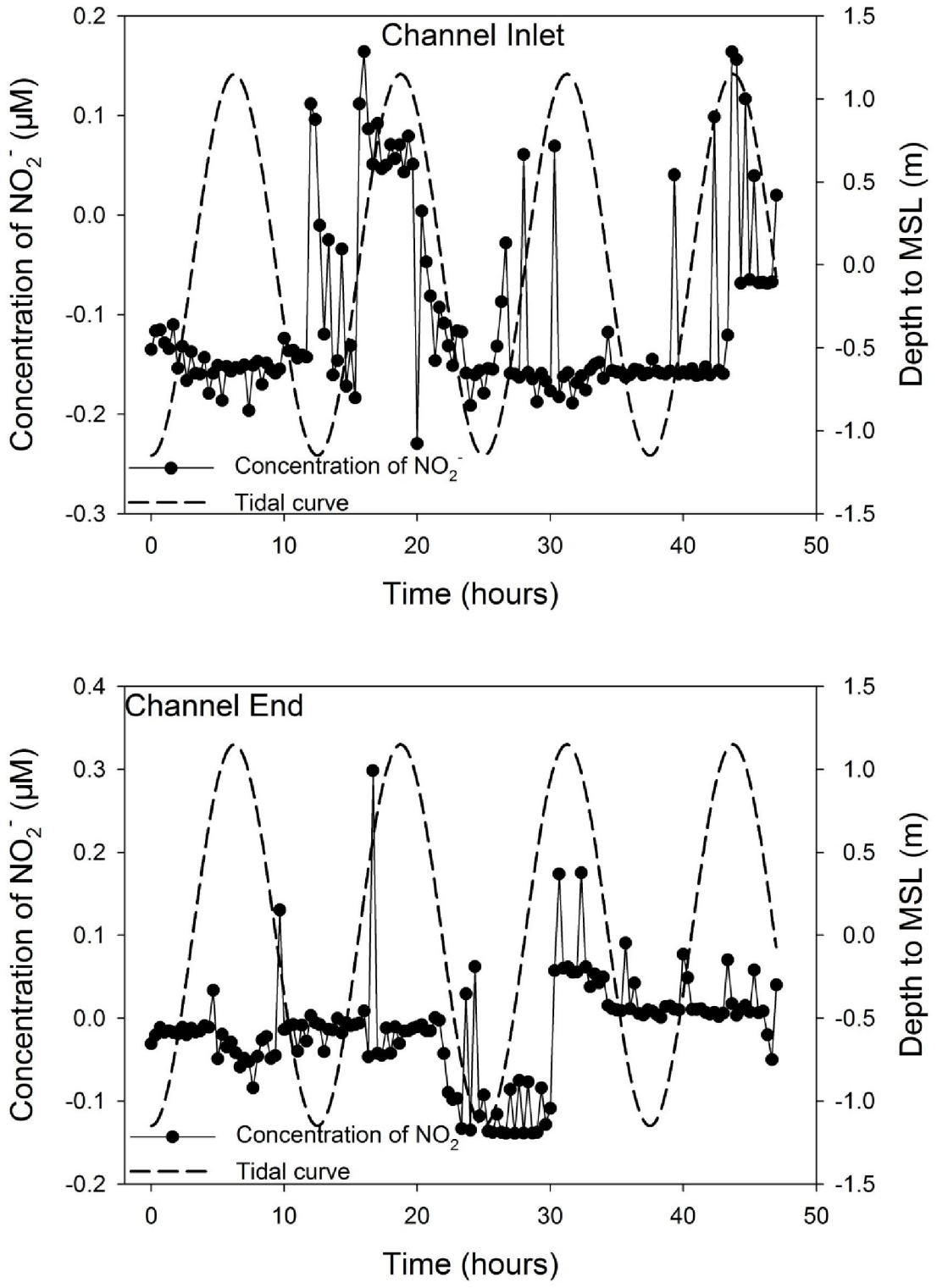

Figure D.1 Concentration of NO_2^- at the Channel inlet and Channel end during time series survey

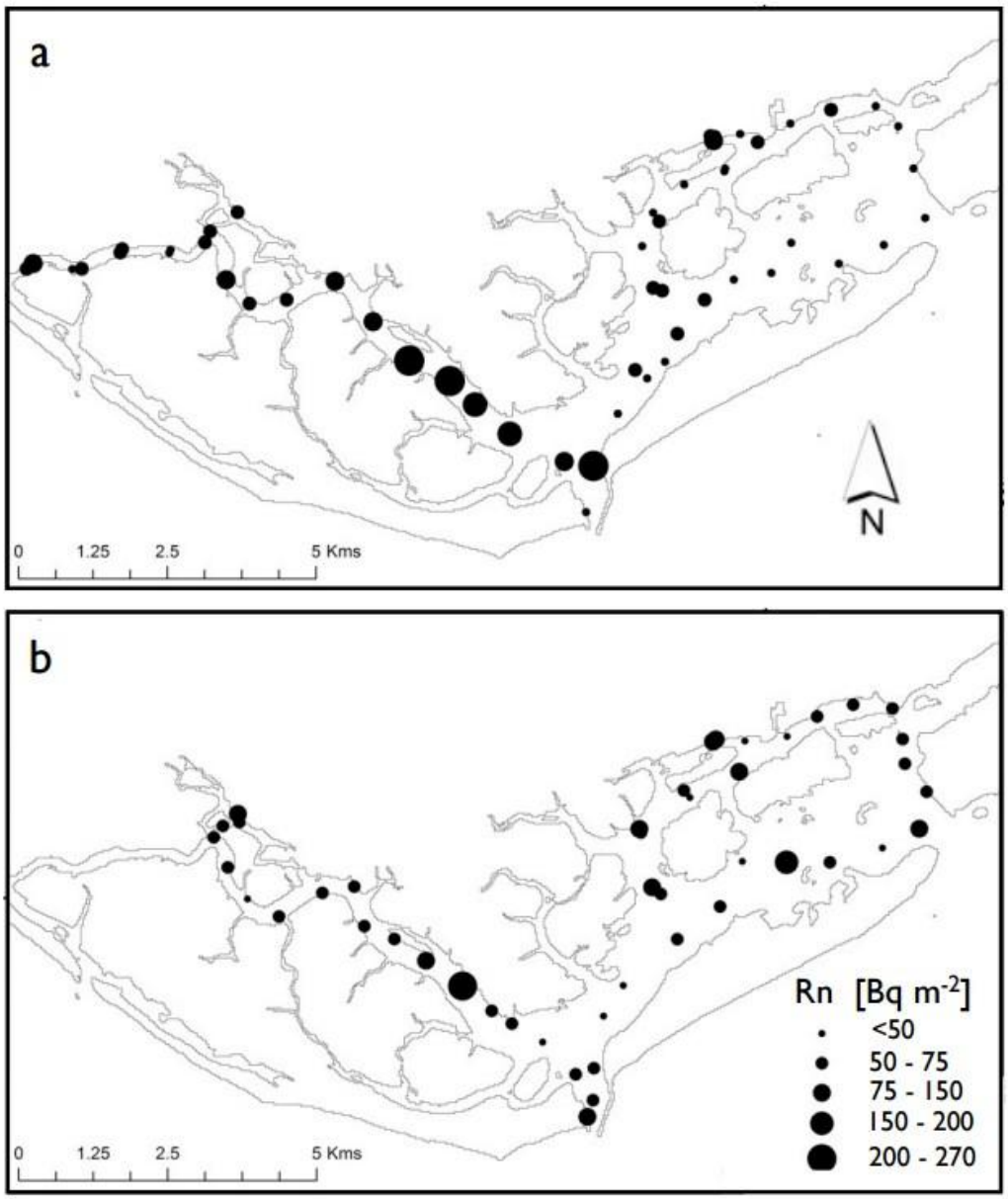

Figure D.2 Radon activity between flood tide (a) and ebbing tide (b) during boat survey, taken from Rocha et al., (in press). Based on the difference between tidal phases, the excess radon flux was 4.14 (±4.87)10^{8} Bq day^{-1} for the entire lagoon.

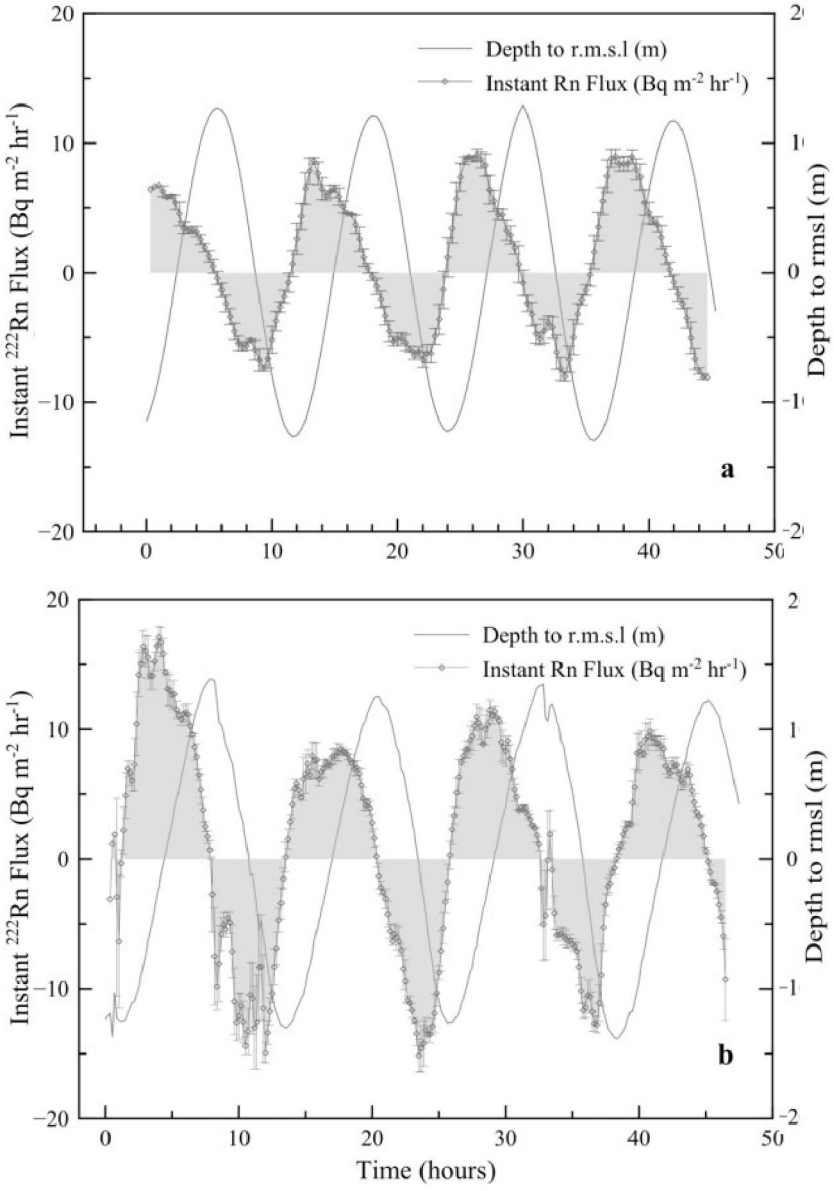

Figure D.3 Radon fluxes at Channel inlet (top) and Channel end (bottom) during time series survey, taken from Rocha et al., (in press) The excess radon flux was 4.14 (±3.00)10^8 Bq day^{-1} for the entire lagoon.

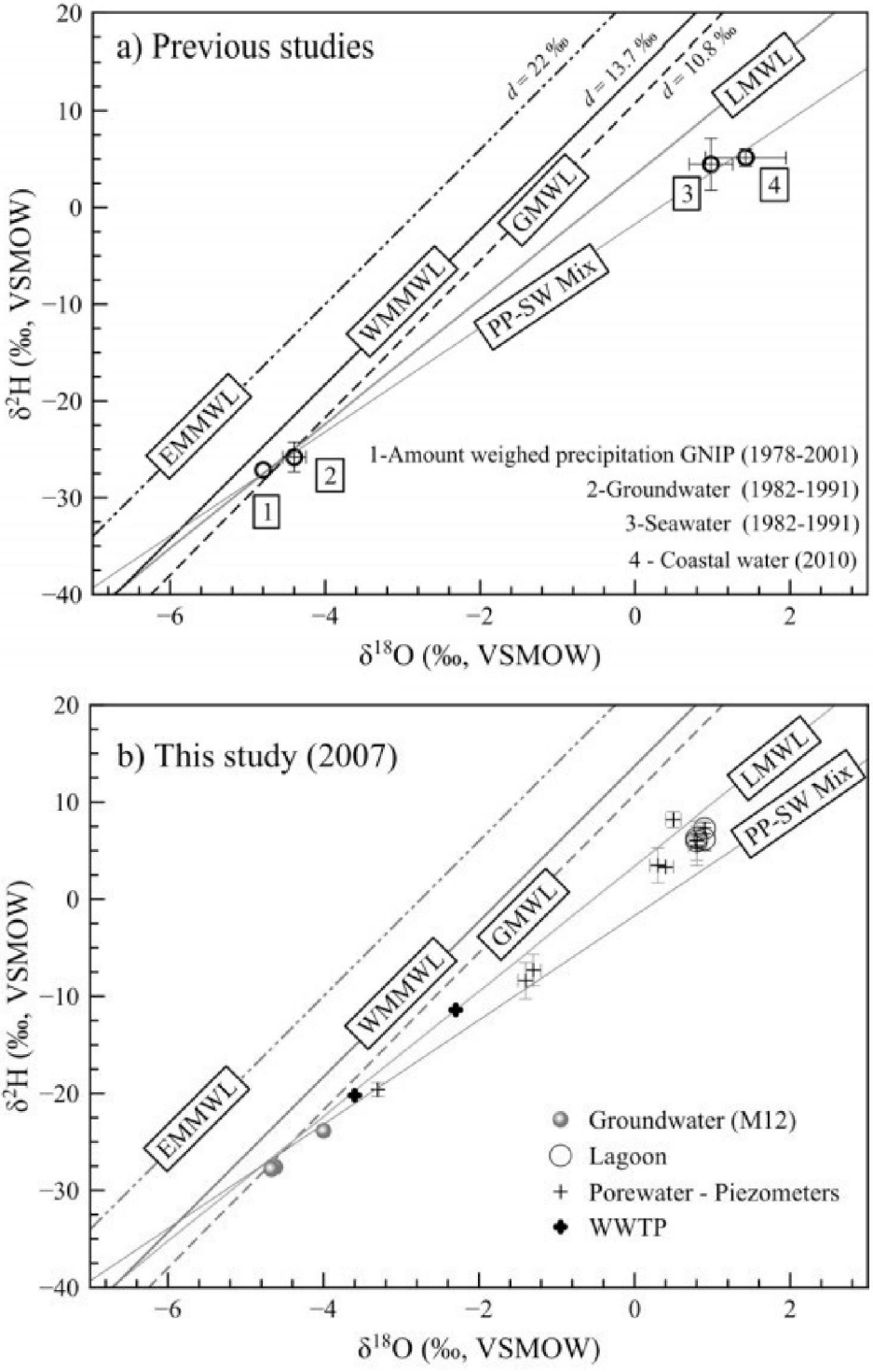

Figure D.4 Catchment isotope hydrology. Plot (A) shows the main meteoric water lines framing the isotopic composition of precipitation within the catchment, including the precipitation-seawater mixing line. B plots the isotopic compositional range of water samples taken during 2007. The mixing suggests that the fresh groundwater in the lagoon is derived from Campino de Faro aquifer system (M12). Taken from Rocha et al., (in press).

Bibliographic list of references

Addy, K., Gold, A., Nowicki, B., McKenna, J., Stolt, M., Groffman, P. (2005) Denitrification capacity in a subterranean estuary below a Rhode Island fringing salt marsh. Estuaries 28, 896-908.

Aller, R.C. (1994) Bioturbation and remineralization of sedimentary organic matter: effects of redox oscillation. Chemical Geology 114, 331-345.

Almeida, C., Mendonça, J., Jesus, M., Gomes, A. (2000) Sistemas aquíferos de Portugal continental. Relatório. INAG, Lisboa. Documento electrónico em CD-ROM.

Almeida, C., Silva, M., (1987) Incidence of agriculture on water quality at Campina de Faro (south Portugal), IV Simposio de Hidrogeología de la Asociación Española de Hidrología Subterránea, Palma de Mallorca.

Almeida, L., Vousdoukas, M., Ferreira, Ó., Rodrigues, B., Matias, A. (2012) Thresholds for storm impacts on an exposed sandy coastal area in southern Portugal. Geomorphology 143, 3-12.

An, S., Gardner, W.S. (2002) Dissimilatory nitrate reduction to ammonium (DNRA) as a nitrogen link, versus denitrification as a sink in a shallow estuary (Laguna Madre/Baffin Bay, Texas). Marine Ecology Progress Series 237.

Andrade, C., Freitas, M., Moreno, J., Craveiro, S. (2004) Stratigraphical evidence of Late Holocene barrier breaching and extreme storms in lagoonal sediments of Ria Formosa, Algarve, Portugal. Marine Geology 210, 339-362.

Aníbal, J., Esteves, E., Rocha, C. (2011) Seasonal variations in gross biochemical composition, percent edibility, and condition index of the clam Ruditapes decussatus cultivated in the Ria Formosa (South Portugal). Journal of Shellfish Research 30, 17-23.

Aníbal, J., Rocha, C., Sprung, M. (2007) Mudflat surface morphology as a structuring agent of algae and associated macroepifauna communities: A case study in the Ria Formosa. Journal of Sea Research 57, 36-46.

Anschutz, P., Smith, T., Mouret, A., Deborde, J., Bujan, S., Poirier, D., Lecroart, P. (2009) Tidal sands as biogeochemical reactors. Estuarine, Coastal and Shelf Science 84, 84-90.

Arnaud-Fassetta, G., Bertrand, F., Costa, S., Davidson, R. (2006) The western lagoon marshes of the Ria Formosa (Southern Portugal): Sediment-vegetation dynamics, long-term to short-term changes and perspective. Continental Shelf Research 26, 363-384.

Azizian, S. (2004) Kinetic models of sorption: a theoretical analysis. Journal of Colloid and Interface Science 276, 47-52.

Balouin, Y., Howa, H., Michel, D. (2001) Swash platform morphology in the ebb-tidal delta of the Barra Nova inlet, South Portugal. Journal of Coastal Research, 784-791.

Balouin, Y., Howa, H., Pedreros, R., Michel, D. (2005) Longshore sediment movements from tracers and models, Praia de Faro, South Portugal. Journal of Coastal Research, 146-156.

Baptista, T. (1993) Microbiological observations in the Ria Formosa. M. Phil, University of Wales.

Barnes, R.S.K. (1980) Coastal lagoons. CUP Archive.

Barreira, L.A., Bebianno, M.J., Mudge, S.M., Ferreira, A.M., Albino, C.I., Veriato, L.M. (2005) Relationship between PCBs in suspended and settled sediments from a coastal lagoon. Ciencias Marinas 31, 179-195.

Batley, G.E. (1989) Trace Element Speciation Analytical Methods and Problems. CRC Press.

Bebianno, M. (1995) Effects of pollutants in the Ria Formosa lagoon, Portugal. Science of the total environment 171, 107-115.

Beck, A.J., Tsukamoto, Y., Tovar-Sanchez, A., Huerta-Diaz, M., Bokuniewicz, H.J., Sañudo-Wilhelmy, S.A. (2007a) Importance of geochemical transformations in determining submarine groundwater discharge-derived trace metal and nutrient fluxes. Applied Geochemistry 22, 477-490.

Beck, M., Dellwig, O., Kolditz, K., Freund, H., Liebezeit, G., Schnetger, B., Brumsack, H.J. (2007b) In situ pore water sampling in deep intertidal flat sediments. Limnology and oceanography: Methods 5, 136-144.

Berg, P., McGlathery, K.J. (2001) A high‐resolution pore water sampler for sandy sediments. Limnology and Oceanography 46, 203-210.

Bernard, R.J., Mortazavi, B., Wang, L., Ortmann, A.C., MacIntyre, H., Burnett, W.C. (2014) Benthic nutrient fluxes and limited denitrification in a sub-tropical groundwater-influenced coastal lagoon. Marine Ecology Progress Series 504, 13-26.

Bettencourt, P., (1994) Les environments sedimentaires de la côte sotavento (Algarve, Sud Portugal) et leurs évolurion holocène et actuelle. 2 volumes. PhD Thesis, Université de Bordeaux I.(unpublished).

Beukema, J., Cadée, G. (1991) Growth rates of the bivalve Macoma balthica in the Wadden Sea during a period of eutrophication: Relationships with concentrations of pelagic diatoms and flagellates. Marine ecology progress series. Oldendorf 68, 249-256.

Beusen, A., Slomp, C., Bouwman, A. (2013) Global land–ocean linkage: direct inputs of nitrogen to coastal waters via submarine groundwater discharge. Environmental Research Letters 8, 034035.

Borggaard, O., Jdrgensen, S., Moberg, J., Raben‐Lange, B. (1990) Influence of organic matter on phosphate adsorption by aluminium and iron oxides in sandy soils. Journal of Soil Science 41, 443-449.

Boudreau, B.P., Huettel, M., Forster, S., Jahnke, R.A., McLachlan, A., Middelburg, J.J., Nielsen, P., Sansone, F., Taghon, G., Van Raaphorst, W. (2001) Permeable marine sediments: overturning an old paradigm. Eos, Transactions American Geophysical Union 82, 133-136.

Bowen, J., Kroeger, K., Tomasky, G., Pabich, W., Cole, M., Carmichael, R., Valiela, I. (2007) A review of land–sea coupling by groundwater discharge of nitrogen to New England estuaries: Mechanisms and effects. Applied Geochemistry 22, 175-191.

Bradley, P., Fernandez Jr, M., Chapelle, F. (1992) Carbon limitation of denitrification rates in an anaerobic groundwater system. Environ Sci Technol 26, 2377-2381.

Brooks, R., Corey, T. (1964) HYDRAU UC PROPERTIES OF POROUS MEDIA.

Brunauer, S., Emmett, P.H., Teller, E. (1938) Adsorption of gases in multimolecular layers. Journal of the American Chemical Society 60, 309-319.

Burgin, A.J., Hamilton, S.K. (2007) Have we overemphasized the role of denitrification in aquatic ecosystems? A review of nitrate removal pathways. Frontiers in Ecology and the Environment 5, 89-96.

Burnett, W., Aggarwal, P., Aureli, A., Bokuniewicz, H., Cable, J., Charette, M., Kontar, E., Krupa, S., Kulkarni, K., Loveless, A. (2006) Quantifying submarine groundwater discharge in the coastal zone via multiple methods. Science of the total environment 367, 498-543.

Burnett, W.C., Bokuniewicz, H., Huettel, M., Moore, W.S., Taniguchi, M. (2003) Groundwater and pore water inputs to the coastal zone. Biogeochemistry 66, 3-33.

Burnett, W.C., Taniguchi, M., Oberdorfer, J. (2001) Measurement and significance of the direct discharge of groundwater into the coastal zone. Journal of Sea Research 46, 109-116.

Cabaço, S., Machás, R., Vieira, V., Santos, R. (2008) Impacts of urban wastewater discharge on seagrass meadows (Zostera noltii). Estuarine, Coastal and Shelf Science 78, 1-13.

Cable, J.E., Burnett, W.C., Chanton, J.P. (1997) Magnitude and variations of groundwater seepage along a Florida marine shoreline. Biogeochemistry 38, 189-205.

Cable, J.E., Burnett, W.C., Chanton, J.P., Weatherly, G.L. (1996) Estimating groundwater discharge into the northeastern Gulf of Mexico using radon-222. Earth and Planetary Science Letters 144, 591-604.

Caetano, M., Falcao, M., Vale, C., Bebianno, M. (1997) Tidal flushing of ammonium, iron and manganese from inter-tidal sediment pore waters. Marine Chemistry 58, 203-211.

Camargo, J.A., Alonso, Á. (2006) Ecological and toxicological effects of inorganic nitrogen pollution in aquatic ecosystems: a global assessment. Environment international 32, 831-849.

Canfield, D.E., Jørgensen, B.B., Fossing, H., Glud, R., Gundersen, J., Ramsing, N.B., Thamdrup, B., Hansen, J.W., Nielsen, L.P., Hall, P.O. (1993) Pathways of organic carbon oxidation in three continental margin sediments. Marine Geology 113, 27-40.

Canuel, E.A., Martens, C.S. (1993) Seasonal variations in the sources and alteration of organic matter associated with recently-deposited sediments. Organic Geochemistry 20, 563-577.

Carey, A.E., Dowling, C.B., Poreda, R.J. (2004) Alabama Gulf Coast groundwaters: 4He and 14C as groundwater-dating tools. Geology 32, 289-292.

Carlson, C., Ducklow, H. (1995) Dissolved organic carbon in the upper ocean of the central equatorial Pacific Ocean, 1992: Daily and finescale vertical variations. Deep Sea Research Part II: Topical Studies in Oceanography 42, 639-656.

References

Carvalho, L.F., Rocha, C., Fleming, A., Veiga-Pires, C., Aníbal, J. (2013) Interception of nutrient rich submarine groundwater discharge seepage on European temperate beaches by the acoel flatworm,< i> Symsagittifera roscoffensis</i>. Mar Pollut Bull 75, 150-156.

Cascalho, J., Taborda, R.d.M., (2006) Heavy mineral placer formation-An example from Algarve, Portugal, Journal of Coastal Research, Proceedings of the 8 International Coastal Symposium, Itajaí, SC, Brazil. SI, pp. 246-249.

Chance, J., Berube, J., Vandersmissen, M., Blanckaert, N. (2009) Evaluation of the BD Vacutainer® PST™ II blood collection tube for special chemistry analytes. Clinical Chemistry and Laboratory Medicine 47, 358-361.

Charbonnier, C., Anschutz, P., Poirier, D., Bujan, S., Lecroart, P. (2013) Aerobic respiration in a high-energy sandy beach. Marine Chemistry 155, 10-21.

Charette, M.A., Buesseler, K.O. (2004) Submarine groundwater discharge of nutrients and copper to an urban subestuary of Chesapeake Bay(Elizabeth River). Limnology and Oceanography 49, 376-385.

Charette, M.A., Sholkovitz, E.R. (2002) Oxidative precipitation of groundwater-derived ferrous iron in the subterranean estuary of a coastal bay. Geophysical Research Letters 29, 1444.

Charette, M.A., Sholkovitz, E.R. (2006) Trace element cycling in a subterranean estuary: Part 2. Geochemistry of the pore water. Geochimica Et Cosmochimica Acta 70, 811-826.

Chassagne, R.L., Lecroart, P., Beaugendre, H., Capo, S., Parisot, J.-P., Anschutz, P. (2012) Silicic acid flux to the ocean from tidal permeable sediments: A modeling study. Computers & Geosciences 43, 52-62.

Chen, N., Peng, B., Hong, H., Turyaheebwa, N., Cui, S., Mo, X. (2013) Nutrient enrichment and N: P ratio decline in a coastal bay–river system in southeast China: The need for a dual nutrient (N and P) management strategy. Ocean & coastal management 81, 7-13.

Cheng, W., Dastgheib, S.A., Karanfil, T. (2005) Adsorption of dissolved natural organic matter by modified activated carbons. Water Research 39, 2281-2290.

Ciavola, P., Taborda, R., Ferreira, Ó., Dias, J. (1997) Field observations of sand-mixing depths on steep beaches. Marine Geology 141, 147-156.

Clayton, C.A., Hines, J.W., Elkins, P.D. (1987) Detection limits with specified assurance probabilities. Analytical Chemistry 59, 2506-2514.

Conley, D.J., (1999) Biogeochemical nutrient cycles and nutrient management strategies, Man and River Systems. Springer, pp. 87-96.

Corbett, D.R., Chanton, J., Burnett, W., Dillon, K., Rutkowski, C., Fourqurean, J.W. (1999) Patterns of groundwater discharge into Florida Bay. Limnology and Oceanography 44, 1045-1055.

Corbett, D.R., Kump, L., Dillon, K., Burnett, W., Chanton, J. (2000) Fate of wastewater-borne nutrients under low discharge conditions in the subsurface of the Florida Keys, USA. Marine Chemistry 69, 99-115.

Cornwell, J.C., Kemp, W.M., Kana, T.M. (1999) Denitrification in coastal ecosystems: methods, environmental controls, and ecosystem level controls, a review. Aquatic Ecology 33, 41-54.

Corre, M.D., Schnabel, R.R., Stout, W.L. (2002) Spatial and seasonal variation of gross nitrogen transformations and microbial biomass in a Northeastern US grassland. Soil Biology and Biochemistry 34, 445-457.

Cravo, A., Cardeira, S., Pereira, C., Rosa, M., Madureira, M., Rita, F., Luís, J., Jacob, J. (2013) Nutrients and particulate matter exchanges through the Ria Formosa coastal lagoon, Portugal. Journal of Coastal Research, 1999-2004.

Cufrey, J.M., Kemp, W.M. (1992) Influence of the submersed plant, Potamogeton perfoliatus, on nitrogen cycling in estuarine sediments. Limnology and Oceanography 37, 1483-1495.

Cunha, A., Assis, J., Serrão, E. (2009) Estimation of available seagrass meadow area in Portugal for transplanting purposes. J. Coast. Res 56, 1100-1104.

Dai, J., Yang, H., Yan, H., Shangguan, Y., Zheng, Q., Cheng, R. (2011) Phosphate adsorption from aqueous solutions by disused adsorbents: chitosan hydrogel beads after the removal of copper (II). Chemical Engineering Journal 166, 970-977.

Dalton, H., Brand‐Hardy, R. (2003) Nitrogen: the essential public enemy. Journal of Applied Ecology 40, 771-781.

Darcy, H. (1856) Les fontaines publiques de la ville de Dijon: exposition et application. Victor Dalmont.

References

Davis, J.A. (1982) Adsorption of natural dissolved organic matter at the oxide/water interface. Geochimica Et Cosmochimica Acta 46, 2381-2393.

De Baar, H.J., De Jong, J.T., Bakker, D.C., Löscher, B.M., Veth, C., Bathmann, U., Smetacek, V. (1995) Importance of iron for plankton blooms and carbon dioxide drawdown in the Southern Ocean.

Dean Jr, W.E. (1974) Determination of carbonate and organic matter in calcareous sediments and sedimentary rocks by loss on ignition: comparison with other methods. Journal of Sedimentary Research 44.

DEMOTT, W., MÜLLER‐NAVARRA, D. (1997) The importance of highly unsaturated fatty acids in zooplankton nutrition: evidence from experiments with Daphnia, a cyanobacterium and lipid emulsions. Freshwater Biology 38, 649-664.

DeMott, W.R. (1998) Utilization of a cyanobacterium and a phosphorus-deficient green alga as complementary resources by daphnids. Ecology 79, 2463-2481.

DeSimone, L.A., Howes, B.L. (1996) Denitrification and nitrogen transport in a coastal aquifer receiving wastewater discharge. Environ Sci Technol 30, 1152-1162.

Dias, J., Boski, T., Rodrigues, A., Magalhães, F. (2000) Coast line evolution in Portugal since the Last Glacial Maximum until present—a synthesis. Marine Geology 170, 177-186.

Dinis, M. (1992) Situação da aquacultura no Algarve: perspectivas e condicionantes. Mesas redondas, Ponte International do Guadiana.

Dionisio, L.P.C., Rheinheimer, G., Borrego, J.J. (2000) Microbiological pollution of Ria Formosa (South of Portugal). Mar Pollut Bull 40, 186-193.

Dodla, S.K., Wang, J.J., DeLaune, R.D., Cook, R.L. (2008) Denitrification potential and its relation to organic carbon quality in three coastal wetland soils. Science of the total environment 407, 471-480.

Dollhopf, S.L., Hyun, J.-H., Smith, A.C., Adams, H.J., O'Brien, S., Kostka, J.E. (2005) Quantification of ammonia-oxidizing bacteria and factors controlling nitrification in salt marsh sediments. Appl Environ Microbiol 71, 240-246.

Dong, J., Robertson, J.D., Markesbery, W.R., Lovell, M.A. (2008) Serum zinc in the progression of Alzheimer's disease. Journal of Alzheimer's Disease 15, 443-450.

Duarte, P., Azevedo, B., Guerreiro, M., Ribeiro, C., Bandeira, R., Pereira, A., Falcão, M., Serpa, D., Reia, J. (2008) Biogeochemical modelling of Ria Formosa (South Portugal). Hydrobiologia 611, 115-132.

Duarte, P., Azevedo, B., Pereira, A. (2005) Hydrodynamic Modelling of Ria Formosa (South Coast of Portugal) with EcoDynamo.

Duce, R., LaRoche, J., Altieri, K., Arrigo, K., Baker, A., Capone, D., Cornell, S., Dentener, F., Galloway, J., Ganeshram, R. (2008) Impacts of atmospheric anthropogenic nitrogen on the open ocean. Science 320, 893-897.

Edwards, V., Icely, J., Newton, A., Webster, R. (2005) The yield of chlorophyll from nitrogen: a comparison between the shallow Ria Formosa lagoon and the deep oceanic conditions at Sagres along the southern coast of Portugal. Estuarine, Coastal and Shelf Science 62, 391-403.

Eisenreich, S., Bannerman, R., Armstrong, D. (1975) A simplified phosphorus analysis technique. Environmental Letters 9, 43-53.

El-Gamal, A.A., Peterson, R.N., Burnett, W.C. (2012) Detecting freshwater inputs via groundwater discharge to Marina Lagoon, Mediterranean Coast, Egypt. Estuaries and Coasts 35, 1486-1499.

Engström, P., Dalsgaard, T., Hulth, S., Aller, R.C. (2005) Anaerobic ammonium oxidation by nitrite (anammox): implications for N 2 production in coastal marine sediments. Geochimica Et Cosmochimica Acta 69, 2057-2065.

Erler, D.V., Santos, I.R., Eyre, B.D. (2014a) Inorganic nitrogen transformations within permeable carbonate sands. Continental Shelf Research 77, 69-80.

Erler, D.V., Santos, I.R., Zhang, Y., Tait, D.R., Befus, K.M., Hidden, A., Li, L., Eyre, B.D. (2014b) Nitrogen transformations within a tropical subterranean estuary. Marine Chemistry 164, 38-47.

Falcão, M., Santos, M., Drago, T., Serpa, D., Monteiro, C. (2009) Effect of artificial reefs (southern Portugal) on sediment–water transport of nutrients: Importance of the hydrodynamic regime. Estuarine, Coastal and Shelf Science 83, 451-459.

Falcao, M., Vale, C. (1990) Study of the Ria Formosa ecosystem: benthic nutrient remineralization and tidal variability of nutrients in the water. Hydrobiologia 207, 137-146.

Falkowski, P.G. (1997) Evolution of the nitrogen cycle and its influence on the biological sequestration of CO 2 in the ocean. Nature 387, 272-275.

Ferguson, A., Eyre, B., Gay, J., Emtage, N., Brooks, L. (2007) Benthic metabolism and nitrogen cycling in a subtropical coastal embayment: spatial and seasonal variation and controlling factors. Aquatic Microbial Ecology 48, 175.

Ferreira, J. (2003) Identification of sensitive areas and vulnerable zones in transitional and coastal portuguese systems: application of the united states national estuarine eutrophication assessment to the Minho, Lima, Douro, Ria de Aveiro, Mondego, Tagus, Sado, Mira, Ria Formosa and Guadiana systems. INAG.

Ferreira, J.P.L., Leitão, T.E. (2014) Demonstrating managed aquifer recharge as a solution for climate change adaptation: results from Gabardine project and asemwaterNet coordination action in the algarve region (Portugal).

Ferreira, J.P.L., Oliveira, M.M., Diamantino, C., Leitão, T.E., (2007) LNEC Contribution to D24: AR needs in Campina de Faro. Julho, (Portuguese), p. 6.

Fields, S. (2004) Global nitrogen: cycling out of control. Environmental Health Perspectives 112, A556.

Finkl, C.W., Krupa, S.L. (2003) Environmental impacts of coastal-plain activities on sandy beach systems: hazards, perception and mitigation. Journal of Coastal Research, 132-150.

Flechard, C., Nemitz, E., Smith, R., Fowler, D., Vermeulen, A., Bleeker, A., Erisman, J., Simpson, D., Zhang, L., Tang, Y. (2011) Dry deposition of reactive nitrogen to European ecosystems: a comparison of inferential models across the NitroEurope network. Atmospheric Chemistry and Physics 11, 2703-2728.

Foster, S. (2000) The Ninth Ineson Lecture Assessing and Controlling the Impacts of Agriculture on Groundwater—from Barley Barons to Beef Bans. Quarterly Journal of Engineering Geology and Hydrogeology 33, 263-280.

Francis, C.A., Beman, J.M., Kuypers, M.M. (2007) New processes and players in the nitrogen cycle: the microbial ecology of anaerobic and archaeal ammonia oxidation. The ISME journal 1, 19-27.

Furnas, M., Alongi, D., McKinnon, D., Trott, L., Skuza, M. (2011) Regional-scale nitrogen and phosphorus budgets for the northern (14 S) and central (17 S) Great Barrier Reef shelf ecosystem. Continental Shelf Research 31, 1967-1990.

Furnas, M., Mitchell, A., Skuza, M., Brodie, J. (2005) In the other 90%: phytoplankton responses to enhanced nutrient availability in the Great Barrier Reef Lagoon. Mar Pollut Bull 51, 253-265.

Galloway, J.N., Aber, J.D., Erisman, J.W., Seitzinger, S.P., Howarth, R.W., Cowling, E.B., Cosby, B.J. (2003) The nitrogen cascade. Bioscience 53, 341-356.

Galloway, J.N., Dentener, F.J., Capone, D.G., Boyer, E.W., Howarth, R.W., Seitzinger, S.P., Asner, G.P., Cleveland, C., Green, P., Holland, E. (2004) Nitrogen cycles: past, present, and future. Biogeochemistry 70, 153-226.

Galloway, J.N., Schlesinger, W.H., Levy, H., Michaels, A., Schnoor, J.L. (1995) Nitrogen fixation: Anthropogenic enhancement - environmental response. Global Biogeochemical Cycles 9, 235-252.

Gamito, S. (1997) Application of canonical correspondence analysis to environmental and benthic macrofauna data of four sites in the Ria Formosa (Portugal). Publicaciones Especiales-Instituto Espanol de Oceanografia.

Gamito, S. (2008) Three main stressors acting on the Ria Formosa lagoonal system (Southern Portugal): physical stress, organic matter pollution and the land–ocean gradient. Estuarine, Coastal and Shelf Science 77, 710-720.

Gao, H., Schreiber, F., Collins, G., Jensen, M.M., Kostka, J.E., Lavik, G., de Beer, D., Zhou, H.-y., Kuypers, M.M. (2010) Aerobic denitrification in permeable Wadden Sea sediments. The ISME journal 4, 417-426.

Gardner, W.S., McCarthy, M.J., An, S., Sobolev, D., Sell, K.S., Brock, D. (2006) Nitrogen fixation and dissimilatory nitrate reduction to ammonium (DNRA) support nitrogen dynamics in Texas estuaries. Limnology and Oceanography 51, 558-568.

Gari, S.R., Newton, A., Icely, J., Lowe, C.D. (2014) Testing the application of the Systems Approach Framework (SAF) for the management of eutrophication in the Ria Formosa. Marine Policy 43, 40-45.

Garrison, G., Glenn, C., McMurtry, G. (2003) Measurement of submarine groundwater discharge in Kahana Bay, O'ahu, Hawai'i. Limnology and Oceanography 48, 920-928.

Gil, A., Assis, F., Albeniz, S., Korili, S. (2011) Removal of dyes from wastewaters by adsorption on pillared clays. Chemical Engineering Journal 168, 1032-1040.

Goldberg, S., Sposito, G. (1985) On the mechanism of specific phosphate adsorption by hydroxylated mineral surfaces: A review. Communications in Soil Science & Plant Analysis 16, 801-821.

Goodchild, R. (1998) EU policies for the reduction of nitrogen in water: the example of the Nitrates Directive. Environmental pollution 102, 737-740.

Grasshoff, K., Kremling, K., Ehrhardt, M. (2009) Methods of seawater analysis. John Wiley & Sons.

Gregg, S.J., Sing, K.S.W., Salzberg, H. (1967) Adsorption surface area and porosity. Journal of The Electrochemical Society 114, 279C-279C.

Griggs, E.M., Kump, L.R., Böhlke, J. (2003) The fate of wastewater-derived nitrate in the subsurface of the Florida Keys: Key Colony Beach, Florida. Estuarine, Coastal and Shelf Science 58, 517-539.

Grundmanis, V., Murray, J.W. (1982) Aerobic respiration in pelagic marine sediments. Geochimica Et Cosmochimica Acta 46, 1101-1120.

Gu, B., Schmitt, J., Chen, Z., Liang, L., McCarthy, J.F. (1994) Adsorption and desorption of natural organic matter on iron oxide: mechanisms and models. Environ Sci Technol 28, 38-46.

Guo, W., Xu, J., Wang, J., Wen, Y., Zhuo, J., Yan, Y. (2010) Characterization of dissolved organic matter in urban sewage using excitation emission matrix fluorescence spectroscopy and parallel factor analysis. Journal of Environmental Sciences 22, 1728-1734.

Hall, S.J. (2002) The continental shelf benthic ecosystem: current status, agents for change and future prospects. Environmental Conservation 29, 350-374.

Halpern, B.S., Walbridge, S., Selkoe, K.A., Kappel, C.V., Micheli, F., D'Agrosa, C., Bruno, J.F., Casey, K.S., Ebert, C., Fox, H.E. (2008) A global map of human impact on marine ecosystems. Science 319, 948-952.

Han, D., Kohfahl, C., Song, X., Xiao, G., Yang, J. (2011) Geochemical and isotopic evidence for palaeo-seawater intrusion into the south coast aquifer of Laizhou Bay, China. Applied Geochemistry 26, 863-883.

Harris, D., Horwáth, W.R., van Kessel, C. (2001) Acid fumigation of soils to remove carbonates prior to total organic carbon or carbon-13 isotopic analysis. Soil science society of America journal 65, 1853-1856.

Hayes, K., Leckie, J. (1987) Modeling ionic strength effects on cation adsorption at hydrous oxide/solution interfaces. Journal of Colloid and Interface Science 115, 564-572.

Haygarth, P.M., Sharpley, A. (2000) Terminology for phosphorus transfer. Journal of environmental quality 29, 10-15.

Hays, R.L., Ullman, W.J. (2007) Dissolved nutrient fluxes through a sandy estuarine beachface (Cape Henlopen, Delaware, USA): contributions from fresh groundwater discharge, seawater recycling, and diagenesis. Estuaries and Coasts 30, 710-724.

Helman, E.Z., Wallick, D.K., Reingold, I. (1971) Vacutainer contamination in trace-element studies. Clinical chemistry 17, 61-62.

Henrichs, S.M., Sugai, S.F. (1993) Adsorption of amino acids and glucose by sediments of Resurrection Bay, Alaska, USA: Functional group effects. Geochimica Et Cosmochimica Acta 57, 823-835.

Herbert, R. (1999) Nitrogen cycling in coastal marine ecosystems. FEMS microbiology reviews 23, 563-590.

Hernández-Terrones, L., Rebolledo-Vieyra, M., Merino-Ibarra, M., Soto, M., Le-Cossec, A., Monroy-Ríos, E. (2011) Groundwater pollution in a karstic region (NE Yucatan): Baseline nutrient content and flux to coastal ecosystems. Water, Air, & Soil Pollution 218, 517-528.

Hill, A.R., Sanmugadas, K. (1985) Denitrification rates in relation to stream sediment characteristics. Water Research 19, 1579-1586.

Ho, Y.-S., McKay, G. (1999) Pseudo-second order model for sorption processes. Process Biochemistry 34, 451-465.

Hodgkiss, I., Ho, K., (1997) Are changes in N: P ratios in coastal waters the key to increased red tide blooms?, Asia-Pacific Conference on Science and Management of Coastal Environment. Springer, pp. 141-147.

Holland, K., Elmore, P. (2008) A review of heterogeneous sediments in coastal environments. Earth-Science Reviews 89, 116-134.

House, W.A., Donaldson, L. (1986) Adsorption and coprecipitation of phosphate on calcite. Journal of Colloid and Interface Science 112, 309-324.

References

Howarth, R.W. (2008) Coastal nitrogen pollution: a review of sources and trends globally and regionally. Harmful Algae 8, 14-20.

Howarth, R.W., Billen, G., Swaney, D., Townsend, A., Jaworski, N., Lajtha, K., Downing, J., Elmgren, R., Caraco, N., Jordan, T., (1996) Regional nitrogen budgets and riverine N & P fluxes for the drainages to the North Atlantic Ocean: Natural and human influences, Nitrogen cycling in the North Atlantic Ocean and its watersheds. Springer, pp. 75-139.

Howarth, R.W., Marino, R. (2006) Nitrogen as the limiting nutrient for eutrophication in coastal marine ecosystems: Evolving views over three decades. Limnology and Oceanography, 364-376.

Huettel, M., Berg, P., Kostka, J.E. (2014) Benthic exchange and biogeochemical cycling in permeable sediments. Marine Science 6.

Hupfer, M., Lewandowski, J. (2008) Oxygen Controls the Phosphorus Release from Lake Sediments – a Long - Lasting Paradigm in Limnology. International Review of Hydrobiology 93, 415-432.

Huysmans, M., Dassargues, A. (2005) Review of the use of Péclet numbers to determine the relative importance of advection and diffusion in low permeability environments. Hydrogeology Journal 13, 895-904.

Hwang, D.-W., Kim, G., Lee, W.-C., Oh, H.-T. (2010) The role of submarine groundwater discharge (SGD) in nutrient budgets of Gamak Bay, a shellfish farming bay, in Korea. Journal of Sea Research 64, 224-230.

Ibánhez, J.S.P., (2012) Alternative nitrate reduction pathways in sandy sediments hosting submarine groundwater discharge (SGD). TCD Document.

Ibánhez, J.S.P., Leote, C., Rocha, C. (2011) Porewater nitrate profiles in sandy sediments hosting submarine groundwater discharge described by an advection–dispersion-reaction model. Biogeochemistry 103, 159-180.

Ibánhez, J.S.P., Leote, C., Rocha, C. (2013) Seasonal enhancement of submarine groundwater discharge (SGD)-derived nitrate loading into the Ria Formosa coastal lagoon assessed by 1-D modeling of benthic NO< sub> 3</sub>< sup>−</sup> profiles. Estuarine, Coastal and Shelf Science 132, 56-64.

Ibánhez, J.S.P., Rocha, C. (2014a) Effects of recirculation of seawater enriched in inorganic nitrogen on dissolved organic carbon processing in sandy seepage face sediments. Marine Chemistry 166, 48-58.

Ibánhez, J.S.P., Rocha, C. (2014b) Porewater sampling for NH4+ with Rhizon Soil Moisture Samplers (SMS): potential artifacts induced by NH4+ sorption. Freshwater Science 33, 1195-1203.

Ibánhez, J.S.P., Rocha, C. (In press) Oxygen transport and reactivity within a sandy seepage face in a mesotidal lagoon (Ria Formosa, Southwestern Iberia).

Isenbeck-Schröter, M., Döring, U., Möller, A., Schröter, J., Mattheß, G. (1993) Experimental approach and simulation of the retention processes limiting orthophosphate transport in groundwater. J Contam Hydrol 14, 143-161.

Israelachvili, J.N. (2011) Intermolecular and surface forces: revised third edition. Academic press.

Jarvie, H.P., Withers, J., Neal, C. (2002) Review of robust measurement of phosphorus in river water: sampling, storage, fractionation and sensitivity. Hydrology and Earth System Sciences Discussions 6, 113-131.

Jensen, M.M., Lam, P., Revsbech, N.P., Nagel, B., Gaye, B., Jetten, M.S., Kuypers, M.M. (2011) Intensive nitrogen loss over the Omani Shelf due to anammox coupled with dissimilatory nitrite reduction to ammonium. The ISME journal 5, 1660-1670.

Jiang, X., Jin, X., Yao, Y., Li, L., Wu, F. (2008) Effects of biological activity, light, temperature and oxygen on phosphorus release processes at the sediment and water interface of Taihu Lake, China. Water Research 42, 2251-2259.

Johannes, R. (1980) Ecological significance of the submarine discharge of groundwater. MARINE ECOL.- PROG. SER. 3, 365-373.

Johannes, R., Hearn, C. (1985) The effect of submarine groundwater discharge on nutrient and salinity regimes in a coastal lagoon off Perth, Western Australia. Estuarine, Coastal and Shelf Science 21, 789-800.

Jones, M.N. (1984) Nitrate reduction by shaking with cadmium: alternative to cadmium columns. Water Research 18, 643-646.

Justić, D., Rabalais, N.N., Turner, R.E., Dortch, Q. (1995) Changes in nutrient structure of river-dominated coastal waters: stoichiometric nutrient balance and its consequences. Estuarine, Coastal and Shelf Science 40, 339-356.

Justić, D., Rabalais, N.N., Turner, R.E., Wiseman, W.J. (1993) Seasonal coupling between riverborne nutrients, net productivity and hypoxia. Mar Pollut Bull 26, 184-189.

Källqvist, T., Svenson, A. (2003) Assessment of ammonia toxicity in tests with the microalga, Nephroselmis pyriformis, Chlorophyta. Water Research 37, 477-484.

Karydis, M., Ignatiades, L., Moschopoulou, N. (1983) An index associated with nutrient eutrophication in the marine environment. Estuarine, Coastal and Shelf Science 16, 339-344.

Keating, K.I. (1978) Blue-green algal inhibition of diatom growth: transition from mesotrophic to eutrophic community structure. Science 199, 971-973.

Kelly, T., Rocha, C., (2014) Analysing Submarine Groundwater Discharge (SGD)-borne Dissolved Organic Matter (DOM) in a karstic aquifer, Co. Galway, Ireland, EGU General Assembly Conference Abstracts, p. 11506.

Ketchum, B.H. (1951) The exchanges of fresh and salt waters in tidal estuaries. Journal of marine research 10, 18-38.

Kharroubi, A., Gzam, M., Jedoui, Y. (2012) Anthropogenic and natural effects on the water and sediments qualities of costal lagoons: case of the Boughrara Lagoon (Southeast Tunisia). Environmental Earth Sciences 67, 1061-1067.

King, J.N., Mehta, A.J., Dean, R.G. (2010) Analytical models for the groundwater tidal prism and associated benthic water flux. Hydrogeology Journal 18, 203-215.

Kim, G., Ryu, J.-W., Yang, H.-S., Yun, S.-T. (2005) Submarine groundwater discharge (SGD) into the Yellow Sea revealed by ^{228}Ra and ^{226}Ra isotopes: Implications for global silicate fluxes. Earth and Planetary Science Letters 237, 156-166.

Kim, T.-W., Lee, K., Najjar, R.G., Jeong, H.-D., Jeong, H.J. (2011) Increasing N abundance in the northwestern Pacific Ocean due to atmospheric nitrogen deposition. Science 334, 505-509.

Kim, T.-H., Kwon, E., Kim, I., Lee, S.-A., Kim, G. (2013) Dissolved organic matter in the subterranean estuary of a volcanic island, Jeju: Importance of dissolved organic nitrogen fluxes to the ocean. Journal of Sea Research 78, 18-24.

Knee, K.L., Layton, B.A., Street, J.H., Boehm, A.B., Paytan, A. (2008) Sources of nutrients and fecal indicator bacteria to nearshore waters on the north shore of Kauai (Hawaii, USA). Estuaries and Coasts 31, 607-622.

Koutitonsky, V., Guyondet, T., St-Hilaire, A., Courtenay, S., Bohgen, A. (2004) Water renewal estimates for aquaculture developments in the Richibucto estuary, Canada. Estuaries 27, 839-850.

Kroeger, K., Charette, M. (2008) Nitrogen biogeochemistry of submarine groundwater discharge. Limnology and Oceanography 53, 1025.

Kroeger, K.D., Swarzenski, P.W., Greenwood, W.J., Reich, C. (2007) Submarine groundwater discharge to Tampa Bay: Nutrient fluxes and biogeochemistry of the coastal aquifer. Marine Chemistry 104, 85-97.

Kurkjian, R., Flegal, A.R. (2003) Isotopic evidence of the persistent dominance of blood lead concentrations by previous gasoline lead emissions in Yerevan, Armenia. Environmental research 93, 308-315.

Kuwae, T., Kibe, E., Nakamura, Y. (2003) Effect of emersion and immersion on the porewater nutrient dynamics of an intertidal sandflat in Tokyo Bay. Estuarine, Coastal and Shelf Science 57, 929-940.

Lam, P., Lavik, G., Jensen, M.M., van de Vossenberg, J., Schmid, M., Woebken, D., Gutiérrez, D., Amann, R., Jetten, M.S., Kuypers, M.M. (2009) Revising the nitrogen cycle in the Peruvian oxygen minimum zone. Proceedings of the National Academy of Sciences 106, 4752-4757.

Lee, C.M., Jiao, J.J., Luo, X., Moore, W.S. (2012) Estimation of submarine groundwater discharge and associated nutrient fluxes in Tolo Harbour, Hong Kong. Science of the total environment 433, 427-433.

Lee, D.R. (1977) A device for measuring seepage flux in lakes and esturies. Limnology and Oceanography 22, 140-147.

Lee, V., Olsen, S. (1985) Eutrophication and management initiatives for the control of nutrient inputs to Rhode Island coastal lagoons. Estuaries 8, 191-202.

Lee, Y.-W., Hwang, D.-W., Kim, G., Lee, W.-C., Oh, H.-T. (2009) Nutrient inputs from submarine groundwater discharge (SGD) in Masan Bay, an embayment surrounded by heavily industrialized cities, Korea. Science of the total environment 407, 3181-3188.

Lee, Y.-W., Kim, G. (2007) Linking groundwater-borne nutrients and dinoflagellate red-tide outbreaks in the southern sea of Korea using a Ra tracer. Estuarine, Coastal and Shelf Science 71, 309-317.

Lehmann, M.F., Sigman, D.M., McCorkle, D.C., Granger, J., Hoffmann, S., Cane, G., Brunelle, B.G. (2007) The distribution of nitrate 15 N/14 N in marine sediments and the impact of benthic nitrogen loss on the isotopic composition of oceanic nitrate. Geochimica Et Cosmochimica Acta 71, 5384-5404.

Leote, C., Epping, E.H. (2015) Sediment–water exchange of nutrients in the Marsdiep basin, western Wadden Sea: Phosphorus limitation induced by a controlled release? Continental Shelf Research 92, 44-58.

Leote, C., Ibánhez, J.S., Rocha, C. (2008) Submarine groundwater discharge as a nitrogen source to the Ria Formosa studied with seepage meters. Biogeochemistry 88, 185-194.

Levenspiel, O. (1972) Chemical reaction engineering. Wiley New York etc.

Levenspiel, O. (1999) Chemical reaction engineering. Industrial & engineering chemistry research 38, 4140-4143.

Li, H., Boufadel, M.C., Weaver, J.W. (2008) Tide-induced seawater–groundwater circulation in shallow beach aquifers. Journal of Hydrology 352, 211-224.

Li, L., Barry, D., Stagnitti, F., Parlange, J.Y. (1999) Submarine groundwater discharge and associated chemical input to a coastal sea. Water Resources Research 35, 3253-3259.

Liu, S.M., Li, R.H., Zhang, G.L., Wang, D.R., Du, J.Z., Herbeck, L.S., Zhang, J., Ren, J.L. (2011) The impact of anthropogenic activities on nutrient dynamics in the tropical Wenchanghe and Wenjiaohe Estuary and Lagoon system in East Hainan, China. Marine Chemistry 125, 49-68.

Liu, Y., Shen, L. (2008) From Langmuir kinetics to first-and second-order rate equations for adsorption. Langmuir 24, 11625-11630.

Lomas, M.W., Glibert, P.M. (1999) Temperature regulation of nitrate uptake: A novel hypothesis about nitrate uptake and reduction in cool‐water diatoms. Limnology and Oceanography 44, 556-572.

Lopes, C., Lillebø, A., Dias, J., Pereira, E., Vale, C., Duarte, A. (2007) Nutrient dynamics and seasonal succession of phytoplankton assemblages in a Southern European Estuary: Ria de Aveiro, Portugal. Estuarine, Coastal and Shelf Science 71, 480-490.

Loureiro, S., Newton, A., Icely, J. (2005) Effects of nutrient enrichments on primary production in the Ria Formosa coastal lagoon (Southern Portugal). Hydrobiologia 550, 29-45.

Loveless, A.M., Oldham, C.E. (2010) Natural attenuation of nitrogen in groundwater discharging through a sandy beach. Biogeochemistry 98, 75-87.

Mackenzie, F.T., Ver, L.M., Lerman, A. (2002) Century-scale nitrogen and phosphorus controls of the carbon cycle. Chemical Geology 190, 13-32.

Mackin, J.E., Aller, R.C. (1984) Ammonium adsorption in marine sediments. Limnol. Oceanogr 29, 250-257.

Maier, C., Pregnall, A. (1990) Increased macrophyte nitrate reductase activity as a consequence of groundwater input of nitrate through sandy beaches. Marine Biology 107, 263-271.

Masselink, G., Turner, I., Conley, D., Ruessink, G., Matias, A., Thompson, C., Castelle, B., Wolters, G. (2013) BARDEX II: Bringing the beach to the laboratory–again. Journal of Coastal Research.

Matson, E.A. (1993) Nutrient flux through soils and aquifers to the coastal zone of Guam (Mariana Islands). Limnology and Oceanography 38, 361-371.

McClelland, J.W., Valiela, I. (1998) Linking nitrogen in estuarine producers to land‐derived sources. Limnology and Oceanography 43, 577-585.

McClelland, J.W., Valiela, I., Michener, R.H. (1997) Nitrogen‐stable isotope signatures in estuarine food webs: a record of increasing urbanization in coastal watersheds. Limnology and Oceanography 42, 930-937.

Michael, H.A., Mulligan, A.E., Harvey, C.F. (2005) Seasonal oscillations in water exchange between aquifers and the coastal ocean. Nature 436, 1145-1148.

Miller, D.C., Ullman, W.J. (2004) Ecological consequences of ground water discharge to Delaware Bay, United States. Groundwater 42, 959-970.

Moore, W., Church, T. (1996) Reply-Submarine groundwater discharge. Nature 382, 121-122.

Moore, W.S. (1996) Large groundwater inputs to coastal waters revealed by 226Ra enrichments. Nature 380, 612-614.

Moore, W.S. (1999) The subterranean estuary: a reaction zone of ground water and sea water. Marine Chemistry 65, 111-125.

Moore, W.S. (2010) The effect of submarine groundwater discharge on the ocean. Ann Rev Mar Sci 2, 59-88.

Mualem, Y. (1976) A new model for predicting the hydraulic conductivity of unsaturated porous media. Water Resources Research 12, 513-522.

Mudge, S.M., Bebianno, M.J.A.F., East, J.A., Barreira, L.A. (1999) Sterols in the Ria Formosa lagoon, Portugal. Water Research 33, 1038-1048.

Mulligan, A.E., Charette, M.A. (2006) Intercomparison of submarine groundwater discharge estimates from a sandy unconfined aquifer. Journal of Hydrology 327, 411-425.

Mullins, E. (2003) Statistics for the quality control chemistry laboratory. Royal Society of Chemistry.

Murray, L., Mudge, S., Newton, A., Icely, J. (2006) The effect of benthic sediments on dissolved nutrient concentrations and fluxes. Biogeochemistry 81, 159-178.

Natarajan, K. (1970) Toxicity of ammonia to marine diatoms. Journal (Water Pollution Control Federation), R184-R190.

Neill, M. (2005) A method to determine which nutrient is limiting for plant growth in estuarine waters—at any salinity. Mar Pollut Bull 50, 945-955.

Newton, A., Icely, J., Falcao, M., Nobre, A., Nunes, J., Ferreira, J., Vale, C. (2003) Evaluation of eutrophication in the Ria Formosa coastal lagoon, Portugal. Continental Shelf Research 23, 1945-1961.

Newton, A., Mudge, S.M. (2003) Temperature and salinity regimes in a shallow, mesotidal lagoon, the Ria Formosa, Portugal. Estuarine, Coastal and Shelf Science 57, 73-85.

Newton, A., Mudge, S.M. (2005) Lagoon-sea exchanges, nutrient dynamics and water quality management of the Ria Formosa (Portugal). Estuarine, Coastal and Shelf Science 62, 405-414.

Nielsen, P. (1990) Tidal dynamics of the water table in beaches. Water Resources Research 26, 2127-2134.

Niencheski, L.F.H., Windom, H.L., Moore, W.S., Jahnke, R.A. (2007) Submarine groundwater discharge of nutrients to the ocean along a coastal lagoon barrier, Southern Brazil. Marine Chemistry 106, 546-561.

Nilsson, C., Reidy, C.A., Dynesius, M., Revenga, C. (2005) Fragmentation and flow regulation of the world's large river systems. Science 308, 405-408.

Nowicki, B.L., Requintina, E., Van Keuren, D., Portnoy, J. (1999) The role of sediment denitrification in reducing groundwater-derived nitrate inputs to Nauset Marsh estuary, Cape Cod, Massachusetts. Estuaries and Coasts 22, 245-259.

Nürnberg, G., Peters, R.H. (1984) Biological availability of soluble reactive phosphorus in anoxic and oxic freshwaters. Canadian Journal of Fisheries and Aquatic Sciences 41, 757-765.

Oliveira, M., Gaspar, M., Paixão, J., Camanho, A. (2009) Productivity change of the artisanal fishing fleet in Portugal: A Malmquist index analysis. Fisheries Research 95, 189-197.

Oude Essink, G., Van Baaren, E.S., De Louw, P.G. (2010) Effects of climate change on coastal groundwater systems: A modeling study in the Netherlands. Water Resources Research 46.

Pacheco, A., Carrasco, A., Vila-Concejo, A., Ferreira, O., Dias, J. (2007) A coastal management program for channels located in backbarrier systems. Ocean & coastal management 50, 119-143.

Pacheco, A., Ferreira, Ó., Williams, J., Garel, E., Vila-Concejo, A., Dias, J. (2010) Hydrodynamics and equilibrium of a multiple-inlet system. Marine Geology 274, 32-42.

Padinha, C., Santos, R., Brown, M. (2000) Evaluating environmental contamination in Ria Formosa (Portugal) using stress indexes of *Spartina maritima*. Marine environmental research 49, 67-78.

Paine, R.T. (1966) Food web complexity and species diversity. American Naturalist, 65-75.

Pallud, C., Meile, C., Laverman, A., Abell, J., Van Cappellen, P. (2007) The use of flow-through sediment reactors in biogeochemical kinetics: methodology and examples of applications. Marine Chemistry 106, 256-271.

Parkes, R.J., Cragg, B.A., Wellsbury, P. (2000) Recent studies on bacterial populations and processes in subseafloor sediments: a review. Hydrogeology Journal 8, 11-28.

Paytan, A., Shellenbarger, G.G., Street, J.H., Gonneea, M.E., Davis, K., Young, M.B., Moore, W.S. (2006) Submarine groundwater discharge: An important source of new inorganic nitrogen to coral reef ecosystems. Limnology and Oceanography 51, 343-348.

Pereira, M.G., Icely, J., Mudge, S., Newton, A., Rodrigues, R. (2007) Temporal and spatial variation of phytoplankton pigments in the western part of Ria Formosa Lagoon, Southern Portugal. Environmental Forensics 8, 205-220.

Pfenning, K., McMahon, P. (1997) Effect of nitrate, organic carbon, and temperature on potential denitrification rates in nitrate-rich riverbed sediments. Journal of Hydrology 187, 283-295.

Pilkey Jr, O., Neal, W., Monteiro, J., Dias, J. (1989) Algarve barrier islands: a noncoastal-plain system in Portugal. Journal of Coastal Research, 239-261.

Platt, T., Fuentes-Yaco, C., Frank, K.T. (2003) Marine ecology: spring algal bloom and larval fish survival. Nature 423, 398-399.

Powlson, D.S., Addiscott, T.M., Benjamin, N., Cassman, K.G., De Kok, T.M., Van Grinsven, H., L'hirondel, J.L., Avery, A.A., Van Kessel, C. (2008) When does nitrate become a risk for humans? Journal of environmental quality 37, 291-295.

Pragay, D.A., Howard, S.F., Chilcote, M.E. (1971) Inorganic ion contaminations in vacutainer tubes and micropipets used for blood collection. Clinical chemistry 17, 350-351.

Puckett, L.J. (1995) Identifying the major sources of nutrient water pollution. Environ Sci Technol 29, 408A-414A.

Pusceddu, A., Sarà, G., Armeni, M., Fabiano, M., Mazzola, A. (1999) Seasonal and spatial changes in the sediment organic matter of a semi-enclosed marine system (W-Mediterranean Sea). Hydrobiologia 397, 59-70.

Rabalais, N.N., Turner, R.E., Díaz, R.J., Justić, D. (2009) Global change and eutrophication of coastal waters. ICES Journal of Marine Science: Journal du Conseil 66, 1528-1537.

Rabalais, N.N., Turner, R.E., Justić, D., Dortch, Q., Wiseman, W.J., Gupta, B.K.S. (1996) Nutrient changes in the Mississippi River and system responses on the adjacent continental shelf. Estuaries 19, 386-407.

Rabouille, C., Mackenzie, F.T., Ver, L.M. (2001) Influence of the human perturbation on carbon, nitrogen, and oxygen biogeochemical cycles in the global coastal ocean. Geochimica Et Cosmochimica Acta 65, 3615-3641.

Ramos, T., Gonçalves, M., Brito, D., Martins, J., Pereira, L. (2013) Development of class pedotransfer functions for integrating water retention properties into Portuguese soil maps. Soil Research 51, 262-277.

Ravishankara, A., Daniel, J.S., Portmann, R.W. (2009) Nitrous oxide (N2O): the dominant ozone-depleting substance emitted in the 21st century. Science 326, 123-125.

Reckhardt, A., Beck, M., Seidel, M., Riedel, T., Wehrmann, A., Bartholomä, A., Schnetger, B., Dittmar, T., Brumsack, H.-J. (2015) Carbon, nutrient and trace metal cycling in sandy sediments: A comparison of high-energy beaches and backbarrier tidal flats. Estuarine, Coastal and Shelf Science 159, 1-14.

Redfield, A.C. (1958) The biological control of chemical factors in the environment. American scientist, 230A-221.

Regnier, P., O'kane, J. (2004) On the mixing processes in estuaries: The fractional freshwater method revisited. Estuaries 27, 571-582.

Reimold, E., Besch, D.J. (1978) Detection and elimination of contaminations interfering with the determination of zinc in plasma. Clinical chemistry 24, 675-680.

Renberg, I., Hansson, H. (2008) The HTH sediment corer. Journal of Paleolimnology 40, 655-659.

Rice, C.W., Tiedje, J.M. (1989) Regulation of nitrate assimilation by ammonium in soils and in isolated soil microorganisms. Soil Biology and Biochemistry 21, 597-602.

Rice, W.R. (1989) Analyzing tables of statistical tests. Evolution, 223-225.

Richards, L.A. (1931) Capillary conduction of liquids through porous mediums. Physics 1, 318-333.

Ridderinkhof, H., Zimmerman, J., Philippart, M. (1990) Tidal exchange between the North Sea and Dutch Wadden Sea and mixing time scales of the tidal basins. Netherlands journal of sea research 25, 331-350.

Rivett, M.O., Buss, S.R., Morgan, P., Smith, J.W., Bemment, C.D. (2008) Nitrate attenuation in groundwater: a review of biogeochemical controlling processes. Water Research 42, 4215-4232.

Robertson, W., Blowes, D., Ptacek, C., Cherry, J. (2000) Long‐term performance of in situ reactive barriers for nitrate remediation. Groundwater 38, 689-695.

Rocha, C. (2008) Sandy sediments as active biogeochemical reactors: compound cycling in the fast lane. Aquatic Microbial Ecology 53, 119.

Rocha, C., Cabral, A. (1998) The influence of tidal action on porewater nitrate concentration and dynamics in intertidal sediments of the Sado estuary. Estuaries 21, 635-645.

Rocha, C., Galvão, H.M., Barbosa, A.B. (2002) Role of transient silicon limitation in the development of cyanobacteria blooms in the Guadiana estuary, south-western Iberia. Marine Ecology Progress Series 228, 35-45.

Rocha, C., Ibanhez, J., Leote, C. (2009) Benthic nitrate biogeochemistry affected by tidal modulation of Submarine Groundwater Discharge (SGD) through a sandy beach face, Ria Formosa, Southwestern Iberia. Marine Chemistry 115, 43-58.

Rocha, C., Wilson, J., Scholten, J., Schubert, M. (2015) Retention and fate of groundwater-borne nitrogen in a coastal bay (Kinvara Bay, Western Ireland) during summer. Biogeochemistry, 1-25.

Rocha, C., Woodward, M. (2011) Nutrients. Chemical Marine Monitoring: Policy Framework and Analytical Trends, 197-221.

Rocha, C.V.-P.S., Knoeller, Grocke, Anibal, Wilson, J (In press) Land-Ocean Connectivity via Submarine Groundwater Discharge (SGD)-Part 1: Combining radon measurements and stable isotopes hydrology to establish SGD sources and transfer pathways in a coastal lagoon. Submittd to Marine Chemistry.

Ruthven, D.M. (1984) Principles of adsorption and adsorption processes. John Wiley & Sons.

Ryther, J.H., Officer, C.B., (1981) Impact of nutrient enrichment on water uses, Estuaries and nutrients. Springer, pp. 247-261.

Salles, P., (2001) Hydrodynamic controls on multiple tidal inlet persistence. DTIC Document.

Santoro, A.E. (2010) Microbial nitrogen cycling at the saltwater–freshwater interface. Hydrogeology Journal 18, 187-202.

Santoro, A.E., Boehm, A.B., Francis, C.A. (2006) Denitrifier community composition along a nitrate and salinity gradient in a coastal aquifer. Appl Environ Microbiol 72, 2102-2109.

Santos, I.R., Burnett, W.C., Dittmar, T., Suryaputra, I.G.N.A., Chanton, J. (2009) Tidal pumping drives nutrient and dissolved organic matter dynamics in a Gulf of Mexico subterranean estuary. Geochimica Et Cosmochimica Acta 73, 1325-1339.

Santos, I.R., Eyre, B.D., Glud, R.N. (2012a) Influence of porewater advection on denitrification in carbonate sands: Evidence from repacked sediment column experiments. Geochimica Et Cosmochimica Acta 96, 247-258.

Santos, I.R., Eyre, B.D., Huettel, M. (2012b) The driving forces of porewater and groundwater flow in permeable coastal sediments: A review. Estuarine, Coastal and Shelf Science 98, 1-15.

Santos, I.R., Lechuga-Deveze, C., Peterson, R.N., Burnett, W.C. (2011) Tracing submarine hydrothermal inputs into a coastal bay in Baja California using radon. Chemical Geology 282, 1-10.

Santos, I.R.S., Burnett, W.C., Chanton, J., Mwashote, B., Suryaputra, I.G., Dittmar, T. (2008) Nutrient biogeochemistry in a Gulf of Mexico subterranean estuary and groundwater ‐ derived fluxes to the coastal ocean. Limnology and Oceanography 53, 705-718.

Scanlon, B.R., Mace, R.E., Barrett, M.E., Smith, B. (2003) Can we simulate regional groundwater flow in a karst system using equivalent porous media models? Case study, Barton Springs Edwards aquifer, USA. Journal of Hydrology 276, 137-158.

Schreiber, B., Brinkmann, T., Schmalz, V., Worch, E. (2005) Adsorption of dissolved organic matter onto activated carbon—the influence of temperature, absorption wavelength, and molecular size. Water Research 39, 3449-3456.

Schubert, M., Knoeller, K., Rocha, C., Einsiedl, F. (2015) Evaluation and source attribution of freshwater contributions to Kinvarra Bay, Ireland, using 222Rn, EC and stable isotopes as natural indicators. Environmental monitoring and assessment 187, 1-15.

Seeberg-Elverfeldt, J., Schlüter, M., Feseker, T., Kölling, M. (2005) Rhizon sampling of pore waters near the sediment/water interface of aquatic systems. Limnology and oceanography: Methods 3, 361-371.

Seitzinger, S., Harrison, J.A., Böhlke, J., Bouwman, A., Lowrance, R., Peterson, B., Tobias, C., Drecht, G.V. (2006) Denitrification across landscapes and waterscapes: a synthesis. Ecological Applications 16, 2064-2090.

Senal, M.I.S., Jacinto, G.S., Siringan, F., Zamora, P., Soria, L., Cardenas, M.B., Villanoy, C., Cabrera, O. (2011) Nutrient inputs from submarine groundwater discharge on the Santiago reef flat, Bolinao, Northwestern Philippines. Mar Pollut Bull 63, 195-200.

Serpa, D., Falcao, M., Duarte, P., da Fonseca, L.C., Vale, C. (2007) Evaluation of ammonium and phosphate release from intertidal and subtidal sediments of a shallow coastal lagoon (Ria Formosa–Portugal): a modelling approach. Biogeochemistry 82, 291-304.

Shah, S., Grabow, G., Westerman, P. (2006) Ammonia adsorption in five types of flexible tubing materials. Applied engineering in agriculture.

Shaw, T.J. (2003) Biogeochemical processes in coastal aquifers and permeable sediments. Aquatic Geochemistry 9, 165-169.

Shellenbarger, G.G., Monismith, S.G., Genin, A., Paytan, A. (2006) The importance of submarine groundwater discharge to the near shore nutrient supply in the Gulf of Aqaba (Israel). Limnology and Oceanography 51, 1876-1886.

Sieyes, N.R.d., Yamahara, K.M., Layton, B.A., Joyce, E.H., Boehm, A.B. (2008) Submarine discharge of nutrient-enriched fresh groundwater at Stinson Beach, California is enhanced during neap tides. Limnology and Oceanography 53, 1434.

Sigman, D., Robinson, R., Knapp, A., Van Geen, A., McCorkle, D., Brandes, J., Thunell, R. (2003) Distinguishing between water column and sedimentary denitrification in the Santa Barbara Basin using the stable isotopes of nitrate. Geochemistry, Geophysics, Geosystems 4.

Sinha, P., Rao, Y., Dube, S., Rao, A., Chatterjee, A. (1996) Modeling of circulation and salinity in Hooghly estuary. Marine Geodesy 19, 197-213.

Slater, J.M., Capone, D.G. (1987) Denitrification in aquifer soil and nearshore marine sediments influenced by groundwater nitrate. Appl Environ Microbiol 53, 1292-1297.

Slomp, C.P., Van Cappellen, P. (2004) Nutrient inputs to the coastal ocean through submarine groundwater discharge: controls and potential impact. Journal of Hydrology 295, 64-86.

Smayda, T.J. (1997) Harmful algal blooms: their ecophysiology and general relevance to phytoplankton blooms in the sea. Limnology and Oceanography 42, 1137-1153.

Smith, S.V., Atkinson, M.J. (1994) Mass balance of nutrient fluxes in coastal lagoons. Elsevier Oceanography Series 60, 133-155.

Smith, V.H. (2003) Eutrophication of freshwater and coastal marine ecosystems a global problem. Environmental Science and Pollution Research 10, 126-139.

Sommer, U. (1985) Comparison between steady state and non-steady state competition: experiments with natural phytoplankton. Limnology and Oceanography 30, 335-346.

Spiteri, C., Regnier, P., Slomp, C.P., Charette, M.A. (2006) pH-Dependent iron oxide precipitation in a subterranean estuary. Journal of Geochemical Exploration 88, 399-403.

Spiteri, C., Slomp, C.P., Charette, M.A., Tuncay, K., Meile, C. (2008) Flow and nutrient dynamics in a subterranean estuary (Waquoit Bay, MA, USA): field data and reactive transport modeling. Geochimica Et Cosmochimica Acta 72, 3398-3412.

Starr, R.C., Gillham, R.W. (1993) Denitrification and organic carbon availability in two aquifers. Groundwater 31, 934-947.

Stedmon, C.A., Bro, R. (2008) Characterizing dissolved organic matter fluorescence with parallel factor analysis: a tutorial. Limnol. Oceanogr. Methods 6, 572-579.

Stigter, T., Dill, A.C., Malta, E.-j., Santos, R. (2013) Nutrient sources for green macroalgae in the Ria Formosa lagoon–assessing the role of groundwater. Selected Papers on Hydrogeology—Groundwater and Ecosystems. Taylor & Francis, Leiden, The Netherlands, 153-167.

Stigter, T., Ribeiro, L., Carvalho Dill, A. (2006a) Application of a groundwater quality index as an assessment and communication tool in agro-environmental policies–Two Portuguese case studies. Journal of Hydrology 327, 578-591.

Stigter, T., Ribeiro, L., Dill, A.C. (2006b) Evaluation of an intrinsic and a specific vulnerability assessment method in comparison with groundwater salinisation and nitrate contamination levels in two agricultural regions in the south of Portugal. Hydrogeology Journal 14, 79-99.

Stigter, T., Van Ooijen, S., Post, V., Appelo, C., Carvalho Dill, A. (1998) A hydrogeological and hydrochemical explanation of the groundwater composition under irrigated land in a Mediterranean environment, Algarve, Portugal. Journal of Hydrology 208, 262-279.

Sun, M.-Y., Aller, R.C., Lee, C., Wakeham, S.G. (2002) Effects of oxygen and redox oscillation on degradation of cell-associated lipids in surficial marine sediments. Geochimica Et Cosmochimica Acta 66, 2003-2012.

Swarzenski, P.W., Simonds, F.W., Paulson, A.J., Kruse, S., Reich, C. (2007) Geochemical and geophysical examination of submarine groundwater discharge and associated nutrient loading estimates into Lynch Cove, Hood Canal, WA. Environ Sci Technol 41, 7022-7029.

Synthesis Report (2003) Development of an Information Technology Tool for the Management of Sourthern Eruopean Lagoons Under the Influence of River Basin Runoff. Porto, University Fernanda Pesson.

Tait, D.R., Erler, D.V., Santos, I.R., Cyronak, T.J., Morgenstern, U., Eyre, B.D. (2014) The influence of groundwater inputs and age on nutrient dynamics in a coral reef lagoon. Marine Chemistry 166, 36-47.

Tait, D.R., Santos, I.R., Erler, D.V., Befus, K.M., Cardenas, M.B., Eyre, B.D. (2013) Estimating submarine groundwater discharge in a South Pacific coral reef lagoon using different radioisotope and geophysical approaches. Marine Chemistry 156, 49-60.

Takano, K., Hino, S. (2000) Effect of temperature and soluble reactive phosphorus on abundance of Aphanizomenon flos‐aquae (Cyanophyceae). Phycological Research 48, 9-13.

Taniguchi, M., Burnett, W.C., Cable, J.E., Turner, J.V. (2002) Investigation of submarine groundwater discharge. Hydrological Processes 16, 2115-2129.

Taniguchi, M., Burnett, W.C., Dulaiova, H., Siringan, F., Foronda, J., Wattayakorn, G., Rungsupa, S., Kontar, E.A., Ishitobi, T. (2008) Groundwater discharge as an important land-sea pathway into Manila Bay, Philippines. Journal of Coastal Research 24, 15-24.

Taniguchi, M., Iwakawa, H. (2004) Submarine groundwater discharge in Osaka bay, Japan. Limnology 5, 25-32.

Tarapchak, S.J., Rubitschun, C. (1981) Comparisons of soluble reactive phosphorus and orthophosphorus concentrations at an offshore station in southern Lake Michigan. Journal of Great Lakes Research 7, 290-298.

Taylor, J.R., Cohen, E. (1998) An introduction to error analysis: the study of uncertainties in physical measurements. Measurement Science and Technology 9, 1015.

Teo, H., Jeng, D.S., Seymour, B., Barry, D., Li, L. (2003) A new analytical solution for water table fluctuations in coastal aquifers with sloping beaches. Advances in Water Resources 26, 1239-1247.

Tett, P., Gilpin, L., Svendsen, H., Erlandsson, C.P., Larsson, U., Kratzer, S., Fouilland, E., Janzen, C., Lee, J.-Y., Grenz, C. (2003) Eutrophication and some European waters of restricted exchange. Continental Shelf Research 23, 1635-1671.

Thibodeau, B., Miyajima, T., Tayasu, I., Wyatt, A., Watanabe, A., Morimoto, N., Yoshimizu, C., Nagata, T. (2013) Heterogeneous dissolved organic nitrogen supply over a coral reef: first evidence from nitrogen stable isotope ratios. Coral reefs 32, 1103-1110.

Thomson, J.M., Easton, A.C., Faragher, E. (1983) The use of vacutainer tubes for collection and storage of blood for coagulation testing. Clinical & Laboratory Haematology 5, 413-421.

Tobias, C., Giblin, A., McClelland, J., Tucker, J., Peterson, B. (2003) Sediment DIN fluxes and preferential recycling of benthic microalgal nitrogen in a shallow macrotidal estuary. Marine Ecology Progress Series 257, 25-36.

Toffaletti, J., Blosser, N., Kirvan, K. (1984) Effects of storage temperature and time before centrifugation on ionized calcium in blood collected in plain vacutainer tubes and silicone-separator (SST) tubes. Clinical chemistry 30, 553-556.

Tse, K.C., Jiao, J.J. (2008) Estimation of submarine groundwater discharge in Plover Cove, Tolo Harbour, Hong Kong by 222 Rn. Marine Chemistry 111, 160-170.

Turner, R.E., Rabalais, N.N. (1991) Changes in Mississippi River water quality this century. Bioscience, 140-147.

Uchiyama, Y., Nadaoka, K., Rölke, P., Adachi, K., Yagi, H. (2000) Submarine groundwater discharge into the sea and associated nutrient transport in a sandy beach. Water Resources Research 36, 1467-1479.

Ueda, S., Go, C.S.U., Suzumura, M., Sumi, E. (2003) Denitrification in a seashore sandy deposit influenced by groundwater discharge. Biogeochemistry 63, 187-205.

Ullman, W.J., Chang, B., Miller, D.C., Madsen, J.A. (2003) Groundwater mixing, nutrient diagenesis, and discharges across a sandy beachface, Cape Henlopen, Delaware (USA). Estuarine, Coastal and Shelf Science 57, 539-552.

Valiela, I., Costa, J., Foreman, K., Teal, J.M., Howes, B., Aubrey, D. (1999) Transport of groundwater-borne nutrients from watersheds and their effects on coastal waters. Biodegradation 10, 177-197.

Van Genuchten, M.T. (1980) A closed-form equation for predicting the hydraulic conductivity of unsaturated soils. Soil science society of America journal 44, 892-898.

Verhoeven, J.T., Arheimer, B., Yin, C., Hefting, M.M. (2006) Regional and global concerns over wetlands and water quality. Trends in ecology & evolution 21, 96-103.

Videira, N., Antunes, P., Santos, R., Gamito, S. (2003) Participatory modelling in environmental decision-making: the ria Formosa natural park case study. Journal of Environmental Assessment Policy and Management 5, 421-447.

Vila-Concejo, A., Ferreira, Ó., Ciavola, P., Matias, A., Dias, J.M. (2004) Tracer studies on the updrift margin of a complex inlet system. Marine Geology 208, 43-72.

Vila-Concejo, A., Ferreira, Ó., Matias, A., Dias, J. (2003) The first two years of an inlet: sedimentary dynamics. Continental Shelf Research 23, 1425-1445.

Vitousek, P.M., Aber, J.D., Howarth, R.W., Likens, G.E., Matson, P.A., Schindler, D.W., Schlesinger, W.H., Tilman, D.G. (1997) Human alteration of the global nitrogen cycle: sources and consequences. Ecological Applications 7, 737-750.

Vitousek, P.M., Howarth, R.W. (1991) Nitrogen limitation on land and in the sea: how can it occur? Biogeochemistry 13, 87-115.

Vogel, T., Van Genuchten, M.T., Cislerova, M. (2000) Effect of the shape of the soil hydraulic functions near saturation on variably-saturated flow predictions. Advances in Water Resources 24, 133-144.

Vousdoukas, M.I., Wziatek, D., Almeida, L.P. (2012) Coastal vulnerability assessment based on video wave run-up observations at a mesotidal, steep-sloped beach. Ocean Dynamics 62, 123-137.

Wada, E., Kadonaga, T., Matsuo, S. (1975) 15N aboundance in nitrogen of naturally occurring substances and global assessment of denitrification from isotopic viewpoint. Geochemical Journal 9, 139-148.

Wakida, F.T., Lerner, D.N. (2005) Non-agricultural sources of groundwater nitrate: a review and case study. Water Research 39, 3-16.

Waska, H., Kim, G. (2011) Submarine groundwater discharge (SGD) as a main nutrient source for benthic and water-column primary production in a large intertidal environment of the Yellow Sea. Journal of Sea Research 65, 103-113.

Wayland, D., Megson, D., Mudge, S., Icely, J., Newton, A. (2008) Identifying the source of nutrient contamination in a lagoon system. Environmental Forensics 9, 231-239.

Weinstein, Y., Yechieli, Y., Shalem, Y., Burnett, W.C., Swarzenski, P.W., Herut, B. (2011) What is the role of fresh groundwater and recirculated seawater in conveying nutrients to the coastal ocean? Environ Sci Technol 45, 5195-5200.

Whalen, S. (2005) Biogeochemistry of methane exchange between natural wetlands and the atmosphere. Environmental Engineering Science 22, 73-94.

Wilson, A.M., Gardner, L.R. (2006) Tidally driven groundwater flow and solute exchange in a marsh: Numerical simulations. Water Resources Research 42.

Windom, H., Niencheski, F. (2003) Biogeochemical processes in a freshwater–seawater mixing zone in permeable sediments along the coast of Southern Brazil. Marine Chemistry 83, 121-130.

Wong, W.W., Grace, M.R., Cartwright, I., Cook, P.L. (2014) Sources and fate of nitrate in a groundwater-fed estuary elucidated using stable isotope ratios of nitrogen and oxygen. Limnol. Oceanogr 59, 1493-1509.

Wu, J.-T., Chou, T.-L. (2003) Silicate as the limiting nutrient for phytoplankton in a subtropical eutrophic estuary of Taiwan. Estuarine, Coastal and Shelf Science 58, 155-162.

Wu, Z., Zhou, H., Zhang, S., Liu, Y. (2013) Using 222 Rn to estimate submarine groundwater discharge (SGD) and the associated nutrient fluxes into Xiangshan Bay, East China Sea. Mar Pollut Bull 73, 183-191.

Yadav, S., Shire, S.J., Kalonia, D.S. (2011) Viscosity analysis of high concentration bovine serum albumin aqueous solutions. Pharmaceutical research 28, 1973-1983.

Yan, L., Fitzgerald, M., Khov, C., Schafermeyer, A., Kupferle, M.J., Sorial, G.A. (2013) Elucidating the role of phenolic compounds in the effectiveness of DOM adsorption on novel tailored activated carbon. Journal of hazardous materials 262, 100-105.

Young, M.B., Gonneea, M.E., Fong, D.A., Moore, W.S., Herrera-Silveira, J., Paytan, A. (2008) Characterizing sources of groundwater to a tropical coastal lagoon in a karstic area using radium isotopes and water chemistry. Marine Chemistry 109, 377-394.

Zektser, I., Loaiciga, H.A. (1993) Groundwater fluxes in the global hydrologic cycle: past, present and future. Journal of Hydrology 144, 405-427.

References

Zhang, J., Mandal, A.K. (2012) Linkages between submarine groundwater systems and the environment. Current Opinion in Environmental Sustainability 4, 219-226.

Zingone, A., Enevoldsen, H.O. (2000) The diversity of harmful algal blooms: a challenge for science and management. Ocean & coastal management 43, 725-748.